

A Study on Heterotic Target Space Duality  
– Bundle Stability/Holomorphy, F-theory and LG Spectra

He Feng

Dissertation submitted to the Faculty of the  
Virginia Polytechnic Institute and State University  
in partial fulfillment of the requirements for the degree of

Doctor of Philosophy  
in  
Physics

Lara B. Anderson, Chair  
Shengfeng Cheng  
James A. Gray  
Eric Sharpe

Aug 1, 2019  
Blacksburg, Virginia

Keywords: Target Space Duality, Heterotic/F-theory Duality, LG spectrum  
Copyright 2019, He Feng

# A Study on Heterotic Target Space Duality – Bundle Stability/Holomorphy, F-theory and LG Spectra

He Feng

(ABSTRACT)

In the context of  $(0, 2)$  gauged linear sigma models, we explore chains of perturbatively dual heterotic string compactifications. The notion of *target space duality* (TSD) originates in non-geometric phases and can be used to generate distinct GLSMs with shared geometric phases leading to apparently identical target space theories. To date, this duality has largely been studied at the level of counting states in the effective theories. We extend this analysis in several ways.

First, we consider the correspondence including the effective potential and loci of enhanced symmetry in dual theories. By engineering vector bundles with non-trivial constraints arising from slope-stability (i.e. D-terms) and holomorphy (i.e. F-terms) the detailed structure of the vacuum space of the dual theories can be explored. Our results give new evidence that GLSM target space duality may provide important hints towards a more complete understanding of  $(0,2)$  string dualities. In addition, we consider TSD theories on elliptically fibered Calabi-Yau manifolds. In this context, each half of the “dual” heterotic theories must in turn have an F-theory dual. Moreover, the apparent relationship between two heterotic compactifications seen in  $(0,2)$  heterotic target space dual pairs should, in principle, induce some putative correspondence between the dual F-theory geometries. It has previously been conjectured in the literature that  $(0,2)$  target space duality might manifest in F-theory as multiple K3- fibrations of the same elliptically fibered Calabi-Yau manifold. In this work we investigate this conjecture in the context of both six-dimensional and four-dimensional effective theories and demonstrate that in general,  $(0,2)$  target space duality cannot be explained by such a simple phenomenon alone. Finally, we consider Landau-Ginzburg (LG) phases of TSD theories and explore their massless spectrum. In particular, we investigate TSD pairs involving geometric singularities. We study resolutions of these singularities and their relationship to the duality.

# A Study on Heterotic Target Space Duality – Bundle Stability/Holomorphy, F-theory and LG Spectra

He Feng

(GENERAL AUDIENCE ABSTRACT)

In string theory, the space-time has “hidden” dimensions beyond the three spatial and one time-like dimensions macroscopically seen in our universe. We want to study how the geometries of this “internal space” can affect observable physics, and which geometries are compatible with our universe. Target space duality is a relationship that connects two or more geometries together. In target space duality, gauged linear sigma models (related to string theories) share a common locus (called a Landau-Ginzburg phase) in their parameter space, but are distinct theories. To date, this duality has largely been studied at the level of counting states in the effective theories. In this dissertation, target space duality is studied in more depth.

First we extend the analysis to the effective potential and loci of enhanced symmetry. By engineering examples with non-trivial constraints, the detailed structure of the vacuum space of the dual theories can be explored. Our results give new evidence that target space duality may provide important hints towards a more complete understanding of string dualities. We also investigate the conjecture that target space duality might manifest in F-theory, a higher dimensional string theory, as multiple fibrations of the same manifold. We demonstrate that in general, target space duality cannot be explained by such a simple phenomenon alone. In our cases, we provide evidence that non-geometric data in F-theory must play at least some role in the induced F-theory correspondence, while leaving the full determination of the putative new F-theory duality to future work. Finally we explore the complete massless spectrum of the Landau-Ginzburg (LG) phase. Specifically, we calculate the full LG spectra for both sides, and compare the theory with the geometric phases. We find examples in which half of the target space dual geometry is singular. We have probed some approaches to resolving the singularity.

# Acknowledgments

During my PhD studies, I received help and support from many people. I wouldn't be able to complete the journey without them, I'm very grateful and I will always remember them. Here I would particularly like to acknowledge the following people:

First, I would like to thank my supervisor Professor Lara Anderson, not only for your guidance and support but also for your kindness, patience and thoughtfulness. It's my good fortune to meet you and have the opportunity to work with you during this journey. When I got confused, you always led me through and inspired me in different ways. I've learned so much from you that will benefit my future.

I would like to thank my collaborators Professor Eric Sharpe, Xin Gao, Mohsen Karkheiran and Hadi Parsian. Your knowledge, enthusiasm and diligence are impressive. I enjoyed working with you and making progress together; it was an unforgettable experience.

I would also like to thank Paul Oehlmann, Wei Gu and Juntao Wang; the discussions with you helped me in so many various situations and problems.

Special thanks to Professor James Gray and Professor Ilarion Melnikov, for helping me adapt into this field, and teaching me a lot of things. Your willingness to guide me from the very beginning allowed me to realize my potential.

# Contents

|  |           |
|--|-----------|
| <b>List of Figures</b>   | <b>ix</b> |
| <b>List of Tables</b>  | <b>x</b>  |
| <b>1 Introduction</b>  | <b>1</b>  |
| 1.1 Steps to String Theory . . . . .   | 1         |
| 1.2 Ten-Dimensional Heterotic Theory . . . . .   | 3         |
| 1.3 GLSM and Target Space Duality . . . . .  | 7         |
| 1.4 Why Duality Matters . . . . .  | 9         |
| 1.5 Structure of This Dissertation . . . . .   | 10        |
| 1.5.1 Stability and Holomorphy Across TSD Pairs . . . . .                                  | 10        |
| 1.5.2 Target Space Duality and Het/F-theory Duality . . . . .                              | 13        |
| 1.5.3 Massless Spectrum of the Landau-Ginzburg Phase . . . . .                             | 17        |
| <b>2 A Brief Review of Target Space Duality</b>  | <b>19</b> |
| 2.1 $(0, 2)$ Gauged Linear Sigma Models . . . . .  | 19        |
| 2.2 Target Space Duality . . . . .   | 23        |
| 2.2.1 Illustration of the Duality Procedure . . . . .                                      | 24        |
| 2.2.2 Target Space Duals with an Additional $U(1)$ . . . . .                               | 25        |
| 2.2.3 Redundant Bundle Geometry and More General Target Space Duals                        | 27        |
| 2.2.4 Summary of Choices for the Target Space Dual Geometries Considered<br>Here . . . . . | 30        |

|          |   |           |
|----------|---|-----------|
| <b>3</b> | <b>Heterotic String Compactifications</b>   | <b>31</b> |
| 3.1      | The Target Space Potential: Supersymmetry Conditions and Vector Bundle Geometry . . . . . | 31        |
| 3.2      | Tools for Probing Slope-Stability of Vector Bundles . . . . .                             | 35        |
| 3.2.1    | Slope Stability . . . . .   | 35        |
| 3.2.2    | Algorithmically Testing Stability . . . . .   | 37        |
| 3.2.3    | Negative Line Bundle Entries in Monad Bundles and Stability . . . . .                     | 38        |
| 3.2.4    | Example Stability Analysis . . . . .  | 39        |
| 3.2.5    | Some Useful Results on Stable Bundles . . . . .   | 41        |
| 3.2.6    | A Few Useful Formulas for Bundle and Manifold Topology . . . . .                          | 43        |
| <b>4</b> | <b>New Evidence for (0,2) Target Space Duality</b>  | <b>46</b> |
| 4.1      | D-terms, Bundle Stability, and Duality . . . . .  | 46        |
| 4.1.1    | Effective Theory Near the Stability Wall . . . . .  | 49        |
| 4.1.2    | Target Space Duals of Theories with D-terms . . . . .                                     | 52        |
| 4.1.3    | Branch Structure in the Vacuum Space of the Dual Theories . . . . .                       | 56        |
| 4.1.4    | Perturbative/Non-perturbative Duality . . . . .   | 61        |
| 4.1.5    | Isomorphic Geometry in Target Space Duality . . . . .                                     | 63        |
| 4.1.6    | On S-Equivalence Classes . . . . .  | 64        |
| 4.2      | F-terms, Bundle Holomorphy, and Duality . . . . .   | 67        |
| 4.2.1    | F-terms in the Effective Theory . . . . .   | 67        |
| 4.2.2    | A Simple Example . . . . .  | 69        |
| 4.2.3    | The Target Space Dual . . . . .   | 72        |
| 4.3      | Target Space Duality, (2, 2) Loci, and Tangent Bundle Deformations . . . . .              | 75        |
| <b>5</b> | <b>Inducing a Duality in F-theory</b>   | <b>80</b> |

|          |  |            |
|----------|--|------------|
| 5.1      | Essential Tools for Heterotic/F-theory Duality . . . . .                           | 80         |
| 5.2      | Spectral Cover Construction . . . . .  | 82         |
| <b>6</b> | <b>Target Space Duality in Heterotic/F-theory Duality</b>                          | <b>88</b>  |
| 6.1      | A Target Space Dual Pair with Elliptically Fibered Calabi-Yau Threefolds . . . . . | 88         |
| 6.1.1    | A Tangent Bundle Deformation . . . . .   | 88         |
| 6.1.2    | More General Vector Bundles . . . . .  | 94         |
| 6.2      | Warm Up: Heterotic/F-theory Duality in Six Dimensions . . . . .                    | 96         |
| 6.2.1    | Spectral Cover of Monads . . . . .   | 97         |
| 6.2.2    | Examples . . . . .   | 99         |
| 6.2.3    | Counter Examples of the Conjecture . . . . .                                       | 102        |
| 6.2.4    | Example 1 . . . . .  | 104        |
| 6.2.5    | Example 2 . . . . .  | 107        |
| 6.3      | F-theory Duals of Four-Dimensional Heterotic TSD Pairs . . . . .                   | 111        |
| <b>7</b> | <b>Massless Spectrum of the Non-Geometric Phase</b>                                | <b>117</b> |
| 7.1      | Method of Computing the Complete Massless Spectrum . . . . .                       | 117        |
| 7.1.1    | Space-time Interpretation of the Massless Spectrum in the Case of $\tilde{r} = 3$  | 122        |
| 7.2      | Example . . . . .  | 123        |
| 7.2.1    | Setup . . . . .  | 124        |
| 7.2.2    | Find Vacuum Charges and Energies . . . . .   | 125        |
| 7.2.3    | k=0 Sector . . . . .   | 126        |
| 7.2.4    | k=1 Sector . . . . .   | 127        |
| 7.2.5    | More Sectors and Summary . . . . .   | 129        |
| 7.3      | Resolution of Singularity . . . . .  | 132        |

|          |   |            |
|----------|---|------------|
| 7.3.1    | Resolution of Ambient Space . . . . .                               | 134        |
| 7.3.2    | Resolution of Manifold/Hypersurfaces . . . . .                      | 135        |
| 7.3.3    | Resolution of the Bundle . . . . .                                  | 136        |
| 7.3.4    | Aside: Getting the Same Result with Linear Combinations . . . . .   | 137        |
| 7.3.5    | Anomaly Cancellation Condition for the Bundle . . . . .             | 137        |
| 7.3.6    | Embed in a Bigger GLSM . . . . .                                    | 139        |
| <b>8</b> | <b>Conclusions and Future Directions</b>                            | <b>141</b> |
|          | <b>Appendices</b>   | <b>145</b> |
|          | <b>Appendix A Examples of Target Space Dual Chains</b>              | <b>146</b> |
| A.1      | A Complete List of Target Space Dual Theories . . . . .             | 146        |
| A.2      | Target Space Dual Chain to a New Description of the Monad . . . . . | 151        |
|          | <b>Appendix B Exotic Cases in Finding Elliptic Fibered Examples</b> | <b>154</b> |
|          | <b>Appendix C Non-trivial Rewriting</b>                             | <b>157</b> |
| C.1      | Non-trivial Rewriting with Tangent Bundle . . . . .                 | 158        |
| C.2      | Non-trivial Rewriting with General Vector Bundle . . . . .          | 160        |
|          | <b>Bibliography</b>   | <b>162</b> |



# List of Figures

|     |   |     |
|-----|---|-----|
| 3.1 | <i>An illustration of the D-term effective potential corresponding to (3.1.7) (and a part of (3.1.6)) and geometrically realized by the bundle failing to be slope-stable for a sub-cone of Kähler moduli space. The white boundary line is referred to as a “stability wall” in the Kähler cone. . . . .</i> | 34  |
| 3.2 | <i>The stable and unstable regions of the Kähler cone associated to the SU(3) bundle in (3.2.19). . . . .</i>   | 41  |
| 4.1 | <i>The stable ray in Kähler moduli space shown for the monad bundle in (4.1.4). Along this co-dimension 1 subcone the bundle takes the poly-stable form shown in (4.1.17). . . . .</i>  | 49  |
| 4.2 | <i>The two-dimensional stable sub-cone in Kähler moduli space shown for the monad bundle in (4.1.20). Along this co-dimension 1 sub-cone the bundle takes the poly-stable form shown in (4.1.29). . . . .</i>   | 53  |
| 4.3 | <i>The stable sub-cone in Kähler moduli space shown for the SU(5) monad bundle in (4.1.37). This corresponds to the branch of vacuum space described by (4.1.34) and (4.1.35). . . . .</i>  | 58  |
| 4.4 | <i>The stable sub-cone in Kähler moduli space shown for the SU(5) monad bundle in (4.1.41). This corresponds to the Higgsed branch of the target space dual theory in (4.1.20) and Figure 4.2. . . . .</i>  | 61  |
| 6.1 | <i>The vertical dotted line on the right hand side is the “vertical <math>\mathbb{P}^1</math>.” After change of fibration on the left hand side the same <math>\mathbb{P}^1</math> will be the base of the dual heterotic K3. . . . .</i>   | 107 |

# List of Tables

|     |  |     |
|-----|--|-----|
| 4.1 | <i>Particle content of the <math>SU(6) \times U(1)</math> theory associated to the bundle (4.1.4) along its reducible and poly-stable locus <math>V = \mathcal{O}(-1, 1) \oplus \mathcal{O}(1, -1) \oplus U_3</math> (i.e. on the stability wall given by (4.1.7) and shown in Figure 4.1).</i> . . . . .  | 51  |
| 4.2 | <i>Particle content of the <math>SU(6) \times U(1)</math> theory associated to the bundle (4.1.20) along its reducible and poly-stable locus <math>V = \tilde{L} \oplus \tilde{L}^\vee \oplus \tilde{U}_3</math> (i.e. on the stability wall given by (4.1.27) and shown in Figure 4.2).</i> . . . . .   | 55  |
| 4.3 | <i>Particle content of the <math>SU(5)</math> theory associated to the indecomposable <math>SU(5)</math> bundle (4.1.37) – the branch of the theory in the stable chamber of Kähler moduli space. See Figure 4.3. The ambiguity (denoted by <math>x</math>) in the <b>5, 5</b> spectrum arises from its dependence on the monad map in (4.1.37).</i> . . . . . | 59  |
| 7.1 | <i>Left and right <math>U(1)</math> charges of fields in a Landau-Ginzburg theory.</i> . . . . .   | 118 |
| 7.2 | <i>Left and right <math>U(1)</math> charges of fields in <math>V(1, 1, 2, 6; 10) \rightarrow \mathbb{P}_{1,2,2,2,3,3}[5, 8]</math>.</i> . . . . .  | 125 |
| 7.3 | <i>Vacuum charges and energy contributed by each field, <math>k=1</math> sector.</i> . . . . .   | 126 |
| 7.4 | <i>The list of vacuum charges and energy for <math>k=0 \sim 10</math> sectors, <math>k &gt; 10</math> is given by symmetry.</i> . . . . .  | 127 |
| 7.5 | <i>The complete massless spectrum of <math>V(1, 1, 2, 6; 10) \rightarrow \mathbb{P}_{1,2,2,2,3,3}[5, 8]</math> for <math>k=0 \sim 19</math> sectors, where <math>k=11 \sim 19</math> sectors are given by symmetry.</i> . . . . .  | 131 |

# Chapter 1

## Introduction

### 1.1 Steps to String Theory

There are 4 fundamental forces in nature that we know of: gravity, electromagnetism, the weak interaction and the strong interaction. However, a major unsolved problem is whether there is a single theory that explains them all, and what it is.

The first successful approach was the combination of electromagnetism and the weak interaction in the 1960s by Glashow, Salam and Weinberg [1–3]. Mathematically the electroweak theory is described by a gauge field theory with  $SU(2) \times U(1)$  gauge group. To this combination, the strong interaction was added and in the 1970s the standard model had its formulation, with the full gauge group  $SU(3) \times SU(2) \times U(1)$  [4]. Despite a wide range of experimental verifications, ranging from the discovery of top quarks (1995) [5], the tau neutrino (2000) [6] and the Higgs boson (2012) [7, 8], and already widely accepted by scientists, the standard model still has deficiencies. These include the hierarchy problem, the failure to explain dark matter and dark energy, and the formal theoretical concern that the standard model is not a unified theory. Perhaps most importantly, it does not include gravity.

At energy scales above  $10^2$  GeV, electromagnetism and the weak force become one electroweak interaction, which has been confirmed by experiments. If strong interactions can unify with electroweak interactions at a higher energy, then the theory is called a Grand Unified Theory (GUT). The first and simplest GUT was proposed by Georgi and Glashow in 1974 [9]. It has  $SU(5)$  gauge group, which contains the  $SU(3) \times SU(2) \times U(1)$  symmetry of the standard model as a subgroup.

There is a large gap between the electroweak scale and gravity, which can be observed by noting that the Higgs mass ( $\sim 125$  GeV) is much smaller than the Planck mass ( $\sim 1.2 \times 10^{19}$  GeV). This is the famous “hierarchy problem” [10]. When calculating the Higgs mass, the quantum correction from the loops could go up as high as Planck scale, which leads to

a quadratic divergence in perturbation theory. One approach to the hierarchy problem is supersymmetry. In supersymmetry (SUSY), the fermions and bosons are superpartners, so the bosonic loop corrections cancel out the fermionic loop corrections with the opposite sign, thus solving the hierarchy problem. Moreover, some SUSY particles can be candidates for dark matter [11]. Even though SUSY is not yet seen in experiments, it's not excluded. In addition, there are also other extensions with SUSY beyond the minimal supersymmetric standard model.

So far none of the theories have included gravity. In the 1970s-1980s, a new approach – string theory – was formulated and developed [12, 13]. As the name suggests, string theory takes the fundamental objects to be strings instead of point-like particles; it naturally includes a graviton. The earliest bosonic string theory has a critical dimension of  $D=26$ , it contains only bosons and has a fundamental instability from tachyons. Incorporating fermions into string theory led to the invention of superstring theory. With SUSY incorporated, string theory is compatible with fermions and is called superstring theory. In superstring theory, to cancel out the central charge from fermionic fields, bosonic fields and ghost contributions, the space time dimension has to be 10. Depending on the SUSY generators and gauge groups, there are 5 consistent superstring theories: type I, type IIA, type IIB, heterotic ( $E_8 \times E_8$ ) and heterotic ( $SO(32)$ ).

During the first superstring revolution in 1985, it was realized the six extra dimensions need to be compact and form a Calabi-Yau manifold [14]. For type I, type IIA and type IIB superstring theories, there are open and closed strings. When open strings propagate, the ends will form a higher dimensional object called D-branes; D-branes describe the gauge interactions and the closed strings describe the gravitational interactions. In heterotic string theories, there are closed strings but not open strings, and gauge interactions are described by gauge bundles attached to the space. There are also NS5-branes. In heterotic ( $E_8 \times E_8$ ) string theory, the  $E_8$  group can break down to the GUT groups  $E_6$ ,  $SO(10)$  or  $SU(5)$  (among others), and can possibly give us the four-dimensional GUT theory. There are lots of examples of this type. We will focus on the heterotic ( $E_8 \times E_8$ ) theory.

During the second superstring revolution in the mid 1990s, it was found by Witten [15] that all 5 superstring theories can be related by dualities, thus can be unified by an eleven-dimensional theory, called M-theory.

In type IIB superstring theory, the action of axion-dilaton is invariant under an  $SL(2, \mathbb{R})$

symmetry. Type IIB theory does not incorporate the D7 brane backreaction. To solve these problems, F-theory was introduced by Vafa in 1996 [16]. By compacting the twelve-dimensional F-theory on a two-torus, one recovers the ten-dimensional type IIB theory. There is no Lagrangian formulation of F-theory as a fundamental theory, but rather as duals to current theories. For example, F-theory as strongly coupled Type IIB theory with 7-branes and varying dilaton, F-theory as dual to  $E_8 \times E_8$  heterotic theory, and F-theory as dual to heterotic-M-theory on a vanishing  $T^2$ . With these observations in mind, we turn now to a review of some of the essential elements of this thesis.

## 1.2 Ten-Dimensional Heterotic Theory

To preserve  $\mathcal{N} = 1$  supersymmetry in the four-dimensional effective theory, we need  $\mathcal{N} = 1$  supersymmetry in ten dimensions. The ten-dimensional effective heterotic action is written:

$$S_{het} = \frac{1}{2\kappa^2} \int d^{10}x (-G)^{1/2} \left[ R - \partial_M \phi \partial^M \phi - \frac{3\kappa^2}{8g^4 \phi^2} |H_3|^2 - \frac{\kappa^2}{4g^2 \phi} Tr(|F_2|^2) + \dots \right], \quad (1.2.1)$$

where  $H_3 = dB_2 - \omega_3$  is the field strength associated to the 2-form and  $F$  is the Yang-Mills field strength.

From the  $\mathcal{N} = 1$  supersymmetric sigma model, the transformations for fermionic fields are [13]:

$$\begin{aligned} \delta\psi_M &= \frac{1}{\kappa} D_M \eta + \frac{\kappa}{32g^2 \phi} (\Gamma_M^{NPQ} - 9\delta_M^N \Gamma^{PQ}) \eta H_{NPQ} + (Fermi)^2, \\ \delta\chi^a &= -\frac{1}{4g\sqrt{\phi}} \Gamma^{MN} F_{MN}^\alpha \eta + (Fermi)^2, \\ \delta\lambda &= -\frac{1}{\sqrt{2}\phi} (\Gamma \cdot \partial\phi) \eta + \frac{\kappa}{8\sqrt{2}g^2 \phi} \Gamma^{MNP} \eta H_{MNP} + (Fermi)^2, \end{aligned} \quad (1.2.2)$$

where  $\psi_M$  is the gravitino,  $\lambda$  the dilatino,  $\chi^a$  the gluino, and the Bianchi identity for H is:

$$dH = tr R \wedge R - tr F \wedge F. \quad (1.2.3)$$

For the simplest class of solutions, we take  $H = 0$  and  $\phi$  constant, and then preserving a

(subset of) supersymmetry requires:

$$\begin{aligned} 0 &= D_M \eta, \\ 0 &= \Gamma^{ij} F_{ij}^\alpha \eta. \end{aligned} \tag{1.2.4}$$

From the first equation  $D_M \eta = 0$ , using the fact that  $M^4$  is Minkowski space, we see that

$$D_i \tilde{\eta} = 0, \tag{1.2.5}$$

where  $\tilde{\eta}$  is a six-dimensional spinor.

This equation indicates that we need a covariantly constant spinor on the six-dimensional internal manifold. The spin connection in six dimensions is an  $\text{SO}(6)$  gauge field,  $\text{SO}(6)$  is isomorphic to  $\text{SU}(4)$ , and the 4 of  $\text{SU}(4)$  contains an  $\text{SU}(3)$  singlet, which means the six-dimensional space has  $\text{SU}(3)$  holonomy, thus is a Calabi-Yau manifold.

We can write out the second equation  $\Gamma^{ij} F_{ij}^\alpha \eta = 0$  more explicitly in terms of local holomorphic coordinates as

$$(F_{\bar{a}\bar{b}} \Gamma^{\bar{a}\bar{b}} + F_{ab} \Gamma^{ab} + 2F_{\bar{a}b} \Gamma^{\bar{a}b}) \eta = 0. \tag{1.2.6}$$

All three terms must vanish separately, which gives the Hermitian Yang-Mills equations:

$$g^{\bar{a}\bar{b}} F_{\bar{a}\bar{b}} = 0, \quad F_{ab} = 0, \quad F_{\bar{a}b} = 0, \tag{1.2.7}$$

where  $F$  is the gauge field strength associated with the vector bundle  $V$ , and  $a$  and  $\bar{b}$  are holomorphic and anti-holomorphic indices on the Calabi-Yau manifold. These equations involve all three types of singlet “moduli” ( $h^{1,1}(X)$ ,  $h^{2,1}(X)$  and  $h^1(X, \text{End}_0(V))$ ) and in general not all possible values of the CY and bundle moduli will correspond to a solution of (1.2.7).

The detailed form of the potential generated in the  $\mathcal{N} = 1$ , four-dimensional effective theory has been developed in recent work [17–21]. By a theorem of Donaldson-Uhlenbeck and Yau [22, 23], the first condition in (1.2.7) is equivalent to the condition of Mumford (slope) polystability of  $V$ . The characterization of slope stability as well as tools to test whether a given bundle is stable are provided in Section 3.2. The condition of stability (equivalently (1.2.7)) manifestly depends on the Kähler moduli through the presence of the metric. The Kähler class can in principle be smoothly varied so that the bundle transitions from being fully

stable in one region of moduli space to poly-stable along a higher co-dimensional boundary (a so-called “stability wall” [18]) to fully unstable (and hence supersymmetry breaking) for some region of moduli space. In the effective theory, this is associated with *D-term breaking* of supersymmetry at stability walls. Along the stability walls the condition of poly-stability forces the bundle  $V$  to become reducible (i.e.  $V \rightarrow \mathcal{F} \oplus V/\mathcal{F}$ ), leading to the presence of enhanced, Green-Schwarz massive  $U(1)$  symmetries in the effective theory. See [17, 18, 21, 24].

Likewise, the second conditions in (1.2.7) correspond geometrically to the condition that the bundle is holomorphic. It is clear that the conditions  $F_{ab} = F_{\bar{a}\bar{b}} = 0$  depend on the definition of holomorphic and anti-holomorphic coordinates on  $X$ . This choice clearly depends on the complex structure. For a fixed topology of the gauge fields, specific changes in the complex structure of the Calabi-Yau threefold may be such that these holomorphy equations no longer have a solution [25, 26]. In the effective theory, this obstruction is associated with the *F-term breaking* of supersymmetry by the complex structure moduli. Geometrically, the flat directions in moduli space corresponding to holomorphic deformations of the complete geometry (manifold + bundle) are described by the “Atiyah class” of  $V$  [27]. More precisely, the infinitesimal complex moduli of the heterotic theory are not the independent bundle moduli ( $h^1(X, \text{End}_0(V))$ ) and complex structure moduli ( $h^{2,1}(X)$ ) but rather the elements of the cohomology group

$$H^1(X, \mathcal{Q}), \tag{1.2.8}$$

which describes the tangent space to *the infinitesimal deformation space of the pair*  $(X, V)$ . Here  $\mathcal{Q}$  is defined by Atiyah Sequence [27]:

$$0 \rightarrow \text{End}_0(V) \rightarrow \mathcal{Q} \rightarrow TX \rightarrow 0. \tag{1.2.9}$$

The geometry and field theory of these F-terms and holomorphy are explored further in Section 4.2.

The gauge group and particle spectrum of the four-dimensional N=1 theory is determined by the structure group of the vector bundle and the associated bundle value cohomology. If the bundle over the internal space has structure group of  $SU(3)$ , then the four-dimensional physical space will see structure group of  $E_6$ , the commutant of  $SU(3)$  in  $E_8$ . This being said, the  $E_8$  group breaks into a product  $G \times H$  where  $G, H \in E_8$ ,  $G$  is the structure group of the bundle and  $H$  is the gauge group observable at low energy [28]. To find the low energy

particle spectrum, we need to decompose the adjoint **248** of  $E_8$  under  $G \times H$ .

$$248 \rightarrow (1, \text{Ad}(H)) \oplus \bigoplus_i (R_i, r_i), \quad (1.2.10)$$

here  $\text{Ad}(H)$  is the adjoint representation of  $H$ , corresponding to the low-energy gauge fields,  $\{(R_i, r_i)\}$  is the set of representations of  $G \times H$ , with  $r_i$  corresponding to the low-energy matter fields.

The fermion fields transforming under the GUT symmetry must be massless modes to be observable at low energy, which can be counted by the dimensions of certain bundle-valued cohomology groups. For each representation  $r_i$ , the number of supermultiplets is given by  $n_{r_i} = h^1(X, V_{R_i})$ .

In our work, we will focus on bundles with  $SU(3)$ ,  $SU(4)$  and  $SU(5)$  groups, corresponding to four-dimensional GUT groups  $E_6$ ,  $SO(10)$  and  $SU(5)$ , respectively. The decomposition for  $SU(3)$ ,  $SU(4)$  and  $SU(5)$  bundles, and the correspondence between number of massless modes and bundle cohomology groups are summarized below:

$$\begin{aligned} SU(3) \times E_6 \in E_8 : \mathbf{248} &\rightarrow (\mathbf{1}, \mathbf{78}) \oplus (\mathbf{3}, \mathbf{27}) \oplus (\mathbf{3}, \overline{\mathbf{27}}) \oplus (\mathbf{8}, \mathbf{1}) \\ n_{\mathbf{27}} &= h^1(V), \quad n_{\overline{\mathbf{27}}} = h^1(V^*) = h^2(V), \\ n_{\mathbf{1}} &= h^1(V \otimes V^*), \\ SU(4) \times SO(10) \in E_8 : \mathbf{248} &\rightarrow (\mathbf{1}, \mathbf{45}) \oplus (\mathbf{4}, \mathbf{16}) \oplus (\mathbf{4}, \overline{\mathbf{16}}) \oplus (\mathbf{6}, \mathbf{10}) \oplus (\mathbf{15}, \mathbf{1}) \\ n_{\mathbf{16}} &= h^1(V), \quad n_{\overline{\mathbf{16}}} = h^1(V^*) = h^2(V), \\ n_{\mathbf{10}} &= h^1(\wedge^2 V), \quad n_{\mathbf{1}} = h^1(V \otimes V^*), \\ SU(5) \times SU(5) \in E_8 : \mathbf{248} &\rightarrow (\mathbf{1}, \mathbf{24}) \oplus (\mathbf{5}, \mathbf{10}) \oplus (\mathbf{5}, \overline{\mathbf{10}}) \oplus (\mathbf{10}, \mathbf{5}) \oplus (\overline{\mathbf{10}}, \mathbf{5}) \oplus (\mathbf{24}, \mathbf{1}) \\ n_{\mathbf{10}} &= h^1(V), \quad n_{\overline{\mathbf{10}}} = h^1(V^*) = h^2(V), \\ n_{\mathbf{5}} &= h^1(\wedge^2 V^*), \quad n_{\overline{\mathbf{5}}} = h^1(\wedge^2 V), \\ n_{\mathbf{1}} &= h^1(V \otimes V^*). \end{aligned} \quad (1.2.11)$$

Moreover, the index of  $V$  is defined as:

$$\text{ind}(V) = \sum_{p=0}^3 (-1)^p h^p(X, V) = \frac{1}{2} \int_X c_3(V), \quad (1.2.12)$$



where  $c_3$  is the third Chern class. For a stable  $SU(n)$  bundle  $V$ ,  $h^0(X, V) = h^3(X, V) = 0$ , so  $\text{ind}(V) = -h^1(X, V) + h^2(X, V)$ , which is the difference between the number of generations and anti-generations.

### 1.3 GLSM and Target Space Duality

Landau-Ginzburg (LG) theories were historically distinct theories from nonlinear sigma models on Calabi-Yau manifolds, until the notion of a gauged linear sigma model (GLSM) was introduced by Witten in 1993 [29]. The GLSM provides a description of the complexified compact stringy Kähler moduli space which is divided into various phases. The freedom to vary a Fayet-Illiopolos parameter links a variety of distinct phases including the geometric phases (associated to target space geometries like Calabi-Yau threefolds  $X$  and holomorphic vector bundle  $V$ ), non-geometric phase (commonly a Landau-Ginzburg phase), and a rich variety of hybrid phases.

Specifically, in an Abelian GLSM, there exists multiple  $U(1)$  gauge fields  $A^{(\alpha)}$  with  $\alpha = 1, \dots, r$ , two sets of chiral superfields as  $X_i$  with  $U(1)$  charges  $Q_i^{(\alpha)}$ , and  $P_l$  with  $U(1)$  charges  $-M_l^{(\alpha)}$ . Furthermore, there are two sets of Fermi superfields:  $\Lambda^a$  with charges  $N_a^{(\alpha)}$ , and  $\Gamma^j$  with charges  $-S_j^{(\alpha)}$ . Here anomaly cancellation condition requires the following linear and quadratic constraints for all  $\alpha, \beta = 1, \dots, r$ :

$$\begin{aligned} \sum_{a=1}^{\delta} N_a^{(\alpha)} &= \sum_{l=1}^{\gamma} M_l^{(\alpha)}, & \sum_{i=1}^d Q_i^{(\alpha)} &= \sum_{j=1}^c S_j^{(\alpha)}, \\ \sum_{l=1}^{\gamma} M_l^{(\alpha)} M_l^{(\beta)} - \sum_{a=1}^{\delta} N_a^{(\alpha)} N_a^{(\beta)} &= \sum_{j=1}^c S_j^{(\alpha)} S_j^{(\beta)} - \sum_{i=1}^d Q_i^{(\alpha)} Q_i^{(\beta)}. \end{aligned} \quad (1.3.1)$$

The GLSM is further described by a superpotential and a scalar potential, while the scalar

potential has contributions from F-terms and D-terms:

$$\begin{aligned}
S &= \int d^2z d\theta \left[ \sum_j \Gamma^j G_j(x_i) + \sum_{l,a} P_l \Lambda^a F_a^l(x_i) \right], \\
V_F &= \sum_j |G_j(x_i)|^2 + \sum_a \left| \sum_l p_l F_a^l(x_i) \right|^2, \\
V_D &= \sum_{\alpha=1}^r \left( \sum_{i=1}^d Q_i^{(\alpha)} |x_i|^2 - \sum_{l=1}^{\gamma} M_l^{(\alpha)} |p_l|^2 - \xi^{(\alpha)} \right)^2.
\end{aligned} \tag{1.3.2}$$

The  $\xi^{(\alpha)} \in \mathbb{R}$  in the D-term potential is the Fayet-Iliopoulos (FI) parameter which determines the structure of the vacuum. Consider the simple case with only one  $U(1)$  so there is only one  $\xi$ . If  $\xi > 0$  then it's the geometric phase, described by a vector bundle over a Calabi-Yau manifold:  $V_{N_1, \dots, N_\delta}[M_1, \dots, M_\gamma] \rightarrow X \equiv \mathbb{P}_{Q_1, \dots, Q_d}[S_1, \dots, S_c]$ .

If  $\xi < 0$  then it's the Landau-Ginzburg phase described by a superpotential:

$$\mathcal{W}(x_i, \Lambda^a, \Gamma^j) = \sum_j \Gamma^j G_j(x_i) + \sum_a \Lambda^a F_a(x_i), \tag{1.3.3}$$

where it would be a hybrid-type non-geometric phases if there are multiple  $U(1)$ 's.

Within (0, 2) GLSMs, the target space duality (TSD) of [30] is manifested by the existence of a shared sub-locus in the moduli space of the paired theories. More precisely each of the “dual” (0, 2) GLSMs shares a non-geometric phase (commonly a Landau-Ginzburg phase). In this web of theories, the geometric phases – consisting of a Calabi-Yau threefold,  $X$ , and a holomorphic bundle  $\pi : V \rightarrow X$  over it – are connected through a wealth of geometric correspondences, including geometric (i.e. conifold) transitions between the base CY geometries  $(X, \tilde{X})$ . However, the relationship between the vector bundles  $(V, \tilde{V})$  is more subtle and no systematic geometric characterization of the full paired geometries,  $(X, V), (\tilde{X}, \tilde{V})$ , has yet been provided. However, one essential feature of this target space duality is that the correspondence between two different geometric phases preserves the net number of moduli of the theory:

$$h^{1,1}(X) + h^{2,1}(X) + h^1(X, \text{End}_0(V)) = h^{1,1}(\tilde{X}) + h^{2,1}(\tilde{X}) + h^1(X, \text{End}_0(\tilde{V})). \tag{1.3.4}$$

Unlike the simple interchange of  $h^{1,1} \leftrightarrow h^{2,1}$  of CY mirror symmetry, the distribution of the

total degrees of freedom given above between the moduli of the base CY manifold and those of the vector bundle can change dramatically across a  $(0, 2)$  dual pair.

In recent work [31, 32], systematic landscape studies of  $(0, 2)$  target space duals were undertaken. In particular, the connected geometric phases were explored in detail and it was found that the gauge symmetry, moduli and charged matter spectrum were generically identical in the geometric phases. This was explored in the context of vector bundles with  $SU(n)$  structure group, for which the charged matter is counted by

$$h^i(X, \wedge^k V) = h^i(\tilde{X}, \wedge^k \tilde{V}), \quad (1.3.5)$$

for  $k = 0, \dots, n - 1$ . In the extensive studies carried out in [31, 32], the complete charged and singlet particle spectra were found to correspond exactly in almost all  $(0, 2)$  target space dual pairs<sup>1</sup>.

## 1.4 Why Duality Matters

Since the first observation of target space duality, it has been an open question whether or not the relationship described above corresponds to a true isomorphism of the target space theories/GLSMs (or indeed full non-linear sigma models) or rather represents a transition – i.e. a shared locus in moduli space for two distinct theories (perhaps similar to conifold transitions in type II theories [33])? To establish which of these possibilities is correct requires a more a detailed study of the “dual” theories and a clear map between them – which could determine whether they can be identified everywhere in their moduli spaces or only at some sublocus.

The goal of this work is to further explore heterotic target space duality, with the hope of moving towards a more fully developed notion of dualities involving the  $(0, 2)$  heterotic string. At present, many heterotic string dualities – including any complete notion of  $(0, 2)$  mirror symmetry [34–37] – remain relatively unexplored compared to their counterparts in  $(2, 2)$  string theories. Heterotic mirror symmetry, for instance, must necessarily exhibit an even more intricate structure than  $(2, 2)$  (Calabi-Yau) mirror symmetry which interchanges

---

<sup>1</sup>In a handful of cases ( $< 2\%$  of roughly 83,000 models analyzed) in the landscape scan, these spectra did not fully agree. The authors conjecture that this is due to the fact that several technical simplification/s/assumptions had been made in the scan. See [31] for details.

a pair of manifolds (and has sparked a rich interchange of ideas with mathematics, including the field of homological mirror symmetry<sup>2</sup>). In the case of heterotic  $(0, 2)$  theories it has been established that duality between  $(0, 2)$  sigma models and their supergravity limits can involve more complicated relationships between the geometry of Calabi-Yau manifolds and vector bundles over them. In many cases, rather than mirror pairs, heterotic dualities could involve whole chains of compactification geometries leading to the same effective theory. One concrete step towards understanding such correspondences has been taken in the direction of “target space duality” originating in  $(0, 2)$  gauged linear sigma models in [30] and further studied in [31, 32, 38, 39].

## 1.5 Structure of This Dissertation

This dissertation is organized as follows: Chapter 2 introduces the origins of target space duality, and the procedure to get target space duals.

After chapter 2 there are three parts, based on three papers.

### 1.5.1 Stability and Holomorphy Across TSD Pairs

The first part mainly comes from our work [41] and includes Chapter 3 and 4. Chapter 3 gives background on heterotic string compactification, as well as cohomology of vector bundles and slope stability. Chapter 4 describes our study in the detailed structure of vacuum space in dual theories, by analyzing vector bundles with non-trivial constraints arising from slope stability (i.e. D-terms) and holomorphy (i.e. F-terms).

In this part of the work, our goal is to test the duality further. Thus far, the study of such pairs has focused primarily on the degrees of freedom (i.e. particle spectra) of the theories as described above. In the present work, we hope to extend this further to explore the *vacuum spaces* of target space dual pairs. This is in general a non-trivial task, since for  $(0, 2)$  theories the full form of the matter field Kähler potential and hence, the full scalar potential, is largely unknown. However, recent work has made progress in explicitly connecting the underlying geometry of  $(X, V)$  with the form of the D-term and F-term contributions to the four-dimensional  $\mathcal{N} = 1$  potential [17–20, 24]. Briefly, explicit obstructions to the slope-

---

<sup>2</sup>See [40] for a review.

stability of the bundle correspond to D-terms (associated to Green-Schwarz anomalous  $U(1)$  symmetries [17, 18, 21, 42, 43]) and holomorphy conditions on  $V$  arise as F-terms in the  $\mathcal{N} = 1$  effective theory [19, 20].

With this link between bundle geometry and the effective potential in mind, the goals of the present work are:

- Generate examples of target space dual pairs in which the vector bundles lead to non-trivial D-terms and/or F-terms in their effective potentials (i.e. bundles that are not everywhere slope stable or holomorphic in the moduli space of the base CY geometry).
- To build examples of such bundles, we must extend the class of monad bundles (see [44, 45]) that have been the primary focus of  $(0, 2)$  GLSMs to date. Thus far, the bundles appearing in the majority of the literature have been of the class of so-called “positive” monad bundles. These consist of bundles defined via a complex built of *ample* line bundles

$$0 \rightarrow \bigoplus_k \mathcal{O}(\mathbf{a}_k) \xrightarrow{E} \bigoplus_i \mathcal{O}(\mathbf{b}_i) \xrightarrow{F} \bigoplus_j \mathcal{O}(\mathbf{c}_j) \rightarrow 0, \quad (1.5.1)$$

where  $f \cdot g = 0$  and  $a_k, b_i, c_j \geq 0$  for all  $i, j, k$ . One motivation for focusing on this simple class of bundles is that they are frequently (though not always) stable with respect to the entire Kähler cone of  $X$  [28]. In this work, we will extend this class to involve some negative degree entries in (1.5.1) and demonstrate that although the bundles are not everywhere stable in Kähler moduli space, none-the-less the associated monad bundles correspond to good  $(0, 2)$  GLSMs. These more general monad bundles have already been considered in a variety of contexts in heterotic vacua and the extension of the class may be an important step towards applying sigma model tools to bundles of interest in string phenomenology [28, 46–48].

- At special points in the vacuum space of the theories, enhanced symmetries can arise. These include enhancements of what would in the full sigma model be worldsheet  $(0, 2)$  to  $(2, 2)$  supersymmetry (when  $V$  is deformable into the holomorphic tangent bundle  $TX$ ) and the loci in moduli space corresponding to “stability walls” in which the bundle  $V$  becomes reducible ( $V \rightarrow V_1 \oplus V_2 \oplus \dots$ ) and enhanced Green-Schwarz massive  $U(1)$  symmetries are present in the effective theory. In the latter case, such loci can lead to complicated branch structure in the vacuum space of the theory in

which many different bundles over the same  $X$  are connected [24].

It is our goal in this context to explore the existence of such loci on each side of a target space dual pair and to explore whether a) such enhancement points always correspond across the target space dual pair? and b) whether the vacuum branch structure is identical in both halves of the pair?

- Finally, to build example geometries  $(X, V)$  with non-trivial D-term and F-term potentials that fit well into GLSMs a number of new technical tools will be needed. In particular, it will be necessary to describe such bundles and their possible deformations via monads. A systematic study of such bundles involves generalizations of the target space duality procedure and developing multiple ways of describing the same bundle to make branch structure in the effective theory evident.

In the later sections we will approach the problems/goals outlined above. It should be noted that this list raises a number of interesting questions in the GLSMs themselves – most prominently how the large volume constraints of bundle holomorphy and stability are realized in the GLSM, and whether the corresponding D- and F-term lifting of moduli in the  $\mathcal{N} = 1$  effective theory extends to other non-geometric phases of the theory? For now, we will leave these important questions unanswered and focus primarily on the structure of the geometric phases and target space theories themselves. It is our goal to test target space duality itself via the geometry and potentials described above.

In Section 3.1, the correspondence between bundle stability/holomorphy and non-trivial D-terms and F-terms in the effective theory is reviewed, as studied in [17–21, 24]. Section 3.2 contains details of bundle stability. In Section 4.1 we provide an example of a bundle with non-trivial D-term constraints and track those conditions through the possible target space dual chains of geometries. In particular, this analysis allows for the exploration of the branch structure arising in the vacuum space in the neighborhood of a stability wall on both sides of a target space dual pair. In addition, examples are given of possible perturbative/non-perturbative dual pairs and examples in which disconnected components of the moduli space are reproduced in the dual theory. In Section 4.2 this procedure is repeated for a bundle with a non-trivial F-term constraint. To probe the target space dual correspondence at yet another point of enhanced symmetry, in Section 4.3 dual pairs are constructed in which the starting bundle is constructed as a deformation of the holomorphic tangent bundle (i.e. the  $(0, 2)$  theory contains a  $(2, 2)$  locus). Finally, our results are summarized and future

directions outlined in Section 8. Appendix A provides a comprehensive list of target space dual chains for several examples.

## 1.5.2 Target Space Duality and Het/F-theory Duality

The second part of this dissertation is from our work [49] and includes Chapter 5 and 6. Chapter 5 introduces the het/F-theory duality. Chapter 6 is our study on the expression of heterotic target space duality in F-theory.

In this part of our work we aim to further explore the consequences of target space duality in the context of yet another duality – that between heterotic string compactifications and F-theory. As has been observed since the first investigations into TSD [38, 50], this non-trivial duality of distinct heterotic backgrounds could potentially also lead to an entirely new duality structure within F-theory. Since heterotic and F-theory vacua consist of two of the most promising frameworks for string model building within four-dimensional string compactifications, it make sense to search for such novel and unexplored dualities to better understand redundancies within the space of such theories. In addition, if new dualities exist, they could also provide deep insights into the structure of the effective physics, or perhaps even new computational tools (as has manifestly proved to be the case with mirror symmetry in Type II compactifications of string theory, see e.g. [51]).

Compactifications of the heterotic string and F-theory can lead to identical effective theories in the situation that the background geometries of the two theories both exhibit fibration structures [52]. Namely, heterotic string theory compactified on a Calabi-Yau  $n$ -fold with an elliptic fibration

$$\pi_h : X_n \xrightarrow{\mathbb{E}} B_{n-1} \quad (1.5.2)$$

over a base manifold  $B_{n-1}$ , leads to the same effective physics as F-theory compactified on a Calabi-Yau  $(n + 1)$ -fold with a  $K3$  fibration over the *same* base manifold,  $B_{n-1}$ :

$$\pi_f : Y_{n+1} \xrightarrow{K3} B_{n-1}. \quad (1.5.3)$$

In order to have a well-defined F-theory background, the  $(n + 1)$ -fold  $Y_{n+1}$  must also be elliptically fibered, with compatible elliptic/ $K3$  fibrations [16, 52].

In the context of (potential) heterotic/heterotic dualities and heterotic/F-theory duality

then, there are a number of natural questions that arise. Suppose that  $(X_3, \pi : V \rightarrow X_3)$  and  $(\tilde{X}_3, \pi : \tilde{V} \rightarrow \tilde{X}_3)$  are the requisite background geometries (i.e. (manifolds, vector bundles)) defining two TSD heterotic theories, then these questions include:

- Can target space dual pairs be found in which both  $X$  and  $\tilde{X}$  are elliptically fibered as in (1.5.2)? In principle, these two fibrations need not be related in any obvious way, for example: two topologically distinct CY 3-folds  $\pi : X_3 \rightarrow B_2$  and  $\tilde{\pi} : \tilde{X}_3 \rightarrow \tilde{B}_2$ , with distinct two (complex) dimensional base manifolds  $B_2, \tilde{B}_2$  to their fibrations.
- If such elliptically fibered CY 3-fold geometries can be found within a TSD pair, this will in principle lead to two CY 4-folds,  $Y_4$  and  $\tilde{Y}_4$ , as dual backgrounds for F-theory. It should follow by construction that these two geometries lead to the same four-dimensional effective theory (or at least the same massless spectrum). How can this apparent duality be understood in the context of F-theory? How are  $Y_4$  and  $\tilde{Y}_4$  related?

For the first point, to our knowledge no explicit pairs of elliptically fibered TSD heterotic geometries have yet appeared in the literature. However, at least one proposal for the latter point has been posited. In [31] it was proposed that if fibered heterotic TSD pairs could be found, one possibility for the induced duality in F-theory would be the existence a CY 4-fold with a single elliptic fibration, but *more than one K3 fibration*:

$$\begin{array}{ccc}
 & Y_4 & \\
 K3 \swarrow & & \searrow \tilde{K}3 \\
 B_2 & \xrightarrow{\pi_f} & \tilde{B}_2 \\
 & \tilde{\pi}_f &
 \end{array}$$

where each fibration can be seen as the F-theory dual of one of the heterotic vacua (associated to  $(X, V)$  or  $(\tilde{X}, \tilde{V})$  respectively). Since by its very definition, F-theory requires that  $Y_4$  is also elliptically fibered, this would imply that each  $K3$ -fiber appearing above is itself also elliptically fibered. Moreover, since the elliptic fibration of F-theory that determines the effective physics (i.e. gauge symmetry, matter spectrum, etc), in order for the two  $K3$  fibrations to lead to identical effective theories, it would be expected that in fact in this scenario,  $Y_4$  has only one elliptic fibration, but that it is compatible with two distinct  $K3$  fibrations. If these compatible fibration structures were to exist it must be that the base of



the elliptic fibration,  $\rho : Y_4 \rightarrow B_3$ , must have two different  $\mathbb{P}^1$ -fibrations:

$$\begin{array}{ccc}
 & Y_4 & \\
 & \downarrow \rho_f \mathbb{E} & \\
 & B_3 & \\
 \swarrow \mathbb{P}^1 \sigma_f & & \searrow \mathbb{P}^1 \tilde{\sigma}_f \\
 B_2 & & \tilde{B}_2
 \end{array}$$

The scenario above is one obvious way in which a “duality” of sorts could arise in F-theory. Of course, in this case the essential F-theory geometry is not changing, only the  $K3$  fibrations which determine the heterotic dual. This is clearly not the only possibility. As one alternative, it could prove that the F-theory duals of heterotic TSD pairs are in fact two distinct CY 4-folds,  $Y_4$  and  $\tilde{Y}_4$ , whose gauge symmetries, massless spectra and effective  $\mathcal{N} = 1$  potentials are ultimately the same through non-trivial G-flux in the background geometry. We can summarize these two options for the induced duality in F-theory as follows

1. (Possibility 1) Heterotic TSD  $\Leftrightarrow$  Multiple  $K3$  fibrations in a single F-theory geometry (and hence manifestly leading to the same effective physics).
2. (Possibility 2) Heterotic TSD  $\Leftrightarrow$  Two distinct pairs of manifolds and G-flux,  $(Y_4, G_4)$  and  $(\tilde{Y}_4, \tilde{G}_4)$  which lead to the same effective physics in F-theory.

In this work we investigate the two questions listed above and provide explicit examples of heterotic target space dual pairs with the requisite fibration structures to lead to F-theory dual theories. As we will outline in the following sections, substantial technical difficulties arise in explicitly computing the full F-theory duals of these heterotic theories. In the present work we do not attempt to fully determine these dual F-theories and instead provide evidence for our primary conclusion: *multiple fibrations in F-theory cannot in general explain the dual physics of (0, 2) TSD.*

To overcome some of the technical obstacles of heterotic/F-theory duality, we begin our analysis by actually considering heterotic/F-theory dual pairs in six-dimensional effective theories rather than in four dimensions. In this context, the heterotic duality is a trivial one – TSD pairs simply generate two bundles over  $K3$  with the same second Chern class, and are thus trivially guaranteed to give rise to the same massless spectrum (see e.g. [53]).

However, this very simple framework for heterotic TSD pairs allows us to explicitly perform Fourier-Mukai transforms to render the data of a holomorphic, stable vector bundle over  $K3$  into its spectral cover [54]. With this data, we are able to explicitly construct examples of F-theory duals and verify that in fact they cannot arise as multiple  $K3$  fibrations of a CY 3-fold,  $Y_3$ , determining an F-theory background. The results of this study are presented in Section 6.2.

Turning once more to our primary area of interest in  $\mathcal{N} = 1$  and heterotic compactifications on CY 3-folds, we outline the essential ingredients determining the dual F-theory geometry. We find that in general a number of technical tools are missing for fully determining the F-theory physics. Some of these we have developed and will appear separately [55, 56] while others we leave to future work. However, we are able to indicate that in general the intermediate Jacobians of the dual F-theory geometries must play some role in the new “F-theory duality” whatever it may prove to be. This leads to the presence of essential data not associated to the complex structure of the CY 4-fold alone, but G-flux as well. In the singular limit such fluxes are well known to have the potential to dramatically change the effective physics through so-called T-brane solutions [57–59] and other possibilities.

In the following sections we will explore these ideas in detail. In Section 6.1, we provide the first non-trivial examples to appear in the literature of heterotic TSD pairs in which both CY 3-folds,  $X$  and  $\tilde{X}$  are elliptically fibered. In these cases, the heterotic geometries are smooth (consisting of smooth so-called CICY threefolds [60] and stable, holomorphic vector bundles defined via the monad construction [44] over them) and lead to well controlled, perturbative heterotic theories. However we will demonstrate in this and subsequent sections that existing techniques in the literature to determine dual F-theory geometries, as outlined in Section 6.3 are insufficient to determine the geometry of  $Y_4$  and  $\tilde{Y}_4$  in these cases. However, we none-the-less still find some evidence indicating that multiple fibrations of  $Y_4$  cannot be the F-theory manifestation of  $(0, 2)$  TSD.

To make concrete the dual F-theory geometry we move to six-dimensional examples in Section 6.2. More precisely, we consider heterotic TSD theories consisting of pairs of bundles over  $K3$  in which the second Chern class of both  $V$  and  $\tilde{V}$  is taken to be 12. In this case, it is possible that the F-theory geometry,  $Y_3$  is multiply fibered as described above. However after finding the spectral data (i.e. Fourier Mukai transform) of these bundles, we can explicitly construct the dual F-theory geometry and find that it does not in general agree with what can be obtained by multiple fibrations. We will argue further that the F-theory “image”

of target space duality under the Heterotic/F-theory map shouldn't be purely geometric even in six dimensions, but rather it can be related to the intermediate Jacobian of the CY 3-fold. With these tools and observations in hand we return to the F-theory duals of four dimensional,  $\mathcal{N} = 1$  heterotic theories in Section 6.3.

Finally, in the Appendices we consider a handful of examples illustrating both the range of possibilities arising in heterotic TSD dual geometries, as well as potential pitfalls that can arise in constructing dual pairs.

### 1.5.3 Massless Spectrum of the Landau-Ginzburg Phase

The third part of this dissertation includes Chapter 7. Chapter 7 gives the massless spectrum of the non-geometric phase in the target space duality process, which will be compared with the geometric phase (Calabi-Yau/vector bundle) on both sides.

In (0,2) heterotic target space duality, one goes from a geometric phase, i.e. Calabi-Yau/vector bundle  $(X, V)$ , to a non-geometric phase (Landau-Ginzburg phase), re-label some of the fields, then leave the non-geometric phase and get a new GLSM with a distinct geometric phase corresponding to a new Calabi-Yau/vector bundle  $(\tilde{X}, \tilde{V})$ . These two geometries share a common Landau-Ginzburg point:

$$(X, V) \Leftrightarrow \text{LG point} \Leftrightarrow (\tilde{X}, \tilde{V})$$

For the simplest case when there exists only a geometric phase and a non-geometric phase, these two LG models can be trivially equivalent, because the LG superpotentials are exactly the same. However, the existence of a pure LG phase is not necessary, a non-geometric phase suffices to provide dual models [31], this gives us some clue that the LG models are not trivially the same. So the question arises: are the two (0,2) NLSMs actually the same, as in mirror symmetry? Or is target space duality a transition between theories, like conifold transition in (2,2) theories?

To answer this question, the exploration of the complete massless spectrum of the LG phase becomes necessary. Specifically, calculate the full LG spectra for  $(X, V)$  and  $(\tilde{X}, \tilde{V})$ .

- We expect that in the trivial case, i.e. there is only one  $p$  field, the two massless spectra will be exactly the same. When there are more than one  $p$  fields, the result may not be

so trivial. However, the calculation of massless spectra for hybrid phases are beyond the scope of the present work. In the following chapters, we will illustrate the calculation when there is only one  $p$  field with pure geometric/non-geometric phases.

- After we have the massless spectra, we want to compare them with the cohomology calculated from geometric phases. The calculation includes charged fields as well as gauge singlets. As discussed in the paper [61], “the number of gauge singlets can vary in the moduli space of a given compactification and can differ from what it would be in the large radius limit of the corresponding Calabi-Yau.” So it’s meaningful to compare the Landau-Ginzburg phase with Calabi-Yau phase on both sides.
- In large radius, one of the geometries is not smooth, even though the GLSM vacuum space is compact so the physics could be fine, the cohomology calculation is not trustworthy. Resolving the singularity of  $(X, V)$  leads to a new  $(X', V')$ , we need to answer the question that whether the three models share the same LG point, or if there is any the relationship between them and what it is.

$$\begin{array}{ccc}
 (X', V') & & \\
 \uparrow \text{resolve} & \searrow ? & \\
 (X, V) & \xleftrightarrow{TSD} \text{LG point} \xleftrightarrow{TSD} & (\tilde{X}, \tilde{V})
 \end{array}$$

- Resolving the singularity is not a trivial task. There are many rules, including smoothness after resolution, anomaly cancellation, stability, agreement on the singularity locus, conservation of certain spectrum counts, etc. But there are not many tools, under certain conditions there may not be a solution. We would like to probe the possibilities in resolving the singularity and provide the results under certain conditions. Embed the model in a bigger GLSM may lead to more solution, which is undergoing work.

In the following sections, we will study these matters. In Section 7.2 we will take a pair of target space duals as examples, which are on weighted projective space. The calculation of massless spectra is beyond hand calculation so we use Mathematica do to the work. In Section 7.2.5 we will summarize the result and compare with the large radius, and compare the results with expectation. In section 7.3 we will discuss about the tools and problems to resolve the singularity. With current tools, there is not a proper resolution. We need more techniques, such as embedding into a bigger GLSM, which will be left to future work.

# Chapter 2

## A Brief Review of Target Space Duality

The notion of  $(0, 2)$  target space duality (TSD) is well-studied in the literature [30–32, 38, 39] (see [31] for a thorough review) and in this section we briefly summarize the basic ingredients as well as clarify the simple class of geometries we will consider in order to explore the vacuum structure of the  $\mathcal{N} = 1$  effective theories. In Section 2.2.3, we extend the algorithm further by applying new redundant descriptions of the bundle geometry. The review work and the observation of adding redundant bundle geometry have previously appeared in our paper [41].

### 2.1 $(0, 2)$ Gauged Linear Sigma Models

Gauged linear sigma models (GLSMs) are massive two-dimensional theories which can flow in the infrared (under suitable conditions) to true superconformal theories (i.e. string sigma models). The famous “phase” structure of GLSMs [29] links the vacuum structure of the two-dimensional theory to the geometric data of toric geometry and string compactifications. The freedom to vary a Fayet-Iliopoulos parameter leads to a variety of distinct solutions including non-linear sigma models (and their associated target space geometries – including CY manifolds), Landau-Ginzburg orbifolds, and a rich variety of hybrid models.

In this work we will restrict our consideration to the simplest, Abelian class of GLSMs. The field content will consist of multiple  $U(1)$  gauge fields  $A^{(\alpha)}$  with  $\alpha = 1, \dots, r$ . Following standard notation in the literature, we will label two sets of chiral superfields as  $\{X_i | i = 1, \dots, d\}$  with  $U(1)$  charges  $Q_i^{(\alpha)}$ , and  $\{P_l | l = 1, \dots, \gamma\}$  with  $U(1)$  charges  $-M_l^{(\alpha)}$ . The essential field content will also include two sets of Fermi superfields:  $\{\Lambda^a | a = 1, \dots, \delta\}$  with charges  $N_a^{(\alpha)}$ , and  $\{\Gamma^j | j = 1, \dots, c\}$  with charges  $-S_j^{(\alpha)}$ .

The  $U(1)$  charges appearing in the GLSM are frequently taken to satisfy positivity conditions

that are compatible with realizing Calabi-Yau manifolds and stable, holomorphic vector bundles over them in some geometric phase. In this work, we will take the charges  $Q_i^{(\alpha)} \geq 0$  and require that for each  $i$ , there exists at least one  $r$  such that  $Q_i^{(r)} > 0$ . This assumption of (semi-) positivity will hold in addition for the charges  $S_j^{(\alpha)}$  and  $M_l^{(\alpha)}$ . However, in some cases we will consider solutions in which charges  $N_a^{(\alpha)}$  may be negative (the suitability of such special cases will be further discussed in Sections 4.1 and 4.2).

The key field content and charges of the GLSM can be concisely summarized by a “charge matrix” of the form:

| $x_i$       |             |          |             | $\Gamma^j$   |              |          |             |
|-------------|-------------|----------|-------------|--------------|--------------|----------|-------------|
| $Q_1^{(1)}$ | $Q_2^{(1)}$ | $\dots$  | $Q_d^{(1)}$ | $-S_1^{(1)}$ | $-S_2^{(1)}$ | $\dots$  | $S_c^{(1)}$ |
| $Q_1^{(2)}$ | $Q_2^{(2)}$ | $\dots$  | $Q_d^{(2)}$ | $-S_1^{(2)}$ | $-S_2^{(2)}$ | $\dots$  | $S_c^{(2)}$ |
| $\vdots$    | $\vdots$    | $\ddots$ | $\vdots$    | $\vdots$     | $\vdots$     | $\ddots$ | $\vdots$    |
| $Q_1^{(r)}$ | $Q_2^{(r)}$ | $\dots$  | $Q_d^{(r)}$ | $-S_1^{(r)}$ | $-S_2^{(r)}$ | $\dots$  | $S_c^{(r)}$ |

(2.1.1)

| $\Lambda^a$ |             |          |                  | $p_l$        |              |          |                   |
|-------------|-------------|----------|------------------|--------------|--------------|----------|-------------------|
| $N_1^{(1)}$ | $N_2^{(1)}$ | $\dots$  | $N_\delta^{(1)}$ | $-M_1^{(1)}$ | $-M_2^{(1)}$ | $\dots$  | $-M_\gamma^{(1)}$ |
| $N_1^{(2)}$ | $N_2^{(2)}$ | $\dots$  | $N_\delta^{(2)}$ | $-M_1^{(2)}$ | $-M_2^{(2)}$ | $\dots$  | $-M_\gamma^{(2)}$ |
| $\vdots$    | $\vdots$    | $\ddots$ | $\vdots$         | $\vdots$     | $\vdots$     | $\ddots$ | $\vdots$          |
| $N_1^{(r)}$ | $N_2^{(r)}$ | $\dots$  | $N_\delta^{(r)}$ | $-M_1^{(r)}$ | $-M_2^{(r)}$ | $\dots$  | $-M_\gamma^{(r)}$ |

Familiar GLSM anomaly cancellation conditions (including gauge and gravitational anomalies) impose the following linear and quadratic constraints on the  $U(1)$  charges to hold for all  $\alpha, \beta = 1, \dots, r$ :

$$\begin{aligned}
\sum_{a=1}^{\delta} N_a^{(\alpha)} &= \sum_{l=1}^{\gamma} M_l^{(\alpha)}, & \sum_{i=1}^d Q_i^{(\alpha)} &= \sum_{j=1}^c S_j^{(\alpha)}, \\
\sum_{l=1}^{\gamma} M_l^{(\alpha)} M_l^{(\beta)} - \sum_{a=1}^{\delta} N_a^{(\alpha)} N_a^{(\beta)} &= \sum_{j=1}^c S_j^{(\alpha)} S_j^{(\beta)} - \sum_{i=1}^d Q_i^{(\alpha)} Q_i^{(\beta)}.
\end{aligned}
\tag{2.1.2}$$

The structure of the GLSM is further determined by a non-trivial scalar potential and

superpotential. The latter is given by

$$S = \int d^2z d\theta \left[ \sum_j \Gamma^j G_j(x_i) + \sum_{l,a} P_l \Lambda^a F_a^l(x_i) \right], \quad (2.1.3)$$

where the functions  $G_j$  and  $F_a^l$  are quasi-homogeneous polynomials whose multi-degrees are determined by  $U(1)$  gauge invariance to be:

|       |       |         |       |
|-------|-------|---------|-------|
| $G^j$ |       |         |       |
| $S_1$ | $S_2$ | $\dots$ | $S_c$ |

|                  |                  |          |                       |
|------------------|------------------|----------|-----------------------|
| $F_a^l$          |                  |          |                       |
| $M_1 - N_1$      | $M_1 - N_2$      | $\dots$  | $M_1 - N_\delta$      |
| $M_2 - N_1$      | $M_2 - N_2$      | $\dots$  | $M_2 - N_\delta$      |
| $\vdots$         | $\vdots$         | $\ddots$ | $\vdots$              |
| $M_\gamma - N_1$ | $M_\gamma - N_2$ | $\dots$  | $M_\gamma - N_\delta$ |

(2.1.4)

Furthermore, the function  $F_a^l$  will be chosen to satisfy a *transversality condition* such that  $F_a^l(x) = 0$  only when  $x_i = 0$

The scalar potential includes contributions from F-terms:

$$V_F = \sum_j |G_j(x_i)|^2 + \sum_a \left| \sum_l p_l F_a^l(x_i) \right|^2, \quad (2.1.5)$$

and D-terms

$$V_D = \sum_{\alpha=1}^r \left( \sum_{i=1}^d Q_i^{(\alpha)} |x_i|^2 - \sum_{l=1}^{\gamma} M_l^{(\alpha)} |p_l|^2 - \xi^{(\alpha)} \right)^2. \quad (2.1.6)$$

In this latter expression the  $\xi^{(\alpha)} \in \mathbb{R}$  is the Fayet-Iliopoulos (FI) parameter which determines the structure of the vacuum. In particular the sign of each of the FI terms (for  $\alpha = 1, \dots, r$ ), determine whether the solution of theory is a geometric, Landau-Ginzburg, or hybrid phase.

This can be easily illustrated in the case of a single  $U(1)$  symmetry: For  $\xi > 0$  the D-term implies that not all  $X_i$  are zero simultaneously, thus not all  $F_a$  are zero, and the F-term implies  $G_j(x_i) = 0$  and  $\langle p \rangle = 0$ . This “geometric” phase contains the data of a (0, 2) non-linear sigma-model on a generally singular complete intersection,  $X$ , in a weighted projective space  $\mathbb{P}_{Q_1, \dots, Q_d}[S_1, \dots, S_c]$ . Moreover, the superpotential in (2.1.3) leads to a mass

term of the form  $\sum_a \pi \lambda^a F_a$ , which makes massive one linear combination of the  $\lambda^a$ . The details of fermionic gauge symmetries, etc can be found in [31, 62, 63]. In brief summary, the remaining massless combinations of the left-moving fermions  $\lambda_a$  couple to a vector bundle over it defined by the monad

$$0 \rightarrow \mathcal{O}_X^{\oplus r_\nu} \xrightarrow{E_i^a} \bigoplus_{a=1}^{\delta} \mathcal{O}_X(N_a) \xrightarrow{F_a^l} \bigoplus_{l=1}^{\gamma} \mathcal{O}_X(M_l) \rightarrow 0 \quad (2.1.7)$$

on the complete intersection CY manifold  $X = \cap_{j=1}^c G_j$ . The rank  $(\delta - \gamma - r_\nu)$  vector bundle  $V \rightarrow X$  is defined as

$$V = \frac{\ker(F_a^l)}{\text{im}(E_i^a)}, \quad (2.1.8)$$

where  $E_i^a$  arises from  $r_\nu$  additional fermionic gauge symmetries that have been introduced leading to a deviation in chirality of  $\overline{D}\Lambda^a = \sqrt{2}\Sigma^i E_i^a$ . Note that although the new, neutral, chiral superfields,  $\Sigma^i$ , contribute to the scalar potential, they will play no role in the analysis undertaken here and will be omitted. In general,  $E_i^a$  obeys a composition rule with  $F_a^l$ :  $E \circ F = 0$  on  $X$ . Furthermore, in this work, we will consider the simple case that  $E_i^a = 0$  and  $V$  is defined as a kernel:  $V = \ker(F_a^l)$  defined by a short exact sequence

$$0 \rightarrow V \rightarrow \bigoplus_{a=1}^{\delta} \mathcal{O}_{\mathcal{M}}(N_a) \xrightarrow{F_a^l} \bigoplus_{l=1}^{\gamma} \mathcal{O}_{\mathcal{M}}(M_l) \rightarrow 0. \quad (2.1.9)$$

The simplest possible “non-geometric” phase can be realized with  $\xi < 0$ . In this case, the D-term implies that  $\langle p \rangle \neq 0$  thus all  $\langle x_i \rangle = 0$ . This vacuum corresponds to a Landau-Ginzburg orbifold with a superpotential:

$$\mathcal{W}(x_i, \Lambda^a, \Gamma^i) = \sum_j \Gamma^j G_j(x_i) + \sum_a \Lambda^a F_a(x_i). \quad (2.1.10)$$

Finally, when  $r > 1$ , the possibility of hybrid phases – with some  $x^{(\alpha)}$  less than and some great than zero – naturally arises.

The simple form of (2.1.10) first inspired the observation in [30] of target space duality. By inspection of (2.1.10) it is clear that an exchange/relabeling of the functions  $G_j$  and  $F_a$  will not affect the Landau-Ginzburg model, as long as anomaly cancellation conditions are satisfied. The natural observation is that two distinct GLSMs could “share” a non-geometric



phase in which the original (large volume) role of  $G_j$  and  $F_a$  is obscured. This notion of duality has been extended in a variety of ways including by allowing for the resolution of singularities in the geometry [50] and extending the duality with a trivial re-writing which allows for a change in the number of  $U(1)$  symmetries in the dual pair [31, 63].

In the following section we review and illustrate the target space duality algorithm as laid out clearly in [31, 32] and extend it still further by applying new redundant descriptions of the bundle geometry that make new target space duals manifest.

## 2.2 Target Space Duality

Given a starting point of a  $(0, 2)$  GLSM, the procedure for generating a target space dual model was laid out succinctly in [31, 32]. We follow the conventions of [31] by taking  $\|X\|$  to indicate the charge of the field  $X$  and  $\|G\|$  to denote the multi-degree of a homogeneous function  $G(X)$ . For completeness we summarize the algorithm here:

### The Algorithm:

1. Find all phases of a smooth  $(0, 2)$  GLSM, including a geometric phase with geometry  $(X, V)$ .
2. Construct a phase in which at least one field  $p_l$  (for illustration, take  $p_1$ ) is required to have a non-zero vacuum,  $\langle p_1 \rangle \neq 0$ .
3. Rescale  $k$  Fermi superfields by the constant vev,  $\langle p_1 \rangle$ , and exchange the role of some  $\lambda^a$  and  $\Gamma^j$ :

$$\tilde{\Lambda}^{a_i} := \frac{\Gamma^{j_i}}{\langle p_1 \rangle}, \quad \tilde{\Gamma}^{j_i} = \langle p_1 \rangle \Lambda^{a_i}, \quad \forall i = 1, \dots, k. \quad (2.2.1)$$

For consistency, this relabeling/rescaling can only be done when  $\sum_i \|G_{j_i}\| = \sum_i \|F_{a_i}^1\|$  for anomaly cancellation.

4. Tune the bundle moduli (i.e. morphisms  $F_a^l$ ) so that  $\Lambda^{a_i}$  appear only in terms with  $P_1$  for all  $i$ . i.e. choose

$$F_{a_i}^l = 0, \quad \forall l \neq 1, \quad i = 1, \dots, k. \quad (2.2.2)$$

5. Move away from this shared non-geometric phase and define the Fermi superfields of the new GLSM such that each term in the superpotential is gauge invariant:

$$\|\tilde{\Lambda}^{a_i}\| = \|\Gamma^{j_i}\| - \|P_1\| \quad , \quad \|\tilde{\Gamma}^{j_i}\| = \|\Lambda^{a_i}\| + \|P_1\|. \quad (2.2.3)$$

6. Allow the moduli to move to a generic point and define a new (dual)  $(0, 2)$  GLSM with a distinct geometric phase corresponding to a new Calabi-Yau and vector bundle,  $(\tilde{X}, \tilde{V})$ .

It was proved in [31] that for the algorithm as described above if the initial  $(0, 2)$  GLSM satisfies the anomaly cancellation conditions in (2.1.2) then so does the constructed dual. Moreover, as mentioned in the Introduction, it was observed in the landscape scan of [31] that throughout this process, in the target space theories the net multiplicities of charged matter, and the total number of massless gauge singlets are preserved for almost all of the examples, where the individual number of complex, Kähler and bundle moduli are interchanged as

$$\begin{aligned} h^*(X, \wedge^k V) &= h^*(\tilde{X}, \wedge^k \tilde{V}), \\ h^{2,1}(X) + h^{1,1}(X) + h_X^1(\text{End}_0(V)) &= h^{2,1}(\tilde{X}) + h^{1,1}(\tilde{X}) + h_X^1(\text{End}_0(\tilde{V})). \end{aligned} \quad (2.2.4)$$

On a technical note, the dimensions of the cohomology groups above can be computed using standard tools such as [64, 65]. This procedure is illustrated explicitly below.

### 2.2.1 Illustration of the Duality Procedure

For concreteness, it is easiest to understand the target space duality algorithm in the context of an example. In principle an arbitrary number of  $G$ 's and  $F$ 's can be interchanged in the non-geometric phase. Below we will consider the simplest case in which two such maps play a role. Note that in this case the quadratic anomaly cancellation conditions are known to be satisfied in the dual theory [31].

In the non-geometric phase, we will make explicit the two terms to be exchanged in the corresponding superpotential (here the first two terms with  $a = 1, 2$ ):

$$\mathcal{W} = \sum_{j=1}^c \Gamma^j G_j + \sum_{a=1}^2 P_1 \Lambda^a F_a^1 + \sum_{a=3}^{\delta} P_1 \Lambda^a F_a^1 + \sum_{l=2}^{\gamma} \sum_{a=1}^{\delta} P_l \Lambda^a F_a^l. \quad (2.2.5)$$

In the GLSM, not all the  $\langle p \rangle$ 's are allowed to vanish simultaneously. Giving  $p_1$  a vev, the superpotential can be written as

$$\mathcal{W} = \Gamma^1 G_1 + \Gamma^2 G_2 + \sum_{j=3}^c \Gamma^j G_j + \langle p_1 \rangle \Lambda^1 F_1^1 + \langle p_1 \rangle \Lambda^2 F_2^1 + \sum_{a=3}^{\delta} \langle p_1 \rangle \Lambda^a F_a^1 + \sum_{l=2}^{\gamma} \sum_{a=1}^{\delta} P_l \Lambda^a F_a^l. \quad (2.2.6)$$

Performing the interchange of the first two  $G_j$ 's and  $F_a$ 's as prescribed above, the equivalent superpotential can be expressed by  $\tilde{G}_j$ 's and  $\tilde{F}_a$ 's

$$\mathcal{W} = \tilde{\Gamma}^1 \tilde{G}_1 + \tilde{\Gamma}^2 \tilde{G}_2 + \sum_{j=3}^c \Gamma^j G_j + \langle p_1 \rangle \tilde{\Lambda}^1 \tilde{F}_1^1 + \langle p_1 \rangle \tilde{\Lambda}^2 \tilde{F}_2^1 + \sum_{a=3}^{\delta} \langle p_1 \rangle \Lambda^a F_a^1 + \sum_{l=2}^{\gamma} \sum_{a=1}^{\delta} P_l \Lambda^a F_a^l. \quad (2.2.7)$$

In this case, the rescalings are

$$\begin{aligned} \tilde{\Gamma}^1 &:= \langle p_1 \rangle \Lambda^1, \tilde{\Gamma}^2 := \langle p_1 \rangle \Lambda^2, \tilde{\Lambda}^1 := \frac{\Gamma^1}{\langle p_1 \rangle}, \tilde{\Lambda}^2 := \frac{\Gamma^2}{\langle p_1 \rangle}, \\ \tilde{G}_1 &:= F_1^1, \tilde{G}_2 := F_2^1, \tilde{F}_1^1 := G_1, \tilde{F}_2^1 := G_2, \end{aligned} \quad (2.2.8)$$

and  $\|G_1\| + \|G_2\| = \|F_1^1\| + \|F_2^1\|$ . From this point, a return to a geometric phase would yield a new configuration corresponding to a geometric pair  $(\tilde{X}, \tilde{V})$ .

### 2.2.2 Target Space Duals with an Additional $U(1)$

As outlined above, it is clear that the “relabeling” of fields at the shared Landau-Ginzburg point can mix the degrees of freedom in  $h^{2,1}(X)$  and  $h^1(X, \text{End}_0(V))$  in the target space dual. More general possibilities are possible however that can *also* change the dimension of  $h^{1,1}$ . As one particular example of such a change, we will be interested here in geometries  $X, \tilde{X}$  which are related by geometric (i.e. conifold-type) transitions.

To change the dimension of  $h^{1,1}$  across the target space dual it is necessary to re-write the initial GLSM in an equivalent/redundant way. Stated briefly, it is always possible to introduce into the GLSM a new coordinate (i.e. a new Fermi superfield)  $y_1$  with multi-degree  $\mathcal{B}$  and a new hypersurface (i.e. a chiral superfield with opposite charge to the new Fermi superfield)  $G^{\mathcal{B}}$  corresponding to a homogeneous polynomial of multi-degree  $\mathcal{B}$ . Denoting the

initial bundle/manifold in terms of its GLSM charges as

$$V_{N_1, \dots, N_\delta}[M_1, \dots, M_\gamma] \longrightarrow \mathbb{P}_{Q_1, \dots, Q_d}[S_1, \dots, S_c], \quad (2.2.9)$$

the above addition can be written

$$V_{N_1, \dots, N_\delta}[M_1, \dots, M_\gamma] \longrightarrow \mathbb{P}_{Q_1, \dots, Q_d, \mathcal{B}}[S_1, \dots, S_c, \mathcal{B}]. \quad (2.2.10)$$

As argued in [31], this addition leaves the GLSM and the corresponding target space geometry completely unchanged. However, as we will demonstrate, this redundant description can play a non-trivial role in the target space duality re-labeling.

Following [31], suppose that in an example as in the previous Subsection, there are two chosen map elements  $F_1^1$  and  $F_2^1$  that have been chosen to be interchanged with a defining relation  $S_1$ . In this case we can choose the redundant new coordinate,  $y_1$ , to have charge

$$\|\mathcal{B}\| = \|F_1^1\| + \|F_2^1\| - S_1, \quad (2.2.11)$$

and under the re-labelings required in the algorithm of Section 2.2 it is possible to choose, for example,

$$\tilde{N}_1 = M_1 - S_1 = 0, \quad \tilde{N}_2 = M_2 - \mathcal{B}, \quad \tilde{S}_1 = \|F_1^1\|, \quad \tilde{\mathcal{B}} = \|F_2^1\|. \quad (2.2.12)$$

That is, a Fermi superfield has now been generated with apparently vanishing charge. This is misleading however because as we will see, this field may be thought of as carrying an additional  $U(1)$  charge. To see the origin of this new  $U(1)$ , it should be noted that the redundancy/relabeling described above can, unfortunately, lead to singular geometries. As pointed out in [63], to avoid such singularities in the new model and have a valid, smooth large volume limit  $(\tilde{X}, \tilde{V})$ , it is possible to add an additional  $U(1)$  gauge symmetry under which the formally uncharged Fermi-superfield carries a non-vanishing charge. Geometrically this corresponds with introducing one further coordinate  $y_2$  and identifying the two new coordinates as the homogeneous coordinates on a  $\mathbb{P}^1$  (i.e. a blow-up of the original geometry). So the charges now read

|       |     |       |               |       |            |     |            |                |             |             |     |                  |        |        |     |             |
|-------|-----|-------|---------------|-------|------------|-----|------------|----------------|-------------|-------------|-----|------------------|--------|--------|-----|-------------|
| $x_1$ | ... | $x_d$ | $y_1$         | $y_2$ | $\Gamma^1$ | ... | $\Gamma^c$ | $\Gamma^B$     | $\Lambda^1$ | $\Lambda^1$ | ... | $\Lambda^\delta$ | $p_1$  | $p_2$  | ... | $p_\gamma$  |
| 0     | ... | 0     | 1             | 1     | 0          | ... | 0          | -1             | 0           | 0           | ... | 0                | -1     | 0      | ... | 0           |
| $Q_1$ | ... | $Q_d$ | $\mathcal{B}$ | 0     | $-S_1$     | ... | $-S_c$     | $-\mathcal{B}$ | $N_1$       | $N_2$       | ... | $N_\delta$       | $-M_1$ | $-M_2$ | ... | $-M_\gamma$ |

(2.2.13)

where once again, this configuration is equivalent to the initial one in (2.2.9). This equivalence can be verified by noting that the constraint  $G^B = y_1 = 0$  can be used to eliminate the coordinate  $y_1$ . Further,  $y_2$  can be fixed by the additional  $U(1)$  gauge symmetry and associated D-term. Thus, this configuration is simply the original space  $\times$  a single point. Use the same method discussed before, we can perform rescalings to this new configuration, resulting in a new target space dual with an additional  $U(1)$ .

Applying the field redefinitions in (2.2.12) we arrive at last to the new configuration

|       |     |       |               |       |                    |     |            |                    |                     |                     |     |                  |        |        |     |             |
|-------|-----|-------|---------------|-------|--------------------|-----|------------|--------------------|---------------------|---------------------|-----|------------------|--------|--------|-----|-------------|
| $x_1$ | ... | $x_d$ | $y_1$         | $y_2$ | $\tilde{\Gamma}^1$ | ... | $\Gamma^c$ | $\tilde{\Gamma}^B$ | $\tilde{\Lambda}^1$ | $\tilde{\Lambda}^1$ | ... | $\Lambda^\delta$ | $p_1$  | $p_2$  | ... | $p_\gamma$  |
| 0     | ... | 0     | 1             | 1     | -1                 | ... | 0          | -1                 | 1                   | 0                   | ... | 0                | -1     | 0      | ... | 0           |
| $Q_1$ | ... | $Q_d$ | $\mathcal{B}$ | 0     | $-(M_1 - N_1)$     | ... | $-S_c$     | $-(M_1 - N_2)$     | $M_1 - S_1$         | $M_1 - \mathcal{B}$ | ... | $N_\delta$       | $-M_1$ | $-M_2$ | ... | $-M_\gamma$ |

(2.2.14)

For simplicity, in this work all examples will be chosen so that the target space duals satisfy  $\mathcal{B} = 0$  which will guarantee that the theories stay within the class of simple complete intersection Calabi-Yau manifolds in products of projective spaces [60, 66].

### 2.2.3 Redundant Bundle Geometry and More General Target Space Duals

It is useful to observe here that the procedure of inducing a redundant description of the manifold,  $X$ , illustrated above can also be applied to the vector bundle,  $V$ . At the level of the GLSM, once again we introduce a new pair consisting of a chiral/fermi superfields of opposite charge, but this time to the GLSM data corresponding to the bundle  $V$ , rather than to  $X$  as in the previous section. Once again denoting the bundle in terms of its GLSM charges as in (2.2.9) this time the addition of fields takes the form

$$V_{N_1, \dots, N_\delta, \mathcal{B}}[M_1, \dots, M_\gamma, \mathcal{B}] \rightarrow \mathbb{P}_{Q_1, \dots, Q_d}[S_1, \dots, S_c]. \quad (2.2.15)$$

Note that this is exactly the redundancy utilized in (2.2.10), only here it is applied to  $V$  rather than to  $X$ .

At the level of the bundle geometry, the procedure involves a simple modification of the monad defining  $V$ . Beginning with the short exact sequence

$$0 \rightarrow V \rightarrow B \xrightarrow{F} C \rightarrow 0, \quad (2.2.16)$$

with  $B, C$  sums of line bundles, we can realize the addition in (2.2.15) by adding the same line bundle  $L$  to both  $B$  and  $C$ :

$$0 \rightarrow V' \rightarrow B \oplus L \xrightarrow{F'} C \oplus L \rightarrow 0. \quad (2.2.17)$$

It is clear that the bundles  $V'$  and  $V$  share a locus in moduli space for which the map  $F'$  takes the form

$$F' = \begin{pmatrix} F & \mathbf{0} \\ \mathbf{0} & \mathbb{C} \end{pmatrix} \quad (2.2.18)$$

where  $F$  is the original fiberwise morphism in (2.2.16) and  $\mathbb{C}$  represents the constant map from  $L \rightarrow L$ . For this choice of  $F'$  the bundles  $V$  and  $V'$  are isomorphic. It is also straightforward to verify that the topology of  $V$  and  $V'$  are identical. Their agreement at a general point in moduli space can be probed via Lemmas 3.2.5 and 3.2.5 in Section 3.2.

For more general maps of the form

$$F' = \begin{pmatrix} F & \alpha \\ \beta & \mathbb{C} \end{pmatrix} \quad (2.2.19)$$

where  $\alpha \in H^0(X, L^\vee \otimes C)$  and  $\beta \in H^0(X, B^\vee \otimes L)$  are non-trivial, it is possible to probe a broader region of the shared moduli space. As we will see below, adding  $L$  such that  $\alpha, \beta \neq 0$  can lead to *new target space dual theories* and is a generalization of the procedure systematically explored in [31]. Moreover, demanding that there exist generic non-trivial maps,  $\alpha, \beta \neq 0$ , bounds the set of possible line bundles  $L$  that can be added to produce new target space duals to a finite set. Roughly, these conditions amount to the constraint that the entries  $O(a, b, \dots)$  in  $L$  are “small enough” to map into  $C$  but “big enough” that some

entries in  $B$  can be mapped non-trivially into  $L$ . For example, starting with the geometry

| $x_i$       | $\Gamma^j$ | $\Lambda^a$      | $p_l$    |
|-------------|------------|------------------|----------|
| 1 1 0 0 0 0 | -2         | 0 0 1 1 1 -1 2 2 | -3 -1 -2 |
| 0 0 1 1 1 1 | -4         | 1 1 0 0 3 1 1 2  | -2 -4 -3 |

(2.2.20)

where  $V$  is defined via the monad

$$\begin{aligned}
0 \rightarrow V \rightarrow \mathcal{O}(0, 1)^{\oplus 2} \oplus \mathcal{O}(1, 0)^{\oplus 2} \oplus \mathcal{O}(1, 3) \oplus \mathcal{O}(-1, 1) \oplus \mathcal{O}(2, 1) \oplus \mathcal{O}(2, 2) \\
\begin{array}{c} \xrightarrow{F} \\ \rightarrow \end{array} \mathcal{O}(3, 2) \oplus \mathcal{O}(1, 4) \oplus \mathcal{O}(2, 3) \rightarrow 0.
\end{aligned}
\tag{2.2.21}$$

For a component  $B_i = \mathcal{O}(b_1, b_2)$  mapping into  $C_j = \mathcal{O}(c_1, c_2)$ ,  $h^0(B_i^* \otimes C_j) = h^0(\mathcal{O}(c_1 - b_1, c_2 - b_2)) \neq 0$ . Which means  $c_1 \geq b_1, c_2 \geq b_2$ , or  $c_1 - b_1 = -1, c_2 - b_2 \geq 4$ .

In this case,  $L$  can only be one of the set

$$\begin{aligned}
\{ & \mathcal{O}(-1, 2), \mathcal{O}(-1, 3), \mathcal{O}(-1, 4), \mathcal{O}(0, 2), \mathcal{O}(0, 3), \mathcal{O}(0, 4), \mathcal{O}(1, 1), \mathcal{O}(1, 2), \\
& \mathcal{O}(1, 3), \mathcal{O}(2, 0), \mathcal{O}(2, 1), \mathcal{O}(2, 2), \mathcal{O}(3, 0), \mathcal{O}(3, 1) \}.
\end{aligned}
\tag{2.2.22}$$

It should be noted finally that another concern is whether each of the line bundles appearing in (2.2.22) can appear in (2.2.17) an arbitrary number of times? Having identified the range of possible line bundles in (2.2.17) such that the maps are non-trivial, we may inquire whether they could each be added an arbitrary (i.e. infinite) number of times to the monad? In principle, such an infinite repetition of a line bundle leads to an equivalent monad, however as we will see in future sections, such additions do not increase the number of non-trivial target space dual theories. For the examples in consideration in this work, we begin with at most two defining relations in the geometric realization of the CY manifold (i.e. the index on the fields,  $\Gamma^j$ , runs only over  $j = 1, 2$  in the present examples). Thus, at most 3 line bundles can play a non-trivial role in the algorithm (i.e.  $\Lambda^1, \Lambda^2$  and  $P_1$  as in (2.2.6) and (2.2.7)). So there nothing to be gained by adding more than 3 additional line bundles,  $\mathcal{L}_i$ . The utility of adding “repeated entires” to the monad bundle will be further illustrated in Appendix A.

### 2.2.4 Summary of Choices for the Target Space Dual Geometries Considered Here

It is worth briefly summarizing the classes of target space duals we will consider in this work. Unless otherwise indicated, we will require that

- All target space duals constructed will increase the number of  $U(1)$  symmetries in the GLSM by 1 and take  $\mathcal{B} = 0$  in the notation of Section 2.2.2 to remain within the class of CICYs [60]. This simple choice furthermore ensures that  $X$  and  $\tilde{X}$  are related by geometric transitions (in general, so-called “effective splits” for CICY configuration matrices [67]).
- For the initial geometric pairs,  $(X, V)$ , we take  $c_2(V) = c_2(TX)$  and it was established in [31] that this will guarantee that  $c_2(\tilde{V}) = c_2(T\tilde{X})$  in the target space dual geometry. The structure group of  $V$  is embedded into a single  $E_8$  factor of the  $E_8 \times E_8$  theory. The second, unbroken  $E_8$  factor to the gauge symmetry will not play a role in our analysis.
- We choose bundles,  $V$ , defined as kernels:  $V = \text{Ker}(f)$  and will allow for repeated line bundle entries in the monad, subject to the constraints described in the previous Section.



# Chapter 3

## Heterotic String Compactifications

In this chapter we briefly review of the structure of the  $\mathcal{N} = 1$  effective potential in the four-dimensional heterotic theory, give the background on cohomology of vector bundles and the tools to probe slope stability. This review was previously published in our paper [41].

### 3.1 The Target Space Potential: Supersymmetry Conditions and Vector Bundle Geometry

To preserve  $\mathcal{N} = 1$  supersymmetry in the four-dimensional effective theory, the geometry of the pair  $(X, V)$  is constrained. The simplest class of solutions are found when  $X$  is a Calabi-Yau threefold and the vector bundle  $\pi : V \rightarrow X$  satisfies the Hermitian Yang-Mills equations [13]:

$$g^{a\bar{b}}F_{a\bar{b}} = 0, F_{ab} = 0, F_{\bar{a}\bar{b}} = 0, \quad (3.1.1)$$

where  $F$  is the gauge field strength associated with the vector bundle  $V$ , and  $a$  and  $\bar{b}$  are holomorphic and anti-holomorphic indices on the Calabi-Yau manifold. These equations involve all three types of singlet “moduli” described in the previous section ( $h^{1,1}(X)$ ,  $h^{2,1}(X)$  and  $h^1(X, \text{End}_0(V))$ ) and in general not all possible values of the CY and bundle moduli will correspond to a solution of (3.1.1).

It is straightforward to see that a solution to (3.1.1) is directly linked to the minimum of the potential in the four-dimensional effective theory [68]. The argument below was given in [19] and we briefly summarize it here:

The structure of the four-dimensional effective potential can be seen by focusing on several

terms in the ten-dimensional effective action,

$$S_{\text{partial}} = -\frac{1}{2\kappa_{10}^2} \frac{\alpha'}{4} \int_{\mathcal{M}_{10}} \sqrt{-g} \{ \text{tr}(F^{(1)})^2 + \text{tr}(F^{(2)})^2 - \text{tr}R^2 + \dots \}. \quad (3.1.2)$$

The notation here is standard [13] with the field strengths  $F^{(1)}$  and  $F^{(2)}$  being associated with the two  $E_8$  factors in the gauge group. In addition to the action, the ten-dimensional Bianchi Identity holds,

$$dH = -\frac{3\alpha'}{\sqrt{2}} (\text{tr}F^{(1)} \wedge F^{(1)} + \text{tr}F^{(2)} \wedge F^{(2)} - \text{tr}R \wedge R). \quad (3.1.3)$$

The associated integrability condition can be phrased as

$$\int_{M_6} \omega \wedge (\text{tr} F^{(1)} \wedge F^{(1)} + \text{tr} F^{(2)} \wedge F^{(2)} - \text{tr} R \wedge R) = 0, \quad (3.1.4)$$

where  $\omega$  is the Kähler form. Working to lowest order, with a Ricci flat metric on a manifold of  $SU(3)$  holonomy, equation (3.1.4) then leads to

$$\int_{M_{10}} \sqrt{-g} \left( \text{tr}(F^{(1)})^2 + \text{tr}(F^{(2)})^2 - \text{tr}R^2 + 2 \text{tr}(F_{ab}^{(1)} g^{a\bar{b}})^2 + 2 \text{tr}(F_{ab}^{(2)} g^{a\bar{b}})^2 \right. \\ \left. - 4 \text{tr}(g^{a\bar{a}} g^{b\bar{b}} F_{ab}^{(1)} F_{\bar{a}\bar{b}}^{(1)}) - 4 \text{tr}(g^{a\bar{a}} g^{b\bar{b}} F_{ab}^{(2)} F_{\bar{a}\bar{b}}^{(2)}) \right) = 0. \quad (3.1.5)$$

Using this relation in (3.1.2), the result is

$$S_{\text{partial}} = -\frac{1}{2\kappa_{10}^2} \alpha' \int_{\mathcal{M}_{10}} \sqrt{-g} \left\{ -\frac{1}{2} \text{tr}(F_{ab}^{(1)} g^{a\bar{b}})^2 - \frac{1}{2} \text{tr}(F_{ab}^{(2)} g^{a\bar{b}})^2 \right. \\ \left. + \text{tr}(g^{a\bar{a}} g^{b\bar{b}} F_{ab}^{(1)} F_{\bar{a}\bar{b}}^{(1)}) + \text{tr}(g^{a\bar{a}} g^{b\bar{b}} F_{ab}^{(2)} F_{\bar{a}\bar{b}}^{(2)}) \right\}. \quad (3.1.6)$$

By inspection, the terms included in (3.1.6) are a part of the ten-dimensional theory which does not contain any four-dimensional derivatives. Thus, under dimensional reduction, they will contribute to the potential energy of the four-dimensional theory. In the case of a supersymmetry preserving field configuration, the terms in the integrand of (3.1.6) vanish, corresponding exactly to a geometric moduli choice which solves (3.1.1). In this case, no potential is generated.

As discussed before, by a theorem of Donaldson-Uhlenbeck and Yau [22, 23], the first condition in (3.1.1) is equivalent to the condition of Mumford (slope) poly-stability of  $V$ . In

the effective theory, this is associated with *D-term breaking* of supersymmetry at stability walls. Along the stability walls the condition of poly-stability forces the bundle  $V$  to become reducible (i.e.  $V \rightarrow \mathcal{F} \oplus V/\mathcal{F}$ ), leading to the presence of enhanced, Green-Schwarz massive  $U(1)$  symmetries in the effective theory, see [17, 18, 21, 24]. In the neighborhood of a stability wall, the D-term can be written in the effective theory as

$$D^{U(1)} \sim FI(t) - \frac{1}{2} \sum_i Q_i G_{P\bar{Q}} C_i^P \bar{C}_i^{\bar{Q}}, \quad (3.1.7)$$

where the first term is a moduli-dependent Fayet-Iliopolous parameter (depending on the Kähler moduli,  $t^r$ ,  $r = 1, \dots, h^{1,1}(X)$  of  $X$ ) and the second arises from matter fields,  $C_i$ , charged under the anomalous  $U(1)$ . Briefly, the form of the FI term to leading order is<sup>1</sup>

$$FI(t) \sim \frac{\mu(\mathcal{F})}{Vol(X)}, \quad (3.1.8)$$

where  $Vol(X)$  is the volume of the CY 3-fold,  $Vol(X) = \int_X J \wedge J \wedge J$ , with  $J$  is the Kähler form on  $X$ . Here  $\mu(\mathcal{F}) = \frac{1}{rk(\mathcal{F})} \int_X c_1(\mathcal{F}) \wedge J \wedge J$  is a quasi-topological number called the “slope” [69], associated to a crucial (geometrically de-stabilizing [17]) sub-sheaf,  $\mathcal{F}$ . This last object,  $\mathcal{F}$ , is defined by the fact that near the stability wall,  $V$  must be decomposed as  $V \rightarrow \mathcal{F} \oplus \frac{V}{\mathcal{F}}$ . See [17] for a review and Section 3.2 for further details.

Likewise, the second conditions in (3.1.1) correspond geometrically to the condition that the bundle is holomorphic. In the effective theory, this obstruction is associated with the *F-term breaking* of supersymmetry by the complex structure moduli. Geometrically, the flat directions in moduli space corresponding to holomorphic deformations of the complete geometry (manifold + bundle) are described by the “Atiyah class” of  $V$  [27]. More precisely, the infinitesimal complex moduli of the heterotic theory are not the independent bundle moduli ( $h^1(X, End_0(V))$ ) and complex structure moduli ( $h^{2,1}(X)$ ) but rather the elements of the cohomology group

$$H^1(X, \mathcal{Q}) \quad (3.1.9)$$

which describes the tangent space to *the infinitesimal deformation space of the pair*  $(X, V)$ . Here  $\mathcal{Q}$  is defined by [27]:

$$0 \rightarrow End_0(V) \rightarrow \mathcal{Q} \rightarrow TX \rightarrow 0, \quad (3.1.10)$$

---

<sup>1</sup>See [17] for a discussion of the one-loop correction to this FI term and its geometric interpretation.

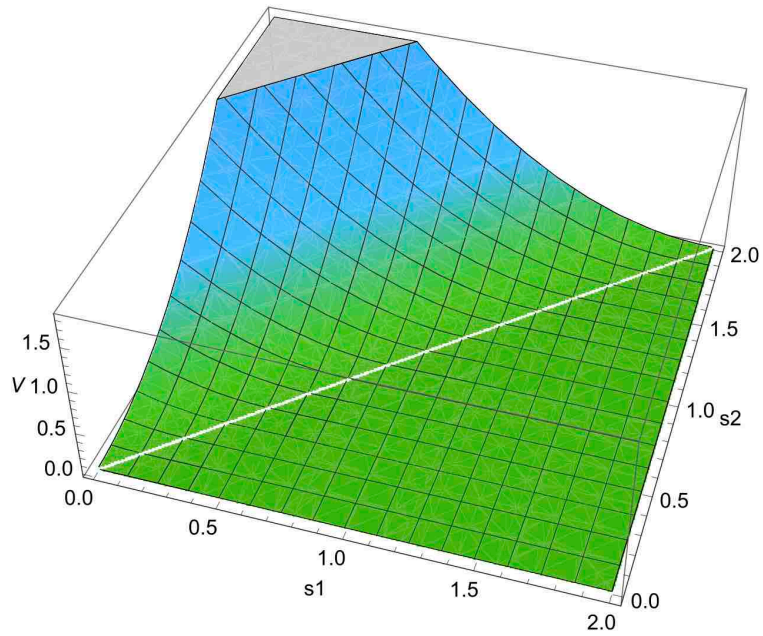


**Figure 3.1:** An illustration of the D-term effective potential corresponding to (3.1.7) (and a part of (3.1.6)) and geometrically realized by the bundle failing to be slope-stable for a sub-cone of Kähler moduli space. The white boundary line is referred to as a “stability wall” in the Kähler cone.

and

$$h^1(X, \mathcal{Q}) = h^1(X, \text{End}_0(V)) \oplus \ker\{H^1(TX) \xrightarrow{[F^{1,1}]} H^2(\text{End}_0(V))\}. \quad (3.1.11)$$

In general, the moduli in (3.1.11) contain the bundle moduli, but only a subset of the complex structure moduli of  $X$ . The scale at which the moduli are “lifted” is generally the compactification scale (and thus, they should be excluded from the start in the zero-mode count given in (1.3.4)), however in some special cases this scale is lowered so that the moduli fixing due to holomorphy of the pair  $(X, V)$  can be realized in the effective theory by the Gukov-Vafa-Witten superpotential [70]:

$$W = \int_X H \wedge \Omega, \quad (3.1.12)$$

and its associated F-terms

$$F_{C_i} = \frac{\partial W}{\partial C_i} \sim \int_X \frac{\partial \omega^{3YM}}{\partial C_i}, \quad (3.1.13)$$

where  $\omega^{3YM} = \text{tr}(F \wedge A - \frac{1}{3} A \wedge A \wedge A)$ . See [19, 20, 25, 26] for further details and computational tools. These moduli considerations have recently been extended to include heterotic non-Kähler vacua [71–74] and a more detailed understanding of moduli space metrics [75, 76].

## 3.2 Tools for Probing Slope-Stability of Vector Bundles

### 3.2.1 Slope Stability

The conditions for supersymmetry in the  $\mathcal{N} = 1$  four-dimensional heterotic theory have been a notorious source of difficulty. With no explicit, non-trivial solutions known<sup>2</sup> for the Ricci-flat, CY metric,  $g_{a\bar{b}}$ , direct solutions of the Hermitian-Yang-Mills equations

$$g^{a\bar{b}} F_{a\bar{b}} = 0 \quad (3.2.1)$$

likewise remain elusive. Progress is possible, however, thanks to the Donaldson-Uhlenbeck-Yau Theorem [22, 23] which states that on each *poly-stable* holomorphic vector bundle  $V$ , there exists a unique connection,  $A$ , satisfying (3.2.1).

A holomorphic vector bundle  $V \rightarrow X$  is called *stable*, if for all subsheaves  $\mathcal{F} \subset V$  with

---

<sup>2</sup>See [77–80] for numerical approaches to the problem of determining Ricci-flat, CY metrics.

$rk(\mathcal{F}) < rk(V)$  the following inequality holds:

$$\mu(\mathcal{F}) < \mu(V), \quad (3.2.2)$$

where

$$\mu(\mathcal{F}) = \frac{1}{rk(\mathcal{F})} \int_X c_1(\mathcal{F}) \wedge J \wedge J, \quad (3.2.3)$$

where  $J$  is the Kähler form on  $X$ .  $V$  is semi-stable if  $\mu(\mathcal{F}) < \mu(V)$  for all subsheaves and is poly-stable if it can be decomposed as a direct sum of stable bundles, all with the same slope:

$$V = \oplus_i V_i \quad \text{with} \quad \mu(V_i) = \mu(V) \quad \forall i. \quad (3.2.4)$$

It is poly-stability which is one-to-one with a solution of (3.2.1). Expanding  $J$  in a basis of harmonic  $\{1, 1\}$  forms as  $J = t^i J_i$ , the slope of any sheaf  $\mathcal{F}$  can be written as

$$\mu(\mathcal{F}) = \frac{1}{rk(\mathcal{F})} d_{ijk} c_1^i(\mathcal{F}) t^j t^k = \frac{1}{rk(\mathcal{F})} s_i c_1^i(\mathcal{F}), \quad (3.2.5)$$

where  $d_{ijk} = \int_X J_i \wedge J_j \wedge J_k$  are the triple intersection numbers of  $X$ ,  $c_1(\mathcal{F}) = c_1^i(\mathcal{F}) J_i$  is the first Chern class of  $\mathcal{F}$ , and  $s_i$  are the so-called “dual” Kähler variables defined by  $s_i = d_{ijk} t^j t^k$ .

For the bundles in consideration in this work,  $c_1(V) = 0$  so  $\mu(V) = 0$ , thus  $V$  is stable if for all  $\mathcal{F} \subset V$ :

$$\mu(\mathcal{F}) = \frac{1}{rk(\mathcal{F})} s_i c_1^i(\mathcal{F}) < 0. \quad (3.2.6)$$

While we have traded a difficult problem in differential geometry (i.e. (3.2.1)) for one in algebraic geometry with the notion of stability, there is still a substantial obstacle to be overcome in determining whether or not a bundle is stable: all possible sub-sheaves  $\mathcal{F} \subset V$  must be characterized. To this end, we employ the tools developed in [28] and we refer the interested reader there for further details. The tools from [28] used in this work are briefly summarized below.

### 3.2.2 Algorithmically Testing Stability

If  $\mathcal{F}$  is a sub-sheaf of  $V$  then it is always possible to describe  $V$  itself in terms of this substructure via the following short exact sequence:

$$0 \rightarrow \mathcal{F} \rightarrow V \rightarrow \frac{V}{\mathcal{F}} \rightarrow 0. \quad (3.2.7)$$

Since  $V$  is a vector bundle it is torsion-free and thus, only subsheaves with rank  $0 < rk(\mathcal{F}) < rk(V)$  need be considered. A central result of [28] is that information about all possible subsheaves  $\mathcal{F}$  above, can be encoded by considering only *line bundle sub-sheaves of  $\wedge^k V$* .

To understand this approach, a good starting point is to note is that for any rank,  $k = rk(\mathcal{F})$  of  $\mathcal{F}$ , the top wedge power,  $\wedge^k \mathcal{F}$  is a rank 1 sheaf. Moreover, the short exact sequence in (3.2.7) guarantees that the inclusion  $0 \rightarrow \mathcal{F} \rightarrow V$  induces an injection

$$0 \rightarrow \wedge^k(\mathcal{F}) \rightarrow \wedge^k(V) \quad (3.2.8)$$

(once again with  $k < rk(V)$ ). Since  $\wedge^k \mathcal{F}$  is rank 1 and torsion-free,  $(\wedge^k \mathcal{F})^{\vee\vee}$  is a line bundle [81] and

$$\wedge^k \mathcal{F} \subset (\wedge^k \mathcal{F})^{\vee\vee} \subset (\wedge^k V)^{\vee\vee} \simeq \wedge^k V. \quad (3.2.9)$$

Let us clarify the utility of this rather opaque chain of results: If there exists a de-stabilizing subsheaf,  $\mathcal{F} \subset V$  as in (3.2.7), this *induces a corresponding line bundle subsheaf*,  $\mathcal{L} = \wedge^k \mathcal{F}$ , s.t.

$$\mathcal{L} \subset \wedge^k V. \quad (3.2.10)$$

As a result, line bundle subsheaves of  $\wedge^k V$  carry information about possibly de-stabilizing subsheaves of  $V$  itself. Finally it should be noted that for any rank  $n$  bundle,  $c_1(\wedge^k \mathcal{F}) = \binom{n-1}{k-1} c_1(V)$  gives  $\mu(\wedge^k V) = 0$ . Thus, to prove that a rank  $n$ ,  $SU(n)$  bundle  $V$  is stable, one needs only to demonstrate that for all  $\mathcal{L} \subset \wedge^k V$

$$\mu(\mathcal{L}) < \mu(V) = 0, \quad (3.2.11)$$

for all  $k < n$ . Note that if a bundle passes the test above it is definitely stable. However, if a line bundle sub-sheaf  $\mathcal{L} \subset \wedge^k$  is found with  $\mu(\mathcal{L}) > 0$  this does not guarantee that it arose from a de-stabilizing subsheaf  $\mathcal{F}$  as in (3.2.7) (i.e. it is not necessarily unstable and further analysis is required).

This algorithmic approach to stability was employed to analyze all the bundles found in this work. We illustrate two important applications of this approach in the following Subsections.

### 3.2.3 Negative Line Bundle Entries in Monad Bundles and Stability

It was a goal of this work to build examples of bundles  $V \rightarrow X$  which are in fact *not stable for the entire Kähler cone of  $X$*  and instead, give rise to stability walls and cone-substructure. Moreover, since we are constrained to work within the framework of  $(0, 2)$  GLSMs, we must represent  $V$  as a monad bundle, (1.5.1). The majority of monads studied in this context have been within the class of so-called “positive” monads in which the degrees of the line bundles in (1.5.1) have been chosen to be  $\geq 0$ . Since the condition of bundle stability is not readily visible within the GLSM itself, this class of positive monads has the added benefit that they are frequently stable everywhere in Kähler moduli space [28, 46–48].

As a result of these observations, in this work we have employed more general classes of monad bundles in which  $V$  is described as the kernel of a map,  $F$ :

$$0 \rightarrow V \rightarrow B \xrightarrow{F} C \rightarrow 0, \quad (3.2.12)$$

and we allow for some non-ample line bundles within  $B$ . We will demonstrate below that generically *any mixed positive/negative degree line bundle in the middle term of the monad,  $B$ , will induce a stability wall in  $V$* . We will illustrate the possibilities here in the simplest case of  $h^{1,1}(X) = 2$ .

To see this, note that one immediate consequence of the analysis in the previous Section is that  $V$  is stable for any choice of Kähler moduli where  $V$  is. As a result, if  $V$  takes the form

$$0 \rightarrow V \rightarrow \mathcal{O}(-a, b) \oplus B' \xrightarrow{F} C \rightarrow 0, \quad (3.2.13)$$

the dual sequence is

$$0 \rightarrow C^\vee \rightarrow \mathcal{O}(a, -b) \oplus B'^\vee \rightarrow V^\vee \rightarrow 0. \quad (3.2.14)$$

By inspection, it is clear that  $\mathcal{O}(a, -b)$  has the potential to be a de-stabilizing line-bundle sub-sheaf of  $V^*$ . It must be checked whether  $\text{Hom}(\mathcal{O}(a, -b), V^\vee) \simeq H^0(X, \mathcal{O}(-a, b) \otimes V^\vee)$



is non-trivial. To this end, note that

$$0 \rightarrow \mathcal{O}(-a, b) \otimes C^\vee \rightarrow \mathcal{O} \oplus \mathcal{O}(-a, b) \otimes B'^\vee \rightarrow \mathcal{O}(-a, b) \otimes V^\vee \rightarrow 0. \quad (3.2.15)$$

Thus, whenever

$$h^0(X, \mathcal{O}(-a, b) \otimes B'^\vee) + 1 > h^0(X, \mathcal{O}(-a, b) \otimes C^\vee), \quad (3.2.16)$$

$\mathcal{O}(a, -b)$  injects into  $V^\vee$  and de-stabilizes it whenever  $\mu(\mathcal{O}(a, -b)) > 0$ . By construction the relationship in (3.2.16) holds for all the examples in this work with non-trivial D-terms. By (3.2.8) and (3.2.9) (as well as the observation that  $\wedge^{N-1}V \simeq V^\vee$  for an  $SU(N)$  bundle,  $V$ ) this leads to information on a non-trivial de-stabilizing subsheaf of  $V$  itself:

$$0 \rightarrow \mathcal{F} \rightarrow V \rightarrow \mathcal{O}(-a, b) \rightarrow 0. \quad (3.2.17)$$

Note that this observation only gives information about one de-stabilizing subsheaf. There can be many others and a full stability analysis is necessary to determine the exact structure of the stable subcone of Kähler moduli space. We provide an example of such an analysis in the next Section.

### 3.2.4 Example Stability Analysis

In this section we employ the techniques described in Section 3.2.2 to test whether or not a monad bundle is stable. Since stability is difficult to probe directly from the GLSM, these tools play a crucial role in verifying the validity of the theory.

Consider an  $SU(3)$  vector bundle  $V$  defined on the familiar co-dimension one CICY  $\begin{matrix} \mathbb{P}^1 \\ \mathbb{P}^3 \end{matrix} \left[ \begin{matrix} 2 \\ 4 \end{matrix} \right]$ :

| $x_i$       | $\Gamma^j$ | $\Lambda^a$ | $p_l$ |
|-------------|------------|-------------|-------|
| 1 1 0 0 0 0 | -2         | -1 1 1 1 2  | -3 -1 |
| 0 0 1 1 1 1 | -4         | 1 1 1 1 2   | -4 -2 |

(3.2.18)

The bundle  $V$  is given by a short exact sequence (SES):

$$0 \rightarrow V \rightarrow \mathcal{O}(-1, 1) \oplus \mathcal{O}(1, 1)^{\oplus 3} \oplus \mathcal{O}(2, 2) \rightarrow \mathcal{O}(3, 4) \oplus \mathcal{O}(1, 2) \rightarrow 0, \quad (3.2.19)$$

and satisfies  $c_1(V) = 0$  and  $c_2(TX) = c_2(V)$ . For simplicity we will denote this as  $0 \rightarrow V \rightarrow B \xrightarrow{F} C \rightarrow 0$ .

Following the arguments of Section 3.2.2, since  $V$  is a rank 3 bundle, to test its stability it is necessary to identify all line bundles  $\mathcal{L}$  that destabilize  $\wedge^k V$ , where  $k = 1, 2$ . We consider each value of  $k$  in turn.

First with  $k = 1$ , take  $\mathcal{L} = \mathcal{O}(a, b)$ . Note that if  $a, b < 0$  then  $\mathcal{L}$  de-stabilizes  $V$  nowhere in Kähler moduli space (since the intersection numbers  $d_{rst}$  for the manifold above are positive) and thus is not of interest. Thus, we are concerned with cases in which  $a, b > 0$  and where  $ab < 0$ , (i.e. one of  $a$  and  $b$  is less than zero). If  $\mathcal{L}$  injects into  $V$ , then the space of maps  $H^0(\mathcal{L}^\vee \otimes V)$  must be non-vanishing and can be calculated from the SES:

$$0 \rightarrow \mathcal{L}^\vee \otimes V \rightarrow \mathcal{L}^\vee \otimes B \rightarrow \mathcal{L}^\vee \otimes C \rightarrow 0. \quad (3.2.20)$$

This sequence in turn induces the long exact sequence in cohomology

$$\begin{aligned} 0 \rightarrow H^0(\mathcal{L}^\vee \otimes V) &\rightarrow H^0(\mathcal{L}^\vee \otimes B) \rightarrow H^0(\mathcal{L}^\vee \otimes C) \\ &\rightarrow H^1(\mathcal{L}^\vee \otimes V) \rightarrow H^1(\mathcal{L}^\vee \otimes B) \rightarrow H^1(\mathcal{L}^\vee \otimes C) \\ &\rightarrow H^2(\mathcal{L}^\vee \otimes V) \rightarrow H^2(\mathcal{L}^\vee \otimes B) \rightarrow H^2(\mathcal{L}^\vee \otimes C) \\ &\rightarrow H^3(\mathcal{L}^\vee \otimes V) \rightarrow H^3(\mathcal{L}^\vee \otimes B) \rightarrow H^3(\mathcal{L}^\vee \otimes C) \rightarrow 0. \end{aligned} \quad (3.2.21)$$

Thus, in each case the question is for which values of  $a, b$  is

$$\ker\{H^0(\mathcal{L}^\vee \otimes B) \rightarrow H^0(\mathcal{L}^\vee \otimes C)\} \quad (3.2.22)$$

non-trivial? To answer this, we use the structure of line bundle cohomology on  $X$  [28, 64, 67]. For any line bundle  $\mathcal{O}(\alpha, \beta)$  which descends from the ambient space  $\mathcal{A} = \mathbb{P}^1 \times \mathbb{P}^4$  we have the Koszul sequence:

$$0 \rightarrow \mathcal{O}_{\mathcal{A}}(-2, 4) \otimes \mathcal{O}_{\mathcal{A}}(\alpha, \beta) \rightarrow \mathcal{O}_{\mathcal{A}}(\alpha, \beta) \rightarrow \mathcal{O}_X(\alpha, \beta) \rightarrow 0. \quad (3.2.23)$$

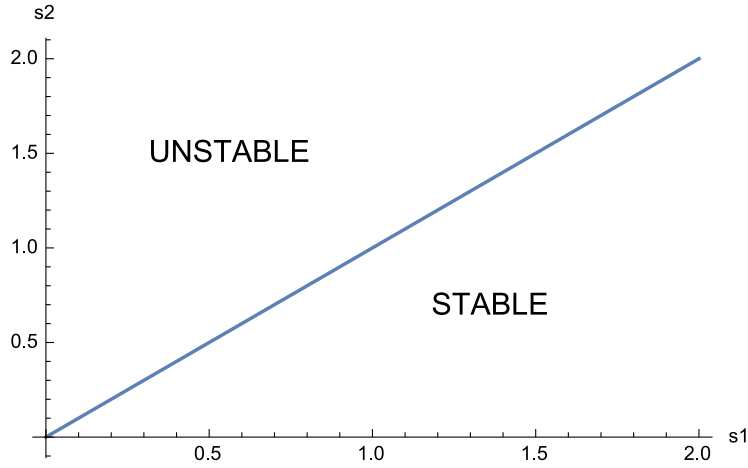


**Figure 3.2:** *The stable and unstable regions of the Kähler cone associated to the  $SU(3)$  bundle in (3.2.19).*

It follows that in this case

$$h^0(X, \mathcal{O}(\alpha, \beta)) \neq 0 \text{ if and only if } \begin{cases} \alpha, \beta \geq 0, \\ \text{or} \\ \alpha = -1, \beta \geq 4. \end{cases} \quad (3.2.24)$$

With these tools, the bundle in (3.2.19) can be analyzed. The only de-stabilizing subsheaves arise as  $\mathcal{L} \subset V^\vee$  (i.e. the  $k = 2$  case) and take the form

$$\mathcal{O}(1, -1) \quad \text{or} \quad \mathcal{O}(2, -p) \quad p \geq 5. \quad (3.2.25)$$

It is clear that the “maximally de-stabilizing” line bundle subsheaf of  $V$  is exactly  $\mathcal{O}(1, -1)$ , the one expected from the arguments of the previous sub-section. Describing the Kähler cone in terms of dual variables  $s_t = d_{trs} t^s t^r$  the sub-cone structure of Kähler moduli space is given in Figure 3.2 below.

### 3.2.5 Some Useful Results on Stable Bundles

The following notion of an “S-equivalence class” plays a useful role in characterization of semi-stable sheaves and the notion of moduli space (both mathematically and physically) [82].

**Theorem 1: Harder-Narasimhan**

Given a holomorphic bundle  $V$  over a closed Kähler manifold  $X$  (with Kähler form  $\omega$ ), there is a filtration (called the Harder-Narasimhan filtration) by sub-sheaves

$$0 = \mathcal{F}_0 \subset \mathcal{F}_1 \subset \dots \mathcal{F}_m = V \quad (3.2.26)$$

such that  $\mathcal{F}_i/\mathcal{F}_{i-1}$  are semi-stable sheaves for  $i = 1, \dots, m$  and the slope of the quotients are ordered

$$\mu(\mathcal{F}_1) > \mu(\mathcal{F}_2/\mathcal{F}_1) > \dots \mu(\mathcal{F}_m/\mathcal{F}_{m-1}) . \quad (3.2.27)$$

If  $V$  is semi-stable, then there is a filtration by sub-sheaves (called the Jordan-Hölder filtration)

$$0 = \mathcal{F}_0 \subset \mathcal{F}_1 \subset \dots \mathcal{F}_m = V \quad (3.2.28)$$

such that the quotients  $\mathcal{F}_i/\mathcal{F}_{i-1}$  are all stable sheaves and have slope  $\mu(\mathcal{F}_i/\mathcal{F}_{i-1}) = \mu(V)$ . In addition

$$Gr(V) = \mathcal{F}_1 \oplus \mathcal{F}_2/\mathcal{F}_1 \oplus \dots \mathcal{F}_m/\mathcal{F}_{m-1} \quad (3.2.29)$$

is uniquely determined up to isomorphism (and is called the ‘graded sum’).

Theorem 3.2.5 plays a crucial role in the notion of a moduli space of semi-stable sheaves. Two semi-stable bundles,  $V_1$  and  $V_2$ , are called *S-equivalent* if  $Gr(V_1) = Gr(V_2)$ . A moduli space of semi-stable sheaves can only be made Hausdorff if each point corresponds to an S-equivalence class [82]. To compare this with the physical notion of a moduli space near the stability wall, it should be noted that each S-equivalence class contains a unique poly-stable representative, namely, the graded sum (3.2.29). Within the effective theory near the stability wall, we will see in Section 4.1.3 that the branch structure of the effective theory is visible near the stability wall. That is, all stable bundles that can be constructed at generic points in moduli space *by non-trivially “gluing” together the reducible bundle at the wall* can be characterized by their poly-stable decomposition on the wall – that is, their S-equivalence class.

As discussed in Section 4.1.3, the possible branches of supersymmetric vacua are determined by the charged bundle moduli appearing in  $U(1)$  D-terms (see the matter content in Table 4.1 and the D-term constraint given in (4.1.32) and (4.1.33)) which in the language of Theorem

3.2.5 are described by

$$\langle C \rangle \sim Ext^1(\mathcal{F}_i/\mathcal{F}_{i-1}, \mathcal{F}_j/\mathcal{F}_{j-1}), \quad (3.2.30)$$

for  $i < j \leq m$  associated with terms  $\mathcal{F}_i/\mathcal{F}_{i-1}$  in the graded sum  $Gr(V)$  of (3.2.29). Thus, for semi- and poly-stable bundles near a stability wall, it is important to observe that the mathematical and physical notions of a moduli space coincide.

Finally, in exploring collections of target space geometries, the following well-known Lemma and its corollary [83] play a valuable role in identifying isomorphic slope-stable vector bundles described by seemingly distinct monad sequences:

### Morphism Lemma

*Let  $\phi : V_1 \rightarrow V_2$  be a non-trivial sheaf homomorphism between semi-stable bundles  $V_1, V_2$ . If at least one of the bundles is properly stable and  $\mu(V_1) = \mu(V_2)$ , then  $\phi$  is a monomorphism or generically, an epimorphism.*

### Corollary

*Let  $\phi : V_1 \rightarrow V_2$  be a nontrivial sheaf homomorphism between two semistable vector bundles  $V_1, V_2$  with  $rk(V_1) = rk(V_2)$  and  $c_1(V_1) = c_1(V_2)$ . Let at least one of the bundles be properly stable. Then  $\phi$  is an isomorphism.*

## 3.2.6 A Few Useful Formulas for Bundle and Manifold Topology

For ease of reference, a few standard formulas for the topology of a monad bundle are included here.

As in (1.5.1), define a two-term monad bundle  $V = Ker(F)$  via a short exact sequence

$$0 \rightarrow V \rightarrow B \xrightarrow{f} C \rightarrow 0, \text{ where}$$

$$B = \bigoplus_{i=1}^{r_B} \mathcal{O}_X(\mathbf{b}_i), \quad C = \bigoplus_{j=1}^{r_C} \mathcal{O}_X(\mathbf{c}_j)$$

are sums of line bundles with ranks  $r_B$  and  $r_C$ , respectively. The rank  $N$  of  $V$  is easily seen,

by exactness of (3.2.31), to be

$$n = \text{rk}(V) = r_B - r_C . \quad (3.2.31)$$

The topology of the monad is

$$\begin{aligned} c_1^r(V) &= \sum_{i=1}^{r_B} b_i^r - \sum_{j=1}^{r_C} c_j^r , \\ c_{2r}(V) &= \frac{1}{2} d_{rst} \left( \sum_{j=1}^{r_C} c_j^s c_j^t - \sum_{i=1}^{r_B} b_i^s b_i^t \right) , \\ c_3(V) &= \frac{1}{3} d_{rst} \left( \sum_{i=1}^{r_B} b_i^r b_i^s b_i^t - \sum_{j=1}^{r_C} c_j^r c_j^s c_j^t \right) . \end{aligned} \quad (3.2.32)$$

These are equivalent to the GLSM formulae given in (2.1.2). Above  $d_{rst}$  is the triple intersection number on  $X$ , a CY 3-fold:

$$d_{rst} = \int_X J_r \wedge J_s \wedge J_t, \quad (3.2.33)$$

with  $J_r$ ,  $r = 1, \dots, h^{1,1}$  a basis of Kähler forms on  $X$ .

Finally, we turn to the topology of a CY manifold,  $X$ , defined as a complete intersection manifold in a product of ordinary projective spaces. Such a manifold is determined by a *configuration matrix*

$$\left[ \begin{array}{c|cccc} \mathbb{P}^{n_1} & q_1^1 & q_1^2 & \cdots & q_1^K \\ \mathbb{P}^{n_2} & q_2^1 & q_2^2 & \cdots & q_2^K \\ \vdots & \vdots & \vdots & \ddots & \vdots \\ \mathbb{P}^{n_m} & q_m^1 & q_m^2 & \cdots & q_m^K \end{array} \right]_{m \times K} \quad (3.2.34)$$

The entry  $q_i^r$  denotes the degree of the  $j$ -th defining polynomial in the factor  $\mathbb{P}^{n_r}$  and each column corresponds to one polynomial constraint. In order that the resulting manifold be Calabi-Yau, the condition

$$\sum_{j=1}^K q_r^j = n_r + 1, \quad \forall r = 1, \dots, m \quad (3.2.35)$$

is imposed. In terms of this data, the topology of  $X$  is given by

$$c_1^r = 0, \quad c_2^{rs} = \frac{1}{2} \left[ -\delta^{rs}(n_r + 1) + \sum_{j=1}^K q_j^r q_j^s \right], \quad c_3^{rst} = \frac{1}{3} \left[ \delta^{rst}(n_r + 1) - \sum_{j=1}^K q_j^r q_j^s q_j^t \right]. \quad (3.2.36)$$

Integration over  $X$  can be done with respect to a measure  $\mu_{q_r^j}$  and pulled back to a simpler integration over the ambient space  $\mathcal{A}$ :

$$\int_X \cdot = \int_{\mathcal{A}} \mu_{q_r^j} \wedge \cdot, \quad \mu_{q_r^j} := \wedge_{j=1}^K \left( \sum_{r=1}^m q_r^j J_r \right). \quad (3.2.37)$$

# Chapter 4

## New Evidence for (0,2) Target Space Duality

In this chapter we will present our result in the exploration of the detailed structure of vacuum space in dual theories, by analyzing vector bundles with non-trivial constraints arising from slope-stability (i.e. D-terms) and holomorphy (i.e. F-terms). The contents of this chapter have previously appeared in our paper [41].

### 4.1 D-terms, Bundle Stability, and Duality

In this section we will begin to explore the role of a non-trivial D-term condition in target space dual chains. One complication in this process is that we do not have a concrete map (i.e. an explicit isomorphism) between the two moduli spaces of the (0,2) theories. In general, the presence of a non-trivial D-term potential does not lift entire flat directions (i.e. change the dimension of the vacuum space) but merely change its shape (see Figure 3.1). At the level of the effective theory, this is a realization of the fact that the vacuum space can be written as a solution to the F-terms, modulo D-term constraints [84]. In the bundle geometry, this same notion plays a crucial role in the definition of bundle moduli spaces, geometric invariant theory (GIT), quotients, etc [69].

To simplify our analysis then, we will take as a first example an extreme case in which the bundle is only stable for a sub-cone of the Kähler moduli space of *strictly smaller dimension*. This will make it possible to simply count and observe whether or not there is a drop in the total degrees of freedom on both sides of the duality. For the details of how to analyze the slope-stability of a vector bundle and how to engineer interesting monad examples, see Section 3.2. Using these tools, we can select a pair,  $(X, V)$ , of CY manifold and vector bundle  $\pi : X \rightarrow V$  with a D-term which “lifts” whole directions of Kähler moduli space.



Below, we will start with a simple example with  $h^{1,1} = 2$  and a bundle over it which contains *two* destabilizing sub-sheaves,  $\mathcal{F}_1, \mathcal{F}_2$ . These sheaves, as described in the previous Section, appear in the associated D-terms as in (3.1.8) and in the slope-stability analysis of  $V$  as described in Section 3.2. Here, the sub-sheaves are chosen such that

$$c_1(\mathcal{F}_1) = -c_1(\mathcal{F}_2). \quad (4.1.1)$$

Since a bundle is only stable if  $\mu(V) > \mu(\mathcal{F})$  for all  $\mathcal{F} \subset V$  (see Section 3.2), it is clear that with two de-stabilizing sub-sheaves as in (4.1.1), and  $c_1(V) = 0$ ,  $V$  cannot be properly stable at all. Indeed it can only solve the Hermitian-Yang-Mills equations, (3.1.1), on the locus in Kähler moduli space for which

$$\mu(\mathcal{F}_1) = -\mu(\mathcal{F}_2) = \mu(V) = 0, \quad (4.1.2)$$

where  $V$  itself must become reducible as a poly-stable bundle  $V \rightarrow V_1 \oplus V_2 \oplus \dots$

For the CY manifold,  $X$ , consider the simple degree  $\{2, 4\}$  hypersurface in  $\mathbb{P}^1 \times \mathbb{P}^3$  with Hodge numbers  $h^{1,1}(X) = 2$  and  $h^{2,1}(X) = 86$ . Expanding the second Chern class of the manifold in a basis of  $\{1, 1\}$  forms as  $c_2(TX)_r = d_{rst}c_2(TX)^{st}$  (where  $d_{rst}$  are the triple intersection numbers and  $r = 1, \dots, h^{1,1}$ ) we have  $c_2(TX)^r = \{24, 44\}$  (see Section 3.2.6). Finally, to complete the geometry, a rank 5 monad bundle,  $V$ , can be chosen over  $X$ , written as a kernel:

$$0 \rightarrow V \rightarrow B \xrightarrow{F} C \rightarrow 0, \quad (4.1.3)$$

where  $V = \ker(F)$  and  $B$  and  $C$  are sums of line bundles over  $X$  as in (2.1.7). In GLSM language, the manifold and bundle are given by the following data:

| $x_i$       | $\Gamma^j$ | $\Lambda^a$      | $p_l$    |
|-------------|------------|------------------|----------|
| 1 1 0 0 0 0 | -2         | 1 -1 0 0 2 1 1 2 | -3 -1 -2 |
| 0 0 1 1 1 1 | -4         | -1 1 1 1 1 2 2 2 | -2 -4 -3 |

(4.1.4)

By inspection,  $c_1(V) = 0$  and using the tools of [28] it can be verified that

$$c_2(V) = c_2(TX) = \{24, 44\}, \quad (4.1.5)$$

and the third Chern class is  $c_3(V) = -80$ . Finally, a straightforward, but lengthy calculation yields the following naive total for the uncharged (geometric) moduli of the theory:

$$\dim(\mathcal{M}_0) = h^{1,1}(X) + h^{2,1}(X) + h^1(X, \text{End}_0(V)) = 2 + 86 + 340 = 428. \quad (4.1.6)$$

Thus far we are in familiar territory. As described in Section 3.1, it is now possible to go further and explore the theory in more depth by considering the structure of its effective potential. As will be shown in the next subsections, the bundle in (4.1.4) is exactly of the form required to generate a non-trivial D-term constraint and a corresponding reduction in the number of flat directions. We will begin by analyzing the effective theory arising from this geometry along the stable ray in the Kähler cone (the “stability wall” [17, 18, 21]).

The non-vanishing triple intersection numbers of the CY 3-fold are  $d_{122} = 4$  and  $d_{222} = 2$ . Expanding the Kähler form in a basis of  $\{1, 1\}$  forms as  $J = t^r J_r$  (with  $t^r$  the Kähler moduli), it is clear that the condition in (4.1.2) restricts the theory to the locus in Kähler moduli space for which  $-8t^1 t^2 + 2(t^2)^2 = 0$ . Choosing perturbative solutions in the interior of the Kähler cone requires  $t^r > 0$  for all  $r$ , and thus the “stability wall” in this case is the one-dimensional ray in Kähler moduli space where

$$t^2 = 4t^1 \quad \text{equivalently} \quad s_2 = s_1 \quad (4.1.7)$$

in the dual Kähler coordinates with  $s_r = d_{rst} t^s t^t$ . The stable subcone for  $V$  is shown in Figure 4.1.

This bundle is an example of one where the naive degree-of-freedom counting given in (1.3.4) fails to capture important structure. In fact, the dimension of the singlet moduli space is not the sum given in (4.1.6). Instead, with the stability constraint in (4.1.7) it is reduced to

$$\dim(\mathcal{M}_1) = \dim(\mathcal{M}_0) - 1 = 427. \quad (4.1.8)$$

This type of example provides a direct new probe of target space duality. Will the dual theories also reflect this reduction in degrees of freedom? What is the structure of the potential in the dual theory and will the moduli lifting happen through D-terms or F-terms? Before answering these questions however, we will see below that in fact the detailed structure of the theory on the stability wall provides many new features that can be compared.

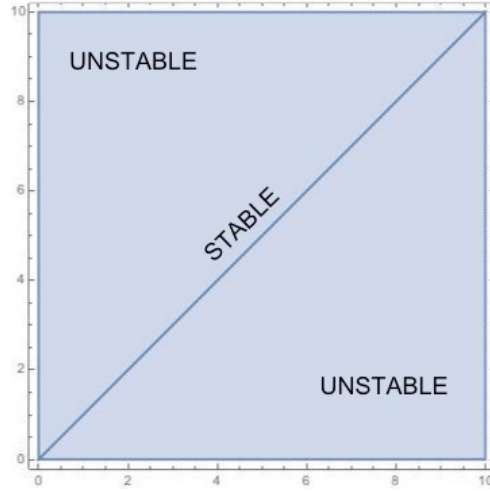


**Figure 4.1:** *The stable ray in Kähler moduli space shown for the monad bundle in (4.1.4). Along this co-dimension 1 subcone the bundle takes the poly-stable form shown in (4.1.17).*

### 4.1.1 Effective Theory Near the Stability Wall

As described in Section 3.2, the presence of each of the line bundles with negative entries in  $B$  (the middle term of the monad) in (4.1.3) implies the existence of a particular sub-sheaf of  $V$ . In this case, following (3.2.17) we see that  $V$  can be written in terms of its de-stabilizing sub-sheaves as

$$0 \rightarrow Q_4 \rightarrow V \rightarrow \mathcal{O}(1, -1) \rightarrow 0, \quad (4.1.9)$$

$$0 \rightarrow \tilde{Q}_4 \rightarrow V \rightarrow \mathcal{O}(-1, 1) \rightarrow 0, \quad (4.1.10)$$

where the rank 4 sheaves,  $Q_4$  and  $\tilde{Q}_4$  are described via the monads

$$0 \rightarrow Q_4 \rightarrow \mathcal{O}(-1, 1) \oplus \mathcal{O}(0, 1)^{\oplus 2} \oplus \mathcal{O}(2, 1) \oplus \mathcal{O}(1, 2)^{\oplus 2} \oplus \mathcal{O}(2, 2) \rightarrow \mathcal{O}(3, 2) \oplus \mathcal{O}(1, 4) \oplus \mathcal{O}(2, 3) \rightarrow 0,$$

$$0 \rightarrow \tilde{Q}_4 \rightarrow \mathcal{O}(1, -1) \oplus \mathcal{O}(0, 1)^{\oplus 2} \oplus \mathcal{O}(2, 1) \oplus \mathcal{O}(1, 2)^{\oplus 2} \oplus \mathcal{O}(2, 2) \rightarrow \mathcal{O}(3, 2) \oplus \mathcal{O}(1, 4) \oplus \mathcal{O}(2, 3) \rightarrow 0. \quad (4.1.11)$$

Since  $Q_4$  and  $\tilde{Q}_4$  are sub-sheaves of  $V$ , with non-trivial first Chern classes, it is clear that supersymmetry will only be preserved if the bundle is poly-stable. This implies a decomposition of  $V$  into each de-stabilizing sub-sheaf as  $V \rightarrow \mathcal{F} \oplus V/\mathcal{F}$ . In this case, for

the two subsheaves of interest:

$$V \rightarrow Q_4 \oplus \mathcal{O}(1, -1), \quad (4.1.12)$$

$$V \rightarrow \tilde{Q}_4 \oplus \mathcal{O}(-1, 1). \quad (4.1.13)$$

Moreover, these descriptions are only compatible if  $Q_4$  and  $\tilde{Q}_4$  decompose still further as

$$Q_4 \rightarrow U_3 \oplus \mathcal{O}(-1, 1), \quad (4.1.14)$$

$$\tilde{Q}_4 \rightarrow U_3 \oplus \mathcal{O}(1, -1). \quad (4.1.15)$$

for *the same* rank 3 sheaf  $U_3$  with  $c_1(U_3) = 0$ . By inspection of (4.1.11) it is straightforward to verify that such a reducible locus in the moduli space of  $Q_4$  and  $\tilde{Q}_4$  does indeed exist and here  $U_3$  is in fact locally free (i.e. an  $SU(3)$  bundle) itself described as a monad:

$$0 \rightarrow U_3 \rightarrow \mathcal{O}(0, 1)^{\oplus 2} \oplus \mathcal{O}(2, 1) \oplus \mathcal{O}(1, 2)^{\oplus 2} \oplus \mathcal{O}(2, 2) \rightarrow \mathcal{O}(3, 2) \oplus \mathcal{O}(1, 4) \oplus \mathcal{O}(2, 3) \rightarrow 0. \quad (4.1.16)$$

One less obvious observation can be made using the tools of Section 3.2: the bundle  $U_3$  is properly stable for the stability wall,  $t^2 = 4t^1$ . Thus, in summary, the only locus in the moduli space of the monad bundle  $V$ , given in (4.1.4) for which the bundle is poly-stable and supersymmetry is preserved is when the map  $f$  is chosen so that the bundle is reducible:

$$V \rightarrow U_3 \oplus L \oplus L^\vee, \quad (4.1.17)$$

with  $L = \mathcal{O}(1, -1)$ .

The consequences of this decomposition are immediate for the effective target space theory. Since we began with a seemingly indecomposable  $SU(5)$  bundle the natural expectation would have been to find a four-dimensional  $SU(5)$  effective theory (since  $SU(5) \times SU(5)$  is a maximal subgroup of  $E_8$ ). However, once the D-term is taken into account we see that the structure group of the bundle on the stability wall has decreased to  $S[U(1) \times U(1)] \times SU(3) \simeq U(1) \times SU(3)$  which has a commutant within  $E_8$  of  $SU(6) \times U(1)$ . The  $U(1)$  symmetry is in general Green-Schwarz massive [42] and as described in Section 3.1, leads to a non-trivial D-term constraint. Thus *the presence of a stability wall in the theory has led not only to a reduction in Kähler moduli, but also to a non-Abelian enhancement of the four-dimensional gauge symmetry.*

| Field                        | Cohom.                      | Multiplicity | Field                        | Cohom.                         | Multiplicity |
|------------------------------|-----------------------------|--------------|------------------------------|--------------------------------|--------------|
| $\mathbf{1}_{+2}$            | $H^1(L \otimes L)$          | 0            | $\mathbf{1}_{-2}$            | $H^1(L^\vee \otimes L^\vee)$   | 10           |
| $\mathbf{15}_0$              | $H^1(U_3^\vee)$             | 0            | $\overline{\mathbf{15}}_0$   | $H^1(U_3)$                     | 80           |
| $\mathbf{20}_{+1}$           | $H^1(L)$                    | 0            | $\mathbf{20}_{-1}$           | $H^1(L^\vee)$                  | 0            |
| $\mathbf{6}_{+1}$            | $H^1(L \otimes U_3)$        | 72           | $\mathbf{6}_{-1}$            | $H^1(L^\vee \otimes U_3)$      | 90           |
| $\overline{\mathbf{6}}_{+1}$ | $H^1(L \otimes U_3^\vee)$   | 0            | $\overline{\mathbf{6}}_{-1}$ | $H^1(L^\vee \otimes U_3^\vee)$ | 2            |
| $\mathbf{1}_0$               | $H^1(U_3 \otimes U_3^\vee)$ | 166          |                              |                                |              |

**Table 4.1:** Particle content of the  $SU(6) \times U(1)$  theory associated to the bundle (4.1.4) along its reducible and poly-stable locus  $V = \mathcal{O}(-1, 1) \oplus \mathcal{O}(1, -1) \oplus U_3$  (i.e. on the stability wall given by (4.1.7) and shown in Figure 4.1).

The charged matter spectrum can be determined by beginning with the decomposition [85]

$$\mathbf{248}_{E_8} \rightarrow [(\mathbf{3}, \mathbf{1}, \mathbf{1}) \oplus (\mathbf{1}, \mathbf{8}, \mathbf{1}) \oplus (\mathbf{1}, \mathbf{1}, \mathbf{35}) \oplus (\mathbf{1}, \mathbf{3}, \overline{\mathbf{15}}) \oplus (\mathbf{1}, \overline{\mathbf{3}}, \mathbf{15}) \oplus (\mathbf{2}, \mathbf{3}, \mathbf{6}) \oplus (\mathbf{2}, \overline{\mathbf{3}}, \overline{\mathbf{6}}) \oplus (\mathbf{2}, \mathbf{1}, \mathbf{20})] \quad (4.1.18)$$

of the adjoint of  $E_8$  into  $SU(2) \times SU(3) \times SU(6)$ . Then the further reduction of  $SU(2) \rightarrow S[U(1) \times U(1)]$  allows us to read off the final charged matter content of the  $SU(6) \times U(1)$  theory<sup>1</sup>. The result is given in Table 4.1.

In addition to the D-terms associated to the non-Abelian  $SU(6)$  gauge symmetry there is a D-term associated to the Green-Schwarz massive  $U(1)$  which is self commuting in the  $S[U(1) \times U(1)]$  factor in  $E_8$ . Written in the expansion parameters of heterotic M-theory, this takes the schematic form (see [17] for details):

$$D^{U(1)} \sim \frac{3}{16} \frac{\epsilon_S \epsilon_R^2 \mu(\mathcal{F})}{\kappa_4^2 \text{Vol}(X)} - \frac{1}{2} \sum_i Q_i G_{P\bar{Q}} C_i^P \bar{C}_i^{\bar{Q}}, \quad (4.1.19)$$

where  $\text{Vol}(X)$  is the volume of the CY threefold  $X$ ,  $G_{P\bar{Q}}$  is the field space metric, and  $C_i$  denotes any of the matter fields charged under the Green-Schwarz massive  $U(1)$  symmetry (with charge  $Q_i$ ) appearing in Table 4.1. Once again, we note the key feature of this example: because of the non-trivial D-term above, when  $\langle C \rangle = 0$  (corresponding to the monad in (4.1.4)), the D-term non-trivially constrains the Kähler moduli through the condition that  $\mu(\mathcal{F}) = 0$  and the moduli of the theory are not those counted in (4.1.6) but rather the  $\dim(\mathcal{M}) = 427$  moduli in (4.1.8).

<sup>1</sup>Note that locally  $S[U(n) \times U(1)] \simeq SU(n) \times U(1)$ . Globally, however, there is a different normalization on the  $U(1)$  which is comprises part of the commutant of this symmetry within  $E_8$ . Because it will not affect the vacuum analysis in this section, for simplicity we will follow the local charge normalization conventions of [85] for all  $U(1)$  charges in this work.

We will explore the vacuum branch structure of this theory in more detail in Section 4.1.3, but for now we turn to the target space dual theories.

### 4.1.2 Target Space Duals of Theories with D-terms

Following the target space duality algorithm as described in Section 2.2 (including repeated line bundles as in Section 2.2.3) it is possible to generate 16 target space duals for the pair  $(X, V)$  given in (4.1.4) in which the new manifolds,  $\tilde{X}_i$ , are still described as CICYs. The complete chain of target space dual theories is given in Appendix A. To investigate these results, a simple starting point is given below – a dual for which the Calabi-Yau manifold,  $X$ , is related to the original threefold by a geometric transition.

| $x_i$           | $\Gamma^j$ | $\Lambda^a$       | $p_t$    |
|-----------------|------------|-------------------|----------|
| 0 0 0 0 0 0 1 1 | -1 -1      | 0 0 1 0 0 0 0 0   | 0 0 -1   |
| 1 1 0 0 0 0 0 0 | -2 0       | 1 -1 0 0 2 1 1 2  | -3 -1 -2 |
| 0 0 1 1 1 1 0 0 | -2 -2      | -1 1 -1 1 3 2 2 2 | -2 -4 -3 |

(4.1.20)

In view of the results of the previous subsection, obvious questions include:

1. Does  $(\tilde{X}, \tilde{V})$  give rise to a stability wall?
2. Is  $\dim(\tilde{\mathcal{M}}_1)$  also reduced in dimension compared to  $\dim(\tilde{\mathcal{M}}_0)$ ? Are the number of lifted moduli the same?
3. Does the structure group of  $\tilde{V}$  also reduce, leading to a four-dimensional non-Abelian enhancement of symmetry (i.e.  $SU(6)$ )?
4. Do the charged matter spectra of the two theories match?

We will address each of these questions in turn.

First, the complete intersection CY (CICY) manifold and rank 5 vector bundle given in (4.1.20) satisfies  $h^{1,1}(\tilde{X}) = 3$ ,  $h^{2,1}(\tilde{X}) = 55$  and

$$c_2(\tilde{V}) = c_2(T\tilde{X}) = \{24, 24, 44\}, \quad (4.1.21)$$

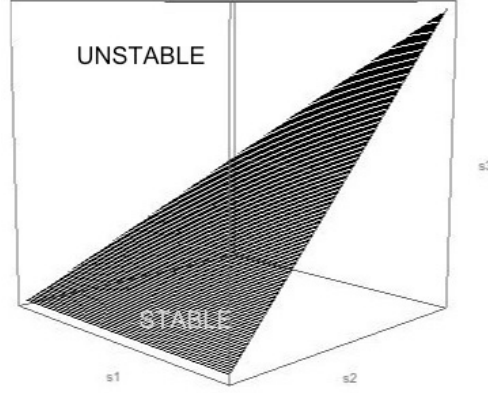


**Figure 4.2:** The two-dimensional stable sub-cone in Kähler moduli space shown for the monad bundle in (4.1.20). Along this co-dimension 1 sub-cone the bundle takes the poly-stable form shown in (4.1.29).

and the third Chern class is  $c_3(\tilde{V}) = -80$  as expected. The comparison to (4.1.4) can begin with the uncharged (geometric) moduli of the theory:

$$\dim(\tilde{\mathcal{M}}_0) = h^{1,1}(\tilde{X}) + h^{2,1}(\tilde{X}) + h^1(X, \text{End}_0(\tilde{V})) = 3 + 55 + 370 = 428. \quad (4.1.22)$$

Once again, it is important to observe that this naive moduli count may not be the correct zero mode count for the theory. As illustrated in the previous Section, this count is only preliminary since we have not yet taken into account any non-trivial D-term potential associated to the geometry above.

By inspection, the negative charges in (4.1.20) indicate that the bundle will possess stability walls (see Section 3.2). For the bundle in (4.1.20) it can be verified that there are now *three* de-stabilizing subsheaves rather than the two of (4.1.4). Explicitly, these are given by

$$0 \rightarrow \tilde{\mathcal{F}}_1 \rightarrow \tilde{V} \rightarrow \mathcal{O}(0, 1, -1) \rightarrow 0 \quad c_1(\tilde{\mathcal{F}}_1) = (0, -1, 1), \quad (4.1.23)$$

$$0 \rightarrow \tilde{\mathcal{F}}_2 \rightarrow \tilde{V} \rightarrow \mathcal{O}(0, -1, 1) \rightarrow 0 \quad c_1(\tilde{\mathcal{F}}_2) = (0, 1, -1), \quad (4.1.24)$$

$$0 \rightarrow \tilde{\mathcal{F}}_3 \rightarrow \tilde{V} \rightarrow \mathcal{O}(1, 0, -1) \rightarrow 0 \quad c_1(\tilde{\mathcal{F}}_3) = (-1, 0, 1). \quad (4.1.25)$$

To proceed, it can be noted that the non-vanishing triple intersection numbers for  $\tilde{X}$  are

$$d_{123} = d_{133} = d_{233} = 4 \quad , \quad d_{333} = 2. \quad (4.1.26)$$

Combining this with the stability conditions that  $\mu(\tilde{\mathcal{F}}_i) \leq 0$  for  $i = 1, 2, 3$  leads to the constraint that (for  $t^i > 0$  in the interior of the Kähler cone) that  $t^2 > t^1$  and  $t^3 = 2t^2 + 2\sqrt{t^1 t^2 + (t^2)^2}$ . In the dual Kähler variables this takes the form of a simple plane the three-dimensional Kähler cone of  $\tilde{X}$ :

$$s_3 < s_1 \quad \text{and} \quad s_2 = s_3. \quad (4.1.27)$$

The two-dimensional stable plane is shown in Figure 4.2.

Although the number of de-stabilizing subsheaves differs in the target space dual theory, the total number of moduli has been precisely matched! That is, in this case we have

$$\dim(\tilde{\mathcal{M}}_1) = \dim(\tilde{\mathcal{M}}_0) - 1 = 427 \quad (4.1.28)$$

exactly as required for a correspondence of the target space theories. Thus, the first two questions posed in the previous section are answered: *The presence of the stability wall (i.e. the locus of enhanced symmetry) and the reduction in moduli due to the D-term constraint are both exactly mirrored in the target space dual theory.*

To see if the enhancement of non-Abelian symmetry is the same as that for the bundle given in (4.1.4) it should be noted that the bundle in (4.1.20) has a poly-stable decomposition along the two-dimensional stability wall given by (4.1.27) as

$$\tilde{V} \rightarrow (\tilde{L} \oplus \tilde{L}^\vee) \oplus \tilde{U}_3, \quad (4.1.29)$$

with  $\tilde{L} = \mathcal{O}(0, 1, -1)$  and the rank 3 bundle  $\tilde{U}_3$  is given by the monad

$$0 \rightarrow \tilde{U}_3 \rightarrow \mathcal{O}(1, 0, -1) \oplus \mathcal{O}(0, 0, 1) \oplus \mathcal{O}(0, 2, 3) \oplus \mathcal{O}(0, 1, 2)^{\oplus 2} \oplus \mathcal{O}(0, 2, 2) \rightarrow \mathcal{O}(0, 3, 2) \oplus \mathcal{O}(0, 1, 4) \oplus \mathcal{O}(1, 2, 3) \rightarrow 0. \quad (4.1.30)$$

The presence of the negative line bundle,  $\mathcal{O}(1, 0, -1)$  in  $\tilde{U}_3$  indicates that there is a sub-locus in moduli space where  $\tilde{V}$  can be decomposed still further (namely, where  $\tilde{U}_3 \rightarrow \mathcal{O}(1, 0, -1) \oplus \tilde{U}_2$ ). However, unlike the decomposition in (4.1.29) which is *required* by stability of  $\tilde{V}$ , this further decomposition is not generic and would correspond to some further tuning in bundle moduli of (4.1.4) in the dual theory.

We are now in a position to answer yet another of our questions. From the form of (4.1.29) it is clear that the *non-Abelian symmetry enhancement is identical*. Once again, on the wall, the four-dimensional gauge symmetry enhances from  $SU(5) \rightarrow SU(6)$ . Furthermore, in this



| Field                        | Cohom.                                      | Multiplicity | Field                        | Cohom.   | Multiplicity |
|------------------------------|---|--------------|------------------------------|--|--------------|
| $\mathbf{1}_{+2}$            | $H^1(\tilde{L} \otimes \tilde{L})$          | 0            | $\mathbf{1}_{-2}$            | $H^1(\tilde{L}^\vee \otimes \tilde{L}^\vee)$   | 10           |
| $\mathbf{15}_0$              | $H^1(\tilde{U}_3^\vee)$                     | 0            | $\overline{\mathbf{15}}_0$   | $H^1(\tilde{U}_3)$                             | 80           |
| $\mathbf{20}_{+1}$           | $H^1(\tilde{L})$                            | 0            | $\mathbf{20}_{-1}$           | $H^1(\tilde{L}^\vee)$                          | 0            |
| $\mathbf{6}_{+1}$            | $H^1(\tilde{L} \otimes \tilde{U}_3)$        | 72           | $\mathbf{6}_{-1}$            | $H^1(\tilde{L}^\vee \otimes \tilde{U}_3)$      | 90           |
| $\overline{\mathbf{6}}_{+1}$ | $H^1(\tilde{L} \otimes \tilde{U}_3^\vee)$   | 0            | $\overline{\mathbf{6}}_{-1}$ | $H^1(\tilde{L}^\vee \otimes \tilde{U}_3^\vee)$ | 2            |
| $\mathbf{1}_0$               | $H^1(\tilde{U}_3 \otimes \tilde{U}_3^\vee)$ | 196          |                              |  |              |

**Table 4.2:** Particle content of the  $SU(6) \times U(1)$  theory associated to the bundle (4.1.20) along its reducible and poly-stable locus  $V = \tilde{L} \oplus \tilde{L}^\vee \oplus \tilde{U}_3$  (i.e. on the stability wall given by (4.1.27) and shown in Figure 4.2).

case the number of Green-Schwarz massive  $U(1)$  symmetries appears to be identical<sup>2</sup>.

To address the final question, that of whether the  $SU(6)$ -charged matter spectra of the theories agree, the cohomology of the reducible bundle in (4.1.20) (equivalently (4.1.29)) can be computed. The results are given in Table 4.2. By inspection, it can be verified that the number of fields in the  $\mathbf{15}$ ,  $\mathbf{20}$ ,  $\mathbf{6}$ , etc representations is identical to the particle content given in Table 4.1. Moreover, the  $U(1)$ -charges under the GS massive  $U(1)$  symmetries are identical and would appear to lead to identical constraints from gauge invariance on the  $\mathcal{N} = 1$  four-dimensional theory!<sup>3</sup>.

Beyond the geometry listed in (4.1.20), there are another 15 target space dual theories in the chain related to (4.1.4). These are listed explicitly in Appendix A and share many of the features of the dual theory described above. In each case we can verify the existence of a stability wall in the new theory and in each case

$$\dim(\tilde{\mathcal{M}}_1) = 427. \quad (4.1.31)$$

<sup>2</sup>Although the Green-Schwarz massive  $U(1)$  symmetry is identical in this example, in general one would not expect that a discrepancy in the number of such symmetries should signal a breakdown of duality. The mass scale of the massive  $U(1)$  symmetries is only just below the compactification scale [17, 18] and care should be taken with how they are included in the effective theories. In general, while the presence of the Green-Schwarz massive  $U(1)$  can affect the structure of the theory (for example in Yukawa textures and the structure of the matter field Kähler potential [86–90]), it should not be expected that the massive  $U(1)$  gauge bosons themselves should be visible in the low-energy effective theory and the difference noted above does not indicate a failure of duality.

<sup>3</sup>It would be illuminating to probe the effect of higher-codimensional loci such as that determined by  $\tilde{U}_3 \rightarrow \mathcal{O}(1, 0, -1) \oplus \tilde{U}_2$  and its effect on Yukawa couplings and compare this with special loci in the moduli space of the target space dual. At the moment however, this is difficult to accomplish without an explicit moduli map between  $(X, V)$  and  $(\tilde{X}, \tilde{V})$ .

However, in 6 out of 16 we find a surprising feature which is that the stability condition forces the theory to the boundary of the Kähler cone. Such a point is a metric singularity and corresponds to a perturbative/non-perturbative duality and will be explored in Section 4.1.4.

### 4.1.3 Branch Structure in the Vacuum Space of the Dual Theories

An intriguing aspect of theories with stability walls is the rich branch structure in the vacuum space of the theories. As described in [17, 18, 24] the distinct branches of the vacuum moduli space near the wall correspond to distinct infinitesimal deformations at the level of the bundle geometry. These walls also provide non-trivial information about discrete symmetries and Yukawa textures in the effective target space theories away from the wall [90, 91].

As a result of this, heterotic theories with stability walls provide a further detailed check of the target space duality correspondence. We have seen in the previous sections that a stability wall in one theory,  $(X, V)$  is reproduced in its target space dual  $(\tilde{X}, \tilde{V})$  and that the charged and singlet matter of the two wall theories matches exactly. In the next sections we briefly explore the branch structures in these two moduli spaces away from the stability walls (i.e. away from the locus of enhanced symmetry). To begin, consider the bundle given in (4.1.4) and its associated  $SU(6) \times U(1)$  theory with the particle spectrum given in Table 4.1.

We will consider deformations away from the stability wall that lead to indecomposable, properly stable, rank 5 vector bundles. Such a deformation of bundle geometry would correspond in the four-dimensional theory to a Higgsing  $SU(6) \rightarrow SU(5)$  of the effective theory along a flat direction. Several such directions can be readily identified. First, there are two non-trivial D-term constraints on the theory corresponding to the Green-Schwarz massive  $U(1)$ , and to the  $U(1)$  associated with  $SU(5) \times U(1) \subset SU(6)$  ( $\mathbf{6} \rightarrow \mathbf{1}_{-5} + \mathbf{5}_{+1}$ ). Note we will take the Vevs of all fields charged under  $SU(5) \subset SU(6)$  to be vanishing.

#### Branches for $(X, V)$

We begin with the geometry in (4.1.4). Taking into account the spectrum of Table 4.1 and adding a second  $U(1)$  charge subscript for the  $U(1) \subset SU(6)$  described above, the D-terms

take the schematic form:

$$D_{GS}^{U(1)} \sim \frac{3}{16} \frac{\epsilon_S \epsilon_R^2 \mu(L^\vee)}{\kappa_4^2 \mathcal{V}} - \frac{1}{2} \left( (-2)|C_{-2,0}|^2 + (+1)|C_{+1,-5}|^2 + (-1)|C_{-1,-5}|^2 + (-1)|C_{-1,+5}|^2 \right), \quad (4.1.32)$$

$$D_{SU(6)}^{U(1)} \sim \frac{1}{2} \left( (-5)|C_{+1,-5}|^2 + (-5)|C_{-1,-5}|^2 + (+5)|C_{-1,+5}|^2 \right). \quad (4.1.33)$$

In the above, sums over multiplicities of each type of term are suppressed and for each category of charged matter field in Table 4.1 we abbreviate  $\sum_i Q_i G_{P\bar{Q}} C_i^P \bar{C}_i^{\bar{Q}} \simeq Q|C|^2$ . In considering the vacuum structure, note that (4.1.33) leads to a condition of the form

$$\langle C_{-1,+5} \rangle^2 \sim \langle C_{-1,-5} \rangle^2 + \langle C_{+1,-5} \rangle^2. \quad (4.1.34)$$

However, it is also clear that substituting this constraint into to (4.1.32) we find that D-flatness requires that

$$\frac{3}{16} \frac{\epsilon_S \epsilon_R^2 \mu(L^\vee)}{\kappa_4^2 \text{Vol}(X)} + \frac{1}{2} \left( \langle C_{-2,0} \rangle^2 + \langle C_{-1,-5} \rangle^2 \right) \sim 0. \quad (4.1.35)$$

Since this involves only matter fields with negative charge under the first (GS massive)  $U(1)$  symmetry, it is clear that *all vacuum solutions breaking  $SU(6) \rightarrow SU(5)$  with  $\langle C \rangle \neq 0$  must involve a non-trivial FI term with  $\mu(L^\vee) < 0$ .*

The indecomposable,  $SU(5)$  bundle corresponding to this deformation will be properly slope-stable only in the region of Kähler moduli space for which  $\mu(L^\vee) < 0$ . This chamber structure is depicted in Figure 4.3.

To describe this bundle as a monad (and hence, build the associated GLSM) we need two facts: 1) the new monad bundle corresponding to this branch of the vacuum space must admit a point in its moduli space for which it can be decomposed as in (4.1.17) and 2) By the results of Section 3.2, if both  $\mathcal{O}(1, -1)$  and  $\mathcal{O}(-1, 1)$  appear in the monad, it cannot be stable in the region shown in Figure 4.3. A useful technical observation is that to accommodate both these facts, it is clear that one of the line bundles  $L$  or  $L^\vee$  must be “replaced” in the monad with an alternate description. To that end, we observe that  $\mathcal{O}(-1, 1)$  itself can be written as a monad:

$$0 \rightarrow L_{new} \rightarrow \mathcal{O}(0, 1)^{\oplus 2} \xrightarrow{g} \mathcal{O}(1, 1) \rightarrow 0. \quad (4.1.36)$$

This monad describes  $L_{new}$  as a rank 1 sheaf given by the kernel of the map  $g$ , with  $c_1(L_{new}) =$

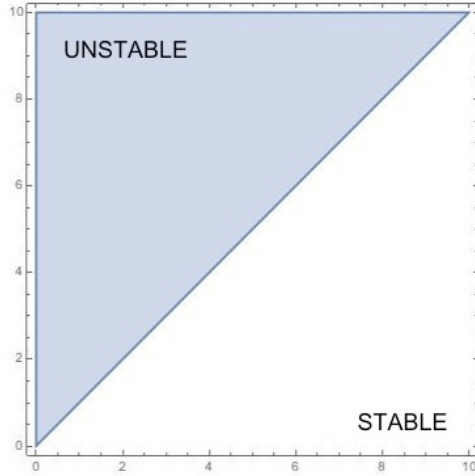


**Figure 4.3:** *The stable sub-cone in Kähler moduli space shown for the  $SU(5)$  monad bundle in (4.1.37). This corresponds to the branch of vacuum space described by (4.1.34) and (4.1.35).*

$-J_1 + J_2$ . Since line bundles on CY 3-folds are classified by their first Chern classes, it remains to show only that (4.1.36) describes a locally free sheaf. To this end, recall that the kernel of a monad sequence defines a locally free sheaf only if the map satisfies the transversality condition described in Section 2.1 (i.e. the condition that the rank of  $g$  does not drop anywhere on  $X$ ). In this case, the map,  $g$ , can be written as a vector of two linear functions of the ambient  $\mathbb{P}^1$  coordinates which manifestly do not vanish simultaneously on  $X$ , thus  $L_{new} \simeq \mathcal{O}(-1, 1)$ .

As a result, the new branch, corresponding to deforming off of the stability wall is given by the following monad:

| $x_i$       | $\Gamma^j$ | $\Lambda^a$        | $p_l$       |
|-------------|------------|--------------------|-------------|
| 1 1 0 0 0 0 | -2         | 1 0 0 0 0 2 1 1 2  | -1 -3 -1 -2 |
| 0 0 1 1 1 1 | -4         | -1 1 1 1 1 1 2 2 2 | -1 -2 -4 -3 |

(4.1.37)

The  $SU(5)$  charged matter spectrum associated to this bundle can be computed directly and is shown in Table 4.3. Note that here

$$h^{1,1}(X) + h^{2,1}(X) + h^1(\text{End}_0(V)) = 2 + 86 + 338 = 426. \quad (4.1.38)$$

In this case *there are no obstructions in moduli* and  $\dim(\mathcal{M}_1) = \dim(\mathcal{M}_0) = 426$  since despite

| Field     | Cohom.                  | Multiplicity | Field                    | Cohom.                 | Multiplicity |
|-----------|-------------------------|--------------|--------------------------|------------------------|--------------|
| <b>1</b>  | $H^1(V \otimes V^\vee)$ | 338          |                          |                        |              |
| <b>10</b> | $H^1(V^\vee)$           | 0            | $\overline{\mathbf{10}}$ | $H^1(V)$               | 80           |
| <b>5</b>  | $H^1(\wedge^2 V)$       | $81 + x$     | $\overline{\mathbf{5}}$  | $H^1(\wedge^2 V^\vee)$ | $1 + x$      |

**Table 4.3:** Particle content of the  $SU(5)$  theory associated to the indecomposable  $SU(5)$  bundle (4.1.37) – the branch of the theory in the stable chamber of Kähler moduli space. See Figure 4.3. The ambiguity (denoted by  $x$ ) in the  $\mathbf{5}, \mathbf{5}$  spectrum arises from its dependence on the monad map in (4.1.37).

the presence of the stability wall forming a sub-chamber of Kähler moduli space, there are still two free degrees of freedom associated to the Kähler moduli. More importantly, the count in Table 4.3 matches exactly with what is expected from the Higgsing in the vacuum analysis above with precisely two degrees of freedom are removed by the D-terms above. This agrees with comparison to (4.1.8) on the branch in moduli space corresponding to  $\langle C \rangle \neq 0$  (i.e. “gluing” the reducible bundle in (4.1.17) back into the irreducible  $SU(5)$  bundle given in (4.1.37)). In addition, in the Higgsing  $SU(6) \rightarrow SU(5)$  a number of  $\mathbf{5}, \mathbf{5}$  pairs can become massive<sup>4</sup>. The exact number depends on the detailed form of the effective potential, for example, the number of non-vanishing couplings of the form

$$\langle 1_{+1,-5} \rangle \mathbf{5}_{0,+4} \mathbf{5}_{-1,+1} \quad \text{and} \quad \langle 1_{-1,-5} \rangle \mathbf{5}_{0,+4} \mathbf{5}_{+1,+1} \quad (4.1.39)$$

induced from the  $\overline{\mathbf{15}}_0 \mathbf{6}_{-1} \mathbf{6}_{+1}$  couplings of the original  $SU(6) \times U(1)$  theory. These moduli-dependent mass terms are realized geometrically in Table 4.3 by the dependence of the  $\mathbf{5}, \mathbf{5}$  spectrum on the monad map.

The fact that we can “see” the complete branch structure of the theory on the stability wall (and off of it) both in terms of the stability and D-term analysis and as monad bundles leads to a complete and clear picture. It only remains to compare these results to those in the target space dual theories.

### Branches for $(\tilde{X}, \tilde{V})$

In the case of the dual geometry in (4.1.20), the symmetry  $SU(6) \times U(1)$  and the charged matter content is precisely identical (see Table 4.2). The only difference arises in the count

<sup>4</sup>We thank J. Gray for useful suggestions on computer algebra methods [92] used in the computation of the particle spectrum in Table 4.3.

of the uncharged singlets  $h^1(\tilde{X}, \tilde{U}_3 \otimes \tilde{U}_3^\vee) = 196$ . Thus, the vacuum structure of the theory under the Higgsing  $SU(6) \rightarrow SU(5)$  is also *manifestly the same*.

As in the previous Section, the vacuum equations, (4.1.34) and (4.1.35) indicate that there will be a solution when  $\mu(\tilde{L}^\vee) < 0$ . It only remains to understand how to geometrically realize this deformation as a monad.

From here, the analysis exactly mirrors that of the previous theory. There is only one branch to the theory leaving the stability wall and breaking  $SU(6) \rightarrow SU(5)$ . As before we can replace one negative entry line bundle in the monad (in this case,  $\mathcal{O}(0, -1, 1)$ ) as

$$0 \rightarrow \tilde{L}_{new} \rightarrow \mathcal{O}(0, 0, 1)^{\oplus 2} \xrightarrow{\tilde{g}} \mathcal{O}(0, 1, 1) \rightarrow 0. \quad (4.1.40)$$

This leads at last to the bundle

| $x_i$           | $\Gamma^j$ | $\Lambda^a$         | $p_l$       |
|-----------------|------------|---------------------|-------------|
| 0 0 0 0 0 0 1 1 | -1 -1      | 0 0 0 1 0 0 0 0 0   | 0 0 0 -1    |
| 1 1 0 0 0 0 0 0 | -2 0       | 1 0 0 0 0 2 1 1 2   | -1 -3 -1 -2 |
| 0 0 1 1 1 1 0 0 | -2 -2      | -1 1 1 -1 1 3 2 2 2 | -1 -2 -4 -3 |

(4.1.41)

The charged matter of this  $SU(5)$  theory matches exactly to that given in Table 4.3. Once again, the only difference arises in the number of uncharged moduli. In this case we find

$$h^{1,1}(\tilde{X}) + h^{2,1}(\tilde{X}) + h^1(\tilde{X}, \text{End}_0(\tilde{V})) = 3 + 55 + 368 = 426, \quad (4.1.42)$$

in agreement with (4.1.38).

This bundle is stable in a three-dimensional chamber of the Kähler cone of  $\tilde{X}$  determined by

$$\mu(\mathcal{O}(0, -1, 1)) < 0 \quad \text{and} \quad \mu(\mathcal{O}(-1, 0, 1)) < 0 \quad \Leftrightarrow \quad s_3 < s_2 \quad \text{and} \quad s_3 < s_1. \quad (4.1.43)$$

This region is shown in Figure 4.4.

With this monad bundle in hand we have formed a complete picture of the local deformation space near the stability wall in both the original theory and its target space dual. It is clear from the above analysis that not only do the loci of enhanced symmetry correspond in the two theories, but their vacuum branch structure is also identical. In the end we have a

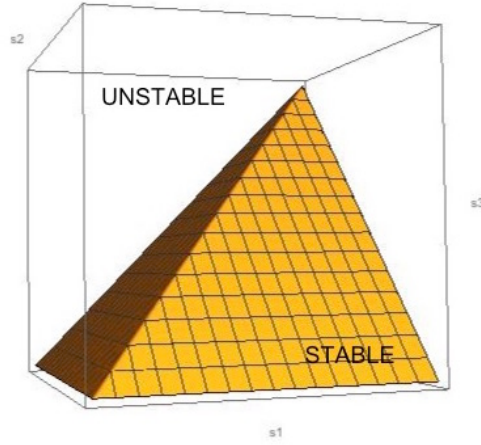


**Figure 4.4:** The stable sub-cone in Kähler moduli space shown for the  $SU(5)$  monad bundle in (4.1.41). This corresponds to the Higgsed branch of the target space dual theory in (4.1.20) and Figure 4.2.

commutative diagram of geometric deformations and target space duals (i.e. “transgressed” [93] geometries):

$$\begin{array}{ccc}
 V_1 & \xrightarrow{\text{dual}} & \tilde{V}_1 \\
 \langle C \rangle \downarrow & & \downarrow \langle \tilde{C} \rangle \\
 V_2 & \xrightarrow{\text{dual}} & \tilde{V}_2
 \end{array} \tag{4.1.44}$$

It can be verified that the deformed manifolds/bundles (labeled as  $V_2$  and  $\tilde{V}_2$  above) given in (4.1.37) and (4.1.41) also form a target space dual pair, as expected. Thus, the correspondence given in (4.1.44) is complete.

#### 4.1.4 Perturbative/Non-perturbative Duality

Of the 17 bundles in the target space dual chain associated to (4.1.4) (see Appendix A), the majority of them exhibit the same essential features seen in the previous example, including: a) new stability walls in the bundle geometry, b) a matching reduction of dimension arising from the associated D-terms, c) Agreement in the degrees of freedom (both charged and uncharged) in the target space effective theory and d) perfect correspondence between the vacuum branch loci near the stability wall as described in (4.1.44).

There are however, several interesting exceptions that arise and we turn to one such now.

The following target space bundle

| $x_i$           | $\Gamma^j$ | $\Lambda^a$        | $p_l$       |
|-----------------|------------|--------------------|-------------|
| 0 0 0 0 0 0 1 1 | -1 -1      | 1 0 0 0 0 0 0 0    | -1 0 0 0    |
| 1 1 0 0 0 0 0 0 | -2 0       | 1 -1 0 0 2 1 1 2 3 | -3 -1 -2 -3 |
| 0 0 1 1 1 1 0 0 | -3 -1      | -2 1 1 1 1 2 2 2 2 | -2 -4 -3 -1 |

(4.1.45)

Once again exhibits a stability wall and shows the exact reduction in Kahler moduli expected by the D-term condition. However, the new feature in this case is that the stability wall is *forced to the boundary of the Kähler cone*. That is, the target space dual leads to a theory that is necessarily at a singular point in moduli space. For the CY 3-fold given in (4.1.45), the Kähler cone is given by the positive octant  $t^a > 0$ ,  $a = 1, 2, 3$  and the D-term condition on the stability wall constrains the Kaähler moduli of  $X$  to

$$t^1 = 0, \quad t^2 \geq 0, \quad t^3 = 2t^2 - 2\sqrt{(t^2)^2} \quad \text{or} \quad t^1 > 0, \quad t^2 = 0, \quad t^3 = \frac{3}{2} \left( t^1 \pm \sqrt{(t^1)^2} \right). \quad (4.1.46)$$

Although the overall volume is still finite when (4.1.46) holds, the presence of small cycles leads us to expect the appearance of non-perturbative physics. Indeed, a closer inspection of (4.1.45) suggests that the metric singularities in  $X$  must play an important role in the effective physics. On the stability wall, the bundle in (4.1.45) splits as

$$V_5 \rightarrow L_1 \oplus L_2 \oplus U_3, \quad (4.1.47)$$

with  $L_1 = \mathcal{O}(1, 1, -2)$ ,  $L_2 = \mathcal{O}(0, -1, 1)$  and  $c_1(U_3) = (-1, 0, 1)$ . The structure group of the bundle on the stability wall is  $S[U(1) \times U(1) \times U(3)]$  which has commutant  $SU(5) \times U(1) \times U(1)$  within  $E_8$ . Thus, this bundle naively does not lead to the same non-Abelian enhancement of symmetry (i.e.  $SU(6)$ ) seen in the initial bundle (4.1.4). This is not wholly unexpected however, since it is well-known that singularities in the base manifold,  $X$ , can force bundles (and more generally small instantons) to exhibit non-Abelian enhancements of symmetry (see for example [94]). We leave a full exploration of this interesting class of examples to further work.



### 4.1.5 Isomorphic Geometry in Target Space Duality

An interesting possibility within the target space duality algorithm includes cases in which the base manifold  $X$  is mapped to an identical or related geometry. As an example, consider the following target space dual to the geometry given in (4.1.4):

| $x_i$           | $\Gamma^j$ | $\Lambda^a$        | $p_l$       |
|-----------------|------------|--------------------|-------------|
| 0 0 0 0 0 0 1 1 | -1 -1      | 1 0 0 0 0 0 0 0 0  | 0 0 -1 0    |
| 1 1 0 0 0 0 0 0 | -1 -1      | 0 -1 0 0 2 1 1 2 2 | -3 -1 -2 -1 |
| 0 0 1 1 1 1 0 0 | -4 0       | -1 1 1 1 1 2 2 2 3 | -2 -4 -3 -3 |

(4.1.48)

It is well known that many CICY threefolds can have redundant descriptions [60] and it is straightforward to verify that the CY threefold given in (4.1.48) is in fact *the same manifold* as the  $\{2, 4\}$  hypersurface in  $\mathbb{P}^1 \times \mathbb{P}^3$  given in (4.1.4) (this is an example of a so-called “ineffective split” [67]). Solving the linear constraint in the defining relation of (4.1.48) leads to  $X \times pt$  with  $X$  defined in (4.1.4). Interestingly, even when  $X = \tilde{X}$  the action on the associated monad bundle is not manifestly trivial. To test whether or not the bundles are also isomorphic, it is possible to employ a useful Lemma (Lemma 3.2.5, Section 3.2) for isomorphisms of stable bundles.

Finally, another quantitatively different possibility can arise which  $X$  and  $\tilde{X}$  are presented as distinct complete intersection manifolds in different ambient products of projective spaces but are “redundant” manifolds from the point of view of their topological data. Wall’s Theorem [95] says that two (simply connected) CY 3-folds which share the same total Chern classes and triple intersection numbers are of the same homotopy type and from the point of view the effective four-dimensional physics, equivalent. For example, the following pair of CY 3-folds have equivalent data in the sense of Wall’s theorem:

$$X_1 = \left[ \begin{array}{c|cc} \mathbb{P}^1 & 1 & 1 \\ \mathbb{P}^1 & 0 & 2 \\ \mathbb{P}^3 & 2 & 2 \end{array} \right], \quad X_2 = \left[ \begin{array}{c|cc} \mathbb{P}^1 & 1 & 1 \\ \mathbb{P}^1 & 1 & 1 \\ \mathbb{P}^3 & 2 & 2 \end{array} \right]. \quad (4.1.49)$$

Both of these manifolds appear in the list of target space duals to (4.1.4) given in Appendix A. Interestingly, the number of bundles appearing over these manifolds in the target space duality procedure can apparently differ (starting with the bundle in (4.1.4) the target space duality algorithm generates 3 bundles over  $X_1$  and 5 over  $X_2$ ). This indicates that the target

space duality procedure probes some properties of the manifolds beyond their topology.

### 4.1.6 On S-Equivalence Classes

Given the strong role played by stability walls in the chain of examples in the previous Sections, it is natural to wonder whether all bundles that “share” a wall must somehow be connected in moduli space? The mathematics associated with this question includes the notion of a so-called “S-equivalence class” [69]. An S-equivalence class is an equivalence class of several bundles, which includes a sum as one bundle in the equivalence class

$$V \rightarrow V_1 \oplus V_2 \oplus \dots \quad (4.1.50)$$

This decomposition on the wall characterizes the physical theory and as we will see below bundles with different S-equivalence classes are generally unconnected in the vacuum space of the  $\mathcal{N} = 1$ , four-dimensional theory. The mathematics of S-equivalence classes and their relationship to stability walls and the decomposition into poly-stable bundles (such as (4.1.17) and (4.1.29)) can be found in Section 3.2.

In this section we provide an example to demonstrate that even for bundles with the same topology and a shared stability wall, there can be disconnected components to the moduli space,  $\mathcal{M}_{bundle}(rk, c_1, c_2, c_3)$  of (semi-) stable bundles with fixed rank and total Chern class.

To illustrate this possibility, consider the following pair of bundles on the bi-cubic hypersurface,  $\{3, 3\}$  in  $\mathbb{P}^2 \times \mathbb{P}^2$ :

| $x_i$       | $\Gamma^j$ | $\Lambda^a$      | $p_l$    |
|-------------|------------|------------------|----------|
| 1 1 1 0 0 0 | -3         | -2 1 1 2 2 2 2 0 | -4 -3 -1 |
| 0 0 0 1 1 1 | -3         | 1 0 1 2 0 0 0 2  | -1 -2 -3 |

(4.1.51)

and

| $x_i$       | $\Gamma^j$ | $\Lambda^a$      | $p_l$    |
|-------------|------------|------------------|----------|
| 1 1 1 0 0 0 | -3         | 2 4 1 0 0 0 0 1  | -4 -3 -1 |
| 0 0 0 1 1 1 | -3         | -1 1 1 1 1 1 2 0 | -1 -2 -3 |

(4.1.52)

The topology for each bundle is identical, both satisfying  $c_2(V) = c_2(TX)$  and  $Ch_3(V) = -63$ . In both cases, the charged matter spectrum is  $h^*(V) = (0, 63, 0, 0)$ . Labeling the bundle in (4.1.51) as  $V_a$  and that in (4.1.52) as  $V_b$ , we see that they are each stable in complementary chambers of Kähler moduli space (determined by whether  $\mu(\mathcal{O}(-2, 1))$  is  $> 0$  or  $< 0$ ). Along the shared stability wall they decompose as

$$V_a \rightarrow \mathcal{O}(-2, 1) \oplus U_a, \quad (4.1.53)$$

$$V_b \rightarrow \mathcal{O}(2, -1) \oplus U_b, \quad (4.1.54)$$

with

$$0 \rightarrow U_a \rightarrow \mathcal{O}(1, 0) \oplus \mathcal{O}(1, 1) \oplus \mathcal{O}(2, 2) \oplus \mathcal{O}(2, 0)^{\oplus 3} \oplus \mathcal{O}(0, 2) \rightarrow \mathcal{O}(4, 1) \oplus \mathcal{O}(3, 2) \oplus \mathcal{O}(1, 3) \rightarrow 0, \quad (4.1.55)$$

$$0 \rightarrow U_b \rightarrow \mathcal{O}(4, 1) \oplus \mathcal{O}(1, 1) \oplus \mathcal{O}(0, 1)^{\oplus 3} \oplus \mathcal{O}(0, 2) \oplus \mathcal{O}(1, 0) \rightarrow \mathcal{O}(4, 1) \oplus \mathcal{O}(3, 2) \oplus \mathcal{O}(1, 3) \rightarrow 0. \quad (4.1.56)$$

Direct calculation yields that for  $V_a$ ,  $H^*(X, \mathcal{O}(-2, 1) \otimes V_a) = (0, 99, 0, 0)$ . Thus, only one possible “direction” of deformation exists to move the bundle away from its reducible locus and off of the stability wall (corresponding to only one sign of charged bundle moduli in (3.1.7), [17, 18]). Furthermore, on the reducible locus,  $Hom(U_a, U_b) = 0$ . Thus, there is no deformation of  $V_a$  can lead to a stable bundle in the region determined by  $V_b$  and the bundles live in different S-equivalence classes.

Just as we saw in Section 4.1.3, where connected branches of moduli space were carried faithfully through the target space duality (see (4.1.44)), it can also be verified that disconnected components of bundle moduli space on  $X$  lead to disconnected components on  $\tilde{X}$ .

For each bundle, there are many possible target space dual theories, but to illustrate that the “disconnected” bundles persist in the dual theories, the following pair is sufficient to illustrate the phenomenon described above.

A target space dual to (4.1.51) is

| $x_i$           | $\Gamma^j$ | $\Lambda^a$      | $p_l$    |
|-----------------|------------|------------------|----------|
| 0 0 0 0 0 0 1 1 | -1 -1      | 0 0 1 0 0 0 0 0  | 0 -1 0   |
| 1 1 1 0 0 0 0 0 | -2 -1      | -2 1 0 2 2 2 3 0 | -4 -3 -1 |
| 0 0 0 1 1 1 0 0 | -1 -2      | 1 0 -1 2 0 0 2 2 | -1 -2 -3 |

(4.1.57)

and the following target space dual to (4.1.52)

| $x_i$           | $\Gamma^j$ | $\Lambda^a$         | $p_l$       |
|-----------------|------------|---------------------|-------------|
| 0 0 0 0 0 0 1 1 | -1 -1      | 0 0 1 0 0 0 0 0 0   | 0 -1 0 0    |
| 1 1 1 0 0 0 0 0 | -2 -1      | 2 4 0 0 0 0 0 1 3   | -4 -3 -1 -2 |
| 0 0 0 1 1 1 0 0 | -1 -2      | -1 1 -1 1 1 1 2 0 2 | -1 -2 -3 0  |

(4.1.58)

Once again, we see that the stability wall structure persists into the target space dual theory and here a similar analysis to that shown above demonstrates that  $\tilde{V}_a$  and  $\tilde{V}_b$  again form a disjoint pair of bundles that share a stability wall.

Finally, a note of caution should be raised that it is possible that seemingly distinct monads can in fact correspond to the same elements of the S-equivalence class:

To see this, consider the following rank 5 bundle defined on the  $\{2, 4\}$  hypersurface in  $\mathbb{P}^1 \times \mathbb{P}^3$ :

| $x_i$       | $\Gamma^j$ | $\Lambda^a$    | $p_l$ |
|-------------|------------|----------------|-------|
| 1 1 0 0 0 0 | -2         | 0 0 0 0 1 1 1  | -1 -2 |
| 0 0 1 1 1 1 | -4         | 1 1 1 2 -1 1 2 | -4 -3 |

(4.1.59)

This bundle shares *identical topology* with the bundle given in (4.1.37) in Section 4.1.3. Moreover it shares a stability wall (given by the condition that  $\mu(\mathcal{O}(1, -1)) = 0$ ) and is stable in the same sub-cone in Kähler moduli space. However, on the stability wall it decomposes as

$$V_5 \rightarrow \mathcal{O}(1, -1) \oplus \mathcal{Q}_4, \quad (4.1.60)$$

where

$$0 \rightarrow \mathcal{Q}_4 \rightarrow \mathcal{O}(0, 1)^{\oplus 3} \oplus \mathcal{O}(0, 2) \oplus \mathcal{O}(1, 1) \oplus \mathcal{O}(1, 2) \rightarrow \mathcal{O}(1, 4) \oplus \mathcal{O}(2, 3) \rightarrow 0. \quad (4.1.61)$$

We can now ask: is this decomposition the same as the one arising on the wall for the  $SU(5)$  bundle given in (4.1.37)? There, the bundle data of (4.1.37) makes it clear that the bundle decomposes as  $V_5 \rightarrow \mathcal{O}(1, -1) \oplus U_4$ , with

$$0 \rightarrow U_4 \rightarrow \mathcal{O}(0, 1)^{\oplus 4} \oplus \mathcal{O}(2, 1) \oplus \mathcal{O}(1, 2)^{\oplus 2} \oplus \mathcal{O}(2, 2) \rightarrow \mathcal{O}(1, 1) \oplus \mathcal{O}(3, 2) \oplus \mathcal{O}(1, 4) \oplus \mathcal{O}(2, 3) \rightarrow 0. \quad (4.1.62)$$

At first pass,  $\mathcal{Q}_4$  and  $U_4$  appear to be different rank 4 monad bundles. However, a direct calculation yields that

$$\dim(\text{Hom}(\mathcal{Q}_4, U_4)) = 1 \quad (4.1.63)$$

and once again it is possible to apply Lemma 3.2.5 in Section 3.2 to determine that these are, in fact, isomorphic stable bundles. Interestingly, the different monad realizations of isomorphic bundles seem in general to lead to new target space dual theories. This effect and the corresponding list of target space dual theories is given in Appendix A.

## 4.2 F-terms, Bundle Holomorphy, and Duality

### 4.2.1 F-terms in the Effective Theory

In this section we will explore examples of  $(0, 2)$  GLSMs with non-trivial F-term contributions to their four-dimensional,  $\mathcal{N} = 1$  potential. At the level of geometry, this corresponds to obstructions to geometric deformations arising from the constraint of bundle holomorphy.

In general, it is exceedingly challenging computationally to calculate directly the Atiyah obstruction (largely due to the difficulty in determining the the class of the Atiyah map  $([F^{1,1}])$  in (3.1.11). To find tractable/computable examples a series of approaches were developed in [17–20]. In particular, one simple way to generate examples employs methods of constructing bundles that *manifestly depend on the complex structure moduli of  $X$* . One such tool is the well-known “jumping” phenomena of bundle-valued cohomology on a CY manifold,  $X$ . This was applied to build examples of monad and extension bundles that presented non-trivial holomorphy obstructions. For a thorough treatment of the deformation theory associated to this idea, see [19]. Here we will briefly review the relevant techniques for monads.

In the case of monad bundles, a simple class of holomorphy obstructions can be realized in

the dependence on  $F_a^l(x^i)$  on the complex structure of  $X$ . In general, elements of  $F_a^l(x^i)$  may be generically zero and only non-vanishing for certain higher co-dimensional sub-loci of complex structure moduli space. Suppose we consider a rank  $n$  monad of the form

$$0 \rightarrow V \rightarrow \mathcal{O}(\mathbf{b}_1) \oplus \dots \oplus \mathcal{O}(\mathbf{b}_{n+1}) \xrightarrow{F} \mathcal{O}(\mathbf{c}) \rightarrow 0 \quad (4.2.1)$$

with the property that a given map element, say  $Hom(\mathcal{O}(\mathbf{b}_1), \mathcal{O}(\mathbf{c}))$  is generically vanishing. That is,

$$h^0(X, \mathcal{O}(\mathbf{c} - \mathbf{b}_1)) = 0. \quad (4.2.2)$$

Such a monad does not define a good, slope stable bundle since in general it will be reducible (since  $\mathcal{O}(\mathbf{b}_1) \in ker(F)$  generically):

$$\mathcal{O}(\mathbf{b}_1) \oplus V'. \quad (4.2.3)$$

Note that in general if  $\mathcal{O}(\mathbf{b}_1)$  is of purely positive or negative degree, then the sum above *cannot* be poly-stable within the Kähler cone. However, on special loci in complex structure moduli space, line bundle cohomology can “jump” to a non-zero value. We will denote this locus as  $\mathcal{CS}_{jump}$ . On that locus,  $h^0(X, \mathcal{O}(\mathbf{c} - \mathbf{b}_1)) \neq 0$  and we find new global holomorphic sections to  $\mathcal{O}(\mathbf{c} - \mathbf{b}_1)$  that can be used to define a stable, holomorphic bundle,  $V = ker(F)$ . As an example, consider the following line bundle on the  $\{2, 4\}$  hypersurface in  $\mathbb{P}^1 \times \mathbb{P}^3$ :

$$h^0(X, \mathcal{O}(-2, 4)) = 0 \quad \text{for generic values of complex structure.} \quad (4.2.4)$$

However, as computed in [19] on a 53-dimensional sub-locus of the 86-dimensional complex structure moduli space, this cohomology can “jump” to

$$\text{On } \mathcal{CS}_{jump}, \quad h^0(X, \mathcal{O}(-2, 4)) = 1. \quad (4.2.5)$$

In the following section, we will make use of this calculation to build a monad bundle with a non-trivial holomorphy obstruction and construct its target space dual theory. Before we begin however, two notes of caution are in order.

First, it should be noted that the inclusion of map elements such as the one above  $F \in H^0(X, \mathcal{O}(-2, 4))$  introduce more dramatic negative charges into the definition of the GLSM than those we previously considered (only negative charges for some  $\Lambda^a$  and all maps,  $F_a^l$  positive in the D-term examples of the previous Sections). This can change the vacuum

structure of the GLSM and care must be taken interpreting these both in the geometric regime and for other phases. For this section, we will consider only examples that we can confirm correspond to good geometric phases (i.e. large volume, perturbative, etc). We leave the important and intriguing question of how many negative degrees can be included<sup>5</sup> in the GLSM to a future publication [96] and focus in this Section only on the well-defined target space theories.

Second, the calculations of holomorphy obstructions in the following sections will be done at the level of the compactification geometry. Caution must be used in describing this reduction in moduli from the naive count in (4.1.6) in the effective theory. In the examples that follow below, the mass scale of the holomorphy obstructions is too high to be included in the effective theory. Instead, the geometric obstructions are directly calculated at the compactification scale (as is done to compute (1.3.5) in the charged matter) and the resulting massless modes (corresponding to the solution of (3.1.11)) are presented. For some steps towards realizing holomorphy obstructions at the level of sigma models, see [97].

As a final comment, it should be noted that compared to the D-term computations of Section 4.1, the holomorphy computations required here are significantly more computationally intensive and introduce a number of difficult problems in geometry/deformation theory. As a result, we focus on one example geometry and leave a broader scan for examples to future work.

We turn now to a simple example of a monad bundle inducing an obstruction in the complex structure of  $X$  and its target space dual.

### 4.2.2 A Simple Example

In this section we will consider a simple vector bundle which was inspired by an example in [19]. This  $SU(3)$  monad bundle:

$$\begin{array}{c|c|c|c}
 & x_i & \Gamma^j & \Lambda^a & p_l \\
 \hline
 1 & 1 & 0 & 0 & 0 & 0 & -2 & 2 & -1 & -1 & 1 & 0 & 0 & -1 \\
 0 & 0 & 1 & 1 & 1 & 1 & -4 & 0 & 2 & 2 & 0 & 2 & -4 & -2
 \end{array} \tag{4.2.6}$$

---

<sup>5</sup>Note this is closely related to the new “generalized complete intersection” (gCICY) method of constructing Calabi-Yau manifolds [98–100].

cannot be defined for generic choices of the complex structure of  $X$  given in (4.2.6). It is clear that by (4.2.4), for generic values of the complex structure the map,  $F$  takes the form

$$F_a^l = \begin{pmatrix} f_{(-2,4)} & f_{(1,2)} & f'_{(1,2)} & f_{(-1,4)} & f_{(0,2)} \\ 0 & f_{(1,0)} & f'_{(1,0)} & f_{(0,2)} & f_{(1,0)} \end{pmatrix} \quad (4.2.7)$$

where  $f_{(a,b)}$  is generic polynomials on  $X$  of multi-degree  $\{a, b\}$ . Of note are the maps with “negative” degree. It is straightforward to verify that on  $X$ ,  $h^0(X, \mathcal{O}(-1, 4)) = 2$  and thus, despite the negative degree this map is an ordinary holomorphic function on  $X$ . In [99] tools were developed to describe such “non-polynomial” functions explicitly. Here we will not require the explicit description of  $f'$  and merely need to know that it is non-trivial.

As noted above however, the map  $f_{(-2,4)}$  is on a different footing since *for generic values of the complex structure*  $h^0(X, \mathcal{O}(-2, 4)) = 0$ . When  $f_{(-2,4)}$  is not available as a non-trivial map, it is clear that this  $F_a^l(x)$  cannot define a good bundle. Here  $V$  is reducible as the sum of a line bundle and rank 2 sheaf:

$$V \sim \mathcal{O}(2, 0) \oplus \mathcal{V} \quad (4.2.8)$$

and *cannot be made poly-stable* in the Kähler cone of  $X$ . Thus, in general, this monad cannot provide a good definition of the background gauge fields in the heterotic theory. However, as shown in [19] and using (4.2.5), on the 53-dimensional sub-locus of complex structure moduli space, there is a new map element available given by  $f_{(-2,4)} \in H^0(X, \mathcal{O}(-2, 4))$ . Once again, despite the negative degree in the line bundle, for the chosen complex structure this is an ordinary, global, holomorphic section to  $\mathcal{O}(-2, 4)$  on  $X$ . Thus on the locus  $\mathcal{CS}_{jump}$ , it is possible to define a stable, *indecomposable* monad,  $V$ . We will begin there and use this example to construct a target space dual.

We have chosen this example because of its simplicity and the fact that the difficult computational exercise of computing  $\mathcal{CS}_{jump}$  and the associated Atiyah calculation was already completed in [19]. However, it should be noted that the monad given above does not satisfy the anomaly cancellation condition alone since  $c_2(V) = \{16, 32\}$ . This can be remedied by choosing to “complete” this example with another monad bundle. We will embed this second



bundle into the second  $E_8$  factor. One such good  $SU(3)$  bundle is

| $x_i$       | $\Gamma^j$ | $\Lambda^a$ | $p_l$ |
|-------------|------------|-------------|-------|
| 1 1 0 0 0 0 | -2         | 1 0 0 0 0   | -1 0  |
| 0 0 1 1 1 1 | -4         | 0 1 1 1 1   | -2 -2 |

(4.2.9)

with  $c_2(V) = \{8, 12\}$  as required so that

$$c_2(V_{total}) = c_2(V_1) + c_2(V_2) = c_2(TX). \quad (4.2.10)$$

With this addition, the full four-dimensional theory has gauge symmetry  $E_6 \times E_6$ .

In what follows the bundle in (4.2.9) plays a trivial, spectating role and thus, we will recall that it must be included, but it will not be central to our further analysis. Focusing first on the rank 3 bundle in (4.2.6), naive moduli count associated to the first  $SU(3)$  bundle and the CY manifold would have produced

$$\dim(\mathcal{M}_0) = h^{1,1} + h^{2,1} + h^1(X, \text{End}_0(V)) = 2 + 86 + 92 = 180. \quad (4.2.11)$$

However, taking into account the constraint that the complex structure lies within the “jumping locus” in order for the bundle to be well-defined we have

$$\dim(\mathcal{M}_1) = \dim(\mathcal{M}_0) - 33 = 147. \quad (4.2.12)$$

See [19] for a discussion of the relationship between this jumping cohomology calculation and the Atiyah obstruction. To complete the degree of freedom count, we note that for  $V$  in (4.2.6) the charged matter is

$$h^1(X, V) = 41 \quad (\text{no. of } \mathbf{27}), \quad (4.2.13)$$

$$h^1(X, V^\vee) = 1 \quad (\text{no. of } \overline{\mathbf{27}}). \quad (4.2.14)$$

For completeness, the spectrum of the second  $E_6$  factor consists of 12  $\mathbf{27}$ s (and no  $\overline{\mathbf{27}}$ s) and 38 singlets.

Finally, one last interesting note about this geometry: despite the negative line bundle entry ( $\mathcal{O}(-1, 2)$ ) in (4.2.6), the  $SU(3)$  bundle presented there is stable throughout the *entire* Kähler cone since  $\mu(\mathcal{O}(-1, 2)) < 0$  for all Kähler moduli,  $t^r$ , on  $X$ . Thus, there is no stability wall

and no non-trivial D-term anywhere in the moduli space of this theory.

With these calculations in hand, we turn finally to the target space dual theory. Once again, we can ask the relevant questions of the duality:

- Is a holomorphy obstruction in  $(X, V)$  reflected in some (deformation theoretic) obstruction in  $(\tilde{X}, \tilde{V})$ ?
- Since in general the dimensions of  $h^{2,1}(X)$  and  $h^{2,1}(\tilde{X})$  (and any Atiyah obstructions within these spaces) are different, is the final set of zero modes the same in each theory?

We will address these questions in turn in the following Section.

### 4.2.3 The Target Space Dual

The target space dual is easy to construct for the rank 3 bundle given in (4.2.6). We obtain

| $x_i$           | $\Gamma^j$ | $\Lambda^a$ | $p_l$ |          |
|-----------------|------------|-------------|-------|----------|
| 0 0 0 0 0 0 1 1 | -1 -1      | 0 1 0 0 0   | -1 0  | (4.2.15) |
| 1 1 0 0 0 0 0 0 | -1 -1      | 2 -2 0 1 0  | 0 -1  |          |
| 0 0 1 1 1 1 0 0 | -2 -2      | 0 0 4 0 2   | -4 -2 |          |

The new CY manifold,  $\tilde{X}$  has Hodge numbers  $h^{1,1} = 3$  and  $h^{2,1} = 55$ .

Now, to answer the first question in our list, we can ask whether the bundle in (4.2.15) provides any obvious obstruction to holomorphy? By inspection, the answer is immediately yes! We see that in fact, the map  $\tilde{F}_a^l(x)$  associated to  $\tilde{V}$  takes the form

$$\tilde{F}_a^l = \begin{pmatrix} f_{(1,-2,4)} & f_{(0,2,4)} & f_{(1,0,0)} & f_{(-1,1,4)} & 0 \\ 0 & f_{(-1,3,2)} & 0 & f_{(0,0,2)} & f_{(0,1,0)} \end{pmatrix}. \quad (4.2.16)$$

All the map entries above are generically non-vanishing polynomials of the given degree with the exception of  $\tilde{F}_1^1$  of degree  $(1, -2, 4)$ . As expected, the line bundle cohomology associated to this

$$h^0(\tilde{X}, \mathcal{O}(1, -2, 4)) = 0 \quad \text{for generic values of the complex structure,} \quad (4.2.17)$$

but once again, *on a higher co-dimensional locus in complex structure moduli space, which can be labeled  $\widetilde{\mathcal{C}S}_{jump}$ ,  $h^0(\widetilde{X}, \mathcal{O}(1, -2, 4)) = 1$* . Once again, it is possible to define a good, indecomposable rank 3 monad bundle, but only by tuning the complex structure moduli of the CY manifold. In this case, the locus has dimension

$$\dim(\widetilde{\mathcal{C}S}_{jump}) = 37. \quad (4.2.18)$$

That is, the jumping of the relevant monad map fixes 18 of the 55 complex structure moduli of  $\widetilde{X}$ . The initial moduli count for this bundle is then

$$\dim(\widetilde{\mathcal{M}}_0) = 3 + 55 + 122 = 180. \quad (4.2.19)$$

With the obvious constraint above this reduces the total to  $\dim(\widetilde{\mathcal{M}}_0) - 18 = 162$ . Moreover, the charged matter of the  $E_6$  theory is identical to that in (4.2.13):

$$h^1(\widetilde{X}, \widetilde{V}) = 41 \quad (\text{no. of } \mathbf{27}), \quad (4.2.20)$$

$$h^1(\widetilde{X}, \widetilde{V}^\vee) = 1 \quad (\text{no. of } \overline{\mathbf{27}}). \quad (4.2.21)$$

This is almost in agreement with the final singlet count of 147 in the original geometry in (4.2.12). We are left however, with an apparent discrepancy of 15 moduli. Could these too be lifted from the count for  $(\widetilde{X}, \widetilde{V})$ ? There are two hints that this is indeed the case.

The first is that the lengthy calculation of  $h^1(\widetilde{X}, \text{End}_0(\widetilde{V})) = 122$  in (4.2.19) was performed by taking all induced monad maps in  $\widetilde{V} \otimes \widetilde{V}^\vee$  to be generic (a necessary computational simplification). However, it is clear that for the special bundle at hand a more detailed calculation is necessary. Two hints at this structure are significant.

First, the line bundle  $\mathcal{O}(0, -2, 4)$  appears in the calculation of  $h^1(\widetilde{X}, \text{End}_0(\widetilde{V}))$  (corresponding to morphisms of the form  $\text{Hom}(\widetilde{B}, \widetilde{B})$ ). As for the similar line bundle on  $X$ , generically this has no global sections. However, if we further tune the complex structure of  $\widetilde{X}$  to make  $h^0(\widetilde{X}, \mathcal{O}(0, -2, 4))$  jump to a non-zero value, this fixes exactly 15 additional moduli<sup>6</sup>. Such a choice might be expected in comparison with the original pair  $(X, V)$  since it is exactly these additional moduli that “pass through” the conifold transition connecting  $X$  and  $\widetilde{X}$  and are in some sense “shared” between the CY manifolds. See [20] for results on how jumping loci

---

<sup>6</sup>This can be verified using the tools of [19, 20].

$(\mathcal{CS}_{jump})$  are fixed across conifold transitions.

Finally, as another hint for where the moduli fixing may arise, it should be noted that unlike the starting geometry, the bundle in (4.2.15) *does display a stability wall in Kähler moduli space*. In general, the bundle is stable for the three-dimensional sub-cone of Kähler moduli space determined by

$$0 < t^1 \quad , \quad 2t^1 < t^2 \quad , \quad 0 < t^3 < 2t^2 - 4t^1. \quad (4.2.22)$$

On the two-dimensional stability wall given by  $t^3 = 2t^2 - 4t^1$  and  $2t^1 < t^2$  the bundle decomposes as

$$\mathcal{O}(1, -2, 0) \oplus \tilde{U}_2, \quad (4.2.23)$$

with

$$0 \rightarrow \tilde{U}_2 \rightarrow \mathcal{O}(0, 2, 0) \oplus \mathcal{O}(0, 0, 4) \oplus \mathcal{O}(0, 1, 0) \oplus \mathcal{O}(0, 0, 2) \rightarrow \mathcal{O}(1, 0, 4) \oplus \mathcal{O}(0, 1, 2) \rightarrow 0. \quad (4.2.24)$$

At this locus the bundle decomposes as  $SU(3) \rightarrow S[U(1) \times U(2)]$  and the full matter spectrum is charged under the Green-Schwarz anomalous  $U(1)$  symmetry as in Section 4.1. Of interest to us are the 123 singlets corresponding to bundle moduli:

$$C_{+3} \quad h^1(\tilde{X}, \tilde{L}^\vee \otimes \tilde{U}_2) = 68, \quad (4.2.25)$$

$$C_{-3} \quad h^1(\tilde{X}, \tilde{L} \otimes \tilde{U}_2^\vee) = 10, \quad (4.2.26)$$

$$C_0 \quad h^1(\tilde{X}, \tilde{U}_2 \otimes \tilde{U}_2^\vee) = 45, \quad (4.2.27)$$

with  $\tilde{L} = \mathcal{O}(1, -2, 0)$ . In this description it is clear that the form of  $U_2$ , itself and the number of fields  $C_0$  depends on the choice complex structure of  $\tilde{X}$ . Moreover, this description makes it clear that additional bundle moduli can acquire a mass. Near the stability wall, one origin for such mass terms is evident from the fact that there are allowed, gauge-invariant trilinear couplings in the superpotential of the form

$$W \sim C_0 C_{+3} C_{-3}. \quad (4.2.28)$$

By leaving the stability wall with  $\langle C_{\pm 3} \rangle \neq 0$ , it is clear that mass terms can be generated for singlets which could lift degrees of freedom, including the significant 15 moduli above. We leave a detailed analysis of the bundle moduli of (4.2.15) and the computation of trilinear couplings such as (4.2.28) for future work.

To complete this example, it should be noted that as before, another bundle in the second  $E_8$  factor is necessary to satisfy anomaly cancellation and the bundle in (4.2.9) trivially carries through the target space duality procedure.

| $x_i$           | $\Gamma^j$ | $\Lambda^a$ | $p_l$ |
|-----------------|------------|-------------|-------|
| 0 0 0 0 0 0 1 1 | -1 -1      | 0 0 0 0 0   | 0 0   |
| 1 1 0 0 0 0 0 0 | -1 -1      | 1 0 0 0 0   | -1 0  |
| 0 0 1 1 1 1 0 0 | -2 -2      | 0 1 1 1 1   | -2 -2 |

(4.2.29)

The charged and singlet matter spectrum for this bundle is identical to that associated to (4.2.9).

In summary then, we have found that F-term obstructions are non-trivially preserved across this target space dual pair and correspond to a sensitive inter-mixing of complex structure and bundle moduli which are non-trivially redefined across the duality.

### 4.3 Target Space Duality, (2, 2) Loci, and Tangent Bundle Deformations

Having seen that loci of enhanced symmetry (i.e. stability walls, etc) were reflected in the target space duals in previous sections, it is natural to investigate whether or not another special locus is preserved – namely, the (2, 2) locus of a (0, 2) theory. Such a locus – realized in the geometric regime by GLSMs in which  $V$  is a deformation of the holomorphic tangent bundle of the CY base manifold,  $X$  – play a crucial role in the study of (0, 2) GLSMs. In this section, we will provide examples of starting GLSMs with a (2, 2) locus and explore the structure of their target space duals.

To begin, we consider perhaps the simplest case available: the rank-changing deformation of the holomorphic tangent bundle to the quintic hypersurface in  $\mathbb{P}^4$ . The following  $SU(4)$  bundle is a non-trivial deformation of  $\mathcal{O}_X \oplus TX$  on the quintic:

| $x_i$     | $\Gamma^j$ | $\Lambda^a$ | $p_l$ |
|-----------|------------|-------------|-------|
| 1 1 1 1 1 | -5         | 1 1 1 1 1   | -5    |

(4.3.1)

Indeed, this  $V_4$  is in fact the most general slope-stable, rank 4 deformation of this type and

the entire local moduli space of deformations can be captured in the moduli of the monad (see [101]). Writing the bundle,  $V_4$ , as

$$0 \rightarrow V \rightarrow \mathcal{O}(1)^{\oplus 5} \xrightarrow{f} \mathcal{O}(5) \rightarrow 0, \quad (4.3.2)$$

the locus in bundle moduli space for which it decomposes as  $\mathcal{O}_X \oplus TX$  is given by

$$f = dP_5, \quad (4.3.3)$$

where  $P_5$  is the homogeneous, degree 5 defining relation of the quintic in  $\mathbb{P}^4$ .

An application of the tangent space duality procedure can produce the following geometry, including a new manifold  $\tilde{X}$  which is related to the quintic via a conifold transition:

| $x_i$         | $\Gamma^j$ | $\Lambda^a$ | $p_l$ |         |
|---------------|------------|-------------|-------|---------|
| 1 1 0 0 0 0 0 | -1 -1      | 1 0 0 0 0 0 | -1 0  | (4.3.4) |
| 0 0 1 1 1 1 1 | -4 -1      | 0 5 1 1 1 1 | -5 -4 |         |

As required by the target space duality algorithm, this bundle leads to the same effective theory as the original geometry in (4.3.1). In particular, it is clear that the chiral index (the difference between  $\mathbf{16}$  and  $\overline{\mathbf{16}}$  representations in the target space  $SO(10)$  theory) is given by

$$Ch_3(\tilde{V}) = -100 \quad (4.3.5)$$

as required by our starting point of  $V = TX$  on the quintic.

However, this fact leads immediately to the observation that this bundle *cannot be a standard deformation of  $T\tilde{X}$* , since for the new manifold<sup>7</sup> in (4.3.4)

$$Ch_3(T\tilde{X}) = -84. \quad (4.3.6)$$

This result is clearly a general feature of the target space duality procedure. Starting from a bundle near the (2, 2) locus on  $X$ , the algorithm produces a bundle with  $ch_2(\tilde{V}) = ch_2(T\tilde{X})$  but with  $ch_3(\tilde{V}) \neq ch_3(T\tilde{X})$ , as required by the  $\mathcal{N} = 1$ , four-dimensional effective theories being identical.

---

<sup>7</sup>This difference in index is precisely arising from the classic conifold transition between  $X$  and  $\tilde{X}$  – the difference corresponding to resolving the 16 singular points on the nodal quintic [102].

If however, the target space dual is really isomorphic in some deeper sense (as a (0, 2) sigma model), it is natural to expect that the (2, 2) locus should still somehow be present. One possibility is that the only deformations leading to the (2, 2) locus in the dual geometry of (4.3.4) force the theory to a non-perturbative regime. A candidate for such a possibility might be the singular shared locus in the moduli space of  $X$  and  $\tilde{X}$ . Since the two CY 3-folds are related by a conifold transition [102], their common locus in moduli space is given by a nodal quintic of the form

$$P_5 = l_1(x)q_2(x) - l_2(x)q_1(x) = 0, \tag{4.3.7}$$

where  $l_i(x)$  and  $q_i(x)$  are linear and quartic polynomials, respectively, in the homogeneous coordinates of  $\mathbb{P}^4$  (and the CY 3-fold in (4.3.4) is the resolution of this singular variety).

A second possibility is that even at general points in complex structure moduli space, the bundle given in (4.3.4) is deformable to the holomorphic tangent bundle through some more general, chirality changing transition. Such possibilities have been previously conjectured in the heterotic literature [103], though explicit geometric realizations have yet to be fully understood (see [104] for some recent, related results). It would be intriguing to explore the geometry of such transitions further in this context.

To conclude, we provide one interesting hint towards the behavior of (2, 2) loci under the duality. A useful observation is that it is possible for some target space duals to lead to a new vector bundle on *an isomorphic CY threefold*. To illustrate this, consider the following rank 5 deformation of the tangent bundle  $TX$  of the  $\{2, 4\}$  hypersurface in  $\mathbb{P}^1 \times \mathbb{P}^3$ :

| $x_i$       | $\Gamma^j$ | $\Lambda^a$ | $p_l$ |         |
|-------------|------------|-------------|-------|---------|
| 1 1 0 0 0 0 | -2         | 1 1 0 0 0 0 | -2    | (4.3.8) |
| 0 0 1 1 1 1 | -4         | 0 0 1 1 1 1 | -4    |         |

The bundle above is a stable deformation of  $TX \oplus \mathcal{O}_X \oplus \mathcal{O}_X$ . This starting point admits a target space dual in which the original manifold appears in a redundant CICY description (achieved by adding the repeated entry  $\mathcal{O}(1, 4)$ ):

| $x_i$           | $\Gamma^j$ | $\Lambda^a$   | $p_l$ |
|-----------------|------------|---------------|-------|
| 0 0 0 0 0 0 1 1 | -1 -1      | 1 0 0 0 0 0 0 | -1 0  |
| 1 1 0 0 0 0 0 0 | -1 -1      | 0 1 0 0 0 0 2 | -2 -1 |
| 0 0 1 1 1 1 0 0 | -4 0       | 0 0 1 1 1 1 4 | -4 -4 |

(4.3.9)

As described in Section 4.1.5, this target space dual exhibits a particularly interesting structure because it has left the CY 3-fold unchanged. As argued in Section 4.1.5, this threefold is equivalent to  $X$  in (4.3.8) times a point. Despite the fact that the manifold has not changed, this example is not trivial however, since the vector bundles given in (4.3.8) and (4.3.9) are not obviously the same, nor is their apparent dependence on the complex structure of  $X = \tilde{X}$ .

To clarify things, it can be noted that although there are three divisors restricted from the ambient hyperplanes in (4.3.9), these divisors are linearly dependent and  $h^{1,1}(\tilde{X}) = 2$ . Furthermore, a simple exploration of linear equivalence of divisors shows that  $\mathcal{O}(a, b, c)$  on  $\tilde{X}$  in (4.3.9) is the same line bundle as  $\mathcal{O}(a+b, c)$  on the threefold in (4.3.8) for any integers,  $a, b, c \in \mathbb{Z}$ . With this observation it is possible to re-write the dual theory in (4.3.9) as

| $x_i$       | $\Gamma^j$ | $\Lambda^a$   | $p_l$ |
|-------------|------------|---------------|-------|
| 1 1 0 0 0 0 | -2         | 1 1 0 0 0 0 2 | -3 -1 |
| 0 0 1 1 1 1 | -4         | 0 0 1 1 1 1 4 | -4 -4 |

(4.3.10)

which is the same manifold  $X$  with an apparently distinct monad bundle  $\tilde{V}$ . Now we can ask the question: are the bundles on  $X$  given in (4.3.8) and (4.3.10) equivalent? To answer this puzzle it is possible to appeal to a useful lemma which establishes when two stable bundles on  $X$  can be identified (see Lemmas 3.2.5 and 3.2.5 in Section 3.2). Briefly, the lemma states if there exists a non-trivial map (in  $Hom(V, \tilde{V})$ ) between two stable bundles on  $X$  with the same slope,  $\mu(V)$ , then they are isomorphic. In this case, a direct calculation leads to

$$\dim(Hom(V, \tilde{V})) = h^0(X, V \otimes \tilde{V}^\vee) = 1. \quad (4.3.11)$$

Thus, the naively distinct monads given in (4.3.8) and (4.3.10) are in fact equivalent stable,



#### 4.3. TARGET SPACE DUALITY, $(\mathbf{2}, \mathbf{2})$ LOCI, AND TANGENT BUNDLE DEFORMATIONS 79

holomorphic vector bundles, complete with the same  $(2, 2)$  locus (though the locus is clearly most easily realized in the first description). Thus in this simple case, the  $(2, 2)$  locus is preserved in the target space dual, though in a subtle way.

# Chapter 5

## Inducing a Duality in F-theory

In this chapter we will review the heterotic/F-theory duality, as well as some tools on finding the dual F-theory model of a specific heterotic model. This chapter of review work is taken from our previous paper [49].

### 5.1 Essential Tools for Heterotic/F-theory Duality

In type IIB superstring theory, the axion-dilaton transforms under  $SL(2, Z)$  while leaving the action invariant. However, it is frequently assumed the string coupling  $g_s$  vanishes and the backreaction from 7-branes is ignored. As a result, many important non-perturbative aspects of the string compactification which are crucial both conceptually and phenomenologically, are missing. This is exactly where F-theory arises as a proper description of orientifold IIB theory with  $(p, q)$  7-branes and varying finite string coupling (i.e. axion-dilaton). The classical  $SL(2, Z)$  self-dual symmetry of Type IIB theory acting on the axion-dilaton is identified as the modular group of a one complex dimensional torus  $T^2$  and as the complex structure of a fictitious elliptic curve. In this way, we formally attach an elliptic curve at each point of the type IIB space time and promote the ten-dimensional IIB theory to auxiliary twelve-dimensional F-theory. This structure defines a genus-one or elliptic fibration. The locus where the fiber degenerates is where the 7-brane is wrapped in the internal CY. F-theory realizes a remarkable synthesis of geometry and field theory in that the structure of the 7-branes/gauge sector, matter content and Yukawa couplings are all encoded in the geometry of the fibration structure and the back-reaction of these branes is taken into account.

There is no description of F-theory as a fundamental theory, but rather, as duals to other theories. A concrete example would be an eight-dimensional duality [16] i.e, F-theory compactified on  $K3$  is dual to type IIB on  $S^2$  with 24 7-branes turned on, which is also dual to heterotic on  $T^2$ . The duality between F-theory and heterotic is described further as F-

theory compactified on  $K3$  fibered Calabi-Yau  $(n+1)$ -fold is dual to  $E_8 \times E_8$  heterotic string compactified on Calabi-Yau  $n$ -fold which is elliptically fibered on the same  $(n-1)$ -fold base:

- Heterotic:  $\pi_h : X_n \xrightarrow{\mathbb{E}} B_{n-1}$  elliptic fibration,
- F-theory:  $\pi_f : Y_{n+1} \xrightarrow{K3} B_{n-1}$  where  $\rho_f : Y_{n+1} \xrightarrow{\mathbb{E}} B_n$ ,  $\sigma_f : B_n \xrightarrow{\mathbb{P}^1} B_{n-1}$ .

The geometries given above involve both  $K3$  and elliptic fibered manifolds. Specifically, in the F-theory geometry,  $Y_{n+1}$  must be both  $K3$  and elliptically fibered. This requirement implies that  $Y_{n+1}$  is elliptically fibered over a complex  $n$ -dimensional base  $B_n$ , which is  $\mathbb{P}^1$  fibered over a complex  $(n-1)$ -dimensional base  $B_{n-1}$ . If there exists a section in any two of the fibrations structures, then it's guaranteed that there exists a section in the third fibration structure (i.e. if  $\rho_f$  and  $\sigma_f$  both admit sections then so does the fibration  $\pi_f$ ).

With different number of  $n$ 's, there are theories in different dimensions. Specifically,  $n = 1, 2, 3$  will lead to eight dimensions, six dimensions, and four dimensions respectively. When  $n = 1$ , the  $(n-1)$ -fold base  $B_{n-1}$  is a point, when  $n = 2$  it is a  $\mathbb{P}^1$ . In four dimensions case, the duality can be written as:

$$\begin{array}{ccc} Y_4 & \xrightarrow{\mathbb{E}} & B_3 \\ K3 \downarrow & & \downarrow \mathbb{P}^1 \\ B_2 & \xrightarrow{=} & B_2 \end{array} \quad (5.1.1)$$

By the fibration structure of the CY 4-fold (5.1.1), the base  $B_3$  must be  $\mathbb{P}^1$ -fibered. As in [54], such a  $\mathbb{P}^1$  bundle can be defined as the projectivization of two line bundles,

$$B_3 = \mathbb{P}(\mathcal{O} \oplus \mathcal{L}) , \quad (5.1.2)$$

where  $\mathcal{O}$  is the trivial bundle and  $\mathcal{L}$  is a general line bundle on  $B_2$ . In this case the topology of  $B_3$  is completely fixed by the choice of line bundle  $\mathcal{L}$  and we can defined a  $(1, 1)$ -form on  $B_2$  as  $T = c_1(\mathcal{L})$ . A special case would be  $R = c_1(\mathcal{O}(1))$  where  $\mathcal{O}(1)$  is a bundle that restricts to the usual  $\mathcal{O}(1)$  on each  $\mathbb{P}^1$  fiber. They satisfy the relation  $R(R+T) = 0$  in cohomology class, which indicates the two corresponding sections don't intersect to each other. This kind of twist allows us to matching the degrees of freedom in the four-dimensional heterotic/F-theory dual pairs.

In the  $E_8 \times E_8$  heterotic side, the vector bundle can be decomposed as  $V = V_1 \oplus V_2$ , and the

curvature splits as

$$c_2(V) = \frac{1}{30} \text{Tr} F_i^2 = \eta_i \wedge \sigma + \xi_i, \quad (5.1.3)$$

where  $\eta_i, \xi_i$  are pullback of 2-forms and 4-forms on  $B_2$ ,  $\sigma$  is the Poincare dual to the section of the elliptic fibration  $\pi_h : X_3 \xrightarrow{\mathbb{E}} B_2$ . For any CY 3-fold in Weierstrass form as described above,  $c_2(TX_3) = 12c_1(B_2) \wedge \omega_0 + (c_2(B_2) + 11c_1(B_2)^2)$  [54]. The heterotic Bianchi identity requires  $\eta_1 + \eta_2 = 12c_1(B_2)$ , which enable us to parameterize a solution as

$$\eta_{1,2} = 6c_1(B_2) \pm T', \quad (5.1.4)$$

where  $T'$  is a (1,1) form on  $B_2$ . By studying the four-dimensional effective theories of these dual heterotic/F-theory compactifications, the defining (1, 1)-forms  $T, T'$  are identical to each other  $T = T'$ . Here  $T$  is referred to as the “twist” of the  $\mathbb{P}^1$ -fibration and is the crucial defining data in the simplest classes of heterotic/F-theory dual pairs. Moreover, this duality map depends on a particular way of constructing Mumford poly-stable vector bundles, which is called the spectral cover construction.

## 5.2 Spectral Cover Construction

To find the dual F-theory model of a specific Heterotic model, we need a description of the moduli space of stable degree zero vector bundles over elliptically fibered manifolds, (the standard formulation works for Weierstrass fibration, but it can be generalized to other types of elliptic fibrations) in terms of two “pieces,” which are called spectral data. This can be done by Fourier-Mukai transform, and we briefly review it in the following. (Fourier-Mukai is an important type of functor between derived categories, but to avoid unnecessary technicalities, we only restrict ourselves to the following special type defined by the Poincare bundle, and ignore general discussions. Interested readers can refer to [105, 106].)<sup>1</sup>

Fourier-Mukai transforms take stable bundles of degree zero and rank  $n$  over  $X$ , and give a torsion sheaf (rank 0) of degree  $n$  over the (compactified) Jacobian fibration  $\tilde{X} \sim X$ . More precisely, consider the following fiber product, and the natural projections,

---

<sup>1</sup>Please note that we restrict ourselves to  $SU(N)$  (degree zero, and stable) vector bundles over a Weierstrass elliptic fibration.

$$\begin{array}{ccccc}
 & & X \times_B \tilde{X} & & \\
 & \swarrow \pi_1 & \downarrow \rho & \searrow \pi_2 & \\
 X & & B & & \tilde{X}
 \end{array}$$

then FM transform is defined as <sup>2</sup>,

$$FM^1(V) = \mathbf{R}^1\pi_{2*}(\pi_1^*V \otimes \mathcal{P}^*). \quad (5.2.1)$$

We emphasize again(compactified) Jacobian of irreducible elliptic curves are isomorphic to the elliptic curve, therefore in the Weierstrass fibration we have  $X \sim \tilde{X}$ . In (5.2.1)  $\mathcal{P}$  is the Poincare bundle,

$$\mathcal{P} = \mathcal{O}(\Delta - \sigma_1 \times \tilde{X} - X \times \sigma_2) \otimes \rho^*\mathcal{K}_B, \quad (5.2.2)$$

where  $\Delta$  is the diagonal divisor in  $X \times_B \tilde{X}$ ,  $\sigma_1$  and  $\sigma_2$  are section of the first and second factor respectively.  $R^1\pi_*$  is the first derived pushforward. Roughly speaking, the presheaf corresponding to  $R\pi_*\mathcal{F}$  over an open set  $U$  is isomorphic to  $H^1(\pi^{-1}U, \mathcal{F})$  (look at [107] III.1 and [108]). Note that the restriction of stable and degree zero vector bundles over generic fibers will be a semistable bundle with degree zero and the same rank [109]. Then, a well known theorem proved by Atiyah<sup>3</sup> [110] tells us the the general form of restriction of the vector bundle over a generic smooth elliptic curve  $E$ ,

$$\begin{aligned}
 V|_E &= \bigoplus_i \mathcal{E}_i \otimes \mathcal{O}_E(p_i - \sigma), \\
 \sum_i \text{rank}(\mathcal{E}_i) \times p_i &= 0,
 \end{aligned} \quad (5.2.3)$$

The second condition is imposed because of the ‘‘S’’ of the  $SU(N)$  gauge group (note that the sum is over the group law of the elliptic curve), and  $\mathcal{E}_i$  is constructed inductively by

<sup>2</sup>In some sense it is similar to the notion of a Fourier transform. In that case one starts with a function  $f(x)$  defined in a space  $X$ , then we pull back the function into a larger space  $X \times Y$ , multiply by a kernel  $e^{ix \cdot y}$  and integrate over  $x$  to get a function in  $Y$ . The pushforward action is similar to the integration over the fibers

<sup>3</sup>Intuitively, one can argue that to construct a non trivial flat bundle over a torus the only way is to embed the fundamental group of the torus inside the Lie group, i.e. turn on the Wilson lines.

extending with trivial bundle,

$$0 \rightarrow \mathcal{O}_E \rightarrow \mathcal{E}_i \rightarrow \mathcal{E}_{i-1} \rightarrow 0. \quad (5.2.4)$$

Therefore using (5.2.3), it's easy to show that the stalk of the Fourier-Mukai transform of  $V$  over some generic point  $p \in \tilde{X}$  takes the following form (the isomorphism can be proved by a the final theorem in [107] III.12),

$$FM^1(V)_p \sim H^1(E_p, \bigoplus_i \mathcal{E}_i \otimes \mathcal{O}_E(p_i - p)). \quad (5.2.5)$$

It's clear that (5.2.5) is non-zero only at point  $p$  that are coincident with one of the points  $p_i$ . To see this consider the  $\mathcal{E}_2$ . By definition we have

$$0 \rightarrow \mathcal{O}_E \rightarrow \mathcal{E}_2 \rightarrow \mathcal{O}_E \rightarrow 0. \quad (5.2.6)$$

If we multiply the whole sequence with  $\mathcal{O}_E(p_i - p)$ , the first cohomology of  $\mathcal{E}_2 \otimes \mathcal{O}(p_i - p)$  will be zero, since  $\mathcal{O}(p_i - p)$  is a line bundle over the elliptic curve corresponding to a degree zero, but non effective divisor (so it doesn't have global section, and by Riemann-Roch, trivial first cohomology). By induction we can get similar conclusions for a general  $\mathcal{E}_i$  in (5.2.3)

Therefore the Fourier-Mukai sheaf  $FM^1(V)$  is supported on a  $n$ -sheeted cover of the base  $\mathcal{S}$  (possibly a non-reduced and/or reducible scheme), which is called a spectral cover. To be more clear consider a special case of (5.2.3),

$$V|_E = \bigoplus_{i=1}^n \mathcal{O}(p_i - \sigma),$$

such that the points  $p_i$  are all different. In fact every semistable bundle over  $E$  is  $\mathcal{S}$ -equivalent to the direct sum written above. In this situation  $\mathcal{S}$  is a non degenerate surface (i.e. non reduced as a scheme), and by (5.2.5) rank of the Fourier-Mukai sheaf when restricted over  $\mathcal{S}$  is one. Therefore the Fourier-Mukai transform of the vector bundle is described by an  $n$ -sheeted cover of the base  $\mathcal{S}$ , and a sheaf (called the spectral sheaf) over that, which if  $\mathcal{S}$  is non degenerate, the restriction of the spectral sheaf will be a line bundle  $\mathcal{L}$  over  $\mathcal{S}$ .<sup>4</sup>

---

<sup>4</sup>More precisely the rank of the spectral sheaf over the modified support (a scheme defined by 0th Fitting

The next question is how the vector bundle can be reconstructed from the spectral data described above. This can be done by using the inverse “functor”, which simply is,

$$V = \pi_{1*}(\pi_2^* FM^1(V) \otimes \mathcal{P}). \quad (5.2.7)$$

The final point is that, technically, Fourier-Mukai is the equivalence of the derived category of coherent sheaves on  $X$  and derived category coherent sheaves on  $\tilde{X}$  (at least when  $X$  and  $\tilde{X}$  are smooth). It roughly means that, Fourier-Mukai transform gives a “one to one” relation between the “space of stable vector bundles  $V$ ” and the “ $(\mathcal{S}, \mathcal{L})$ .” The logic is that the latter seems easier to study rather than the original bundles.

In principle, it is possible to find the F-theory dual by using the spectral data. We review this briefly in the following. Suppose we have two vector bundles  $(V_1, V_2)$  over a Weierstrass elliptically fibered manifold  $X$  (suppose there are no NS5 branes), then heterotic anomaly cancellation requires,

$$c_2(V_1) + c_2(V_2) = c_2(X).$$

Then second Chern classes (which can be computed by Grothendieck-Riemann-Roch, if we have the spectral data [54]), can be written generally as,

$$\begin{aligned} c_2(V_i) &= \sigma\eta_i + \omega_i, \\ \eta_i &= 6C_1(B_H) \pm T, \end{aligned} \quad (5.2.8)$$

where  $\eta_i$  is a divisor in the base  $(B_H)$ , and  $\omega_i$  is the intersection of two divisor in  $B_H$ . Now, the first statement about the Heterotic and F-theory duality is that the topology of the F-theory geometry is fixed by the “twist”  $T$  in (5.2.8) as,

---

ideal [106] is one. For example is the support is defined as  $z^2 = 0$ , rank of the spectral sheaf over the topological support,  $z = 0$  locus, is 2, but over the modified support, which roughly looks two copies of  $z = 0$  infinitesimally close to each other, the rank of the sheaf is one

$$B_F = \mathbb{P}(\mathcal{O}_{B_H} \oplus \mathcal{O}_B(T)). \quad (5.2.9)$$

The second statement is that the complex structure of  $\mathcal{S}$ , (partially) fix the complex structure of the Calabi-Yau in the F-theory side. It's easier to describe this with an example. Suppose we have a  $SU(2)$  bundle  $V$ , and it's spectral cover is non degenerate,

$$S = a_0 z^2 + a_2 x. \quad (5.2.10)$$

Since one of the  $E_8$  factors breaks to  $E_7$ , we should have an  $E_7$  singularity in the F-theory geometry, which is described by the following Weierstrass equation,

$$\begin{aligned} Y^2 &= X^3 + F(u, z)x + G(u, z), \\ F &= \sum_{i=1}^8 F_i(z)u^i, \\ G &= \sum_{i=1}^{12} G_i(z)u^i, \end{aligned} \quad (5.2.11)$$

where  $u$  is the affine coordinate of the  $\mathbb{P}^1$  fiber of (5.2.9), and  $z$  is the “collective” coordinate for  $B_H$ . Now, the conjectured duality tells us the corresponding  $E_7$  singularity should be located near  $u = 0$ , therefore  $F_0 = F_1 = F_2 = 0$ , and  $G_0 = \dots = G_4 = 0$ . Also  $a_0$  is identified with  $G_5$ , and  $a_2$  with  $F_3$ .

The other vector bundle (which is embedded in the other  $E_8$  factor) determines the singularity near  $u \rightarrow \infty$ , and higher polynomials ( $F_5, \dots$  and  $G_7 \dots$ ) are determined by the spectral cover of that vector bundle (which we didn't write here). The middle polynomials  $F_4$  and  $G_6$  are determined by the Heterotic Weierstrass equation.

The last piece of data which is remained is the spectral sheaf  $\mathcal{L}$ , which is an element of the Picard group  $Pic(S)$ . The “space of line bundles” itself is made by two pieces, the “discrete” part  $H^{1,1}(S)$ , and the “continuous” part which is  $J(S)$  (space of degree zero (flat) line bundles),

$$0 \rightarrow J(S) \rightarrow Pic(S) \rightarrow H_{\mathbb{Z}}^{1,1}(S) \rightarrow 0. \quad (5.2.12)$$

In six-dimensional theories, the discrete part can be fixed uniquely by using Fourier-Mukai transform, and the Jacobian of the curve is mapped to the intermediate Jacobian of the



Calabi-Yau threefold in F-theory. In type IIA or M-theory language, the “space of three forms”,  $H^3(X, \mathbb{R})/H^3(X, \mathbb{Z})$ , is described by intermediate Jacobian [54, 111, 112].

The situation in four-dimensional theories are even more complicated. In such cases, it is possible to have non trivial 4-form fluxes which can be introduced in various (equivalent) ways. One way is to define as 4-form induced by the field strength of the 3-form in M-theory limit. Another way is to define as a (1,1)-form flux over the 7-branes wrapping the divisors in the base times another (1,1)-form localized around the 7-brane locus [113, 114]. In general, the 4-flux data is parameterized by the Deligne cohomology (see the lectures [115], and references therein)

$$0 \rightarrow J^2(\hat{X}_4) \rightarrow H_D^4(\hat{X}_4, \mathbb{Z}(2)) \rightarrow H_{\mathbb{Z}}^{2,2}(\hat{X}_4) \rightarrow 0, \quad (5.2.13)$$

where  $\hat{X}_4$  is the resolved geometry in M-theory limit,  $J^2$  is the intermediate Jacobian,

$$J^2(\hat{X}_4) = H^3(\hat{X}_4, \mathbb{C})/(H^{3,0}(\hat{X}) \oplus H^{2,1}(\hat{X}_4)), \quad (5.2.14)$$

which corresponds to the space of flat 3-forms in M theory .The third, and most difficult part, of the Heterotic F-theory duality, is that continuous part of the spectral sheaf data,  $J(S)$  maps to  $J^2(X_4)$ , and discrete part,  $H^{1,1}(S)$  (which is determined by the divisor class (first Chern class) of the spectral line bundle), maps to the discrete part of the 4-flux data  $H^{2,2}(X)$ .

# Chapter 6

## Target Space Duality in Heterotic/F-theory Duality

This chapter contains the main results as appeared in our paper [49]. Here we will provide several heterotic TSD pairs which both halves of the geometry exhibit Calabi-Yau threefolds with elliptic fibrations. For these examples, we will study their behavior in F-theory, specifically, whether they come from the same F-theory with multiple fibrations.

### 6.1 A Target Space Dual Pair with Elliptically Fibered Calabi-Yau Threefolds

Before we can begin to investigate the consequences of  $(0, 2)$  target space duality for F-theory, a non-trivial first step is to establish if examples exist in which both halves of a TSD pair in turn lead to F-theory dual geometries. In this section we explicitly provide a first example of such a pair.

In the following example, we will find that the CY manifolds,  $X$  and  $\tilde{X}$ , consist of two complete intersection Calabi-Yau 3-folds (so-called “CICYs” [60, 67]), each of which is fibered over (a different) complex surface  $B_2$ . These two CICY 3-folds are related by a conifold transition [67] and can be constructed via the target space duality algorithm in which an additional  $U(1)$  symmetry is added to the dual GLSM as in Section 2.

#### 6.1.1 A Tangent Bundle Deformation

To investigate these results, a simple starting point is given below – a dual pair for which the Calabi-Yau manifolds,  $X$  and  $\tilde{X}$ , are related by a conifold transition. Consider the following

CICY 3-fold, described by a so-called “configuration matrix” [67]

$$X = \left[ \begin{array}{c|cc} \mathbb{P}^1 & 1 & 1 \\ \mathbb{P}^2 & 1 & 2 \\ \mathbb{P}^2 & 1 & 2 \end{array} \right]. \quad (6.1.1)$$

Here the columns indicate the ambient space (a product of complex projective spaces) and the degrees of the defining equations in that space. The Hodge numbers are  $h^{1,1}(X) = 3$  and  $h^{2,1}(X) = 60$ . Over this manifold, we choose a simple vector bundle built as a deformation of the holomorphic tangent bundle to  $X$ . In the present case we will choose this bundle to be a rank 6 smoothing deformation of the reducible bundle

$$V_{red} = \mathcal{O}^{\oplus 3} \oplus TX. \quad (6.1.2)$$

The smooth, indecomposable bundle will be defined<sup>1</sup> as a kernel  $V \equiv \ker(F_a^l)$  via the short exact sequence

$$0 \rightarrow V \rightarrow \bigoplus_{a=1}^{\delta} \mathcal{O}_{\mathcal{M}}(N_a) \xrightarrow{F_a^l} \bigoplus_{l=1}^{\gamma} \mathcal{O}_{\mathcal{M}}(M_l) \rightarrow 0, \quad (6.1.3)$$

which is the simple case of (2.1.7) when  $E_i^a = 0$ .

In the language of GLSM charge matrices, the manifold and rank 6 monad bundle  $(X, V)$  are given by the following charge matrix:

| $x_i$           | $\Gamma^j$ | $\Lambda^a$     | $p_l$ |         |
|-----------------|------------|-----------------|-------|---------|
| 1 1 0 0 0 0 0 0 | -1 -1      | 1 1 0 0 0 0 0 0 | -1 -1 | (6.1.4) |
| 0 0 1 1 1 0 0 0 | -1 -2      | 0 0 1 1 1 0 0 0 | -1 -2 |         |
| 0 0 0 0 0 1 1 1 | -1 -2      | 0 0 0 0 0 1 1 1 | -1 -2 |         |

The reason that this rank 6 bundle makes for a particularly simple choice of gauge bundle is that in this case the GLSM charges associated to the manifold and the bundle are identical (as can be seen above). As a result, anomaly cancellation conditions such as the requirement that

$$c_2(TX) = c_2(V) \quad (6.1.5)$$

(realized as (2.1.2) in the GLSM) are automatically satisfied.

---

<sup>1</sup>See [28] for discussions of this deformation problem and local moduli space.

Expanding the second Chern class of the manifold in a basis of  $\{1, 1\}$  forms  $J_r$ ,  $r = 1, \dots, h^{1,1}$  we have

$$c_2(TX) = 3J_1J_2 + J_2^2 + 3J_1J_3 + 5J_2J_3 + J_3^2. \quad (6.1.6)$$

Following the standard  $(0, 2)$  target space duality procedure, it is easy to produce the TSD geometry  $(\tilde{X}, \tilde{V})$ . In this case, the duals we consider mix all three types of heterotic geometry moduli and induce an additional  $U(1)$  gauge symmetry in the GLSM. As an intermediate step we form the equivalent GLSM charge matrix with an additional  $U(1)$  outlined in Section 2 (choosing  $\mathcal{B} = 0$ ) and introduce a repeated entry in the monad bundle charges which does not change either the geometry of GLSM field theory<sup>2</sup> This leads us to the following charge matrix with a new  $\mathbb{P}^1$  row and a new column  $\Gamma^{\mathcal{B}}$  as in (2.2.13):

| $x_i$               | $\Gamma^j$ | $\Lambda^a$       | $p_l$    |
|---------------------|------------|-------------------|----------|
| 1 1 0 0 0 0 0 0 0 0 | 0 -1 -1    | 1 1 0 0 0 0 0 0 1 | -1 -1 -1 |
| 0 0 1 1 1 0 0 0 0 0 | 0 -1 -2    | 0 0 1 1 1 0 0 0 2 | -1 -2 -2 |
| 0 0 0 0 0 1 1 1 0 0 | 0 -1 -2    | 0 0 0 0 0 1 1 1 1 | -1 -2 -1 |
| 0 0 0 0 0 0 0 0 1 1 | -1 0 0     | 0 0 0 0 0 0 0 0 0 | 0 -1 0   |

(6.1.7)

Finally, we can perform the field redefinitions in this intermediate geometry to obtain the final TSD. Here we choose two map elements – in this case,  $F_8^2$  and  $F_9^2$  – to be interchanged with a defining relation  $G_2$  with degree  $\|S_2\| = \{1, 2, 2\}$ . Such a choice satisfies the linear anomaly cancelation (2.2.11) since  $\|S_2\| + \mathbf{0} = \|F_8^2\| + \|F_9^2\|$ . In the intermediate configuration, applying the field redefinitions (2.2.12) gives:

$$\tilde{N}_8 = M_2 - S_2 = 0, \quad \tilde{N}_9 = M_2, \quad \tilde{S}_2 := F_9^2, \quad \tilde{\mathcal{B}} := F_8^2. \quad (6.1.8)$$

This leads us at last to the dual charge matrix associated to  $(\tilde{X}, \tilde{V})$  with  $h^{1,1}(\tilde{X}) = 4$  and  $h^{2,1}(\tilde{X}) = 60$ :

| $x_i$               | $\Gamma^j$ | $\Lambda^a$       | $p_l$    |
|---------------------|------------|-------------------|----------|
| 1 1 0 0 0 0 0 0 0 0 | 0 -1 -1    | 1 1 0 0 0 0 0 0 1 | -1 -1 -1 |
| 0 0 1 1 1 0 0 0 0 0 | 0 -1 -2    | 0 0 1 1 1 0 0 0 2 | -1 -2 -2 |
| 0 0 0 0 0 1 1 1 0 0 | -1 -1 -1   | 0 0 0 0 0 1 1 0 2 | -1 -2 -1 |
| 0 0 0 0 0 0 0 0 1 1 | -1 0 -1    | 0 0 0 0 0 0 0 1 0 | 0 -1 0   |

(6.1.9)

Again, in the new configurations the anomaly cancellation condition are satisfied (as was

<sup>2</sup>See [31] for details of this argument.

proved in general to happen in [31]). To make sure they are true target space duals, we will show that these two different geometric phases preserve the net multiplicities of charged matter, and the total number of massless gauge singlets, while the individual number of complex, Kähler and bundle moduli are changed. First, it is clear that the low-energy gauge group  $G$  in the four-dimensional gauge theory is given by the commutant of the structure group,  $H$  in  $E_8 \times E_8$  of the bundles defined over the CY manifold. Here there is only one bundle (saturating the anomaly cancellation condition on  $c_2(V)$ ). We choose to embed this structure group into one of the two  $E_8$  factors and considering the other  $E_8$  factor as an unbroken, hidden sector gauge symmetry.

In order to find the matter field representations, the adjoint **248** of  $E_8$  must be decomposed under the subgroup  $G \times H$ . In the present case, the rank 6 bundles with  $c_1 = 0$  indicates the structure group  $H = SU(6)$ , which leads the charged matter spectrum can be determined by the decomposition of  $E_8$  into representations of the maximal subgroup  $SU(2) \times SU(3) \times SU(6)$ :

$$\mathbf{248}_{E_8} \rightarrow [(\mathbf{3}, \mathbf{1}, \mathbf{1}) \oplus (\mathbf{1}, \mathbf{8}, \mathbf{1}) \oplus (\mathbf{1}, \mathbf{1}, \mathbf{35}) \oplus (\mathbf{1}, \mathbf{3}, \overline{\mathbf{15}}) \oplus (\mathbf{1}, \overline{\mathbf{3}}, \mathbf{15}) \oplus (\mathbf{2}, \mathbf{3}, \mathbf{6}) \oplus (\overline{\mathbf{2}}, \overline{\mathbf{3}}, \overline{\mathbf{6}}) \oplus (\mathbf{2}, \mathbf{1}, \mathbf{20})]. \quad (6.1.10)$$

As a result, the multiplicity of fields in the four-dimensional theory transforming in representations of  $SU(2) \times SU(3)$  is counted by those transforming in an  $SU(6)$  representation over the CY. The latter are counted by the dimension of bundle valued cohomology groups,  $H^*(X, \wedge^k V)$ , for assorted values of  $k$  (see [116, 117] for details).

It is helpful to note that for a vector bundle  $V$ , on a Calabi-Yau 3-fold,  $X$ , the cohomology groups of the bundle and its dual are related by Serre duality as  $H^i(X, V) = H^{3-i}(X, V^*)^*$  and when  $H = SU(n)$ ,  $H^*(X, \wedge^k V) \simeq H^*(X, \wedge^{n-k} V^*)$ . Finally, a necessary condition for  $\mu$ -stability of the vector bundle  $V$  is  $h^0(X, V) = 0$  which is satisfied for tangent bundle deformations considered here (by direct computation).

With these observations in hand, the multiplicity of the charged chiral matter spectrum of these dual pair theories can be determined by computing corresponding vector bundle valued

cohomology classes on the Calabi-Yau 3-fold:

$$\begin{aligned}
(\mathbf{2}, \mathbf{3})'_s &: & h^1(V) &= 57, & h^1(\tilde{V}) &= 57, \\
(\bar{\mathbf{2}}, \bar{\mathbf{3}})'_s &: & h^1(V^*) &= 0, & h^1(\tilde{V}^*) &= 0, \\
(\mathbf{1}, \mathbf{3})'_s &: & h^1(\wedge^2 V) &= 115, & h^1(\wedge^2 \tilde{V}) &= 115, \\
(\mathbf{1}, \bar{\mathbf{3}})'_s &: & h^1(\wedge^2 V^*) &= 1, & h^1(\wedge^2 \tilde{V}^*) &= 1, \\
(\mathbf{2}, \mathbf{1})'_s &: & h^1(\wedge^3 V) &= 2, & h^1(\wedge^3 \tilde{V}) &= 2.
\end{aligned} \tag{6.1.11}$$

Furthermore, the low-energy theory has massless gauge singlets,  $(\mathbf{1}, \mathbf{1})$ , which are counted by  $h^1(V \otimes V^*) = h^1(\text{End}_0(V))$ . There are additional singlets, beyond those related to the complex structure and Kähler deformations of the Calabi-Yau 3-fold, which are counted by  $h^{2,1}(X)$  and  $h^{1,1}(X)$ . The total number of singlet moduli are counted by:

$$\begin{aligned}
h^{1,1}(X) + h^{2,1}(X) + h^1(\text{End}_0(V)) &= 3 + 60 + 292 = 355, \\
h^{1,1}(\tilde{X}) + h^{2,1}(\tilde{X}) + h^1(\text{End}_0(\tilde{V})) &= 4 + 53 + 298 = 355.
\end{aligned} \tag{6.1.12}$$

From the point of view of the massless heterotic spectrum, it is clear that in the theories associated to the TSD geometries,  $(X, V)$  and  $(\tilde{X}, \tilde{V})$ , all the degree of freedom appear to match.

Moreover, we have chosen this pair of geometries to have a further special property. Each CY 3-fold appearing in the dual pair exhibits an elliptic fibration structure. As a result, by the arguments laid out in Section 2, we expect each heterotic background in the pair to lead to its own F-theory dual.

A closer inspection yields the following elliptic fibration structures:

$$\pi_h : X \xrightarrow{\mathbb{E}} \mathbb{P}^2 \quad \text{and} \quad \tilde{\pi}_h : \tilde{X} \xrightarrow{\mathbb{E}} dP_1. \tag{6.1.13}$$

The fibrations of  $X$  and  $\tilde{X}$  can be seen very explicitly from the form of the complete intersection descriptions of the manifolds (so-called ‘‘obvious’’ fibrations [118]). Below we use

dotted lines to separate the “base” and “fiber” of the manifold:

$$X = \left[ \begin{array}{c|cc} \mathbb{P}^1 & 1 & 1 \\ \mathbb{P}^2 & 1 & 2 \\ \hline \mathbb{P}^2 & 1 & 2 \end{array} \right], \quad \tilde{X} = \left[ \begin{array}{c|ccc} \mathbb{P}^1 & 0 & 1 & 1 \\ \mathbb{P}^2 & 0 & 1 & 2 \\ \hline \mathbb{P}^2 & 1 & 1 & 1 \\ \mathbb{P}^1 & 1 & 0 & 1 \end{array} \right], \quad (6.1.14)$$

where the base for the elliptically fibered  $X$  is  $B_2 = \mathbb{P}^2$  (the bottom row of the configuration matrix) while the  $dP_1$  base for  $\tilde{X}$  is given as  $\tilde{B}_2 = \left[ \begin{array}{c|c} \mathbb{P}^2 & 1 \\ \hline \mathbb{P}^1 & 1 \end{array} \right]$ .

Employing the techniques of [119, 120], we find that the fibrations in both  $X$  and  $\tilde{X}$  in fact admit rational sections and as a result are elliptically fibered (as opposed to genus-one fibered only). Moreover, each fibration contains two rational sections (i.e. a higher rank Mordell-Weil group). In an abuse of notation, we will use  $\sigma_i$  to denote both the two sections to the elliptic fibration of  $X$  (respectively  $\tilde{X}$ ) and the associated Kähler forms dual to the divisors. In terms of the basis of the Kähler  $(1, 1)$ -forms  $J_r$  inherited from the ambient space factors  $\mathbb{P}_r^n$  of each CICY 3-fold:

$$\begin{aligned} \sigma_1(X) &= -J_1 + J_2 + J_3, & \sigma_2(X) &= 2J_1 - J_2 + 5J_3, \\ \sigma_1(\tilde{X}) &= -J_1 + J_2 + J_3, & \sigma_2(\tilde{X}) &= 2J_1 - J_2 + 4J_3 + J_4. \end{aligned} \quad (6.1.15)$$

With a choice of zero section for each manifold from the set above, the CY 3-fold can in principle be put into Weierstrass form [121, 122]. For explicit techniques to carry out this process we refer the reader to [119].

In summary then, we have produced an explicit example of a TSD pair in which both sides are elliptically fibered manifolds, admitting four-dimensional,  $\mathcal{N} = 1$  F-theory duals in principle. This is an important point of principle, since we have demonstrated that *some* F-theory correspondence should exist for the dual F-theory EFTs. In practice however, it should be noted that explicitly determining the F-theory duals for the geometries given above is difficult. We will begin untangling this process explicitly in Section 5.

For now we close this example by observing an interesting feature of the TSD pair above: Since we began with a deformation of the tangent bundle, the associated  $(0, 2)$  GLSM admits a  $(2, 2)$  locus. However, in the TSD geometry the bundle we obtain is no longer manifestly a holomorphic deformation of the tangent bundle on  $\tilde{X}$ . It remains an open question whether

this second theory admits a  $(2, 2)$  locus in some subtle way. For the moment, we will turn to one further TSD pair in which neither vector bundle is related to the tangent bundle.

### 6.1.2 More General Vector Bundles

Here we present a second example in which the same CY manifolds appear, but with different vector bundles. Once again, we start with the GLSM charge matrix determining the pair  $(X, V)$  as in (6.1.16) where in this time we have a rank 4 bundle with structure group  $SU(4)$ :

| $x_i$           | $\Gamma^j$ | $\Lambda^a$ | $p_l$ |
|-----------------|------------|-------------|-------|
| 1 1 0 0 0 0 0 0 | -1 -1      | 1 0 0 0 0 1 | -1 -1 |
| 0 0 1 1 1 0 0 0 | -1 -2      | 0 1 1 0 0 2 | -2 -2 |
| 0 0 0 0 0 1 1 1 | -1 -2      | 0 0 0 1 1 1 | -2 -1 |

(6.1.16)

In this case, the second Chern class of  $(X, V)$  is different from (6.1.6):

$$c_2(V) = 2J_1J_2 + J_2^2 + 2J_1J_3 + 4J_2J_3 + J_3^2. \quad (6.1.17)$$

However, in this case,  $c_2(V) \leq c_2(TX)$  and thus it is expected that this bundle could be embedded into one factor of the  $E_8 \times E_8$  heterotic string, where another bundle  $V'$  is embedded into the second factor. By completing the geometry in this way, with  $c_2(V) + c_2(V') = c_2(TX)$ , the anomaly cancellation conditions can be satisfied (alternatively, NS5/M5 branes might be considered).

Following the standard procedure described above, the target space duality data is given by  $(\tilde{X}, \tilde{V})$  with the following charge matrix:

| $x_i$             | $\Gamma^j$ | $\Lambda^a$ | $p_l$ |
|-------------------|------------|-------------|-------|
| 1 1 0 0 0 0 0 0 0 | 0 -1 -1    | 1 0 0 0 0 1 | -1 -1 |
| 0 0 1 1 1 0 0 0 0 | 0 -1 -2    | 0 1 1 0 0 2 | -2 -2 |
| 0 0 0 0 0 1 1 1 0 | -1 -1 -1   | 0 0 0 1 0 2 | -2 -1 |
| 0 0 0 0 0 0 0 0 1 | -1 0 -1    | 0 0 0 0 1 0 | -1 0  |

(6.1.18)

Here the second chern classes of the tangent bundle and the monad vector bundle are re-



spectively:

$$\begin{aligned} c_2(TX) &= 3J_1J_2 + J_2^2 + 2J_1J_3 + 3J_2J_3 + J_1J_4 + 2J_2J_4 + 2J_3J_4, \\ c_2(V) &= 2J_1J_2 + J_2^2 + J_1J_3 + 2J_2J_3 + J_1J_4 + 2J_2J_4 + 2J_3J_4, \end{aligned} \quad (6.1.19)$$

which could also satisfy the  $c_2$  matching condition with the addition of a hidden sector bundle.

In this background, the bundle structure group of  $H = SU(4)$  breaks  $E_8$  to  $SO(10)$ . As above, the charged matter content can be determined by the decomposition under  $SO(10) \times SU(4)$ :

$$248_{E_8} \rightarrow (\mathbf{1}, \mathbf{15}) \oplus (\mathbf{10}, \mathbf{6}) \oplus (\overline{\mathbf{16}}, \overline{\mathbf{4}}) \oplus (\mathbf{16}, \mathbf{4}) \oplus (\mathbf{45}, \mathbf{1}). \quad (6.1.20)$$

The multiplicity of the spectrum is then determined via bundle-valued cohomology as:

$$\begin{aligned} \mathbf{16}'_s : \quad & h^1(V) = 48, & h^1(\tilde{V}) &= 48, \\ \overline{\mathbf{16}}'_s : \quad & h^1(V^*) = 0, & h^1(\tilde{V}^*) &= 0, \\ \mathbf{10}'_s : \quad & h^1(\wedge^2 V) = 0, & h^1(\wedge^2 \tilde{V}) &= 0. \end{aligned} \quad (6.1.21)$$

Furthermore, the counting of the gauge singlets appearing in this TSD pair match as well:

$$\begin{aligned} h^{1,1}(X) + h^{2,1}(X) + h^1(\text{End}_0(V)) &= 3 + 60 + 159 = 222, \\ h^{1,1}(\tilde{X}) + h^{2,1}(\tilde{X}) + h^1(\text{End}_0(\tilde{V})) &= 4 + 53 + 165 = 222. \end{aligned} \quad (6.1.22)$$

With these two examples in hand, it is clear that at least the first question outlined in Section 1.5.2 can be answered in the positive. *Heterotic TSD pairs can indeed be found in which both halves of the dual pair exhibit elliptic fibrations.* However, it is clear that the manifolds in our examples above are not in simple Weierstrass form (and exhibit higher rank Mordell-Weil group) as a result, their F-theory dual geometries may be difficult to determine using standard tools.

## 6.2 Warm Up: Heterotic/F-theory Duality in Six Dimensions

In this section, we'll begin in earnest the process of attempting to determine the induced duality in F-theory given by TSD and whether the multiple fibrations conjecture outlined in previous sections could be a viable realization. In this simpler context both the geometry of the F-theory compactification as well as the process of reparameterizing (i.e. performing a FM-transform) of the heterotic data are more readily accomplished.

To begin, it should be noted that in the context of heterotic target space duals we will consider smooth geometries (i.e. smooth bundles over  $K3$  manifolds) in the large volume, perturbative limit of the theory. We will consider solutions without NS 5-branes so that the six-dimensional theory exhibits a single tensor multiple (associated to the heterotic dilaton) (see [123] for a review). Within the context of six-dimensional F-theory EFTs with a single tensor and a heterotic dual it is clear that we must restrict ourselves to CY 3-folds that are elliptically fibered over Hirzebruch surfaces:

$$\pi_f : Y_3 \rightarrow \mathbb{F}_n \tag{6.2.1}$$

with  $n \leq 12$  [52, 124].

It is our goal in this section to test the multiple fibrations conjecture in the context of target space duality. At the level of GLSMs TSD in heterotic compactifications on  $K3$  works mechanically exactly as in the case of CY 3-folds. However, the associated geometry is dramatically simpler. It is clear that the two TSD GLSMs will parameterize at best two different descriptions of a  $K3$  surface and that the process must by construction preserve the second chern class of the vector bundle  $V$  over  $K3$  (see [31] for a proof valid for either CY 2- or 3-folds). Since the massless spectrum of the six-dimensional heterotic theory compactified on a smooth  $K3$  is entirely determined by the rank and second Chern class of  $V$  (see e.g. [53])<sup>3</sup>, it is clear that TSD is only a simple re-writing of the same geometry and six-dimensional EFT.

However, there remains something interesting to compare to in that it can still be asked: *Does the concrete process of heterotic TSD duality in six dimensions correspond to exchanging*

---

<sup>3</sup>The moduli space of stable sheaves over  $K3$  with fixed Chern character has only one component.

*K3 fibrations in the dual F-theory geometry?* In the context of F-theory 3-folds that are elliptically fibered over a Hirzebruch surface as described above, there is in fact only one geometry where multiple  $K3$  fibrations can arise. It was established in the very first papers on F-theory [52, 124], that in order to have different  $K3$  fibrations within a CY threefold with a perturbative heterotic dual, the base twofold must be  $F_0$ . Indeed, the remarkable observation of Morrison and Vafa was that the existence of two  $K3$  fibrations in  $\pi_f : Y_3 \rightarrow \mathbb{F}_0$  (only a simple relabeling in F-theory) was dual to a highly non-perturbative heterotic/heterotic duality discovered by Duff, Minasian and Witten [125].

With these observations in mind, we can immediately make several observations. To begin, we must recall that a base manifold for the F-theory fibration of  $\mathbb{F}_n$  in this context is correlated to bundles with  $c_2 = 12 \pm n$  in the  $E_8 \times E_8$  heterotic dual. Thus

- For any purely perturbative heterotic TSD pair in six dimensions with  $c_2(V) = c_2(\tilde{V}) \neq 12$ ,  $(0, 2)$  TSD *cannot correspond to multiple fibrations in F-theory* (since as described above, such multiple  $K3$  fibrations arise only for  $n = 0$ ).
- With the point above, we have established that in general the multiple fibrations conjecture outlined in introduction the *must be false in general* at least in the six-dimensional heterotic theories.
- This demonstrates that not all TSD pairs can be described by F-theory multiple fibrations, but the converse question, namely – *can multiple fibrations in F-theory give rise to dual heterotic TSD pairs?* – in principle remains open.

Thus, in this section we chose to look at this last point in closer detail by considering an example TSD pair over  $K3$  in which  $c_2(V) = c_2(\tilde{V}) = 12$  (the so-called symmetric embedding), corresponding to an  $\mathbb{F}_n = \mathbb{P}^1 \times \mathbb{P}^1$  base in F-theory. This will at least make it possible in principle for the two duals to consider.

### 6.2.1 Spectral Cover of Monads

To begin, we observe that since the vector bundles defined by GLSMs (in their geometric phases) are usually presented as monads [44], we must deal with how to convert this description of a bundle into one compatible with heterotic/F-theory duality. As discussed in

Section 5, it is necessary to perform an FM transform to compute the spectral cover in this case. As a result, here we briefly review the method first introduced in [126].

Suppose we are given a general monad such as,

$$0 \rightarrow \mathcal{V} \rightarrow \mathcal{H} \xrightarrow{F} \mathcal{N} \rightarrow 0, \quad (6.2.2)$$

where  $\mathcal{H}$  and  $\mathcal{F}$  are direct sum of line bundles of appropriate degrees. If we assume  $\mathcal{V}$  is stable and degree zero, then from the previous subsection we know that its restriction over a generic elliptic fiber will look like  $\bigoplus_i \mathcal{O}(p_i - \sigma)$ . So if we twist the whole monad by  $\mathcal{O}(\sigma)$ ,

$$\tilde{\mathcal{V}} := \mathcal{V} \otimes \mathcal{O}(\sigma)|_E = \bigoplus_i \mathcal{O}(p_i). \quad (6.2.3)$$

Each factor has only one global section over the fiber, and it becomes zero exactly at the point  $p_i$  which is the intersection of the spectral cover with the fiber. So the idea is try to find the global section of the twisted vector bundle over elliptic fibers, then check at what points the dimension of the vector space generated by global sections drop. To illustrate how this can be done explicitly, first consider twisting the full monad sequence by  $\mathcal{O}(\sigma)$ ,

$$0 \rightarrow \tilde{\mathcal{V}} \rightarrow \tilde{\mathcal{H}} \xrightarrow{F} \tilde{\mathcal{N}} \rightarrow 0, \quad (6.2.4)$$

and follow this by next taking the action of the left exact functor  $\pi_*$  on the above sequence ( $\bar{F}$  is the induced map, corresponding to  $F$ ):

$$0 \rightarrow \pi_* \tilde{\mathcal{V}} \rightarrow \pi_* \tilde{\mathcal{H}} \xrightarrow{\bar{F}} \pi_* \tilde{\mathcal{N}} \rightarrow R^1 \pi_* \tilde{\mathcal{V}} \rightarrow \dots \quad (6.2.5)$$

If we assume the vector bundle is semistable over every elliptic fiber (this need not be true always, as we'll see. It is only necessary that vector bundle be semistable over generic elliptic fibers), then  $R^1 \pi_* \tilde{\mathcal{V}}$  is identically zero, because its presheaf is locally of the form  $H^1(E, \mathcal{O}(p_i))$ . Now consider the action of the right exact functor  $\pi^*$  over the last sequence, since the elliptic fibration map  $\pi$  is a flat morphism, it doesn't have higher left derived functors (we have  $Tor_{1S}(M, R) = 0$  due to the flatness, where  $S$  is the ring that corresponds to  $\mathcal{O}_B$ ,  $R$  corresponds to  $\mathcal{O}_X$ , and  $M$  is the free module corresponding to  $\mathcal{V}$  (see e.g. [108], Chapter 3) ). So we get,

$$0 \rightarrow \pi^* \pi_* \tilde{\mathcal{V}} \rightarrow \pi^* \pi_* \tilde{\mathcal{H}} \xrightarrow{\bar{F}} \pi^* \pi_* \tilde{\mathcal{N}} \rightarrow 0. \quad (6.2.6)$$

Note,  $\pi^* \pi_* \tilde{\mathcal{V}}$  is vector bundle that its fibers over a point  $p$  are generated by the global sections of  $\tilde{\mathcal{V}}$  over elliptic curve  $E_b$ , where  $b = \pi(p)$ . So (6.2.6) tells us that if we find the global sections of  $\tilde{\mathcal{H}}$  and  $\tilde{\mathcal{N}}$ , then the kernel of the induced map  $F$  is isomorphic to  $\pi^* \pi_* \tilde{\mathcal{V}}$ . So the locus where the rank of the kernel drop, coincides with the spectral cover. To clarify these rather abstract ideas, in the following subsection, we explicitly compute the spectral cover of two examples which will be used in the final subsection.

## 6.2.2 Examples

To begin we assume that the  $K3$  can be written in the following simple toric form,

| $x_i$     | $\Gamma^j$ |
|-----------|------------|
| 3 2 1 0 0 | -6         |
| 6 4 0 1 1 | -12        |

(6.2.7)

- **Example 1** The first example is the following  $SU(2)$  monad,

| $\Lambda$ | $p$   |
|-----------|-------|
| 1 1 2 3   | -3 -4 |
| 1 5 3 7   | -9 -7 |

(6.2.8)

The second Chern class of this monad is 12. The map  $F$  of the monad is given by the following generic matrix,

$$F \sim \begin{bmatrix} x f_4 + z^2 f_8 & a x + z^2 g_4 & z f_6 & f_2 \\ b y + x z g_2 + z^3 g_6 & z^3 h_2 & c x + z^2 h_4 & d z \end{bmatrix} \quad (6.2.9)$$

where subscripts indicate the degree of homogeneous polynomials over  $\mathbb{P}^1$ . With this choice,

it can be verified that the kernel of  $\bar{F}$  in (6.2.6) takes the following generic form,

$$\left[ \begin{array}{cc} x - z^2 \frac{-f_2 h_4 + d f_6}{c f_2} & 0 \\ 0 & x \frac{c f_2}{f_2 h_4 - d f_6} + z^2 \\ -\frac{b}{c} y - x z \frac{f_2 g_2 - b f_4}{c f_2} - z^3 \frac{f_2 g_6 - d f_8}{c f_2} & -z^3 \frac{f_2 h_2 - d g_4}{f_2 h_4 - d f_6} + -x z \frac{a d}{d f_6 - f_2 h_4} \\ -x^2 \frac{f_4}{f_2} + y z \frac{b f_6}{c f_2} - x z^2 \frac{c f_8 + f_4 h_4 - g_2 f_6}{c f_2} - z^4 \frac{f_8 h_4 - f_6 g_6}{c f_2} & x^2 \frac{a c}{d f_6 - f_2 h_4} - x z^2 \frac{c g_4 + a h_4}{f_2 h_4 - d f_6} - z^4 \frac{-f_6 h_2 + g_4 h_4}{f_2 h_4 - d f_6} \end{array} \right] \quad (6.2.10)$$

where  $f_i, g_i, h_i$  are polynomials in terms of base coordinates with degree  $i$ , and  $a, b, c, d$  are constant. The common factor of the minors of (6.2.10) is,

$$c f_2 x + (f_2 h_4 - d f_6) z^2. \quad (6.2.11)$$

From the previous discussion naively we might conclude that (6.2.11) must be the spectral cover. However, in the Fourier-Mukai discussion it was noted that the divisor class of the spectral cover should be  $2\sigma + 12D$ . So, in the expression above we are clearly missing a degree 6 polynomial in (6.2.11). The correct spectral cover should be

$$S = F_6(c f_2 x + (f_2 h_4 - d f_6) z^2). \quad (6.2.12)$$

But why then is  $F_6$  is missing? The reason is that in the previous subsection we assumed the vector bundles are semistable over every fiber. This not necessarily true. It is possible to start from a stable bundle, and modify it in a way that it becomes semistable over every fiber [127].

To see clearly what happens, let us first find the elliptic fibers such that vector bundle over them is unstable. Note that from (6.2.11) it can be seen that the spectral cover is a non degenerate two sheeted surface, and over generic  $E$ ,  $V|_E = \mathcal{O}(p - \sigma) \oplus \mathcal{O}(q - \sigma)$ , where  $p + q = 2\sigma$ . So  $V|_E$  does not have global section over almost every fiber except when  $p = q = \sigma$ . These points are on the intersection of  $z = 0$  and the spectral cover, which are the zeros of  $f_2 F_6$ . The idea then is to see if we can find the elliptic fibers which over the vector bundle (not its twisted descendant) can have global section. So all we need to do to find  $F_6$  is to study the kernel of the induced map in the following sequence:

$$0 \rightarrow \pi_* \mathcal{V} \rightarrow \pi_* \mathcal{H} \xrightarrow{F_{ind}} \pi_* \mathcal{N} \rightarrow R^1 \pi_* \mathcal{V} \rightarrow \dots \quad (6.2.13)$$

where the induced map,  $F_{ind}$ , in the above case is a  $7 \times 7$  matrix in terms of the base coordinates. Generically it's rank is 7, excepts over the zeros of  $f_2 F_6$ , so we can read the missing polynomial from this form. Please note that the above computations are local, globally  $\pi_* \mathcal{V} = 0$ . Because  $\mathcal{V}$  is locally free, and  $\pi$  is a flat morphism, so the pushforward of  $\mathcal{V}$  should also be torsion-free (see [107], Ch. III.9.2).

Interestingly, when we repeat the same analysis after twisting with  $\mathcal{O}(\sigma)$  and  $\mathcal{O}(2\sigma)$ , the rank of the corresponding induced map drops over  $F_6$ , and nowhere respectively. This means that the bundle over those fibers takes the following form,

$$\mathcal{V}|_{E_{\text{missing}}} = \mathcal{O}(p) \oplus \mathcal{O}(-p), \quad (6.2.14)$$

therefore  $h^0(E, \mathcal{V} \otimes \mathcal{O}(\sigma)) \geq 2$ , and the rank of the kernel in (6.2.6) (which generically is the same as the rank of the bundle, in this case, 2) doesn't drop over the points of these fibers. So the algorithm suggested in [126] doesn't find them. But it can be seen from (5.2.1) that these (whole) elliptic fibers are in the support of the spectral sheaf. In summary, a detailed analysis along the lines sketched above shows that the missing component is given by,

$$F_6 = h_2 c f_2^2 - c d f_2 g_4 + a d f_2 h_4 - a d^2 f_6. \quad (6.2.15)$$

where each in the expression polynomial above is defined from the monad map in (6.2.9).

• **Example 2** The second example is interesting because its spectral cover is degenerate (in this case, a non reduced scheme):

| $\Lambda$ | $p$   |
|-----------|-------|
| 0 1 2 3   | -2 -4 |
| 2 1 3 7   | -6 -7 |

(6.2.16)

The second Chern class of this monad is  $c_2(V) = 6$ , so from the previous discussion, it is clear that the divisor class of its spectral cover must be  $2\sigma + 6D$ . The number of global sections of  $\mathcal{H}$  and  $\mathcal{N}$  is seven and six respectively, which tells us that the kernel of  $F_{ind}$  is at least one dimensional over almost every elliptic fiber. Since  $\mathcal{V}$  is a stable, rank two bundle with  $c_1(\mathcal{V}) = 0$ , we conclude either  $\mathcal{V}|_E = \mathcal{O} \oplus \mathcal{O}$  or  $\mathcal{V}|_E = \epsilon_2$ <sup>4</sup>. In both cases the spectral

---

<sup>4</sup>By  $\mathcal{V}|_E = \epsilon_2$  we mean the unique non trivial extension of the trivial bundles over the elliptic curve.

cover must have the following general form,

$$S = F_6 z^2. \quad (6.2.17)$$

In fact, by computing the  $F_{ind}$  directly, we can see the rank of the kernel is always one, so  $\mathcal{V}|_E = \epsilon_2$ . As before we can compute the kernel of (6.2.6), to generate the spectral cover,

$$\begin{bmatrix} z & 0 \\ 0 & z^2 \\ -\frac{xz}{f_3} - z^3 \frac{f_4}{f_3} & z^3 \frac{f_5}{f_3} \\ a \frac{x^2}{f_3} + xz^2 \frac{f_4}{f_3} + z^4 \frac{f_8}{f_3} & byz + xz^2 \frac{g_5}{f_3} + z^4 \frac{f_9}{f_3} \end{bmatrix} \quad (6.2.18)$$

Then we look at the minors, and common factor should be spectral cover. However, as in the previous examples, the algorithm in [126] miss the polynomial  $F_6$ . The reason is similar to the previous example, the bundle is unstable over the zeros of  $F_6$ . It can be shown that the correct spectral cover is indeed,

$$S = (F_3)^2 z^2, \quad (6.2.19)$$

where  $F_3$  is the entry (1,3) of the monad's map (i.e. the map between the line bundles  $\mathcal{O}_X(2,3)$  and  $\mathcal{O}_X(2,6)$ ).<sup>5</sup>

### 6.2.3 Counter Examples of the Conjecture

Here we return to the main goal of this section. Suppose we have two target space dual GLSMs that describe different stable bundles over elliptic  $K3$  surfaces. The goal is to check whether their F-theory dual geometries can be related via a change in  $K3$ - fibrations (i.e. a change in  $\mathbb{P}^1$  fibrations in the two-fold base of the CY 3-fold). Generally the base of the F-theory threefold will be a Hirzebruch surface  $F_n$ , where  $n$  is given by the twist in (5.2.8). The only situation that can accommodate such multiple fibration structures is when  $n = 0$ .

---

<sup>5</sup>After a thorough computation we can show that,

$$0 \longrightarrow \mathcal{J} \longrightarrow FM^1(V) \longrightarrow \mathcal{O}_\sigma \longrightarrow 0,$$

where  $\mathcal{J}$  is a torsion sheaf supported over  $\{z = 0\} \cup \{F_3 = 0\}$ , and its rank over  $\{F_3 = 0\}$  is 2.  $\mathcal{J}$  can be computed explicitly, but it is outside of the scope of this paper.



So here we focus on this case and demand that the second Chern class of both heterotic vector bundles be 12.

We assume that one of the target space dual geometries is given by monads on the toric  $K3$  (6.2.7). We also write the elliptically fibered  $K3$  in Weierstrass form,

$$y^2 = x^3 + f_8(x_1, x_2)xz^4 + f_{12}(x_1, x_2)z^6, \quad (6.2.20)$$

where  $x_1$  and  $x_2$  are the coordinates of the base  $\mathbb{P}^1$ . To find explicit examples for target space duality, recall there are several constraints that must be met. First, it is necessary to have a well defined GLSM. This means the first Chern class of both bundles should be zero, and the second Chern class of both bundles (or sheaves) should be 12.

In addition we must make sure that the hybrid phase in which we do the TSD “exchange” of  $G$  and  $F$  actually exists. In the process of generating the TSD pairs, it may happen that singularities arise in the bundle or manifold (we expect that crepant resolutions should exist for the manifold and that the singularities in the “bundle” should be codimension 2 in the base, so that the sheaf is torsion-free). In addition to these constraints for the GLSM, there is another practical requirement for finding the F-theory geometry, we prefer to work with  $SU(N)$  bundles which have a non-degenerate spectral cover. If this is not satisfied it is still possible to find the F-theory dual, but we should remember that the form of the spectral sheaves can be vastly more rich/complex in these cases. This enhanced data in the Picard group will not be manifest in the spectral cover, or in the complex structure moduli of the dual F-theory geometry. Instead it will be related in the dual F-theory to nilpotent Higgs bundles over singular curves [57, 128–130].

It is straightforward to find many GLSMs where at least one of the bundles (say  $\mathcal{V}_1$ ) has  $SU(N)$  structure, and spectral cover is non degenerate, for example consider (6.2.8) once again,

| $\Lambda$ | $p$   |
|-----------|-------|
| 1 1 2 3   | -3 -4 |
| 1 5 3 7   | -9 -7 |

with Chern class

$$C_2(V_1) = 5\sigma^2 + 22\sigma D + 23D^2 = 12. \quad (6.2.21)$$

It should be noted that the algorithm for determining the spectral cover, using the methods of [126] was sketched above, but when the spectral cover becomes reducible (which can still be reduced), it is not guaranteed that those methods find the full spectral cover (i.e. usually some (vertical) components will be missed). One can find these components by closer examination of the morphisms that define the bundle and elliptic fibration, as we saw in the last subsection. The spectral cover (schematically) is then given by (6.2.12)

$$S = F_6(f_2x + f_6z^2).$$

Note that (6.2.8) by itself is not a well defined linear sigma model, therefore we need another bundle such that it's structure group embedded in the other  $E_8$  factor. This second bundle must also have GLSM description over the same  $K3$ , and it's second Chern class should be,

$$C_2(V_2) = 6\sigma^2 + 24\sigma D + 21D^2 = 12. \quad (6.2.22)$$

Since the existence of this bundle with above properties may not be quite obvious, we turn now to constructing appropriate examples explicitly.

### 6.2.4 Example 1

We can construct an example  $\mathcal{V}_2$  (though not the most general such bundle) as a direct sum of two bundles, each defined by the monad in (6.2.16) (which we denote it here by  $\mathcal{V}_0$ ), with  $c_2(\mathcal{V}_0) = 6$ :

$$\mathcal{V}_2 = \mathcal{V}_0 \oplus \mathcal{V}_0. \quad (6.2.23)$$

For this monad bundle, the spectral cover was found to be of the form given in (6.2.19). In addition, the rank 1 sheaf on the spectral cover can be readily constrained. Here  $FM^0(\mathcal{V}_0)$  is zero by results in [107] (see Section III.12, the final theorem). So we actually have the following short exact sequence:

$$FM^1(\mathcal{V}_2) = FM^1(\mathcal{V}_0) \oplus FM^1(\mathcal{V}_0), \quad (6.2.24)$$

where the support of  $FM^1(\mathcal{V}_2)$ , which is the spectral cover of  $\mathcal{V}_2$ , is the union of the spectral covers associated to the two copies of  $\mathcal{V}_0$ . The resulting spectral cover is a non-reduced

scheme, which can be realized by the following polynomial<sup>6</sup>

$$S(V_2) = (F_3)^2(G_3)^2z^4. \quad (6.2.25)$$

Before turning to the F-theory dual of this geometry, let us first construct a target space dual model for the above GLSM. To do that we add new chiral fields, in a way that after integrating them out, we return to the initial model. This can be done by adding “repeated entries” to the charge matrix of the  $K3$ , and can lead to multiple TSD geometries (all still of the same topological type of manifold and bundle, of course). One possibility is

| $x$         | $\Gamma$ | $\Lambda_1$ | $p_1$    | $\Lambda_2$ | $p_2$ |
|-------------|----------|-------------|----------|-------------|-------|
| 3 2 1 0 0 0 | −6 0     | 1 1 2 3 2   | −3 −4 −2 | 0 1 2 3     | −2 −4 |
| 3 2 0 1 1 1 | −6 −2    | 0 4 1 5 6   | −6 −3 −7 | 2 0 1 4     | −4 −3 |

(6.2.26)

This heterotic geometry ( $K3$  manifold and bundle) has point like singularities in the would-be bundle – that is, it is a rank 2 torsion-free sheaf rather than a vector bundle [63].

With this pair of TSD bundles over  $K3$  in hand, we are now in a position to consider the dual F-theory geometry. In this case we will ask the key question: *are the two GLSMs/geometries (i.e. that defined by  $\mathcal{V}_1$  and  $\mathcal{V}_2$ , and its TSD dual in (6.2.26), realized as different fibrations of a single F-theory geometry?*

By the results of the previous subsection, the complex structure of the Calabi-Yau threefold can be readily determined:

$$\begin{aligned}
Y^2 &= X^3 + F(u_1, u_2, x_1, x_2)XZ^4 + G(u_1, u_2, x_1, x_2)z^6, \\
F(u_1, u_2, x_1, x_2) &= u_1^4u_2^4f_8(x_1, x_2) + u_1^3u_2^5F_6(x_1, x_2)f_2(x_1, x_2), \\
G(u_1, u_2, x_1, x_2) &= u_1^7u_2^5(F_3(x_1, x_2))^2(G_3(x_1, x_2))^2 + u_1^6u_2^6f_{12}(x_1, x_2) + u_1^5u_2^7F_6(x_1, x_2)f_6(x_1, x_2).
\end{aligned} \quad (6.2.27)$$

As frequently happens with degenerate spectral data, we find that the apparent F-theory gauge symmetry seems in contradiction with what is expected from the heterotic theory we

---

<sup>6</sup>Generally the two  $\mathcal{V}_0$  in the above construction can be related by a continuous deformation, so we consider  $F_3$  and  $G_3$  as different generic degree 3 polynomials.

have engineered. By inspection of the discriminant of (6.2.27), it is straightforward to see that there appears to be an  $E_7$  symmetry on  $u_1 \rightarrow 0$ , and an apparent  $E_8$  singularity above the curve  $u_1 \rightarrow \infty$ . This might seem in contradiction with the expected gauge symmetry of  $SO(12)$  in the hidden sector (determined as the commutant of the  $SU(2) \times SU(2)$  structure group defined by the reducible bundle in (6.2.23)). However, in the case of degenerate spectral covers, we naturally expect that T-brane type solutions [57, 128] may well arise in the dual F-theory geometry. That is, we expect a nilpotent  $SU(2) \times SU(2)$  Higgs bundle over the 7-brane which wraps around this curve ( $u_2 = 0$ ) and breaks the space time gauge group to  $SO(12)$  as expected (see [59] for a similar construction).

Next, as demonstrated in [124], changing the  $K3$ -(resp.  $\mathbb{P}^1$ -)fibration in the F-theory geometry simply amounts to exchanging the vertical  $\mathbb{P}^1$  (whose coordinates are  $u_1$  and  $u_2$ ) with the horizontal  $\mathbb{P}^1$  which is the base in the initial heterotic  $K3$  surface in (6.2.7). This means that the vertical  $\mathbb{P}^1$  becomes the base of a dual heterotic  $K3$ -surface. To determine gauge groups in the dual heterotic theory, the discriminant curve must be considered. This is shown in Figure 6.1. The figure on the right hand side, shows the discriminant of the F-theory Calabi-Yau 3-fold. The line at the top is the locus of the  $E_7$  singularity and the one at the bottom corresponds to  $E_8$ . The curve is the locus of the  $I_1$  singularities. It intersects eight times with the  $III^*$  curve, where on six of them it has triple point singularities. These six points are exactly the zeros of  $F_6$  in Figure 6.1, which naively correspond to point like instantons that are responsible for the vertical components in spectral cover of  $\mathcal{V}_1$  (not taking into account the spectral sheaf/T-brane data). Similarly the  $I_1$  curve intersect with  $II^*$  at two sets of three points, which are the zeros of  $F_3$  and  $G_3$  in (6.2.25), and over all of them the curve has double point singularities.

We can expand the polynomials in (6.2.27) in terms of  $x_1$  and  $x_2$ , and read the dual heterotic complex structure from there. Clearly we see that the elliptic  $K3$  in the new Heterotic dual *must be singular*. In particular, it exhibits singular  $E_8$  and  $E_7$  located at  $u_1 = 0$  and  $u_1 \rightarrow \infty$  respectively (with expected instanton number of 12 on each locus). This is a highly non-perturbative limit of the string theory. This exchange of gauge symmetry with singularities in the base  $K3$  surface arising in the heterotic theory seems to be a generic feature of exchanging F-theory fibrations [120]. As a result, it seems is impossible to get something which is purely smooth/perturbative on both sides like (6.2.26) from such a change of fibrations. This shows that at least some of the TSD dual pairs cannot be seen simply as different fibrations of the F-theory geometry. We explore these possibilities a little more in one further example.

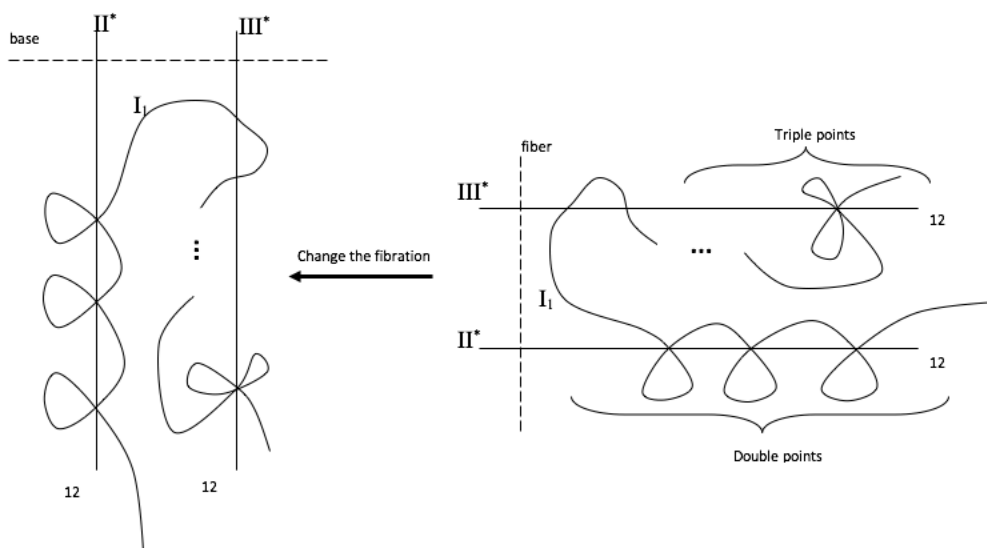


**Figure 6.1:** The vertical dotted line on the right hand side is the “vertical  $\mathbb{P}^1$ .” After change of fibration on the left hand side the same  $\mathbb{P}^1$  will be the base of the dual heterotic  $K3$ .

### 6.2.5 Example 2

In this example, the starting geometry/bundles, are the same as before, but here we present another TSD geometry that can also be described easily by spectral cover. So once again we take as our starting point the manifold/bundle:

| $x_i$     | $\Gamma^j$ | $\Lambda^a$ | $p_l$ |
|-----------|------------|-------------|-------|
| 3 2 1 0 0 | −6         | 1 1 2 3     | −3 −4 |
| 6 4 0 1 1 | −12        | 1 5 3 7     | −9 −7 |

(6.2.28)

and embed it into a larger GLSM by adding a new gauge field, and fermionic and chiral fields:

| $x_i$           | $\Gamma^j$ | $\Lambda^a$ | $p_l$       |
|-----------------|------------|-------------|-------------|
| 3 2 1 0 0 0 0 0 | −6 0 0     | 1 1 2 3 3 3 | −3 −4 −3 −3 |
| 6 4 0 1 1 0 0 1 | −12 0 −1   | 1 5 3 7 8 9 | −9 −7 −8 −9 |
| 0 0 0 0 0 1 1 0 | 0 −1 0     | 0 0 0 0 0 0 | −1 0 0 0    |

(6.2.29)

After performing the combinatoric “exchange” (i.e. the usual TSD procedure), this yields the new TSD geometry

| $x_i$           | $\Gamma^j$ | $\Lambda^a$ | $p_l$    |          |
|-----------------|------------|-------------|----------|----------|
| 3 2 1 0 0 0 0 0 | -6 0 0     | 1 1 2 3 3   | -3 -4 -3 | (6.2.30) |
| 6 4 0 1 1 0 0 1 | -12 -1 0   | 1 5 3 7 8   | -9 -7 -8 |          |
| 0 0 0 0 0 1 1 0 | 0 -1 -1    | 0 0 0 0 1   | -1 0 0   |          |

The advantage of this new example is that, it is possible to compute the spectral cover of both sides easily<sup>7</sup> and they are both reducible but still reduced

$$S_1 = F_6(f_2X + f_6Z^2), \quad (6.2.31)$$

$$S_2 = F_7(f_1X + f_5Z^2). \quad (6.2.32)$$

As in the previous example, we can readily construct the F-theory geometry of both sides, and check whether they are related by exchanging the fibration or not. The Weierstrass polynomials,  $F$  and  $G$ , of the dual F-theories is given by,

$$F_1 = \mathcal{O}(u_1^5) + u_1^4 u_2^4 f_1^8(v_1, v_2) + u_1^3 u_2^5 F_6(v_1, v_2) f_2(v_1, v_2), \quad (6.2.33)$$

$$G_1 = \mathcal{O}(u_1^7) + u_1^6 u_2^6 g_1^{12}(v_1, v_2) + u_1^5 u_2^7 F_6(v_1, v_2) f_6(v_1, v_2), \quad (6.2.34)$$

$$(6.2.35)$$

$$F_2 = \mathcal{O}(v_1^5) + v_1^4 v_2^4 f_2^8(u_1, u_2) + v_1^3 v_2^5 F_7(u_1, u_2) f_1(u_1, u_2), \quad (6.2.36)$$

$$G_2 = \mathcal{O}(v_1^7) + v_1^6 v_2^6 g_2^{12}(u_1, u_2) + v_1^5 v_2^7 F_7(u_1, u_2) f_5(u_1, u_2). \quad (6.2.37)$$

As in the previous example, the change in fibration can be realized in  $F_1$  and  $G_1$  by re-expanding these polynomials in terms of  $v_1$  and  $v_2$ . Then if the dual (F-theory) geometries are related through changing the fibration, after this rearrangement,  $F_1$  and  $G_1$  must be equal to  $F_2$  and  $G_2$ .

---

<sup>7</sup>In the previous example the base,  $\mathbb{P}^1$ , was defined as a conic inside  $\mathbb{P}^2$ . However, the spectral cover equations would be in terms of the ambient space coordinates and imposing the non linear relations between the coordinates to define the  $\mathbb{P}^1$  makes the situation somewhat obscure.

But since  $F_2$  and  $G_2$  have an order three zero at  $v_1 = 0$ , it means that  $f_1^8(v_1, v_2)$  and  $g_1^{12}(v_1, v_2)$  must have an order three zero at  $v_1 = 0$ . Recall that these two polynomials are the  $f$  and  $g$  of the dual heterotic  $K3$  surface, so the above argument tells us if the TSD geometries are related to the different fibrations of the same geometry in F-theory, both TSD Calabi-Yau 2-folds must have an  $E_7$  singularity at some point on the base. Thus once again, we see that exchange of fibration leads to a perturbative/non-perturbative duality in heterotic [124] and not the apparent correspondence arising from TSD.

In summary, if we start with two perfectly smooth TSD geometries, they cannot be related through different  $K3$ -fibrations of a single F-theory 3-fold. But if we allow both  $K3$  surfaces to be singular, and at the same time put bundles/small instantons over them, they might be dual to a single geometry in F-theory<sup>8</sup>.

Having determined that the multiple fibrations are not describing the TSD exchange in six dimensions, we can take a step back and ask *what F-theory correspondence is induced by TSD in six dimensions?* Since the spectral covers in (6.2.31) and (6.2.32) are relatively simple, we can try to roughly figure out some generalities about the F-theory duals of each of them. Let us start with the first one. The topology of the vector bundle fixes the dimension of the moduli space of the bundle,

$$h^1(V_1 \otimes V_1^*) = 42. \quad (6.2.38)$$

We can describe them in terms of the spectral data as follows,

$$\dim(\mathcal{M}_V) = \dim(\text{cplx}(C)) + \dim(\text{Jac}(C)) + 6\text{pts} + 6 \times \dim(\text{Jac}(E)) + \text{gluing}, \quad (6.2.39)$$

where  $C$  is the irreducible smooth curve defined by  $f_2X + f_6Z^2$ , by  $6\text{pts}$  we mean the degrees of freedom in choosing the location of the six points defined by the zero set of  $F_6 = 0$ , and over them we have 6 elliptic curves (whose Jacobians must also be taken into account), and finally “gluing” denotes the degrees of freedom associated with the choice of spectral sheaf at the intersection of the 6 vertical fiber with  $C$ . The genus of  $C$  can be computed easily,

$$g(C) = 9. \quad (6.2.40)$$

---

<sup>8</sup>But we should recall that the GLSM is only a perturbative formulation and clearly lacks information about the full string theory in such a context.

Therefore, the dimension of the Jacobian and the complex structure of  $C$  must be 9. On the other hand, obviously, Jacobian of  $E$  is one-dimensional, and the contribution of the “gluing” is twelve-dimensional (each vertical fiber intersects  $C$  at 2 points). Therefore the total dimension of the moduli space is,

$$\dim(\mathcal{M}_V) = 9 + 9 + 6 + 6 + 12 = 42. \quad (6.2.41)$$

Now, to obtain the F-theory EFT we must use the spectral data as explained before, and infer the form of the complex structure of the CY 3-fold. From this procedure it can be seen that there are 6 (4,6,12) points in the F-theory geometry. Since the heterotic dual is a perturbative model, we should consider these singularities as the singular limit of the following deformations,

$$F_1 = \mathcal{O}(u_1^5) + u_1^4 u_2^4 f_1^8(v_1, v_2) + u_1^3 u_2^5 (F_6(v_1, v_2) f_2(v_1, v_2) + \epsilon F_8(v_1, v_2)), \quad (6.2.42)$$

$$G_1 = \mathcal{O}(u_1^7) + u_1^6 u_2^6 g_1^{12}(v_1, v_2) + u_1^5 u_2^7 (F_6(v_1, v_2) f_6(v_1, v_2) + \lambda F_{12}(v_1, v_2)), \quad (6.2.43)$$

where  $\epsilon$  and  $\lambda$  correspond to deforming the Higgs field over the 7-branes [57, 131]. Therefore we can deform these two theories into each other by continuously deforming the Higgs bundle. This reflects the fact the moduli space of the vector bundles on  $K3$  is connected. Phrased differently, the existence of apparent (4, 6, 12) points in the putative dual F-theory indicates that such solutions can *only be dual to the expected perturbative heterotic theories* in the case that T-brane solutions arise. This has been seen before in [128] and is a substantial hint that G-flux must play an important role in the non-trivial F-theory correspondence expected in four-dimensional compactifications.

It is worth commenting briefly also on another branch of the theory visible from this singular limit. We can increase the number of tensor multiplets in the six-dimensional YM theory by performing small instanton transitions (i.e. moving NS5/M5 branes off the  $E_8$  fixed plane in the language of heterotic M-theory). For bundles described as spectral covers, this small instanton limit is visible by the spectral cover becoming reducible and vertical components (corresponding to small instantons) appearing (note that this limit must also set all gluing data to zero). Naively it seems that this limit appears different for the TSD pair of bundles defined by (6.2.31) and (6.2.32) since they exhibit different degree polynomials defining their vertical components (i.e.  $F_6$  vs.  $F_7$ ). However, this is simply a statement that the mapping of moduli in this case may exchange what are spectral cover deformations in one description



with data associated to the Jacobian of the spectral cover (i.e. gluing data in this singular case). To really obtain the same point in moduli space, we must consider a scenario in which both halves of the TSD gain the same number of tensor multiplets (i.e. we pull either 6 or 7 5-branes into the bulk). In this case it would be intriguing to analyze the dual F-theory geometry – which would correspond to blowing up the base of the elliptic fibration. We expect in this case that the F-theory 3-fold will still be  $K3$  fibered but no longer of such a simple form. In particular, the elliptic fibration over a Hirzebruch surface would be modified to become a more general conic bundle [120]. We will return to questions of a similar geometric nature in the following section.

Let us briefly summarize the results of our six-dimensional investigation. We have seen that after exchanging  $K3$ -fibrations within the F-theory geometry, the dual heterotic  $K3$  surface must become singular, and therefore perturbative smooth heterotic geometries arising in TSD pairs cannot in general be realized as different fibrations within F-theory. On the other hand we saw that the dual F-theory EFTS arising from the chosen TSD pairs must crucially rely on data from the intermediate Jacobian of the CY 3-fold – so-called T-brane solutions – in order to give rise to the same physical theories. Starting from such points we can deform back to smooth points in the CY 3-fold moduli space and identify the theories. Any possible correspondences within the tensor branch of the six-dimensional theories must involve more complicated  $K3$ -fibrations (i.e. conic bundles) and we leave this exploration to future work.

### 6.3 F-theory Duals of Four-Dimensional Heterotic TSD Pairs

In Section 6.1 we provided a non-trivial example of a heterotic TSD pair in which both  $X$  and  $\tilde{X}$  were elliptically fibered. It is now natural to ask – *what are the F-theory duals of these heterotic theories?* As we will explain below, this example (and others like it that we have found) seem to force beyond the arena of “standard” heterotic/F-theory duality (as in the canonical reference [54]) by including several important features in the dual geometries. In this section, we will not try to solve all the obstacles that arise at once. Instead, we will outline what can be determined about the dual F-theory geometries and where new tools will be needed to fully probe this correspondence. Many of these we are currently developing [55, 56] and we hope to definitively answer these questions in future work.

As a first step towards determining the dual F-theory geometry, the data of the heterotic bundle must be taken through a Fourier-Mukai transform to be presented as spectral data (see the discussion in Section 6.2). However in this we immediately encounter several problems. The first of these is that unlike in the case of heterotic/F-theory dual pairs studied in the literature to date, neither of these heterotic CY elliptic 3-folds is in Weierstrass form.

To be specific we focus on the examples in Section 6.1 (though similar obstacles will arise in general in this context). Recall that each of the CY 3-folds listed in (6.1.14) admitted two rational sections. Those for  $X$  in (6.1.14) lie in the following classes

$$[\sigma_1(X)] = -D_1 + D_2 + D_3, \quad [\sigma_2(X)] = 2D_1 - D_2 + 5D_3.$$

where  $D_i$  are a basis of divisors on  $X$  (inherited from the ambient space hyperplanes by restriction). By “rational” it is meant that these divisors are isomorphic to blow ups of the base manifold (in this case  $P^2$ ). The first difficulty with this example is that the standard Fourier-Mukai transformation with Poincare bundle is not applicable here. The reason is we need the zero section to intersect exactly one point on *every fiber*, but both of the sections described above wrap around a finite number of rational curves (which are components of reducible fibers). We have shown [55] that in specific situations one can use flop transitions to make one of the sections holomorphic, and since derived categories are invariant under the flop transitions (i.e. there is a specific Fourier-Mukai functor for flops), it is still possible to define the spectral data in the “flopped” geometry. However the example given in (6.1.14) proves to be too complicated to be analyzed in this manner since  $\sigma_1$  and  $\sigma_2$  wrap around 27 and 127 rational curves respectively, rendering the necessary birational transformations (i.e. flops) impractical.

In principle, one might hope to bypass this difficulty by transitioning  $X$  directly to its Weierstrass form (by blowing down the reducible components of fibers), following the Deligne procedure outlined in [119, 120]. However, this poses difficulties in a heterotic theory in that it is unclear how the heterotic bundle data should be appropriately mapped to this singular limit of  $X$ .

Nonetheless, if we choose  $\sigma_1$  as the zero section, it can be demonstrated that the spectral cover in the singular Weierstrass limit, has the same divisor class as before (this is seen by taking the FM transform before blowing down the reducible fiber components). In other

words, if we write the second Chern class as

$$c_2(V) = 36\sigma_1 H + 14S_{sh}H + 156f, \quad (6.3.1)$$

where  $H$  is the (pull-back of the) hyperplane divisor in the base,  $S_{sh}$  is the divisor corresponding to the Shioda map [132–134] for non trivial Mordell-Weil group,

$$S_{sh} = \sigma_2 - \sigma_1 - 18H \quad (6.3.2)$$

and  $f$  is the fiber class. In terms of these divisors, the class of the spectral cover,  $S$ , in the singular limit will be,

$$[S] = 6\sigma_1 + 36H. \quad (6.3.3)$$

We might hope to get some information about the F-theory geometry just from the spectral cover alone. Naively, we may write the algebraic formula for the spectral cover whose class is given in (6.3.3) as

$$S = f_{36}z^3 + f_{30}xz + f_{27}y. \quad (6.3.4)$$

where  $f_i$  are generic polynomials of degree  $i$  over  $\mathbb{P}^2$ . A generic deformation of the spectral cover of the form (6.3.4) can be obtained by counting the degrees of freedom in the polynomials  $f_{36}, f_{30}, f_{27}$  which contain 703, 496 and 406 parameters, respectively. Immediately we see that these numbers much higher than the dimension of the vector bundle moduli space in our example, which is 292-dimensional. Thus, we can see that the FM-transform of the monad in (6.1.4) is certainly *not* a generic spectral cover. This is not too surprising. We have seen examples of the spectral cover of monads in Section 6.2 and there it was clear that the polynomials are not generic, rather they are dictated by the monad's map (see also [126, 130]). In principle, a similar story happens in the current case. We expect that the spectral cover may also be non-reduced/reducible [126]. However, regardless of its explicit form, the question arises, why is the spectral cover forbidden from assuming a generic form? That is, given an explicit starting point (in which the polynomials are determined by the monad map as in (6.1.4)) why is the deformation space restricted?

We expect that the answer to this lies with the other half of the spectral data of this monad, that is, the rank 1 sheaf [54] supported over the spectral cover in (6.3.3) and (6.3.4). It

has been observed previously [135] that the Picard group of  $S$  may “jump” at higher co-dimensional loci in moduli space – i.e. so-called Noether-Lefschetz loci. This phenomenon could “freeze” the moduli of the spectral cover to a sub-space compatible with the form of the monad map (see also [136]). In terms of the four-dimensional,  $\mathcal{N} = 1$  EFT, the reduction in the apparent number of singlets (i.e. the non generic form of the spectral cover) is a symptom of existence of a specific superpotential – arising from the Gukov-Vafa-Witten form [70]:

$$W \sim \int_X H \wedge \Omega \quad (6.3.5)$$

where  $H \sim dB + \omega_3^{YM} - \omega_3^{Lorentz}$ , and  $\omega_3 = F \wedge A - \frac{1}{3}A \wedge A \wedge A$  is the Chern Simons 3-form (and the associated Lorentz quantity built from the spin connection in  $\omega_3^{Lorentz}$  and  $\Omega$  is the holomorphic  $(0, 3)$  form on  $X$ . The existence of this superpotential arises from the presence of the gauge bundle (rather than from quantized flux) (see [19, 26, 135] for related discussions) but none-the-less stabilizes vector bundle moduli.

As a result, in the dual F-theory EFT, we also expect the existence of a superpotential. Geometrically, since the spectral cover determines part of the complex structure moduli of the Calabi-Yau fourfold, it is clear that the dual of the bundle data given in (6.1.4) should include a specific G-flux that stabilizes the moduli through the GVW superpotential. It should be noted that there is another way to see the requirement for this flux: since there are no  $D3$  branes in the F-theory dual (since we have chosen  $c_2(X) = c_2(V)$  in the heterotic theory), G-flux is also necessary for anomaly cancellation.

Although we have not yet explicitly calculated the FM transform of the heterotic bundle or determined the dual F-theory geometry. The arguments above show that whatever the F-theory geometry, G-flux must play a prominent role and therefore it cannot be ignored. A similar set of arguments can also be made about the F-theory dual of the heterotic TSD geometry  $(\tilde{X}, \tilde{V})$ . In this case as well, the naive deformations of the spectral cover are much larger than the dimension of the vector bundle moduli space, and therefore we conclude that Noether-Lefschetz loci/G-flux should be in play.

Despite the fact that flux must be involved in the putative F-theory duality, it still remains to be asked whether the dual F-theory 4-folds might still exhibit multiple fibration structure? That is could the geometric scenario described in the introduction with these compatible

elliptic/ $\mathbb{P}^1$  (and hence  $K3$ ) fibrations exist?

$$\begin{array}{ccc}
 & Y_4 & \\
 & \downarrow \rho_f \mid \mathbb{E} & \\
 & B_3 & \\
 \swarrow \mathbb{P}^1 \sigma_f & & \searrow \mathbb{P}^1 \tilde{\sigma}_f \\
 B_2 & & \tilde{B}_2
 \end{array}$$

On this front, once again we see that we must quickly leave behind the “standard” geometry of heterotic/F-theory duality. As reviewed in Section 5, if the heterotic CY 3-fold is in Weierstrass form, the construction of [54] generates a threefold base,  $B_3$  (see (5.1.2)) for the CY 4-fold that is a  $\mathbb{P}^1$ -bundle over the base  $B_2$  (which is the base of the dual elliptically fibered CY 3-fold and  $K3$ -fibered 4-fold). The topology of this bundle (i.e.  $B_3$  itself) is determined by the second Chern class of the heterotic bundle  $c_2(V)$ . In this context then, we can ask whether or not such a base could admit two different descriptions as a  $\mathbb{P}^1$  bundle? While multiply fibered  $\mathbb{P}^1$  bundles certainly exist (for example the “generalized Hirzebruch” toric 3-fold defined as the zero twist over  $\mathbb{F}_n$  or the  $n$ -twist over  $\mathbb{F}_0$  [94, 120]), it is easy to demonstrate that

$$h^{1,1}(B_3) = 1 + h^{1,1}(B_2) \tag{6.3.6}$$

for any  $\mathbb{P}^1$  bundle. As a result, it is clear that *there exists no multiply fibered  $\mathbb{P}^1$ -bundles compatible with the  $B_2$  and  $\tilde{B}_2$  arising in Section 6.1* since for those manifolds  $B_2 = \mathbb{P}^2$  and  $\tilde{B}_2 = dP_1$ . Hence  $h^{1,1}(B_2) < h^{1,1}(\tilde{B}_2)$  and  $h^{1,1}(B_3) \neq h^{1,1}(\tilde{B}_3)$  for 3-fold bases constructed as  $\mathbb{P}^1$ -bundles.

From the results above we would be tempted to conclude that the hypothesis we set out to test in the literature (i.e. is heterotic TSD dual to multiply fibered geometries in F-theory?) is manifestly false. However, we must first recall that the construction of  $K3$  fibrations in terms of  $\mathbb{P}^1$ -bundle bases  $B_3$  as commonly used in the literature is not the only possible structure. More general 3-fold bases,  $B_3$  are possible which are  $\mathbb{P}^1$  fibrations *but not  $\mathbb{P}^1$  bundles*. These fibrations degenerate (as multiple  $\mathbb{P}^1$ s) over higher co-dimensional loci in the base  $B_2$  and are known as “conic bundles” in the literature (see e.g. [137]).

If we consider this more general class of bases for CY 4-folds it seems that some possibilities

remain. For example, the following threefold

$$B_3 = \left[ \begin{array}{c|cc} \mathbb{P}^2 & 0 & 1 \\ \mathbb{P}^1 & 1 & 0 \\ \mathbb{P}^2 & 1 & 1 \end{array} \right] \quad (6.3.7)$$

is manifestly fibered over both  $\mathbb{P}^2$  and  $dP_1$  as required. However, it is unclear that the generic “twist” of such a fibration is compatible with the topology of the bundles defined in Section 6.1. It is possible to generalize simple constructions like the one above to accommodate more general twists by choosing more general toric ambient spaces. However, in each case we hit a new problem in that the stable degeneration limits of  $\mathbb{P}^1$  bundles such as that in (6.3.7) are not yet understood in the literature (though we are considering such geometries in separate work [56]). As a result, it is a non-trivial task to determine whether such a geometry might arise in the F-theory duals of the examples outlined in Section 6.1. To check this we need precise spectral data. But as explained before, finding the Fourier-Mukai transforms of the heterotic bundles, while possible in principle, is beyond our current computational limits for the bundles in Section 6.1.

For now though, we can conclude that whatever the F-theory correspondence induced from (0, 2) target space duality may be, it must expand the current understanding of heterotic/F-theory duality both via the crucial inclusion of G-fluxes (including possibly limits and T-brane solutions) and via more general geometry – in particular  $K3/\mathbb{P}^1$ -fibrations – than has previously been considered.

# Chapter 7

## Massless Spectrum of the Non-Geometric Phase

This chapter contains our unpublished work. In this chapter we will compute the massless spectra for a pair of TSD. In section 7.1 the computation of massless states arising from a (0,2) Landau-Ginzburg background is reviewed briefly, following the procedure developed in [61, 138]. In Section 7.2 our calculation for a pair of TSD is described, then the result is compared with the cohomology from Calabi-Yau geometry. Because one of the large radius geometries is singular, in Section 7.3 we will try to resolve the singularity to get a new model.

### 7.1 Method of Computing the Complete Massless Spectrum

In a supersymmetric (0, 2) Landau-Ginzburg theory, there are two different types of superfields. One is called chiral superfield and can be expanded in components as

$$\Phi = \phi + \theta^+ \psi_+ + \bar{\theta}_+ \theta_+ \bar{\partial} \phi, \quad (7.1.1)$$

where  $\psi_+$  is a right moving fermion, the superpartner of  $\phi$ . Also, it includes Fermi superfield  $\Lambda$ , which can be expanded in components to

$$\Lambda = \lambda + \theta^+ l + \bar{\theta}_+ \theta_+ \bar{\partial} \lambda, \quad (7.1.2)$$

where  $\lambda$  is a left moving fermion and  $l$  is an auxiliary field. Now let's consider a (0, 2) Landau-Ginzburg theory with the following superpotential

$$\mathcal{W}(\Phi_i, \Lambda^a) = \Lambda^a F_a(\Phi_i). \quad (7.1.3)$$

| Field       | Left U(1) charge $q$ | Right U(1) charge $\bar{q}$ |
|-------------|----------------------|-----------------------------|
| $\phi_i$    | $q_i$                | $q_i$                       |
| $\psi^i$    | $q_i$                | $q_i - 1$                   |
| $\lambda^a$ | $q_a - 1$            | $q_a$                       |

**Table 7.1:** Left and right  $U(1)$  charges of fields in a Landau-Ginzburg theory.

In particular, if this superpotential is a Landau-Ginzburg  $\mathbb{Z}_m$ -orbifold phase of a  $U(1)$  gauge theory, such that the charges of  $\Phi_i$  are  $w_i$  and charges of  $\Lambda^a$  are  $n_a$ , then the superpotential is a quasi-homogeneous polynomial of the fields satisfying

$$\mathcal{W}(\epsilon^{w_i}\Phi_i, \epsilon^{n_a}\Lambda^a) = \epsilon^m \mathcal{W}(\Phi_i, \Lambda^a). \quad (7.1.4)$$

The quasi-homogeneity of the superpotential guarantees the existence of a right-moving  $U(1)$  R-symmetry which plays an important role in  $(0, 2)$  models. In addition, there is a global left-moving  $U(1)$  symmetry. Let's define:

$$q_i = \frac{w_i}{m}, \quad q_a = \frac{n_a}{m}, \quad (7.1.5)$$

then the left and right  $U(1)$  charges of the fields are given in Table 7.1.

In compactification of a heterotic string theory to four dimensions with  $E_6$ ,  $SO(10)$  or  $SU(5)$  gauge groups, the internal part of the theory needs to be a  $(0, 2)$  superconformal field theory with central charge  $(c, \bar{c}) = (6 + \tilde{r}, 9)$ , where  $\tilde{r}$  is 3 for  $E_6$ , 4 for  $SO(10)$ , and 5 for  $SU(5)$ .

In application of the Landau-Ginzburg theory in string theory,  $16 - 2\tilde{r}$  extra left moving free fermions

$$L' = \int \sum_{I=1}^{16-2\tilde{r}} \lambda^I \bar{\partial} \lambda^I \quad (7.1.6)$$

are added to the theory. In a case where the Landau-Ginzburg theory is the other phase of a geometric Calabi-Yau phase with a rank  $\tilde{r}$  bundle for a  $U(1)$  gauge theory, the central charge of the geometric phase is  $(c, \bar{c}) = (6 + \tilde{r}, 9)$ , so adding  $L'$  is essential for matching central charges of both phases and gaining the desired gauge group in four dimensions. There are also 16 left-moving free fermions which generate the hidden  $E_8$  space-time gauge symmetry. We will leave them in NS sector, and only consider states which are singlets under the hidden gauge group.



In string theory, four different boundary conditions need to be imposed: (R,R), (NS,R), (R,NS), and (NS,NS) on right and left moving fermions. Here, we will consider (R,R) and (NS,R) sectors, which yield space time fermions. The (R,NS) and (NS,NS) sectors give the spacetime bosons which are related to the fermions by supersymmetry. To find both (R,R) and (NS,R) sectors simultaneously, the Landau-Ginzburg  $\mathbb{Z}_m$  orbifold is combined with the  $\mathbb{Z}_2$  orbifold due to two different boundary conditions on the left moving fermions. In this case, we get a  $\mathbb{Z}_{2m}$ -orbifold and the different sectors are labelled by  $k = 0, \dots, 2m - 1$ . States in even  $k$  sector correspond to  $(R, R)$  sector, and states in odd  $k$  sector correspond to  $(NS, R)$  sector.

Not all the states in the twisted sectors survive, most of them are projected out and states with  $g = 1$  survive,

$$g = \exp(-i\pi J)(-1)^{N_\lambda}, \quad (7.1.7)$$

where

$$J_L = \oint dx^1 \left( i \sum_i q_i \phi_i \overset{\leftrightarrow}{\partial}_0 \bar{\phi}_i + \sum_i q_i \psi_i \bar{\psi}_i + \sum_a (q_a - 1) \lambda_a \bar{\lambda}_a \right) \quad (7.1.8)$$

is the operator which transforms the fields according to Table 7.1, and  $N_\lambda$  is the number of the free fermions  $\lambda_I$ . In practice this projection is equivalent to restricting states to states with half integer left  $U(1)$  charge  $q$ .

Specially, we are interested in the massless spectrum of the Landau-Ginzburg orbifold. The right moving supersymmetry algebra is

$$\{Q_+, \bar{Q}_+\} = \bar{L}_0, \quad Q_+^2 = \bar{Q}_+^2 = 0. \quad (7.1.9)$$

Massless states are annihilated by  $\bar{L}_0$ . By (7.1.9), finding such states is equivalent to calculating the cohomology of  $\bar{Q}_+$  operators. (Also the massless states annihilated by  $L_0$  need to be considered, but we actually look at the subspace, i.e. states with vanishing  $L_0$ , then compute  $\bar{Q}_+$  cohomology.)

The  $\bar{Q}_+$  operator, as provided in [139, 140], can be written explicitly:

$$\begin{aligned} \bar{Q}_+ &= i \oint dx^1 \left( \mathcal{W}|_{\theta=0} + i \bar{\psi}^i \bar{\partial} \phi_i \right), \\ &= i \oint dx^1 \left( \lambda^a F_a(\phi) + i \bar{\psi}^i \bar{\partial} \phi_i \right), \end{aligned} \quad (7.1.10)$$

The computation of  $\bar{Q}_+$  cohomology can be separated into two parts:

$$\bar{Q}_{+,L} = i \oint dx^1 \left( \lambda^a F_a(\phi) \right), \quad \bar{Q}_{+,R} = i \oint dx^1 \left( i\bar{\psi}^i \bar{\partial} \phi_i \right). \quad (7.1.11)$$

Then computing  $\bar{Q}_+$ -cohomology is equivalent to computing  $\bar{Q}_{+,R}$  and then calculate  $\bar{Q}_{+,L}$  inside of that which means:

$$H_{\bar{Q}_+} \equiv H_{\bar{Q}_{+,L}} \Big|_{H_{\bar{Q}_{+,R}}}. \quad (7.1.12)$$

$\bar{Q}_{+,R}$ -cohomology simply removes all the right moving fermions  $\psi_i$  from the massless spectrum, so calculating  $\bar{Q}_{+,L}$ -cohomology is our main task.

Now let's see how to convert the above procedure to a model. The first thing that should be noticed is that the world-sheet is a cylinder, which is parameterized by  $(x^0, x^1)$ , with  $x^1 \sim x^1 + 2\pi$ .

As mentioned before, we have to calculate the massless spectrum in  $2m$  sectors which are labeled by  $k = 0, \dots, 2m - 1$ . Massless states in the  $k$ -th sector with charges  $(q, \bar{q})$  are in one to one correspondence with massless states in the  $(2m - k)$ -th sector with charges  $(-q, -\bar{q})$ . So we only need to calculate the massless states of the sectors  $k = 0, \dots, m$ .

In the  $k$ -th sector the boundary conditions on the bosonic and fermionic fields are

$$\phi(x^0, x^1 + 2\pi) = e^{-i\pi q k} \phi(x^0, x^1) \quad (7.1.13)$$

where  $q$  is the left  $U(1)$  charge associated to the fields. Given this, the fields can be expanded using a Fourier series

$$\phi(x^0, x^1) = \sum_{r \in \mathbb{Z} - iqk/2} \phi_r(x^0) e^{irx^1}. \quad (7.1.14)$$

After quantization,  $\phi_r$  is an operator. For bosonic and fermionic fields we have the following commutation and anti-commutation relations between these operators ( $r > 0$ ):

$$\begin{aligned} [\phi_r, \bar{\phi}_{-r}] &= [\bar{\phi}_r, \phi_{-r}] = [\bar{\phi}_0, \phi_0] = \mathbb{1}, \\ \{\lambda_r, \bar{\lambda}_{-r}\} &= \{\bar{\lambda}_r, \lambda_{-r}\} = \{\lambda_0, \bar{\lambda}_0\} = \mathbb{1}, \end{aligned} \quad (7.1.15)$$

with vanishing commutation and anti-commutation relation for all other pairs of fields. These relations are true for a free field theory, here we will use them in our Born-Oppenheimer approximation of the fields which keeps only the lowest modes of the fields, as argued in [61].

Denoting the Fock vacuum of the  $k$ -th sector by  $|0\rangle_k$ , it is annihilated by the following operators:

$$\begin{aligned}\phi_r |0\rangle_k &= \bar{\phi}_r |0\rangle_k = \bar{\phi}_0 |0\rangle_k = 0, \\ \lambda_r |0\rangle_k &= \bar{\lambda}_r |0\rangle_k = \lambda_0 |0\rangle_k = 0.\end{aligned}\tag{7.1.16}$$

The left and right  $U(1)$  charges of the Fock vacuum  $|0\rangle_k$  are

$$\begin{aligned}q_k &= -\sum_i q_i \left( \frac{q_i k}{2} - \left[ \frac{q_i k}{2} \right] - \frac{1}{2} \right) + \sum_a (q_a - 1) \left( \left[ \left[ \frac{q_a - 1}{2} k \right] \right] - \frac{1}{2} \right), \\ \bar{q}_k &= -\sum_i (q_i - 1) \left( \frac{q_i k}{2} - \left[ \frac{q_i k}{2} \right] - \frac{1}{2} \right) + \sum_a q_a \left( \left[ \left[ \frac{q_a - 1}{2} k \right] \right] - \frac{1}{2} \right),\end{aligned}\tag{7.1.17}$$

where the function  $[[x]]$  is modified from the Floor function, as is introduced to unify all the cases:

$$[[x]] = \begin{cases} x - [x], & x \notin \mathbb{Z}, \\ 1, & x \in \mathbb{Z}. \end{cases}\tag{7.1.18}$$

The reason for this choice is that, for fermions, when  $(q_a - 1)k\pi$  is an integer multiple of  $2\pi$ , there is a discontinuity and both values should be kept. The energy of  $|0\rangle_k$ , i.e. the eigenvalue of  $L_0$ , for even  $k$ , is:

$$E_k = -\frac{(\tilde{r} - 3)}{8} - \frac{1}{2} \sum_i \left( \frac{q_i k}{2} - \left[ \frac{q_i k}{2} \right] - \frac{1}{2} \right)^2 + \frac{1}{2} \sum_a \left( \left[ \left[ \frac{q_a - 1}{2} k \right] \right] - \frac{1}{2} \right)^2,\tag{7.1.19}$$

for odd  $k$ :

$$E_k = -\frac{5}{8} - \frac{1}{2} \sum_i \left( \frac{q_i k}{2} - \left[ \frac{q_i k}{2} \right] - \frac{1}{2} \right)^2 + \frac{1}{2} \sum_a \left( \left[ \left[ \frac{q_a - 1}{2} k \right] \right] - \frac{1}{2} \right)^2.\tag{7.1.20}$$

With these equations we can construct states with zero eigenvalue of  $L_0$ . If the vacuum  $|0\rangle_k$  has negative energy (eigenvalue of  $L_0$ ) then its energy can be raised by an amount  $r$ , using  $\phi_{-r}$ ,  $\bar{\phi}_{-r}$ ,  $\lambda_{-r}$ , and  $\bar{\lambda}_{-r}$  operators. Note that, the operators  $\phi_0$  and  $\bar{\lambda}_0$  do not change the energy of the vacuum.

Our next step is to compute zero eigenvalues of  $\bar{L}_0$ . As argued before, this is equivalent to ignoring right moving fermions and computing  $\bar{Q}_{+,L}$ -cohomology. The  $\bar{Q}_{+,L}$  operator, which is written in integral form

$$\bar{Q}_{+,L} = i \oint dx^1 \left( \lambda^a F_a(\phi) \right),\tag{7.1.21}$$

can be simplified using the Born-Oppenheimer approximation, which simply amounts to replacing bosonic and fermionic fields in the above expression by ( $0 \leq r < 1$ )

$$\begin{aligned}\phi &\rightarrow \phi_{-r}e^{-irx^1} + \phi_{-r+1}e^{i(-r+1)x^1}, \\ \lambda &\rightarrow \lambda_{-r}e^{-irx^1} + \lambda_{-r+1}e^{i(-r+1)x^1}.\end{aligned}\tag{7.1.22}$$

After this replacement in (7.1.21) and the integration, only the terms with a vanishing sum of the modes of fields are relevant, because otherwise  $\bar{Q}_{+,L}$  would change the energy (eigenvalue of  $L_0$ ) of the states, which are out of our interest.

In each sector the massless states can be classified (with respect to  $L_0$ ) by their left and right  $U(1)$  charges  $(q, \bar{q})$ , denoted by  $V_{(q,\bar{q})}$ . The  $\bar{Q}_{+,L}$  operator doesn't change left  $U(1)$  charge, but increases the right  $U(1)$  charge by 1. So, in each sector we get the following complex:

$$0 \rightarrow V_{(q,\bar{q})} \xrightarrow{\bar{Q}_{+,L}} V_{(q,\bar{q}+1)} \xrightarrow{\bar{Q}_{+,L}} \dots \xrightarrow{\bar{Q}_{+,L}} V_{(q,\bar{q}+n)} \rightarrow 0.\tag{7.1.23}$$

In the last step we compute  $\bar{Q}_{+,L}$ -cohomology in each space  $V_{(q,\bar{q})}$  to get the spectrum of massless states with zero eigenvalues of both  $L_0$  and  $\bar{L}_0$ .

### 7.1.1 Space-time Interpretation of the Massless Spectrum in the Case of $\tilde{r} = 3$

Generally, based on the left and right  $U(1)$  charges  $(q, \bar{q})$ , and the number of free fermions  $\lambda^I$  of a state, we can determine the space-time interpretation of the fields. In our case where  $\tilde{r} = 3$ , the following rules apply [61]:

- states with  $q - 1/2$  even transform as a **16** of  $SO(10)$ ,
- states with  $q - 1/2$  odd transform as a  $\overline{\mathbf{16}}$  of  $SO(10)$ ,
- states with  $\bar{q} - 1/2$  even are left-handed spin one-half massless fermions,
- states with  $\bar{q} - 1/2$  odd are right-handed spin one-half massless fermions,
- states with integer charge  $q$  are singlets of  $SO(10)$ ,
- states with one free fermion  $\lambda^I$ , transform as the fundamental representation **10** of  $SO(10)$ ,

- states with two free fermions  $\lambda^I \lambda^J$ , transform as the adjoint representation **45** of  $SO(10)$ .

With left  $U(1)$  charge of the states taken into account, the states can be combined to make **27**, or  $\overline{\mathbf{27}}$  or **78** representations of  $E_6$ . To do that, recall that  $E_6$  includes  $SO(10) \times U(1)$  as its maximal subgroup, and different representations of  $E_6$  decompose under  $SO(10) \times U(1)$  in the following form:

$$\begin{aligned}
 \mathbf{27} &\rightarrow \mathbf{1}_2 \oplus \mathbf{10}_{-1} \oplus \mathbf{16}_{1/2}, \\
 \overline{\mathbf{27}} &\rightarrow \mathbf{1}_{-2} \oplus \mathbf{10}_1 \oplus \overline{\mathbf{16}}_{-1/2}, \\
 \mathbf{78} &\rightarrow \mathbf{1}_0 \oplus \mathbf{16}_{-3/2} \oplus \overline{\mathbf{16}}_{3/2} \oplus \mathbf{45}_0.
 \end{aligned} \tag{7.1.24}$$

We turn now to an explicit realization of these ideas.

## 7.2 Example

In the last section of the paper [138], a pair of TSD are discussed briefly. Here we will perform the calculation of the massless spectra for these examples. The two Calabi-Yau manifold/vector bundles are given as below:

$(X, V) =$

| $x_i$       | $\Gamma^j$ | $\Lambda^a$ | $p_l$ |
|-------------|------------|-------------|-------|
| 1 2 2 2 3 3 | -5 -8      | 1 1 2 6     | -10   |

(7.2.1)

where for  $(X, V)$ , the singlet spectrum in the low energy theory is counted by  $h^{1,1}(X) = 1$ ,  $h^{2,1}(X) = 53$ ,  $h(V \otimes V^*) = (1, 174, 174, 1)$ , and the charged matter is  $h(V) = (0, 72, 0, 0)$ .

$(\tilde{X}, \tilde{V}) =$

| $x_i$       | $\Gamma^j$ | $\Lambda^a$ | $p_l$ |
|-------------|------------|-------------|-------|
| 1 2 2 2 3 3 | -4 -9      | 1 2 2 5     | -10   |

(7.2.2)

Likewise, for  $(\tilde{X}, \tilde{V})$ ,  $h^{1,1}(X) = 1$ ,  $h^{2,1}(X) = 59$ ,  $h(V \otimes V^*) = (1, 168, 168, 1)$ ,  $h(V) = (0, 72, 0, 0)$ .

These CY manifolds are defined as complete intersections in weighted projective spaces and are  $(0,2)$  models instead of  $(2,2)$ .

### 7.2.1 Setup

These two examples have identical Landau-Ginzburg phases, so the calculation for one example would be exactly the same as the other. Here we will do the first example in detail.

$(X, V) =$

| $x_i$ |   |   |   |   |   | $\Gamma^j$ |    | $\Lambda^a$ |   |   |   | $p_l$ |
|-------|---|---|---|---|---|------------|----|-------------|---|---|---|-------|
| 1     | 2 | 2 | 2 | 3 | 3 | -5         | -8 | 1           | 1 | 2 | 6 | -10   |

(7.2.3)

In the Landau-Ginzburg phase this is a  $\mathbb{Z}_{10}$  orbifold. The superpotential

$$W = W(\epsilon\phi_1, \epsilon^2\phi_2, \epsilon^2\phi_3, \epsilon^2\phi_4, \epsilon^3\phi_5, \epsilon^3\phi_6, \epsilon^5\Sigma_1, \epsilon^2\Sigma_2, \epsilon\Lambda_1, \epsilon\Lambda_2, \epsilon^2\Lambda_3, \epsilon^6\Lambda_4) \quad (7.2.4)$$

is quasi-homogeneous:

$$\begin{aligned} W &= \Sigma_1 G_5(\phi) + \Sigma_2 G_8(\phi) + P(\Lambda^1 F_9(\phi) + \Lambda^2 F_9(\phi) + \Lambda^3 F_8(\phi) + \Lambda^4 F_4(\phi)) \\ &= \epsilon^{10} W. \end{aligned} \quad (7.2.5)$$

The quasi-homogeneity indicates a right-moving  $U(1)$  R-symmetry. As discussed in the previous section, the left and right  $U(1)$  charges of the fields can be written as in Table 7.2.

The calculation of massless states is the same as the calculation of  $\bar{Q}_{+,L}$  cohomology. The  $\bar{Q}_{+,L}$  operator can be written explicitly in integral form:

$$\bar{Q}_{+,L} = i \oint dx^1 \left( \sigma_1 G_5(\phi) + \sigma_2 G_8(\phi) + \lambda_1 F_9(\phi) + \lambda_2 F_9(\phi) + \lambda_3 F_8(\phi) + \lambda_4 F_4(\phi) \right). \quad (7.2.6)$$

The  $\bar{Q}_{+,L}$  operator can be simplified using the Born-Oppenheimer approximation by replacing bosonic and fermionic fields in the above expression with the following expression ( $0 \leq r < 1$ ), and keeping only the terms with vanishing sum of the modes of fields.

$$\begin{aligned} \phi &\rightarrow \phi_{-r} e^{-irx^1} + \phi_{-r+1} e^{i(-r+1)x^1}, \\ \lambda &\rightarrow \lambda_{-r} e^{-irx^1} + \lambda_{-r+1} e^{i(-r+1)x^1}. \end{aligned} \quad (7.2.7)$$

Now let's find the vacuum charges and energies corresponding to different twisted sectors.

| Field           | $\mathbf{q}_-$ | $\mathbf{q}_+$ |
|-----------------|----------------|----------------|
| $\phi_1$        | 1/10           | 1/10           |
| $\psi_1$        | 1/10           | -9/10          |
| $\phi_{2,3,4}$  | 2/10           | 2/10           |
| $\psi_{2,3,4}$  | 2/10           | -8/10          |
| $\phi_{5,6}$    | 3/10           | 3/10           |
| $\psi_{5,6}$    | 3/10           | -7/10          |
| $\sigma_1$      | -5/10          | 5/10           |
| $\sigma_2$      | -8/10          | 2/10           |
| $\lambda_{1,2}$ | -9/10          | 1/10           |
| $\lambda_3$     | -8/10          | 2/10           |
| $\lambda_4$     | -4/10          | 6/10           |

**Table 7.2:** Left and right  $U(1)$  charges of fields in  $V(1, 1, 2, 6; 10) \rightarrow \mathbb{P}_{1,2,2,2,3,3}[5, 8]$ .

## 7.2.2 Find Vacuum Charges and Energies

In this Landau-Ginzburg  $\mathbb{Z}_{10}$  orbifold, the sectors are twisted by  $g^k$  where  $k = 1, \dots, 19$ . The  $U(1)$  charges will pick up the phases when going around the circle, for example the  $\phi_1$  field transforms as:

$$\phi_1 \rightarrow \phi_1 e^{-i\pi q k} = \phi_1 e^{-i\theta} \quad 0 \leq \theta < 2\pi. \quad (7.2.8)$$

From the previous section, the vacuum charges and energy can be determined from the following equations:

$$\begin{aligned}
q_k &= -\sum_i q_i \left( \frac{q_i k}{2} - \left[ \frac{q_i k}{2} \right] - \frac{1}{2} \right) + \sum_a (q_a - 1) \left( \left[ \left[ \frac{q_a - 1}{2} k \right] \right] - \frac{1}{2} \right), \\
\bar{q}_k &= -\sum_i (q_i - 1) \left( \frac{q_i k}{2} - \left[ \frac{q_i k}{2} \right] - \frac{1}{2} \right) + \sum_a q_a \left( \left[ \left[ \frac{q_a - 1}{2} k \right] \right] - \frac{1}{2} \right), \\
E_{k \text{ even}} &= -\frac{(\tilde{r} - 3)}{8} - \frac{1}{2} \sum_i \left( \frac{q_i k}{2} - \left[ \frac{q_i k}{2} \right] - \frac{1}{2} \right)^2 + \frac{1}{2} \sum_a \left( \left[ \left[ \frac{q_a - 1}{2} k \right] \right] - \frac{1}{2} \right)^2, \\
E_{k \text{ odd}} &= -\frac{5}{8} - \frac{1}{2} \sum_i \left( \frac{q_i k}{2} - \left[ \frac{q_i k}{2} \right] - \frac{1}{2} \right)^2 + \frac{1}{2} \sum_a \left( \left[ \left[ \frac{q_a - 1}{2} k \right] \right] - \frac{1}{2} \right)^2,
\end{aligned} \quad (7.2.9)$$

|   | Left $q$  | Right $\bar{q}$                                      | E   |
|---|---|--|---|
| $\phi_1 \rightarrow \phi_1 e^{-i\pi \frac{1}{10}}$                | $-\frac{1}{10}(\frac{1}{20} - \frac{1}{2})$           | $\frac{9}{10}(\frac{1}{20} - \frac{1}{2})$           | $-\frac{1}{2}(\frac{1}{20} - \frac{1}{2})^2$          |
| $\phi_{2,3,4} \rightarrow \phi_{2,3,4} e^{-i\pi \frac{2}{10}}$    | $-\frac{2}{10}(\frac{2}{20} - \frac{1}{2}) \times 3$  | $\frac{8}{10}(\frac{2}{20} - \frac{1}{2}) \times 3$  | $-\frac{1}{2}(\frac{2}{20} - \frac{1}{2})^2 \times 3$ |
| $\phi_{5,6} \rightarrow \phi_{5,6} e^{-i\pi \frac{3}{10}}$        | $-\frac{3}{10}(\frac{3}{20} - \frac{1}{2}) \times 2$  | $\frac{7}{10}(\frac{3}{20} - \frac{1}{2}) \times 2$  | $-\frac{1}{2}(\frac{3}{20} - \frac{1}{2})^2 \times 2$ |
| $\sigma_1 \rightarrow \sigma_1 e^{-i\pi \frac{15}{10}}$           | $-\frac{5}{10}(\frac{15}{20} - \frac{1}{2})$          | $\frac{5}{10}(\frac{15}{20} - \frac{1}{2})$          | $\frac{1}{2}(\frac{15}{20} - \frac{1}{2})^2$          |
| $\sigma_2 \rightarrow \sigma_2 e^{-i\pi \frac{12}{10}}$           | $-\frac{8}{10}(\frac{12}{20} - \frac{1}{2})$          | $\frac{2}{10}(\frac{12}{20} - \frac{1}{2})$          | $\frac{1}{2}(\frac{12}{20} - \frac{1}{2})^2$          |
| $\lambda_{1,2} \rightarrow \lambda_{1,2} e^{-i\pi \frac{11}{10}}$ | $-\frac{9}{10}(\frac{11}{20} - \frac{1}{2}) \times 2$ | $\frac{1}{10}(\frac{11}{20} - \frac{1}{2}) \times 2$ | $\frac{1}{2}(\frac{11}{20} - \frac{1}{2})^2 \times 2$ |
| $\lambda_3 \rightarrow \lambda_3 e^{-i\pi \frac{12}{10}}$         | $-\frac{8}{10}(\frac{12}{20} - \frac{1}{2})$          | $\frac{2}{10}(\frac{12}{20} - \frac{1}{2})$          | $\frac{1}{2}(\frac{12}{20} - \frac{1}{2})^2$          |
| $\lambda_4 \rightarrow \lambda_4 e^{-i\pi \frac{16}{10}}$         | $-\frac{4}{10}(\frac{16}{20} - \frac{1}{2})$          | $\frac{6}{10}(\frac{16}{20} - \frac{1}{2})$          | $\frac{1}{2}(\frac{16}{20} - \frac{1}{2})^2$          |

**Table 7.3:** Vacuum charges and energy contributed by each field,  $k=1$  sector.

in our case  $\tilde{r} = 3$ .

To see these formula more explicitly, take the  $k=1$  sector as an example, the charges and energy corresponding to the twisted sector can be calculated as in Table 7.3, taking the sum of each column gives left  $q = 0$ , right  $\bar{q} = -\frac{3}{2}$ , and  $E = -1$ .

Similar to the  $k=1$  sector we can calculate left  $q$ , right  $\bar{q}$  and  $E$  for  $k=0$  and  $k=2 \sim 10$  sectors. The result is summarized in Table 7.4.

### 7.2.3 $k=0$ Sector

Let us consider the  $k=0$  sector explicitly:  $k=0$  is the untwisted sector, the charges and energy for ground states are:  $E=0$ ,  $(q, \bar{q}) = (-\frac{3}{2}, -\frac{3}{2})$ . There is only one state  $|0\rangle$ .

Because of the zero modes  $\phi_{i,0}$ , states with  $E=0$  and half integer  $U(1)$  charges are simply  $P_{10}(\phi)|0\rangle$ ,  $P_{20}(\phi)|0\rangle$ ,  $P_{30}(\phi)|0\rangle \dots$ . Here  $P_{10}(\phi)$  will lift  $(q, \bar{q})$  by 1 such that  $(q, \bar{q}) = (-\frac{1}{2}, -\frac{1}{2})$ . It is subject to the equivalence relation:

$$P_{10} \sim P_{10} + \sigma_1 G_5(\phi) + \sigma_2 G_8(\phi) + \lambda_1 F_9(\phi) + \lambda_2 F_9(\phi) + \lambda_3 F_8(\phi) + \lambda_4 F_4(\phi). \quad (7.2.10)$$

There are  $130-58=72$  independent degree 10 polynomials modulo these relations.



|      | Left $q$         | Right $\bar{q}$ | E                |
|------|------------------|-----------------|------------------|
| k=0  | $-\frac{3}{2}$   | $-\frac{3}{2}$  | 0                |
| k=1  | 0                | $-\frac{3}{2}$  | -1               |
| k=2  | $\frac{3}{2}$    | $-\frac{3}{2}$  | 0                |
| k=3  | $-\frac{2}{5}$   | $-\frac{9}{10}$ | $-\frac{3}{5}$   |
| k=4  | $\frac{3}{5}$    | $-\frac{2}{5}$  | $\frac{1}{5}$    |
| k=5  | $-\frac{17}{10}$ | $\frac{4}{5}$   | $-\frac{1}{4}$   |
| k=6  | $-\frac{1}{5}$   | $\frac{4}{5}$   | $-\frac{1}{10}$  |
| k=7  | $\frac{1}{10}$   | $-\frac{2}{5}$  | $-\frac{13}{20}$ |
| k=8  | $-\frac{1}{2}$   | $\frac{1}{2}$   | 0                |
| k=9  | $-\frac{4}{5}$   | $\frac{7}{10}$  | $-\frac{3}{5}$   |
| k=10 | $-\frac{7}{10}$  | $-\frac{7}{10}$ | 0                |

**Table 7.4:** *The list of vacuum charges and energy for  $k=0\sim 10$  sectors,  $k>10$  is given by symmetry.*

Similarly for  $P_{20}(\phi)$ ,  $(q, \bar{q}) = (\frac{1}{2}, \frac{1}{2})$ , there are  $1463-1391=72$  independent degree 20 polynomials. For  $P_{30}(\phi)$ ,  $(q, \bar{q}) = (\frac{3}{2}, \frac{3}{2})$ , there are  $7364-7363=1$  independent degree 30 polynomials.

### 7.2.4 k=1 Sector

The k=1 sector has the longest calculation because it has the most states. We need to find all the states with energy -1, left and right charges half integer. We have implemented a simple algorithm in Mathematica to determine the number of such states.

There are 4498 such states: 2 with charges  $(0, -\frac{5}{2})$ , 136 with charges  $(0, -\frac{3}{2})$ , 346 with charges  $(0, -\frac{1}{2})$ , 21 with charges  $(2, -\frac{5}{2})$ , 580 with charges  $(2, -\frac{3}{2})$ , 1950 with charges  $(2, -\frac{1}{2})$ , 1463 with charges  $(2, \frac{1}{2})$ .

Because the Q operator increases the right U(1) charge by 1, these states can be written in sequences. The first sequence is given as below:

$$0 \rightarrow (0, -\frac{5}{2}) \xrightarrow{Q_1} (0, -\frac{3}{2}) \xrightarrow{Q_2} (0, -\frac{1}{2}) \xrightarrow{Q_3} 0. \quad (7.2.11)$$

where  $(q, \bar{q})$  means states  $V_{(q, \bar{q})}$ . After calculating the kernels and images of the  $Q$ 's, the cohomologies are given as:

$$\begin{aligned} \text{Im } Q_1 &= 2, \\ \text{Ker } Q_1 &= 0, \\ \text{Im } Q_2 &= 133, \\ \text{Ker } Q_2 &= 3, \end{aligned} \tag{7.2.12}$$

$$\begin{aligned} H^1 &= 0 \rightarrow (0, -\frac{5}{2}), \\ H^2 &= \frac{\text{Ker } Q_2}{\text{Im } Q_1} = 3 - 2 = 1 \rightarrow (0, -\frac{3}{2}), \\ H^3 &= \frac{\text{Ker } Q_3}{\text{Im } Q_2} = 346 - 133 = 213 \rightarrow (0, -\frac{1}{2}). \end{aligned} \tag{7.2.13}$$

The second sequence and the corresponding cohomologies are given as below:

$$0 \rightarrow (2, -\frac{5}{2}) \xrightarrow{Q_1} (2, -\frac{3}{2}) \xrightarrow{Q_2} (2, -\frac{1}{2}) \xrightarrow{Q_3} (2, \frac{1}{2}) \xrightarrow{Q_4} 0. \tag{7.2.14}$$

$$\begin{aligned} \text{Im } Q_1 &= 21, \\ \text{Ker } Q_1 &= 0, \\ \text{Im } Q_2 &= 559, \\ \text{Ker } Q_2 &= 21, \\ \text{Im } Q_3 &= 1391, \\ \text{Ker } Q_3 &= 559, \end{aligned} \tag{7.2.15}$$

$$\begin{aligned} H^5 &= 0 \rightarrow (2, -\frac{5}{2}) \\ H^6 &= \frac{\text{Ker } Q_2}{\text{Im } Q_1} = 21 - 21 = 0 \rightarrow (2, -\frac{3}{2}), \\ H^7 &= \frac{\text{Ker } Q_3}{\text{Im } Q_2} = 559 - 559 = 0 \rightarrow (2, -\frac{1}{2}), \\ H^8 &= \frac{\text{Ker } Q_4}{\text{Im } Q_3} = 1463 - 1391 = 72 \rightarrow (2, \frac{1}{2}). \end{aligned} \tag{7.2.16}$$

In addition to the above, we also need to find the  $\mathbf{10}$ 's of  $\text{SO}(10)$ , which correspond to the massless gauge singlets in the Calabi-Yau phase [61]. These states are annihilated by  $G_{-1/2}$  or  $\bar{G}_{-1/2}$ , so the previous procedure can be used with the energy reduced by  $\frac{1}{2}$ . There are 190 such states: 1 with charges  $(1, -\frac{5}{2})$ , 59 with charges  $(1, -\frac{3}{2})$ , 130 with charges  $(1, -\frac{1}{2})$ .

The sequence is given by:

$$0 \rightarrow (1, -\frac{5}{2}) \xrightarrow{Q_1} (1, -\frac{3}{2}) \xrightarrow{Q_2} (1, -\frac{1}{2}) \xrightarrow{Q_3} 0. \quad (7.2.17)$$

After calculating the kernel and image of the  $Q$ 's, the cohomologies are given as:

$$\begin{aligned} \text{Im } Q_1 &= 1, \\ \text{Ker } Q_1 &= 0, \\ \text{Im } Q_2 &= 58, \\ \text{Ker } Q_2 &= 1, \end{aligned} \quad (7.2.18)$$

$$\begin{aligned} H^1 &= 0 \rightarrow (1, -\frac{5}{2}), \\ H^2 &= \frac{\text{Ker } Q_2}{\text{Im } Q_1} = 1 - 1 = 0 \rightarrow (1, -\frac{3}{2}), \\ H^3 &= \frac{\text{Ker } Q_3}{\text{Im } Q_2} = 130 - 58 = 72 \rightarrow (1, -\frac{1}{2}). \end{aligned} \quad (7.2.19)$$

With all the states required for the  $k=1$  sector found, in the next step we apply the same procedure for other sectors.

### 7.2.5 More Sectors and Summary

Similarly to the  $k=1$  sector, for other sectors we can find the states with corresponding charges and energy, and calculate the maps between them. The states in sectors  $k=11$  to 19 are given by symmetry.

The space-time interpretation of the states is given as follows (as we also mentioned in Section 7.1.1):

- states with  $q - 1/2$  even transform as a **16** of  $SO(10)$ ,
- states with  $q - 1/2$  odd transform as a  $\overline{\mathbf{16}}$  of  $SO(10)$ ,
- states with  $\bar{q} - 1/2$  even are left-handed spin one-half massless fermions,
- states with  $\bar{q} - 1/2$  odd are right-handed spin one-half massless fermions,
- states with integer charge  $q$  are singlets of  $SO(10)$ ,

- states with one free fermion  $\lambda^I$ , transform as the fundamental representation **10** of  $SO(10)$ ,
- states with two free fermions  $\lambda^I \lambda^J$ , transform as the adjoint representation **45** of  $SO(10)$ .

Table 7.5 lists the correspondence between massless states in the 4-dimensional theory and the representations.

Under the maximal subalgebra  $E_6 \supset SO(10) \times U(1)$ , the **27**, or  $\overline{\mathbf{27}}$  or **78** representations of  $E_6$  decompose as follows:

$$\begin{aligned}
 \mathbf{27} &\rightarrow \mathbf{1}_2 \oplus \mathbf{10}_{-1} \oplus \mathbf{16}_{1/2} \\
 \overline{\mathbf{27}} &\rightarrow \mathbf{1}_{-2} \oplus \mathbf{10}_1 \oplus \overline{\mathbf{16}}_{-1/2} \\
 \mathbf{78} &\rightarrow \mathbf{1}_0 \oplus \mathbf{16}_{-3/2} \oplus \overline{\mathbf{16}}_{3/2} \oplus \mathbf{45}_0
 \end{aligned} \tag{7.2.20}$$

Combining states into the representations **27**, or  $\overline{\mathbf{27}}$  or **78** of  $E_6$ , we find:

- 1 vector multiplet in Adj rep (**78**) of  $E_6$  (right handed), arising from the contributions in the  $k = 0, 19, 18$  sectors;
- 1 vector multiplet in Adj rep (**78**) of  $E_6$  (left handed), arising from the contributions in the  $k = 0, 1, 2$  sectors;
- Chiral Multiplet (**27**): 75 (left handed) from the  $k=0, 1, 19, 9, 10, 11$  sectors; 3 (right handed) from the  $k=15, 14, 13, 12, 11$  sectors;
- Anti-Chiral Multiplet ( $\overline{\mathbf{27}}$ ): 75 (right handed) from the  $k=0, 1, 19, 9, 10, 11$  sectors; 3 (left handed) from the  $k=5, 6, 7, 8, 9$  sectors;
- Singlets: 258 (right handed) from the  $k=1, 3, 5, 15, 13, 11$  sectors; 258 (left handed) from the  $k=19, 17, 15, 5, 7, 9$  sectors;
- 1+1 with charge (0,0) from the  $k=8, 12$  sectors.

Comparing the spectrum of the LG theory to that obtained from the geometric (i.e. large volume, CY) phase of the (0,2) GLSM where  $h^1(V) = 72$ , we can see that the *net* number of generations is protected by  $75-3=72$ . Note there is a little subtlety here, the manifold  $X$

|      | # of states | charges                        | representation                 |      | # of states | charges                       | representation      |
|------|-------------|--------------------------------|--------------------------------|------|-------------|-------------------------------|---------------------|
| k=0  | 1           | $(-\frac{3}{2}, -\frac{3}{2})$ | $16_{-\frac{3}{2}}$            |      |             |                               |                     |
|      | 72          | $(-\frac{1}{2}, -\frac{1}{2})$ | $\overline{16}_{-\frac{1}{2}}$ |      |             |                               |                     |
|      | 72          | $(\frac{1}{2}, \frac{1}{2})$   | $16_{\frac{1}{2}}$             |      |             |                               |                     |
|      | 1           | $(\frac{3}{2}, \frac{3}{2})$   | $\overline{16}_{\frac{3}{2}}$  |      |             |                               |                     |
| k=1  | 1           | $(0, -\frac{3}{2})$            | $1_0$                          | k=19 | 1           | $(0, \frac{3}{2})$            | $1_0$               |
|      | 213         | $(0, -\frac{1}{2})$            | $1_0$                          |      | 213         | $(0, \frac{1}{2})$            | $1_0$               |
|      | 72          | $(2, \frac{1}{2})$             | $1_2$                          |      | 72          | $(-2, -\frac{1}{2})$          | $1_{-2}$            |
|      | 72          | $(1, -\frac{1}{2})$            | $10_1$                         |      | 72          | $(-1, \frac{1}{2})$           | $10_{-1}$           |
|      | 1           | $(0, -\frac{3}{2})$            | $45_0$                         |      | 1           | $(0, \frac{3}{2})$            | $45_0$              |
| k=2  | 1           | $(\frac{3}{2}, -\frac{3}{2})$  | $\overline{16}_{\frac{3}{2}}$  | k=18 | 1           | $(-\frac{3}{2}, \frac{3}{2})$ | $16_{-\frac{3}{2}}$ |
| k=3  | 17          | $(0, -\frac{1}{2})$            | $1_0$                          | k=17 | 17          | $(0, \frac{1}{2})$            | $1_0$               |
| k=4  | 0           |                                |                                | k=16 | 0           |                               |                     |
| k=5  | 3           | $(0, -\frac{1}{2})$            | $1_0$                          | k=15 | 3           | $(0, \frac{1}{2})$            | $1_0$               |
|      | 4           | $(0, \frac{1}{2})$             | $1_0$                          |      | 4           | $(0, -\frac{1}{2})$           | $1_0$               |
|      | 2           | $(-2, \frac{1}{2})$            | $1_{-2}$                       |      | 2           | $(2, -\frac{1}{2})$           | $1_2$               |
| k=6  | 2           | $(-\frac{1}{2}, \frac{1}{2})$  | $\overline{16}_{-\frac{1}{2}}$ | k=14 | 2           | $(\frac{1}{2}, -\frac{1}{2})$ | $16_{\frac{1}{2}}$  |
| k=7  | 8           | $(0, \frac{1}{2})$             | $1_0$                          | k=13 | 8           | $(0, -\frac{1}{2})$           | $1_0$               |
|      | 1           | $(-2, \frac{1}{2})$            | $1_{-2}$                       |      | 1           | $(2, -\frac{1}{2})$           | $1_2$               |
|      | 2           | $(1, \frac{1}{2})$             | $10_1$                         |      | 2           | $(-1, -\frac{1}{2})$          | $10_{-1}$           |
| k=8  | 1           | $(-\frac{1}{2}, \frac{1}{2})$  | $\overline{16}_{-\frac{1}{2}}$ | k=12 | 1           | $(\frac{1}{2}, -\frac{1}{2})$ | $16_{\frac{1}{2}}$  |
|      | 1           | $(0, 0)$                       | $1_0$                          |      | 1           | $(0, 0)$                      | $1_0$               |
| k=9  | 13          | $(0, \frac{1}{2})$             | $1_0$                          | k=11 | 13          | $(0, -\frac{1}{2})$           | $1_0$               |
|      | 3           | $(-2, -\frac{1}{2})$           | $1_{-2}$                       |      | 3           | $(2, \frac{1}{2})$            | $1_2$               |
|      | 1           | $(1, \frac{1}{2})$             | $10_1$                         |      | 1           | $(-1, -\frac{1}{2})$          | $10_{-1}$           |
|      | 3           | $(-1, \frac{1}{2})$            | $10_{-1}$                      |      | 3           | $(1, -\frac{1}{2})$           | $10_1$              |
| k=10 | 3           | $(-\frac{1}{2}, -\frac{1}{2})$ | $\overline{16}_{-\frac{1}{2}}$ |      |             |                               |                     |
|      | 3           | $(\frac{1}{2}, \frac{1}{2})$   | $16_{\frac{1}{2}}$             |      |             |                               |                     |

**Table 7.5:** The complete massless spectrum of  $V(1, 1, 2, 6; 10) \rightarrow \mathbb{P}_{1,2,2,2,3,3}[5, 8]$  for  $k=0\sim 19$  sectors, where  $k=11\sim 19$  sectors are given by symmetry.

itself contains a  $\mathbb{Z}_3$  orbifold singularity, so the geometric calculation may not be accurate. However, the zero mode calculation can also be done in the other half of the TSD dual geometry (7.2.2) and there the geometry is smooth. Since we expect these two theories to have the same massless spectrum, we can conclude that  $h^1(V) = 72$ .

For the 258 singlets, the geometric phase calculation (i.e. the Calabi-Yau calculation) gives  $h^{1,1}(X) + h^{2,1}(X) + h(V \otimes V^*) = 1 + 53 + 174 = 228$  for  $(X, V)$ , and  $h^{1,1}(X) + h^{2,1}(X) + h(V \otimes V^*) = 1 + 59 + 168 = 228$  for  $(\tilde{X}, \tilde{V})$ . These 228 complex, Kähler and bundle moduli account for the 258 singlets found, while the others are expected to pick up a mass as moving away from the LG point.

### 7.3 Resolution of Singularity

In the previous section we encountered a TSD pair  $(X, V)$  and  $(\tilde{X}, \tilde{V})$  where  $(X, V)$  contained orbifold singularities. Even though the singularity is “mild” in that the GLSM vacuum space is still compact, the question arises: can we resolve the singularity to get  $(X', V')$ ? If so, does the resolved geometry play any role in the target space duality? Is it related to the LG point? Can we find any relationship as summarized schematically below?

$$\begin{array}{ccc}
 (X', V') & & \\
 \uparrow \text{resolve} & \searrow ? & \\
 (X, V) & \xleftrightarrow{TSD} \text{LG point} \xleftrightarrow{TSD} & (\tilde{X}, \tilde{V})
 \end{array}$$

In the following section, we will attempt to find appropriate resolutions of the singular geometry. It should be noted that the resolution is not unique. The resolution needs to satisfy a set of rules. For a specific geometry, there may be many resolutions, or there may be none. We list the restrictions below, and will provide examples for the conditions:

1. The singularity needs to be resolved (i.e. after resolution, the geometry needs to be smooth);
2. All anomaly cancellation conditions need to be satisfied;
3. For the manifold,  $h^{2,1}$  stays the same (there should be no motion in the complex

structure moduli space),  $h^{1,1}$  increases (a singularity is removed by introducing (at least) one new dimension in Kähler moduli space);

4. The manifold can reduce to the singular limit;
5. The resolved bundle needs to agree with the old one on the singular locus;
6. The bundle needs to be stable;
7. For isolated singularities, we would be intrigued to find those resolutions for which  $h(V)$  does not change (and could thus still be potentially involved in TSD as described above).

To resolve the singularity, we need to do a blow-up. There are two ways to perform the resolution, and they are equivalent. One is described in Distler, Greene and Morrison [63], which separates the charges as linear combinations of two  $U(1)$ 's. The other is described in Blumenhagen [38], which blows up the singular points by subdividing the cone. These two approaches are related by a linear combination of charges in the GLSM charge matrix.

Now we will explain the resolution in detail in an example. Specifically, there are 3 steps: 1) resolve the ambient space; 2) resolve the hypersurfaces; 3) resolve the bundle.

We begin by considering the initial, singular geometry  $(X, V)$ :

| $x_i$       | $\Gamma^j$ | $\Lambda^a$ | $p_l$ |
|-------------|------------|-------------|-------|
| 1 2 2 2 3 3 | -5 -8      | 1 1 2 6     | -10   |

(7.3.1)

For  $(X, V)$ ,  $h^{1,1}(X) = 1$ ,  $h^{2,1}(X) = 53$ ,  $h(V) = (0, 72, 0, 0)$ ,  $h(V \otimes V^*) = (1, 174, 174, 1)$ .

The ambient space has  $\mathbb{Z}_2$  and  $\mathbb{Z}_3$  singularities, but the  $\mathbb{Z}_2$  singularity is avoided by the hypersurfaces, so the Calabi-Yau only has a  $\mathbb{Z}_3$  singularity.

The singular curve is  $x_1 = x_2 = x_3 = x_4 = 0$ . On the singular locus,  $P_5 = 0$ ,  $P_8 = 0$ , the degree 5 and 8 hypersurfaces pass through this locus, so it's not avoided by the CY. In the GLSM, the F-term and D-term potentials are:

$$V_F = \sum_j |G_j(x_i)|^2 + \sum_a \left| \sum_l p_l F_a^l(x_i) \right|^2, \quad (7.3.2)$$

$$V_D = \sum_{\alpha=1}^r \left( \sum_{i=1}^d Q_i^{(\alpha)} |x_i|^2 - \sum_{l=1}^{\gamma} M_l^{(\alpha)} |p_l|^2 - \xi^{(\alpha)} \right)^2. \quad (7.3.3)$$

The defining map of the bundle  $V$  has degrees  $(9,9,8,4)$ . On the singular locus  $x_1 = x_2 = x_3 = x_4 = 0$ , a generic degree 9 polynomial can not go to 0, which means not all  $F$ 's go to 0, then  $\langle p \rangle = 0$  which is constrained. So the vacuum space is compact. However, it is still unclear how the presence of this singularity affects the conclusions of TSD. We turn now to approaches to resolving the  $Z_3$  singularity.

Now we are going to try to resolve the  $\mathbb{Z}_3$  singularity.

### 7.3.1 Resolution of Ambient Space

We begin by torically resolving the ambient space. In a toric description of (7.3.1), the vertices can be written as:

$$\begin{aligned} v_1 &= (-2, -2, -2, -3, -3), \\ v_2 &= (1, 0, 0, 0, 0), \\ v_3 &= (0, 1, 0, 0, 0), \\ v_4 &= (0, 0, 1, 0, 0), \\ v_5 &= (0, 0, 0, 1, 0), \\ v_6 &= (0, 0, 0, 0, 1). \end{aligned}$$

Then a new vertex  $v_7$  is added to the ambient space to resolve the singularity s.t.  $v_5 + v_6 + v_7 = 0$ :

$$v_7 = (0, 0, 0, -1, -1).$$

The resolved ambient space is described by fields with  $U(1)$  charges:

| $x_i$ |   |   |   |   |   |   |
|-------|---|---|---|---|---|---|
| 0     | 0 | 0 | 0 | 1 | 1 | 1 |
| 1     | 2 | 2 | 2 | 3 | 3 | 0 |

(7.3.4)

The SI ideal requires that  $(x_1, x_2, x_3, x_4)$  are not equal to 0 simultaneously, and  $(x_5, x_6, x_7)$  are not equal to 0 simultaneously. So the singular curve  $x_1 = x_2 = x_3 = x_4 = 0$  is resolved.



With this resolution of the ambient space, we turn to the second step to find the resolution of the hypersurfaces.

### 7.3.2 Resolution of Manifold/Hypersurfaces

Let's consider how the ambient space resolution affects the CY hypersurfaces. Our initial manifold is described in the GLSM by

| $x_i$       | $\Gamma^j$ |
|-------------|------------|
| 1 2 2 2 3 3 | -5 -8      |

(7.3.5)

The hypersurfaces are:

$$\begin{aligned}
G_1 &= P_5(x_1) + P_3(x_1)P_1(x_{2-4}) + P_1(x_1)P_2(x_{2-4}) \\
&\quad + P_2(x_1)P_1(x_{5,6}) + P_1(x_{2-4})P_1(x_{5,6}), \\
G_2 &= P_8(x_1) + P_6(x_1)P_1(x_{2-4}) + P_4(x_1)P_2(x_{2-4}) + P_2(x_1)P_3(x_{2-4}) + P_4(x_{2-4}) \\
&\quad + P_5(x_1)P_1(x_{5,6}) + P_3(x_1)P_1(x_{2-4})P_1(x_{5,6}) + P_1(x_1)P_2(x_{2-4})P_1(x_{5,6}) \\
&\quad + P_2(x_1)P_2(x_{5,6}) + P_1(x_{2-4})P_2(x_{5,6}).
\end{aligned}
\tag{7.3.6}$$

The resolved manifold is described in the GLSM by

| $x_i$         | $\Gamma^j$ |
|---------------|------------|
| 0 0 0 0 1 1 1 | -1 -2      |
| 1 2 2 2 3 3 0 | -5 -8      |

(7.3.7)

The hypersurfaces are:

$$\begin{aligned}
G'_1 &= \left( P_5(x_1) + P_3(x_1)P_1(x_{2-4}) + P_1(x_1)P_2(x_{2-4}) \right) x_7 \\
&\quad + P_2(x_1)P_1(x_{5,6}) + P_1(x_{2-4})P_1(x_{5,6}), \\
G'_2 &= \left( P_8(x_1) + P_6(x_1)P_1(x_{2-4}) + P_4(x_1)P_2(x_{2-4}) + P_2(x_1)P_3(x_{2-4}) + P_4(x_{2-4}) \right) x_7^2 \\
&\quad + \left( P_5(x_1)P_1(x_{5,6}) + P_3(x_1)P_1(x_{2-4})P_1(x_{5,6}) + P_1(x_1)P_2(x_{2-4})P_1(x_{5,6}) \right) x_7 \\
&\quad + P_2(x_1)P_2(x_{5,6}) + P_1(x_{2-4})P_2(x_{5,6}).
\end{aligned}
\tag{7.3.8}$$

When  $x_7$  goes to 1,  $G'_1$  and  $G'_2$  become the same as  $G_1$  and  $G_2$ .

Additionally,  $h^{1,1}(X) = 2$ ,  $h^{2,1}(X) = 53$ , so it is clear that this is a resolution of the manifold.

### 7.3.3 Resolution of the Bundle

To lift the monad bundle in (7.3.1) to the resolved geometry in (7.3.7), we have the constraint [38, 63] that the bundle on the resolution must satisfy anomaly cancellation. From the definition, the new bundle should reduce to the old one in the blow-down (i.e. singular) limit. Such bundle resolutions are not unique. Here we will write down the defining map of bundle  $V$ , and compare with the defining map of the resolved one.

Our initial GLSM is described by the data

| $x_i$       | $\Gamma^j$ | $\Lambda^a$ | $p_l$ |
|-------------|------------|-------------|-------|
| 1 2 2 2 3 3 | -5 -8      | 1 1 2 6     | -10   |

(7.3.9)

The defining map  $F$  of the bundle has degrees

$$\|F_1^1\| = 9, \quad \|F_2^1\| = 9, \quad \|F_3^1\| = 8, \quad \|F_4^1\| = 4. \quad (7.3.10)$$

Now we write down the polynomials in  $F$  in terms of  $x_{1-4}$  and  $x_{5,6}$ . Note that the subscript is the same as the degree if written in  $x_1$ , for example  $P_9(x_5)$  means  $x_5^9$ .

$$F = \left[ \begin{array}{cccc} P_9(x_{5,6}) & P_9(x_{5,6}) & P_6(x_{5,6})P_2(x_{1-4}) & P_3(x_{5,6})P_1(x_{1-4}) \\ +P_6(x_{5,6})P_3(x_{1-4}) & +P_6(x_{5,6})P_3(x_{1-4}) & +P_3(x_{5,6})P_5(x_{1-4}) & +P_4(x_{1-4}) \\ +P_3(x_{5,6})P_6(x_{1-4}) & +P_3(x_{5,6})P_6(x_{1-4}) & +P_8(x_{1-4}) & \\ +P_9(x_{1-4}) & +P_9(x_{1-4}) & & \end{array} \right] \quad (7.3.11)$$

To match the old bundle in the singular limit, we make (part of)  $\tilde{F}$  the same as  $F$ . The solution  $(\tilde{X}, \tilde{V})$  is written below in terms of GLSM data:

| $x_i$         | $\Gamma^j$ | $\Lambda^a$ | $p_l$ |
|---------------|------------|-------------|-------|
| 0 0 0 0 1 1 1 | -1 -2      | 0 0 1 2     | -3    |
| 1 2 2 2 3 3 0 | -5 -8      | 1 1 2 6     | -10   |

(7.3.12)

This example has  $h(V) = (0, 72, 0, 0)$ . In addition, every line bundle has the same cohomol-

ogy as before blowing up. Also  $h(V \times V^*) = (1, 174, 174, 1)$ .

If we write out the map  $F$  defining the bundle, it has degrees

$$\|F_1^1\| = \binom{3}{9}, \quad \|F_2^1\| = \binom{3}{9}, \quad \|F_3^1\| = \binom{2}{8}, \quad \|F_4^1\| = \binom{1}{4}. \quad (7.3.13)$$

write down the polynomials in  $F$ , where the subscript of  $P$  indicates the degree of the second  $U(1)$ :

$$F = \begin{bmatrix} P_9(x_{5,6}) & P_9(x_{5,6}) & P_6(x_{5,6})P_2(x_{1-4}) & P_3(x_{5,6})P_1(x_{1-4}) \\ +x_7P_6(x_{5,6})P_3(x_{1-4}) & +x_7P_6(x_{5,6})P_3(x_{1-4}) & +x_7P_3(x_{5,6})P_5(x_{1-4}) & +x_7P_4(x_{1-4}) \\ +x_7^2P_3(x_{5,6})P_6(x_{1-4}) & +x_7^2P_3(x_{5,6})P_6(x_{1-4}) & +x_7^2P_8(x_{1-4}) & \\ +x_7^3P_9(x_{1-4}) & +x_7^3P_9(x_{1-4}) & & \end{bmatrix} \quad (7.3.14)$$

When  $x_7$  goes to 1, it's exactly the same form as the old map. So it matches the old bundle in the singular limit. Unfortunately, anomaly cancellation is not satisfied in this model. We will return to this soon.

### 7.3.4 Aside: Getting the Same Result with Linear Combinations

It is worth mentioning that the above result can also be acquired by a linear combination of charges. If we define  $Q = 3Q_1 + Q_2$ , and add a charge neutral scalar  $\mathcal{O}(1, -3)$ , then the original charge matrix can be written as:

| $x_i$          | $\Gamma^j$ | $\Lambda^a$ | $p_l$ |          |
|----------------|------------|-------------|-------|----------|
| 0 0 0 0 1 1 1  | -1 -2      | 0 0 1 2     | -3    | (7.3.15) |
| 1 2 2 2 0 0 -3 | -2 -2      | 1 1 -1 0    | -1    |          |

If we multiply the first row by 3 and add to the second row, this recovers the above resolution.

### 7.3.5 Anomaly Cancellation Condition for the Bundle

As we have seen, the linear combination of charges does not protect anomaly cancellation automatically. However, the linear combination of charges is not unique. In case anything is missed, we decide to solve for all the possibilities. We'll consider three cases, choosing

different forms for the monad on the resolved manifold:

1. with 4 entries in  $\Lambda$  and 1 entry in  $p$  (the minimal choice),
2. with 5 entries in  $\Lambda$  and 1 entry in  $p$ , plus one fermionic symmetry (to bring back the rank of the bundle to 4),
3. with 6 entries in  $\Lambda$  and 1 entry in  $p$ , plus two fermionic symmetries (to bring back the rank of the bundle to 4).

In all cases, we keep part of the map as the form of  $\|F_1^1\| = 9, \|F_2^1\| = 9, \|F_3^1\| = 8, \|F_4^1\| = 4$ .

The first case is quite restrictive. To keep part of the map in the same form as the original degree (9,9,8,4) map, and to satisfy anomaly cancellation, it has to have degree (1,1,2,6) mapping to (10), this leads to the following parametric charge matrix data:

| $\Lambda^a$ |       |       |       | $p_l$                      |
|-------------|-------|-------|-------|----------------------------|
| $x_1$       | $x_2$ | $x_3$ | $x_4$ | $-(x_1 + x_2 + x_3 + x_4)$ |
| 1           | 1     | 2     | 6     | -10                        |

(7.3.16)

Unfortunately, the two anomaly cancellation constraints (arising from the first row and the cross rows) have no solution.

For the second case, keep part of the map as (9,9,8,4) and to satisfy anomaly cancellation, we can write it in the form below:

| $\Lambda^a$ |         |         |         |       | $p_l$                            |
|-------------|---------|---------|---------|-------|----------------------------------|
| $x_1$       | $x_2$   | $x_3$   | $x_4$   | $x_5$ | $-(x_1 + x_2 + x_3 + x_4 + x_5)$ |
| $1 + a$     | $1 + a$ | $2 + a$ | $6 + a$ | $-3a$ | $-(10 + a)$                      |

(7.3.17)

For the quadratic anomaly cancellation, there are three conditions. The second row indicates  $a = 0$ ; solve for the first row and the cross rows, there is only one solution:

| $\Lambda^a$ |   |   |   |    | $p_l$ |
|-------------|---|---|---|----|-------|
| 0           | 1 | 1 | 2 | -1 | -3    |
| 1           | 1 | 2 | 6 | 0  | -10   |

(7.3.18)

In this solution, the  $\mathcal{O}(-1, 0)$  may cause stability problem as  $h^3(\mathcal{O}(-1, 0)) = 1$ . We should recall however that the fermionic symmetry may change the structure. The bundle is defined

in the monad:

$$0 \rightarrow \mathcal{O} \rightarrow \mathcal{O}(0,1) \oplus \mathcal{O}(1,1) \oplus \mathcal{O}(1,2) \oplus \mathcal{O}(2,6) \oplus \mathcal{O}(-1,0) \rightarrow \mathcal{O}(3,10) \rightarrow 0. \quad (7.3.19)$$

Because  $h^0(V) = h^3(V) = 0$ , it is consistent with stability. In addition, here  $h(V \times V^*) = (1, 174, 174, 1)$ , the bundle is smooth.

Calculating the cohomology of  $V$  gives  $h(V) = (0, 73, 0, 0)$ . Note that  $h^1(V)$  is 73 instead of 72. Furthermore, this example exhibits another troubling feature. Namely when  $x_7$  goes to 1, the degree (2,9) component in the defining map does not recover the original degree 9 component. which means the resolved bundle does not match the original one in the singular locus.

The third case does not give any new solution.

In this scenario, there is no bundle resolution. However, more complicated models may lead to new solutions, for example, embedding the model in a bigger GLSM by adding repeated entries, and tuning the diagonal map components to zero.

### 7.3.6 Embed in a Bigger GLSM

Here we return to the resolution described in (7.3.12), which keeps part of the map but not satisfying anomaly cancellation. We will attempt to overcome the problems outlined in the previous section by embedding the bundle into a bigger GLSM, i.e. add more entries to compensate for the anomaly cancellation conditions, and tune the off-diagonal components to zero afterwards.

There is more than one way to enlarge the GLSM. One candidate described in GLSM data is:

| $x_i$         | $\Gamma^j$ | $\Lambda^a$ | $p_l$     |
|---------------|------------|-------------|-----------|
| 0 0 0 0 1 1 1 | -1 -2      | 0 0 1 2 2 0 | -3 -1 -1  |
| 1 2 2 2 3 3 0 | -5 -8      | 1 1 2 6 2 1 | -10 -2 -1 |

(7.3.20)

Here the  $O(1,2)$  entries cancel out. The anomaly cancellation condition is satisfied, and  $h(V) = (0, 72, 0, 0)$ .  $h(V \times V^*) = (1, 177, 177, 1)$ .

However this bundle is not smooth, the singularity is dimension 2 and the GLSM vacuum

space is not compact.

Adding different/more entries gives more possibilities, but the requirements of stability and smoothness will reduce the number of solutions.

In summary, we have not yet determined a fully satisfactory resolution of the singular geometry  $(X, V)$  in that the bundles on the resolved manifold exhibit problematic features. The methods employed above are not exhaustive. Although we have yet to find a good bundle on the resolved geometry, it is not yet clear whether or not any such bundle exists (which limits correctly to the singular monad), or whether it simply requires different tools than currently available to determine it.

# Chapter 8

## Conclusions and Future Directions

In this work we have explored the notion of  $(0, 2)$  target space duality in three aspects. In the first part of the work, we have studied in detail the four-dimensional effective potential in dual theories and the associated vacuum spaces. It has been an open question whether or not  $(0, 2)$  target space duality may correspond to a true string duality or merely a shared sub-locus in the moduli space of two distinct theories. While a full correspondence of  $(0, 2)$  heterotic string theories has yet to be established, our results appear to provide evidence for the former possibility. As in [31], we find that the full massless spectrum of the dual theories (in the geometric phase) is preserved

$$\begin{aligned} h^*(X, \wedge^k V) &= h^*(\tilde{X}, \wedge^k \tilde{V}), \\ h^{2,1}(X) + h^{1,1}(X) + h^1(X, \text{End}_0(V)) &= h^{2,1}(\tilde{X}) + h^{1,1}(\tilde{X}) + h^1(X, \text{End}_0(\tilde{V})). \end{aligned} \tag{8.0.1}$$

with  $k = 1 \dots rk(V)$  and that the anomaly cancellation conditions and equations of motion are automatically satisfied in the dual theories. Moreover, we make the novel observation that non-trivial geometric obstructions –corresponding to D- and F-term potentials – lead to the same vacuum space in the low energy theories. The central results of this work include the following

1. D-term and F-term constraints associated to stability and holomorphy constraints in the pair  $(X, V)$  appear to be faithfully reflected in the dual geometry  $(\tilde{X}, \tilde{V})$  for all the examples studied in this work.
2. The structure of the  $\mathcal{N} = 1$  vacuum space of the dual theories is identical. That is, beginning at given points in moduli space infinitesimal fluctuations are preserved, leading to commutative diagrams of bundle deformations as in (4.1.44).
3. We find that loci of enhanced symmetry – including stability walls (with enhanced Green-Schwarz massive  $U(1)$  symmetries) and  $(2, 2)$  loci are preserved across the dual-

ity (though the identification of such enhancement points can be subtle and not always in the perturbative regime of the theory).

To make the observations above we have developed a number of new technical tools including a generalization of the target space duality procedure itself (in Section 2.2.3) and the ability to describe complete infinitesimal bundle deformation spaces as monads (see Sections 4.1.3 and 4.1.3).

In the present work, our primary goal has been to compare the structure of the target space effective theories. A natural next step is to explore the examples considered here more fully at the level of GLSMS (or indeed full sigma models when possible). In this work, we have not considered the possible contributions from world sheet instantons to the potential (though in many cases for simple CICY GLSMs such as considered here, they may be expected to vanish [141–143]) or indeed the full structure of even the perturbative Yukawa couplings (see [90, 144–146] for example). Both should be studied to more fully understand the validity of the effective theories considered here and their possible duality. Other interesting future comparisons might include a calculation of spectra of the target space dual GLSMS in non-geometric phases (for example the Landau-Ginsburg spectra [61]), a study of the quantum cohomology rings in some simple cases [147] and perhaps even applying tools from localization [148] to investigate the detailed structure of the GLSMS themselves in more detail. We hope to address some of these questions in future work.

In the second part of the work we have taken a first step towards exploring the consequences of  $(0, 2)$  target space duality for heterotic/F-theory duality. In an important proof of principle, we have illustrated that heterotic TSD pairs exist in which both halves of the geometry exhibit Calabi-Yau threefolds with elliptic fibrations. As a result, it is clear that some F-theory correspondence should be induced in these cases. We take several steps to explore the properties of this putative duality. First, we consider the conjecture made previously in the literature that the F-theory realization of TSD could be multiple  $K3$  fibrations of the same elliptically fibered Calabi-Yau 4-fold background of F-theory. To explore this possibility in earnest, we begin in six-dimensional compactifications of heterotic string theory/F-theory and demonstrate that in general multiple fibrations within F-theory CY backgrounds cannot correspond to the (topologically trivial) TSD realizable for bundles on  $K3$  surfaces. Finally, we provide a sketch of the open questions that arise when attempting to directly compute the F-theory duals of four-dimensional heterotic TSD geometries. In particular, we demonstrate



that multiple  $K3$  fibrations in F-theory cannot account for  $(0, 2)$  TSD in the case that the threefold base,  $B_3$  of the F-theory elliptic fibration takes the form normally assumed – that of a  $\mathbb{P}^1$  bundle over a two (complex) dimensional surface,  $B_2$ .

There are a number of future directions that naturally lead on from this study, most importantly to explicitly determine the F-theory mechanism that generates dual theories from potentially disparate 4-fold geometries. We hope to understand this correspondence in future work. The present study has shed light on these questions however, and highlighted areas where the current state-of-the art in the literature is insufficient to determine the dual heterotic/F-theory geometries.

As noted in Section 6.3, it is clear that new tools will be needed to fully determine this duality. The new geometric features that must be understood in heterotic/F-theory duality in this context clearly extend beyond the canonical assumptions made in [54] and new tools must be developed. These include the following open problems in heterotic/F-theory duality

- Heterotic compactifications on elliptic threefolds with higher rank Mordell-Weil group (as in the examples in Section 6.1).
- F-theory compactifications on threefold bases that are  $\mathbb{P}^1$  fibered, but not  $\mathbb{P}^1$  bundles. I.e. F-theory on elliptic fibrations with *conic bundle* (see e.g. [137]) bases.
- F-theory duals of degenerate (i.e. non-reduced and reducible) heterotic spectral covers. These seem to be a ubiquitous feature in the context of  $(0, 2)$  target space duality since the spectral data of monad bundles appear to be generically singular [126].
- Four-dimensional T-brane solutions of F-theory (expected to arise in the context of degenerate spectral covers above [57, 59, 149]).

This last point seems to be an essential part of the story for four-dimensional heterotic/F-theory pairs since degenerate spectral data naturally arise for monad bundles (and hence geometries arising from  $(0, 2)$  GLSMs). Moreover, the arguments of Section 6.3 make it clear that the degrees of freedom of an expected dual F-theory 4-fold must be constrained by flux in order to match the moduli count of the heterotic theory. Several of these “missing ingredients” are currently being studied (see [55] for generalizations of heterotic geometries in heterotic/F-theory duality and [56] for a study of F-theory on conic bundles). We hope that the present work illustrates the need for these new tools and demonstrates that there remain

many interesting open questions within the context of four-dimensional heterotic/F-theory duality. We will return to these open questions in future work.

In the last part of the work, we have extended the analysis of target space duality to the non-geometric phases. To date, the study of target space duality is mainly within geometric phases, with little knowledge about the LG phase or hybrid phase to perform the dual procedure. In trivial cases the dual models share identical Landau-Ginzburg phases, but this is not necessary for producing target space duals. To find whether the dual pair are the same LG models, we calculated the massless spectra for a pair of target space duals. Even though they share identical LG phase in this case, resolving the singularity in large radius leads to a new configuration, the relationship between them is a potential topic under exploration.

$$\begin{array}{ccc}
 (X', V') & & \\
 \uparrow \text{resolve} & \searrow ? & \\
 (X, V) & \xleftrightarrow{TSD} \text{LG point} \xleftrightarrow{TSD} & (\tilde{X}, \tilde{V})
 \end{array}$$

Our results include:

1. We have calculated the massless spectra for a pair of target space duals on weighted projective space, which is comparable with the cohomology in geometric phase.
2. We have listed the constraints and tools to resolve the singularity in geometric space, the step-by-step procedure for the resolution, and some new tools developed.

The primary goal of the work is to probe target space duality in the level of GLSMs. In the next step we could extend the massless spectra calculation to hybrid phases. In target space duality, two sides may have quite different phases, they share only one common LG/hybrid phase. The calculation of full massless spectra will give us the answer that whether they are the same GLSM. Another interesting direction is the resolution of singularity. Even though there may be more than one resolution, a systematic way, or at least the judgement of whether there exists a resolution, is needed.

# Appendices

# Appendix A

## Examples of Target Space Dual Chains

### A.1 A Complete List of Target Space Dual Theories

This appendix is from our previous paper [41]. In this appendix, we provide the complete mirror chain of the bundle investigated in Section 4.1. Specifically, we apply the version of the algorithm which enhances the number of  $U(1)$  symmetries (see Section 2.2.2) and choose the field redefinitions such that the target space duals will remain within the class of CICYs [60]. To generate the complete list of target space dual theories within this class, the generalized procedure outlined in Section 2.2.3 (which allows for repeated line bundles in the monad) is applied.

The bundle given in (4.1.4) was studied in detail in Section 4.1. Once again, the GLSM data of this starting point is given by

| $x_i$       | $\Gamma^j$ | $\Lambda^a$      | $p_l$    |
|-------------|------------|------------------|----------|
| 1 1 0 0 0 0 | -2         | 1 -1 0 0 2 1 1 2 | -3 -1 -2 |
| 0 0 1 1 1 1 | -4         | -1 1 1 1 1 2 2 2 | -2 -4 -3 |

(A.1.1)

As in Section 2.2.3, the complete list of repeated line bundles, leading to new target space duals, must be determined. Following the criteria of non-trivial morphisms in (2.2.19) yields the following set:

$$\{\mathcal{O}(1, 0), \mathcal{O}(2, 0), \mathcal{O}(3, 0), \mathcal{O}(0, 1), \mathcal{O}(1, 1), \mathcal{O}(2, 1), \mathcal{O}(3, 1), \\ \mathcal{O}(0, 2), \mathcal{O}(1, 2), \mathcal{O}(2, 2), \mathcal{O}(0, 3), \mathcal{O}(1, 3), \mathcal{O}(0, 4)\}.$$
(A.1.2)

The complete list of dual geometries is given here, categorized by repeated entry:

1. No repeated entries, analyzed in Section 4.1.

| $x_i$          | $\Gamma^j$ | $\Lambda^a$       | $p_l$    |
|----------------|------------|-------------------|----------|
| $\mathbb{P}^1$ | -1 -1      | 0 0 1 0 0 0 0 0 0 | 0 0 -1   |
| $\mathbb{P}^1$ | -2 0       | 1 -1 0 0 2 1 1 2  | -3 -1 -2 |
| $\mathbb{P}^3$ | -2 -2      | -1 1 -1 1 3 2 2 2 | -2 -4 -3 |

(A.1.3)

2. Repeated entry  $\mathcal{O}(1, 0) \oplus \mathcal{O}(3, 0)$

| $x_i$          | $\Gamma^j$ | $\Lambda^a$           | $p_l$          |
|----------------|------------|-----------------------|----------------|
| $\mathbb{P}^1$ | -1 -1      | 0 0 0 0 0 0 0 0 1 0   | -1 0 0 0 0     |
| $\mathbb{P}^1$ | -2 0       | 1 -1 0 0 2 1 1 2 1 3  | -3 -1 -2 -1 -3 |
| $\mathbb{P}^3$ | -2 -2      | -1 1 1 1 1 2 2 2 -2 2 | -2 -4 -3 0 0   |

(A.1.4)

3. Repeated entry  $\mathcal{O}(1, 0)$

| $x_i$          | $\Gamma^j$ | $\Lambda^a$         | $p_l$       |
|----------------|------------|---------------------|-------------|
| $\mathbb{P}^1$ | -1 -1      | 0 0 0 0 0 1 0 0 0   | 0 0 -1 0    |
| $\mathbb{P}^1$ | -1 -1      | 1 -1 0 0 2 0 1 2 2  | -3 -1 -2 -1 |
| $\mathbb{P}^3$ | -1 -3      | -1 1 1 1 1 -1 2 2 3 | -2 -4 -3 0  |

(A.1.5)

4. Repeated entry  $\mathcal{O}(0, 3)$ .

| $x_i$          | $\Gamma^j$ | $\Lambda^a$         | $p_l$       |
|----------------|------------|---------------------|-------------|
| $\mathbb{P}^1$ | -1 -1      | 0 0 1 0 0 0 0 0 0   | 0 -1 0 0    |
| $\mathbb{P}^1$ | -1 -1      | 1 -1 -1 0 2 1 1 2 1 | -3 -1 -2 0  |
| $\mathbb{P}^3$ | -3 -1      | -1 1 0 1 1 2 2 2 4  | -2 -4 -3 -3 |

(A.1.6)

5. Repeated entry  $\mathcal{O}(3, 1)$

| $x_i$          | $\Gamma^j$ | $\Lambda^a$         | $p_l$       |
|----------------|------------|---------------------|-------------|
| $\mathbb{P}^1$ | -1 -1      | 1 0 0 0 0 0 0 0 0 0 | -1 0 0 0    |
| $\mathbb{P}^1$ | -2 0       | 1 -1 0 0 2 1 1 2 3  | -3 -1 -2 -3 |
| $\mathbb{P}^3$ | -3 -1      | -2 1 1 1 1 2 2 2 2  | -2 -4 -3 -1 |

(A.1.7)

6. Repeated entry  $\mathcal{O}(1, 3)$

| $x_i$          | $\Gamma^j$ | $\Lambda^a$         | $p_l$       |
|----------------|------------|---------------------|-------------|
| $\mathbb{P}^1$ | -1 -1      | 0 1 0 0 0 0 0 0 0 0 | 0 -1 0 0    |
| $\mathbb{P}^1$ | -2 0       | 1 -1 0 0 2 1 1 2 1  | -3 -1 -2 -1 |
| $\mathbb{P}^3$ | -3 -1      | -1 0 1 1 1 2 2 2 4  | -2 -4 -3 -3 |

(A.1.8)

7. Repeated entry  $\mathcal{O}(2, 0) \oplus \mathcal{O}(2, 0)$

| $x_i$          | $\Gamma^j$ | $\Lambda^a$           | $p_l$          |
|----------------|------------|-----------------------|----------------|
| $\mathbb{P}^1$ | -1 -1      | 0 0 0 0 0 0 0 0 1 0   | -1 0 0 0 0     |
| $\mathbb{P}^1$ | -1 -1      | 1 -1 0 0 2 1 1 2 1 3  | -3 -1 -2 -2 -2 |
| $\mathbb{P}^3$ | -2 -2      | -1 1 1 1 1 2 2 2 -2 2 | -2 -4 -3 0 0   |

(A.1.9)

8. Repeated entry  $\mathcal{O}(1, 1) \oplus \mathcal{O}(1, 1)$

| $x_i$          | $\Gamma^j$ | $\Lambda^a$           | $p_l$          |
|----------------|------------|-----------------------|----------------|
| $\mathbb{P}^1$ | -1 -1      | 0 0 0 0 0 0 0 0 1 0   | 0 0 -1 0 0     |
| $\mathbb{P}^1$ | -1 -1      | 1 -1 0 0 2 1 1 2 0 2  | -3 -1 -2 -1 -1 |
| $\mathbb{P}^3$ | -2 -2      | -1 1 1 1 1 2 2 2 -1 3 | -2 -4 -3 -1 -1 |

(A.1.10)

9. Repeated entry  $\mathcal{O}(0, 2) \oplus \mathcal{O}(0, 2)$

| $x_i$          | $\Gamma^j$ | $\Lambda^a$           | $p_l$          |
|----------------|------------|-----------------------|----------------|
| $\mathbb{P}^1$ | -1 -1      | 0 0 0 0 0 0 0 0 1 0   | 0 -1 0 0 0     |
| $\mathbb{P}^1$ | -1 -1      | 1 -1 0 0 2 1 1 2 -1 1 | -3 -1 -2 0 0   |
| $\mathbb{P}^3$ | -2 -2      | -1 1 1 1 1 2 2 2 0 4  | -2 -4 -3 -2 -2 |

(A.1.11)

10. Repeated entry  $\mathcal{O}(1, 3)$

| $x_i$          | $\Gamma^j$ | $\Lambda^a$         | $p_l$       |
|----------------|------------|---------------------|-------------|
| $\mathbb{P}^1$ | -1 -1      | 0 1 0 0 0 0 0 0 0 0 | 0 0 0 -1    |
| $\mathbb{P}^1$ | -1 -1      | 1 -1 -1 1 2 1 1 2 1 | -3 -1 -2 -1 |
| $\mathbb{P}^3$ | -2 -2      | -1 -1 1 3 1 2 2 2 3 | -2 -4 -3 -3 |

(A.1.12)

11. Repeated entry  $\mathcal{O}(1, 3)$ . Note that this CY 3-fold is known to be equivalent to the initial  $\{2, 4\}$  manifold in (A.1.1) by CICY equivalences [60]. See Section 4.1.5 for a discussion.

| $x_i$          | $\Gamma^j$ | $\Lambda^a$         | $p_l$       |
|----------------|------------|---------------------|-------------|
| $\mathbb{P}^1$ | -1 -1      | 1 0 0 0 0 0 0 0 0 0 | 0 0 -1 0    |
| $\mathbb{P}^1$ | -1 -1      | 0 -1 0 0 2 1 1 2 2  | -3 -1 -2 -1 |
| $\mathbb{P}^3$ | -4 0       | -1 1 1 1 1 2 2 2 3  | -2 -4 -3 -3 |

(A.1.13)

12. Repeated entry  $\mathcal{O}(0, 2) \oplus \mathcal{O}(2, 0)$

| $x_i$          | $\Gamma^j$ | $\Lambda^a$           | $p_l$         |
|----------------|------------|-----------------------|---------------|
| $\mathbb{P}^1$ | -1 -1      | 0 0 0 0 0 0 0 0 1 0   | 0 0 -1 0 0    |
| $\mathbb{P}^1$ | 0 -2       | 1 -1 0 0 2 1 1 2 0 2  | -3 -1 -2 -2 0 |
| $\mathbb{P}^3$ | -3 -1      | -1 1 1 1 1 2 2 2 -1 3 | -2 -4 -3 0 -2 |

(A.1.14)

13. Repeated entry  $\mathcal{O}(1, 2)$

| $x_i$          | $\Gamma^j$ | $\Lambda^a$         | $p_l$       |
|----------------|------------|---------------------|-------------|
| $\mathbb{P}^1$ | -1 -1      | 1 0 0 0 0 0 0 0 0 0 | 0 0 0 -1    |
| $\mathbb{P}^1$ | 0 -2       | -1 1 0 0 2 1 1 2 1  | -3 -1 -2 -1 |
| $\mathbb{P}^3$ | -3 -1      | -2 2 1 1 1 2 2 2 2  | -2 -4 -3 -2 |

(A.1.15)

14. Repeated entry  $\mathcal{O}(1, 0) \oplus \mathcal{O}(1, 0) \oplus \mathcal{O}(2, 2)$

| $x_i$          | $\Gamma^j$ | $\Lambda^a$             | $p_l$             |
|----------------|------------|-------------------------|-------------------|
| $\mathbb{P}^1$ | -1 -1      | 0 0 0 0 0 0 0 0 0 1 0   | 0 0 0 -1 0 0      |
| $\mathbb{P}^1$ | -1 -1      | 1 -1 0 0 2 1 1 2 2 0 2  | -3 -1 -2 -2 -1 -1 |
| $\mathbb{P}^3$ | -2 -2      | -1 1 1 1 1 2 2 2 2 -2 2 | -2 -4 -3 -2 0 0   |

(A.1.16)

15. Repeated entry  $\mathcal{O}(1, 1) \oplus \mathcal{O}(2, 2)$

| $x_i$          | $\Gamma^j$ | $\Lambda^a$           | $p_l$          |
|----------------|------------|-----------------------|----------------|
| $\mathbb{P}^1$ | -1 -1      | 1 0 0 0 0 0 0 0 0 0 0 | 0 0 0 -1 0     |
| $\mathbb{P}^1$ | -1 -1      | 0 -1 0 0 2 1 1 2 2 2  | -3 -1 -2 -2 -1 |
| $\mathbb{P}^3$ | -3 -1      | -2 1 1 1 2 2 2 2 2 2  | -2 -4 -3 -2 -1 |

(A.1.17)

16. Repeated entry  $\mathcal{O}(1, 3) \oplus \mathcal{O}(1, 3)$

| $x_i$          | $\Gamma^j$ | $\Lambda^a$           | $p_l$          |
|----------------|------------|-----------------------|----------------|
| $\mathbb{P}^1$ | -1 -1      | 0 1 0 0 0 0 0 0 0 0 0 | 0 0 0 -1 0     |
| $\mathbb{P}^1$ | -2 0       | 1 -1 0 0 2 1 1 2 1 1  | -3 -1 -2 -1 -1 |
| $\mathbb{P}^3$ | -2 -2      | -1 -1 1 1 1 2 2 2 3 3 | -2 -4 -3 -3 -1 |

(A.1.18)



## A.2 Target Space Dual Chain to a New Description of the Monad

Here we provide the complete list of 10 target space duals beginning from the bundle given in (4.1.59). In Section 4.1.6, it was argued that this bundle shares a stability wall with the bundle given in (A.1.1) in the previous subsection, and is in fact isomorphic to  $V$  given in (4.1.37), though described as a new monad. This alternative description of the same geometry leads to yet another chain of target space dual geometries. This list can contain different representations of the same geometries listed in Section 4.1.3 as well as new pairs  $(\tilde{X}, \tilde{V})$ . To begin we consider:

| $x_i$       | $\Gamma^j$ | $\Lambda^a$    | $p_l$ |
|-------------|------------|----------------|-------|
| 1 1 0 0 0 0 | -2         | 0 0 0 0 1 1 1  | -1 -2 |
| 0 0 1 1 1 1 | -4         | 1 1 1 2 -1 1 2 | -4 -3 |

(A.2.1)

On the stability wall given by  $\mu(\mathcal{O}(1, -1)) = 0$ , this bundle is equivalent to the reducible bundle given in (4.1.17).

Once again, it is possible to generate a chain of inequivalent target space duals by adding repeated line bundle entries to the monad. The relevant set of line bundles is

$$\{\mathcal{O}(1, 0), \mathcal{O}(2, 0), \mathcal{O}(1, 1), \mathcal{O}(2, 1), \mathcal{O}(0, 2), \mathcal{O}(1, 2), \mathcal{O}(2, 2), \mathcal{O}(0, 3), \mathcal{O}(1, 3), \mathcal{O}(0, 4)\}.$$
(A.2.2)

The list of 10 target space duals for which the 3-fold is a CICY in products of projective spaces is given below.

1. Repeated entry  $\mathcal{O}(1, 0)$

| $x_i$          | $\Gamma^j$ | $\Lambda^a$       | $p_l$    |
|----------------|------------|-------------------|----------|
| $\mathbb{P}^1$ | -1 -1      | 0 0 0 0 0 0 1 0   | 0 -1 0   |
| $\mathbb{P}^1$ | -1 -1      | 0 0 0 0 1 1 0 2   | -1 -2 -1 |
| $\mathbb{P}^3$ | -1 -3      | 1 1 1 2 -1 1 -1 3 | -4 -3 0  |

(A.2.3)

2. Repeated entry  $\mathcal{O}(0, 3)$

| $x_i$          | $\Gamma^j$ | $\Lambda^a$      | $p_l$    |
|----------------|------------|------------------|----------|
| $\mathbb{P}^1$ | -1 -1      | 0 0 1 0 0 0 0 0  | -1 0 0   |
| $\mathbb{P}^1$ | -1 -1      | 0 0 -1 0 1 1 1 1 | -1 -2 0  |
| $\mathbb{P}^3$ | -3 -1      | 1 1 0 2 -1 1 2 4 | -4 -3 -3 |

(A.2.4)

3. Repeated entry  $\mathcal{O}(2,0)$

| $x_i$          | $\Gamma^j$ | $\Lambda^a$       | $p_l$    |
|----------------|------------|-------------------|----------|
| $\mathbb{P}^1$ | -1 -1      | 0 0 0 1 0 0 0 0   | 0 -1 0   |
| $\mathbb{P}^1$ | -2 0       | 0 0 0 0 1 1 1 2   | -1 -2 -2 |
| $\mathbb{P}^3$ | -1 -3      | 1 1 1 -1 -1 1 2 3 | -4 -3 0  |

(A.2.5)

4. Repeated entry  $\mathcal{O}(1,1)$

| $x_i$          | $\Gamma^j$ | $\Lambda^a$       | $p_l$    |
|----------------|------------|-------------------|----------|
| $\mathbb{P}^1$ | -1 -1      | 0 0 0 0 0 1 0 0   | 0 -1 0   |
| $\mathbb{P}^1$ | -1 -1      | 0 0 0 0 1 0 1 2   | -1 -2 -1 |
| $\mathbb{P}^3$ | -2 -2      | 1 1 1 2 -1 -1 2 3 | -4 -3 -1 |

(A.2.6)

5. Repeated entry  $\mathcal{O}(0,2)$

| $x_i$          | $\Gamma^j$ | $\Lambda^a$      | $p_l$    |
|----------------|------------|------------------|----------|
| $\mathbb{P}^1$ | -1 -1      | 0 0 0 1 0 0 0 0  | -1 0 0   |
| $\mathbb{P}^1$ | -1 -1      | 0 0 0 -1 1 1 1 1 | -1 -2 0  |
| $\mathbb{P}^3$ | -2 -2      | 1 1 1 0 -1 1 2 4 | -4 -3 -2 |

(A.2.7)

6. Repeated entry  $\mathcal{O}(1,3)$

| $x_i$          | $\Gamma^j$ | $\Lambda^a$       | $p_l$    |
|----------------|------------|-------------------|----------|
| $\mathbb{P}^1$ | -1 -1      | 1 0 0 0 0 0 0 0   | 0 0 -1   |
| $\mathbb{P}^1$ | -1 -1      | -1 1 0 0 1 1 1 1  | -1 -2 -1 |
| $\mathbb{P}^3$ | -2 -2      | -1 3 1 2 -1 1 2 3 | -4 -3 -3 |

(A.2.8)

7. Repeated entry  $\mathcal{O}(2,1)$

| $x_i$          | $\Gamma^j$ | $\Lambda^a$       | $p_l$    |
|----------------|------------|-------------------|----------|
| $\mathbb{P}^1$ | -1 -1      | 0 0 1 0 0 0 0 0   | 0 -1 0   |
| $\mathbb{P}^1$ | -2 0       | 0 0 0 0 1 1 1 2   | -1 -2 -2 |
| $\mathbb{P}^3$ | -2 -2      | 1 1 -1 2 -1 1 2 3 | -4 -3 -1 |

(A.2.9)

8. Repeated entry  $\mathcal{O}(1, 3)$

| $x_i$          | $\Gamma^j$ | $\Lambda^a$      | $p_l$    |
|----------------|------------|------------------|----------|
| $\mathbb{P}^1$ | -1 -1      | 0 0 0 0 1 0 0 0  | 0 -1 0   |
| $\mathbb{P}^1$ | -1 -1      | 0 0 0 0 0 1 1 2  | -1 -2 -1 |
| $\mathbb{P}^3$ | -4 0       | 1 1 1 2 -1 1 2 3 | -4 -3 -3 |

(A.2.10)

9. Repeated entry  $\mathcal{O}(2, 2)$

| $x_i$          | $\Gamma^j$ | $\Lambda^a$      | $p_l$    |
|----------------|------------|------------------|----------|
| $\mathbb{P}^1$ | -1 -1      | 0 0 0 0 1 0 0 0  | 0 0 -1   |
| $\mathbb{P}^1$ | -1 -1      | 0 0 0 0 0 2 1 2  | -1 -2 -2 |
| $\mathbb{P}^3$ | -3 -1      | 1 1 1 2 -2 2 2 2 | -4 -3 -2 |

(A.2.11)

10. Repeated entry  $\mathcal{O}(1, 0) \oplus \mathcal{O}(1, 0) \oplus \mathcal{O}(2, 2)$

| $x_i$          | $\Gamma^j$ | $\Lambda^a$           | $p_l$          |
|----------------|------------|-----------------------|----------------|
| $\mathbb{P}^1$ | -1 -1      | 0 0 0 0 0 0 0 1 0 0   | 0 0 0 0 -1     |
| $\mathbb{P}^1$ | -1 -1      | 0 0 0 0 1 1 1 0 2 2   | -1 -2 -1 -1 -2 |
| $\mathbb{P}^3$ | -2 -2      | 1 1 1 2 -1 1 2 -2 2 2 | -4 -3 0 0 -2   |

(A.2.12)

# Appendix B

## Exotic Cases in Finding Elliptic Fibered Examples

This appendix has appeared in our paper [49]. In this appendix we present some of the exotic cases we encountered during the search for finding “good examples” of stable, smooth vector bundles over bases that are Weierstrass elliptic fibrations. All of these examples pass the usual necessary conditions for stability such as  $h^0(V) = 0$  and Bogomolov topological constraint, but either the spectrum charged hypermultiplets of the four-dimensional effective are different or the total moduli is not conserved. By using careful Fourier-Mukai analysis we can show that the first example is indeed unstable, so it explains the discrepancy, but the other two are perfectly stable vector bundles, and we are unable to explain the reason. In the third example that spectrum match on both sides one may suggest that the existence of the flux (which must exist due to the generically non-reduced spectral cover) may stabilize the moduli space.

| $x_i$          | $\Gamma^j$ | $\Lambda^a$ | $p_l$ |
|----------------|------------|-------------|-------|
| 3 2 1 0 0 0 0  | -6         | 1 0 1 1 1   | -1 -3 |
| 0 0 -2 1 1 0 0 | 0          | 1 3 -2 2 1  | -1 -4 |
| 0 0 -2 0 0 1 1 | 0          | 0 3 -2 3 0  | -1 -3 |

(B.0.1)

with the second Chern classes as:

$$\begin{aligned}
 c_2(X) &= 11\sigma^2 + 2\sigma D_1 + 2\sigma D_2 - 3D_1^2 - 4D_1 D_2 - 3D_2^2 = 24\sigma D_1 + 24\sigma D_2 - 4D_1 D_2, \\
 c_2(V) &= 3\sigma^2 + 11\sigma D_1 + 9\sigma D_2 - D_1^2 - 6D_1 D_2 - 6D_2^2 = 17\sigma D_1 + 15\sigma D_2 - 6D_1 D_2,
 \end{aligned}$$

where  $\sigma$ ,  $D_1$ , and  $D_2$  are the section and base divisors correspondingly, with  $D_1^2 = D_2^2 = 0$ , and  $D_1 D_2 = f$  the class of the generic fiber  $f$ . The anomaly cancellation is not satisfied in the strong sense, but we can still make sense of it at least as heterotic string theory (may be

not GLSM, but well defined as heterotic string theory). Again we embed this GLSM into a larger one:

| $x_i$               | $\Gamma^j$ | $\Lambda^a$ | $p_l$ |
|---------------------|------------|-------------|-------|
| 3 2 1 0 0 0 0 1 0   | -6 -1 0    | 1 0 1 1 1   | -1 -3 |
| 0 0 -2 1 1 0 0 -3 1 | 0 3 -1     | 1 3 -2 2 1  | -1 -4 |
| 0 0 -2 0 0 1 1 -2 1 | 0 2 -1     | 0 3 -2 3 0  | -1 -3 |

(B.0.2)

with the degrees of the monad maps is as follows:

| $F^1$       | $F^2$     |
|-------------|-----------|
| 0 1 0 0 0   | 2 3 2 2 2 |
| 0 -2 3 -1 0 | 3 1 6 2 3 |
| 1 -2 3 -2 1 | 3 0 5 0 3 |

(B.0.3)

After exchanging  $\Gamma^2, \Gamma^3$  (degree  $\|G_2\|, \|G_3\|$  respectively) with  $F_1^1, F_2^1$  respectively, and integrating out the repeated entries, the dual  $(\tilde{X}, \tilde{V})$  can be written as follows:

| $x_i$          | $\Gamma^j$ | $\Lambda^a$ | $p_l$ |
|----------------|------------|-------------|-------|
| 3 2 1 0 0 0 0  | -6         | 1 0 1 1 1   | -1 -3 |
| 0 0 -3 1 1 1 0 | 0          | 0 4 -2 2 1  | -1 -4 |
| 0 0 -2 0 0 1 1 | 0          | 0 3 -2 3 0  | -1 -3 |

(B.0.4)

The dual geometry is perfectly smooth and anomaly cancellation condition can also be make sense as before. However, the spectrum of charged scalars is not the same (i.e,  $h^1(V) = 121$  while  $h^1(\tilde{V}) = 101$ ). So there should be a problem. We can argue that it is related to the stability.

After a detailed calculation of Fourier-Mukai transform of  $V$ , it becomes clear that  $FM^1(V)$  is of relative rank 1 and degree 2. On the other hand  $FM^0(V)$  is also non zero with relative rank and degree 1 and -1. It is well known that the Fourier-Mukai transformation of a sheaf of relative rank and degree  $(n, d)$  is a *complex* of relative rank and degree  $(d, -n)$ . So it is clear from the above data that the restriction of  $V$  on a generic elliptic fiber  $E$  is roughly of the form  $\mathcal{O}_E(\sigma) \oplus \mathcal{V}_2$ , where  $\mathcal{V}_2$  is a rank 2 irreducible bundle of degree -1 on  $E$ . Obviously it tells us that the bundle must be unstable because it is unstable on generic fibers (even though

it seems  $h^0(V) = 0$ ). As a sanity check we can compute the rank of  $\pi_*V$  and  $\pi_*(V \otimes \mathcal{O}_X(\sigma))$ , and they are 1 and 3 respectively. This is consistent because  $h^*(\mathcal{V}_2) = (0, 1)$ <sup>1</sup>. A similar statement can be made about the TSD set up.

---

<sup>1</sup>One can also get the same numbers from semi stable bundles with rank 3 and degree zero, so they are just necessary conditions.

# Appendix C

## Non-trivial Rewriting

This appendix has appeared in our paper [49]. In this appendix, we present an example of a TSD pair in which the geometries  $(X, V)$  and  $(\tilde{X}, \tilde{V})$  are actually equivalent geometries, even though they are described by different algebraic descriptions (of manifolds and monad bundles). Another interesting feature in this case is that both sides of this “trivial” correspondence are elliptically fibered, however the base manifolds are two *different* Hirzebruch surfaces,  $\mathbb{F}_0$  and  $\mathbb{F}_2$ . These base surfaces are distinct as complex manifolds but identical as real (and the elliptic CY 3-fold over these different surfaces is the *same* complex manifold). This demonstrates that even “trivial” TSD correspondences may involve interesting geometric structure.

In the following example the bundle  $\tilde{V}$  on  $\tilde{X}$  as a non-trivial rewriting of bundle  $V$  on  $X$ . Both of the CY 3-folds are weighted projective space  $\mathbb{P}^2[123]$  fibered Calabi-Yau 3-folds. For  $X$  the base is Hirzebruch surface  $\mathbb{F}_0$ , i.e,  $B_2 = \mathbb{P}^3[2]$  while for  $\tilde{X}$  the base is  $\tilde{B}_2 = \left[ \begin{array}{c|cc} \mathbb{P}^3 & 1 & 1 \\ \mathbb{P}^1 & 1 & 1 \end{array} \right]$ , which is generically  $\mathbb{F}_0$  but at special complex structure moduli it “jumps” to become  $\mathbb{F}_2$  [67]. A  $(0, 2)$  target space map can be found that takes  $X$  to  $\tilde{X}$  (this can be achieved by adding a  $\mathbb{P}^1$  to the configuration as usual for a  $U(1)$ -changing TSD pair). On this manifold, both tangent bundle and non-tangent bundle will be studied.

## C.1 Non-trivial Rewriting with Tangent Bundle

Let us first consider the case of a deformation of the tangent bundle. The GLSM charge matrix is a general deformation of  $(X, V = TX + \mathcal{O}^{\oplus 2})$  and can be written as follows:

| $x_i$          | $\Gamma^j$ | $\Lambda^a$    | $p_l$ |
|----------------|------------|----------------|-------|
| 3 2 1 0 0 0 0  | -6 0       | 3 2 1 0 0 0 0  | -6 0  |
| 0 0 -2 1 1 1 1 | 0 -2       | 0 0 -2 1 1 1 1 | 0 -2  |

(C.1.1)

Following the procedure described in previous section, we will end up with the new charge matrix of the target space dual  $(\tilde{X}, \tilde{V})$  as:

| $x_i$              | $\Gamma^j$ | $\Lambda^a$    | $p_l$ |
|--------------------|------------|----------------|-------|
| 3 2 1 0 0 0 0 0 0  | -6 0 0     | 3 2 1 0 0 0 0  | -6 0  |
| 0 0 -2 1 1 1 1 0 0 | 0 -1 -1    | 0 0 -2 1 1 0 2 | 0 -2  |
| 0 0 0 0 0 0 0 1 1  | 0 -1 -1    | 0 0 0 0 0 1 0  | 0 -1  |

(C.1.2)

The number of both charged and uncharged geometric moduli of the theories on these two manifolds are the same, which suggests that they are indeed target space dual to each other. Such degree of freedom counting is given by:

$$\begin{aligned}
 h^*(V) &= (0, 241, 1, 0) & h^{1,1}(X) + h^{2,1}(X) + h^1(\text{End}_0(V)) &= 3 + 243 + 1074 = 1320, \\
 h^*(\tilde{V}) &= (0, 241, 1, 0) & h^{1,1}(\tilde{X}) + h^{2,1}(\tilde{X}) + h^1(\text{End}_0(\tilde{V})) &= 3 + 243 + 1074 = 1320
 \end{aligned}$$
(C.1.3)

### Calculate twist of $V$ and $\tilde{V}$

Starting with heterotic theory, without loss of generality, the second chern class can be splits as (5.1.3) and the heterotic Bianchi identity will implies further that  $\eta$  can be parameterized as (5.1.4) with the twist of the theory  $T' = T$ . In order to get the twist in our example, one can first calculate the second chern class of  $V$  and  $\tilde{V}$  as

$$\begin{aligned}
 c_2(V) &= c_2(TX) = 11J_1^2 + 2J_1J_2 - 2J_2^2, \\
 c_2(\tilde{V}) &= c_2(\tilde{TX}) = 11J_1^2 + 2J_1J_2 - 3J_2^2 + 2J_2J_3.
 \end{aligned}$$
(C.1.4)



For both  $X$  and  $\tilde{X}$ , the section can be parameterized as  $\sigma = J_1 - 2J_2$ , and the section satisfy the birational condition  $\sigma^2 = -c_1(B)\sigma$ . Then by applying eq.(5.1.3, 5.1.4) we get:

$$\eta = 24J_2, \quad T = 12J_2 = 6c_1(B) \quad (\text{C.1.5})$$

for both  $V$  and  $\tilde{V}$ . This indicates that if we start from a deformation of the tangent bundle, after target space dual we will at least end up with a TSD bundle over the same manifold that is topologically equivalent.

## Complex deformation of Bundle Moduli

We can further compare  $V$  and  $\tilde{V}$  by analyzing the deformation of these vector bundles. Consider the difference of  $V$  and  $\tilde{V}$  defined on  $B_2$  and  $\tilde{B}_2$  in the sequence separately, they are:

$$\begin{aligned} 0 \rightarrow V \rightarrow \mathcal{O}(0, 1)^{\oplus 2} \rightarrow \mathcal{O}(0, 2) \rightarrow 0, \\ 0 \rightarrow \tilde{V} \rightarrow \mathcal{O}(0, 0, 1) \oplus \mathcal{O}(0, 2, 0) \rightarrow \mathcal{O}(0, 2, 1) \rightarrow 0, \end{aligned} \quad (\text{C.1.6})$$

where  $V$  is the kernel of map with two degree  $\|1\|$  polynomials on  $B_2 = \left[ \mathbb{P}^3 \mid 2 \right]$ ,  $\tilde{V}$  is the kernel of the map  $F$  of degree  $\|0, 1\|$  and  $\|2, 0\|$  on  $\tilde{B}_2 = \left[ \begin{array}{c} \mathbb{P}^3 \\ \mathbb{P}^1 \end{array} \mid \begin{array}{cc} 1 & 1 \\ 1 & 1 \end{array} \right]$ . However for  $(\tilde{B}_2, \tilde{V})$ , if we first solve the polynomial of degree  $\|0, 1\|$  and put the constraint on the second map with degree  $\|2, 0\|$ , the second map will exactly reduce to a degree  $\|2\|$  polynomial on the manifold  $\left[ \mathbb{P}^3 \mid 1 \quad 1 \right]$ . So it seems that the bundle moduli in  $(\tilde{B}_2, \tilde{V})$  are transformed to the complex moduli in  $(B_2, V)$ . Then one would be interesting to ask whether it is possible that the complex structure and bundle moduli exchange in  $(X, V)$  and  $(\tilde{X}, \tilde{V})$ .

Before answering this question, there is an important observation as  $\tilde{B}_2$  is generically  $\mathbb{F}_0$ , but at a special point it ‘‘jumps’’ to become  $\mathbb{F}_2$ . Write down the defining equations for  $\tilde{B}_2 = \left[ \begin{array}{c} \mathbb{P}^3 \\ \mathbb{P}^1 \end{array} \mid \begin{array}{cc} 1 & 1 \\ 1 & 1 \end{array} \right]$  as:

$$\begin{aligned} z_0 w_0 + z_1 w_1 &= 0, \\ z_2 w_0 + \left( \sum_{i=0}^2 a_i z_i + \epsilon z_3 \right) w_1 &= 0, \end{aligned} \quad (\text{C.1.7})$$

with  $[z_0, z_1, z_2, z_3] \in \mathbb{P}^3$  and  $[w_0, w_1] \in \mathbb{P}^1$ . If  $\epsilon \neq 0$ , this system defines  $\mathbb{F}_0$ . When  $\epsilon = 0$ , a  $\mathbb{P}^1$  blows up at  $(0, 0, 0, 1) \in \mathbb{P}^3$ , which makes it becomes  $\mathbb{F}_2$ . So the question about whether the complex structure and bundle moduli exchange in  $(B_2, V)$  and  $(\tilde{B}_2, \tilde{V})$  changes to what happens for the geometric moduli of  $(\tilde{B}_2, \tilde{V})$  when  $\tilde{B}_2$  becomes  $\mathbb{F}_2$ , and the same for tuning the map of bundle in the  $(B_2, V)$  system.

So in calculating the line bundle cohomology in the new system  $(\tilde{B}_2, \tilde{V})$ , we will not only count the dimension of the cohomology group appearing in the sequence but also their polynomial representations and the explicit map. More specifically, we will set  $z_3 \in \mathbb{P}^3$  in our calculation to be zero to deform the  $\tilde{B}_2$  to be  $F_2$  and see what happens. In this case, the line bundle cohomology are  $h^*(\mathcal{O}(0, 1)) = \{2, 0, 0\}$ ,  $h^*(\mathcal{O}(2, 0)) = \{9, 0, 0\}$ ,  $h^*(\mathcal{O}(1, 1)) = \{12, 0, 0\}$  with and without turning the base manifold. Furthermore, we can check that the cohomology of bundle  $h^*(\tilde{B}_2, \tilde{V}) = \{4, 5, 0\}$  will not be affected by the tuning. On the other hand, we can also tune the complex structure of the map ( $x_7 = 0$  in  $F$ ) in defining the map of  $V$  in the  $(B_2, V)$  system. Again the deformation of the map does not change the bundle valued cohomology  $h^*(B_2, V) = \{1, 2, 0\}$ .

## C.2 Non-trivial Rewriting with General Vector Bundle

Similarly, we can consider another example with the same manifolds but different bundles. Again, we start from the following manifold with charge matrix for the form  $(X, V)$ :

| $x_i$          | $\Gamma^j$ | $\Lambda^a$ | $p_l$ |         |
|----------------|------------|-------------|-------|---------|
| 3 2 1 0 0 0 0  | -6 0       | 4 2 0 0 0   | -6 0  | (C.2.1) |
| 0 0 -2 1 1 1 1 | 0 -2       | 0 -2 2 2 1  | 0 -3  |         |

The second Chern classes of  $(X, TX)$  and  $(X, V)$  are given by

$$\begin{aligned}
 c_2(TX) &= 11J_1^2 + 2J_1J_2 - 2J_2^2, \\
 c_2(V) &= 8J_1^2 + 4J_1J_2 - 2J_2^2,
 \end{aligned}
 \tag{C.2.2}$$

which satisfy the  $c_2$  condition  $c_2(V) \leq c_2(TX)$ . The target space dual of this theory is given by the form of  $(\widetilde{X}, \widetilde{V})$ :

| $x_i$              | $\Gamma^j$ | $\Lambda^a$ | $p_l$ |         |
|--------------------|------------|-------------|-------|---------|
| 3 2 1 0 0 0 0 0 0  | -6 0 0     | 4 2 0 0 0   | -6 0  | (C.2.3) |
| 0 0 -2 1 1 1 1 0 0 | 0 -1 -1    | 0 -2 1 3 1  | 0 -3  |         |
| 0 0 0 0 0 0 0 1 1  | 0 -1 -1    | 0 0 1 0 0   | 0 -1  |         |

with second Chern classes:

$$\begin{aligned}
 c_2(\widetilde{TX}) &= 11J_1^2 + 2J_1J_2 - 3J_2^2 + 2J_2J_3, \\
 c_2(\widetilde{V}) &= 8J_1^2 + 4J_1J_2 - 3J_2^2 + 2J_2J_3.
 \end{aligned}
 \tag{C.2.4}$$

Once again we get their twists of the base to be the same:

$$\eta = 20J_2 \quad T = 8J_2$$

for both  $V$  and  $\widetilde{V}$ . These result indicates that this target space dual is just a kind of rewriting of the origin  $(X, V)$ .

# Bibliography

- [1] S. L. Glashow, “Partial Symmetries of Weak Interactions,” Nucl. Phys. **22**, 579 (1961).
- [2] A. Salam and J. C. Ward, “Electromagnetic and weak interactions,” Phys. Lett. **13**, 168 (1964).
- [3] S. Weinberg, “A Model of Leptons,” Phys. Rev. Lett. **19**, 1264 (1967).
- [4] F. Halzen and A. D. Martin, “Quarks And Leptons: An Introductory Course In Modern Particle Physics,” New York, USA: Wiley ( 1984) 396p
- [5] F. Abe *et al.* [CDF Collaboration], “Observation of top quark production in  $\bar{p}p$  collisions,” Phys. Rev. Lett. **74**, 2626 (1995) [hep-ex/9503002].
- [6] K. Kodama *et al.* [DONUT Collaboration], “Observation of tau neutrino interactions,” Phys. Lett. B **504**, 218 (2001) [hep-ex/0012035].
- [7] S. Chatrchyan *et al.* [CMS Collaboration], “Observation of a new boson at a mass of 125 GeV with the CMS experiment at the LHC,” Phys. Lett. B **716**, 30 (2012) [arXiv:1207.7235 [hep-ex]].
- [8] G. Aad *et al.* [ATLAS Collaboration], “Observation of a new particle in the search for the Standard Model Higgs boson with the ATLAS detector at the LHC,” Phys. Lett. B **716**, 1 (2012) [arXiv:1207.7214 [hep-ex]].
- [9] H. Georgi and S. L. Glashow, “Unity of All Elementary Particle Forces,” Phys. Rev. Lett. **32**, 438 (1974).
- [10] S. P. Martin, “A Supersymmetry primer,” Adv. Ser. Direct. High Energy Phys. **21**, 1 (2010) [Adv. Ser. Direct. High Energy Phys. **18**, 1 (1998)] [hep-ph/9709356].
- [11] C. Munoz, “Models of Supersymmetry for Dark Matter,” EPJ Web Conf. **136**, 01002 (2017) [arXiv:1701.05259 [hep-ph]].
- [12] M. B. Green, J. H. Schwarz and E. Witten, “Superstring Theory. Vol. 1: Introduction,” Cambridge, Uk: Univ. Pr. ( 1987) 469 P. ( Cambridge Monographs On Mathematical Physics)

- [13] M. B. Green, J. H. Schwarz and E. Witten, “Superstring Theory. Vol. 2: Loop Amplitudes, Anomalies And Phenomenology,” Cambridge, Uk: Univ. Pr. ( 1987) 596 P. ( Cambridge Monographs On Mathematical Physics)
- [14] P. Candelas, G. T. Horowitz, A. Strominger and E. Witten, “Vacuum Configurations for Superstrings,” Nucl. Phys. B **258**, 46 (1985).
- [15] E. Witten, “String theory dynamics in various dimensions,” Nucl. Phys. B **443**, 85 (1995) [hep-th/9503124].
- [16] C. Vafa, “Evidence for F theory,” Nucl. Phys. B **469**, 403 (1996) [hep-th/9602022].
- [17] L. B. Anderson, J. Gray, A. Lukas and B. Ovrut, “Stability Walls in Heterotic Theories,” JHEP **0909**, 026 (2009) [arXiv:0905.1748 [hep-th]].
- [18] L. B. Anderson, J. Gray, A. Lukas and B. Ovrut, “The Edge Of Supersymmetry: Stability Walls in Heterotic Theory,” Phys. Lett. B **677**, 190 (2009) [arXiv:0903.5088 [hep-th]].
- [19] L. B. Anderson, J. Gray, A. Lukas and B. Ovrut, “The Atiyah Class and Complex Structure Stabilization in Heterotic Calabi-Yau Compactifications,” JHEP **1110**, 032 (2011) [arXiv:1107.5076 [hep-th]].
- [20] L. B. Anderson, J. Gray, A. Lukas and B. Ovrut, “Vacuum Varieties, Holomorphic Bundles and Complex Structure Stabilization in Heterotic Theories,” JHEP **1307**, 017 (2013) [arXiv:1304.2704 [hep-th]].
- [21] E. R. Sharpe, “Kahler cone substructure,” Adv. Theor. Math. Phys. **2**, 1441 (1999) [hep-th/9810064].
- [22] K. Uhlenbeck and S. T. Yau, “On the existence of Hermitian Yang-Mills connections in stable bundles”, Comm. Pure App. Math., 39, 257, (1986).
- [23] S. Donaldson, “Anti Self-Dual Yang-Mills Connections over Complex Algebraic Surfaces and Stable Vector Bundles”, Proc. London Math. Soc., 3, 1, (1985).
- [24] L. B. Anderson, J. Gray and B. A. Ovrut, “Transitions in the Web of Heterotic Vacua,” Fortsch. Phys. **59**, 327 (2011) [arXiv:1012.3179 [hep-th]].

- [25] L. B. Anderson, J. Gray, A. Lukas and B. Ovrut, “Stabilizing All Geometric Moduli in Heterotic Calabi-Yau Vacua,” *Phys. Rev. D* **83**, 106011 (2011) [arXiv:1102.0011 [hep-th]].
- [26] L. B. Anderson, J. Gray, A. Lukas and B. Ovrut, “Stabilizing the Complex Structure in Heterotic Calabi-Yau Vacua,” *JHEP* **1102**, 088 (2011) [arXiv:1010.0255 [hep-th]].
- [27] M. F. Atiyah, “Complex Analytic Connections in Fibre Bundles”, *Trans. Amer. Math. Soc.*, Vol. 85, No. 1 (May 1957), pg. 181-207.
- [28] L. B. Anderson, “Heterotic and M-theory Compactifications for String Phenomenology,” arXiv:0808.3621 [hep-th].
- [29] E. Witten, “Phases of N=2 theories in two-dimensions,” *Nucl. Phys. B* **403**, 159 (1993) [hep-th/9301042].
- [30] J. Distler and S. Kachru, “Duality of (0,2) string vacua,” *Nucl. Phys. B* **442**, 64 (1995) [hep-th/9501111].
- [31] R. Blumenhagen and T. Rahn, “Landscape Study of Target Space Duality of (0,2) Heterotic String Models,” *JHEP* **1109**, 098 (2011) [arXiv:1106.4998 [hep-th]].
- [32] T. Rahn, “Target Space Dualities of Heterotic Grand Unified Theories,” *Proc. Symp. Pure Math.* **85**, 423 (2012) [arXiv:1111.0491 [hep-th]].
- [33] A. Strominger, “Massless black holes and conifolds in string theory,” *Nucl. Phys. B* **451**, 96 (1995) [hep-th/9504090].
- [34] A. Adams, A. Basu and S. Sethi, “(0,2) duality,” *Adv. Theor. Math. Phys.* **7**, no. 5, 865 (2003) [hep-th/0309226].
- [35] R. Blumenhagen, R. Schimmrigk and A. Wisskirchen, “(0,2) mirror symmetry,” *Nucl. Phys. B* **486**, 598 (1997) [hep-th/9609167].
- [36] I. Melnikov, S. Sethi and E. Sharpe, “Recent Developments in (0,2) Mirror Symmetry,” *SIGMA* **8**, 068 (2012) [arXiv:1209.1134 [hep-th]].
- [37] I. V. Melnikov and M. R. Plesser, “A (0,2) Mirror Map,” *JHEP* **1102**, 001 (2011) [arXiv:1003.1303 [hep-th]].

- [38] R. Blumenhagen, “Target space duality for (0,2) compactifications,” Nucl. Phys. B **513**, 573 (1998) [hep-th/9707198].
- [39] R. Blumenhagen, “(0,2) Target space duality, CICYs and reflexive sheaves,” Nucl. Phys. B **514**, 688 (1998) [hep-th/9710021].
- [40] A. Kapustin, M. Kreuzer, and K. G. Schlesinger, “Homological Mirror Symmetry: New Developments and Perspectives”, Springer, (2009).
- [41] L. B. Anderson and H. Feng, “New Evidence for (0,2) Target Space Duality,” J. Phys. A **50**, no. 6, 064004 (2017) [arXiv:1607.04628 [hep-th]].
- [42] A. Lukas and K. S. Stelle, “Heterotic anomaly cancellation in five-dimensions,” JHEP **0001**, 010 (2000) [hep-th/9911156].
- [43] R. Blumenhagen, G. Honecker and T. Weigand, “Loop-corrected compactifications of the heterotic string with line bundles,” JHEP **0506**, 020 (2005) [hep-th/0504232].
- [44] G. Horrocks and D. Mumford, “A rank 2 vector bundle on  $\mathbb{P}^4$  with 15000 symmetries,” Topology, 12:63-81, (1973).
- [45] A. Beilinson, “Coherent sheaves on  $\mathbb{P}^n$  and problems in linear algebra, “Funktional. Anal. i Prilozhen. 12 (1978), no. 3, 68-69.
- [46] L. B. Anderson, Y. H. He and A. Lukas, “Heterotic Compactification, An Algorithmic Approach,” JHEP **0707**, 049 (2007) [hep-th/0702210 [HEP-TH]].
- [47] L. B. Anderson, Y. H. He and A. Lukas, “Monad Bundles in Heterotic String Compactifications,” JHEP **0807**, 104 (2008) [arXiv:0805.2875 [hep-th]].
- [48] L. B. Anderson, J. Gray, Y. H. He and A. Lukas, “Exploring Positive Monad Bundles And A New Heterotic Standard Model,” JHEP **1002**, 054 (2010) [arXiv:0911.1569 [hep-th]].
- [49] L. B. Anderson, H. Feng, X. Gao and M. Karkheiran, “Heterotic/Heterotic and Heterotic/F-theory Duality,” [arXiv:1907.04395 [hep-th]].
- [50] T. M. Chiang, J. Distler and B. R. Greene, “Some features of (0,2) moduli space,” Nucl. Phys. B **496**, 590 (1997) [hep-th/9702030].

- [51] K. Hori, S. Katz, A. Klemm, R. Pandharipande, R. Thomas, C. Vafa, R. Vakil and E. Zaslow, “Mirror symmetry,”
- [52] D. R. Morrison and C. Vafa, “Compactifications of F theory on Calabi-Yau threefolds. 1,” Nucl. Phys. B **473**, 74 (1996) [hep-th/9602114].
- [53] M. Bershadsky, K. A. Intriligator, S. Kachru, D. R. Morrison, V. Sadov and C. Vafa, “Geometric singularities and enhanced gauge symmetries,” Nucl. Phys. B **481**, 215 (1996) [hep-th/9605200].
- [54] R. Friedman, J. Morgan and E. Witten, “Vector bundles and F theory,” Commun. Math. Phys. **187**, 679 (1997) [hep-th/9701162].
- [55] L. B. Anderson, X. Gao and M. Karkheiran, “Extending Fourier-Mukai Transforms in Heterotic Geometry,” To appear.
- [56] L. B. Anderson, J. Gray, M. Karkheiran, P. Oehlmann, and N. Raghuram, “Conic Bundles in F-theory”, To appear.
- [57] L. B. Anderson, J. J. Heckman and S. Katz, “T-Branes and Geometry,” JHEP **1405**, 080 (2014) [arXiv:1310.1931 [hep-th]].
- [58] S. Cecotti, C. Cordova, J. J. Heckman and C. Vafa, “T-Branes and Monodromy,” JHEP **1107**, 030 (2011) [arXiv:1010.5780 [hep-th]].
- [59] L. B. Anderson, J. J. Heckman, S. Katz and L. P. Schaposnik, “T-Branes at the Limits of Geometry,” JHEP **1710**, 058 (2017) [arXiv:1702.06137 [hep-th]].
- [60] P. Candelas, A. M. Dale, C. A. Lutken and R. Schimmrigk, “Complete Intersection Calabi-Yau Manifolds,” Nucl. Phys. B **298**, 493 (1988).
- [61] S. Kachru and E. Witten, “Computing the complete massless spectrum of a Landau-Ginzburg orbifold,” Nucl. Phys. B **407**, 637 (1993) [hep-th/9307038].
- [62] J. Distler, “Notes on (0,2) superconformal field theories,” Trieste HEP Cosmology 1994:0322-351 [hep-th/9502012].
- [63] J. Distler, B. R. Greene and D. R. Morrison, “Resolving singularities in (0,2) models,” Nucl. Phys. B **481**, 289 (1996) [hep-th/9605222].



- [64] R. Blumenhagen, B. Jurke, T. Rahn and H. Roschy, “Cohomology of Line Bundles: A Computational Algorithm,” *J. Math. Phys.* **51**, 103525 (2010) [arXiv:1003.5217 [hep-th]].
- [65] L. B. Anderson, J. Gray, Y.-H. He, S.-J. Lee, and A. Lukas, “CICY package”, based on methods described in arXiv:0911.1569, arXiv:0911.0865, arXiv:0805.2875, hep-th/0703249, hep-th/0702210.
- [66] T. Hubsch, “Calabi-Yau Manifolds: Motivations and Constructions,” *Commun. Math. Phys.* **108**, 291 (1987).
- [67] T. Hubsch, “Calabi-Yau manifolds: A Bestiary for physicists,” World Scientific (1994).
- [68] E. Witten, “New Issues in Manifolds of SU(3) Holonomy,” *Nucl. Phys. B* **268**, 79 (1986).
- [69] D. Huybrechts and M. Lehn, “The Geometry of Moduli Spaces of Sheaves”, Cambridge University Press (1997).
- [70] S. Gukov, C. Vafa and E. Witten, “CFT’s from Calabi-Yau four folds,” *Nucl. Phys. B* **584**, 69 (2000) Erratum: [*Nucl. Phys. B* **608**, 477 (2001)] [hep-th/9906070].
- [71] L. B. Anderson, J. Gray and E. Sharpe, “Algebroids, Heterotic Moduli Spaces and the Strominger System,” *JHEP* **1407**, 037 (2014) [arXiv:1402.1532 [hep-th]].
- [72] X. de la Ossa and E. E. Svanes, “Holomorphic Bundles and the Moduli Space of N=1 Supersymmetric Heterotic Compactifications,” *JHEP* **1410**, 123 (2014) [arXiv:1402.1725 [hep-th]].
- [73] X. de la Ossa, E. Hardy and E. E. Svanes, “The Heterotic Superpotential and Moduli,” *JHEP* **1601**, 049 (2016) [arXiv:1509.08724 [hep-th]].
- [74] X. de la Ossa, E. Hardy and E. E. Svanes, “The Massless Spectrum of Heterotic Compactifications,” *Fortsch. Phys.* **64**, 365 (2016) [arXiv:1511.02812 [hep-th]].
- [75] P. Candelas, X. de la Ossa and J. McOrist, “A Metric for Heterotic Moduli,” arXiv:1605.05256 [hep-th].
- [76] J. McOrist, “On the Effective Field Theory of Heterotic Vacua,” arXiv:1606.05221 [hep-th].

- [77] V. Braun, T. Brelidze, M. R. Douglas and B. A. Ovrut, “Calabi-Yau Metrics for Quotients and Complete Intersections,” JHEP **0805**, 080 (2008) [arXiv:0712.3563 [hep-th]].
- [78] M. R. Douglas, R. L. Karp, S. Lukic and R. Reinbacher, “Numerical Calabi-Yau metrics,” J. Math. Phys. **49**, 032302 (2008) [hep-th/0612075].
- [79] M. Headrick and A. Nassar, “Energy functionals for Calabi-Yau metrics,” Adv. Theor. Math. Phys. **17**, no. 5, 867 (2013) [arXiv:0908.2635 [hep-th]].
- [80] L. B. Anderson, V. Braun, R. L. Karp and B. A. Ovrut, “Numerical Hermitian Yang-Mills Connections and Vector Bundle Stability in Heterotic Theories,” JHEP **1006**, 107 (2010) [arXiv:1004.4399 [hep-th]].
- [81] R. Hartshorne, “Algebraic Geometry, Springer,” GTM 52, Springer-Verlag, 1977.
- [82] D. Huybrechts and M. Lehn, “The geometry of the moduli space of stable of sheaves”. Aspects of Mathematics, E 31 (1997).
- [83] C. Okonek, M. Schneider, and H. Spindler, “Vector bundles on complex projective spaces”. Birkhuser Boston, Mass., 1980.
- [84] M. A. Luty and W. Taylor, “Varieties of vacua in classical supersymmetric gauge theories,” Phys. Rev. D **53**, 3399 (1996) [hep-th/9506098].
- [85] R. Slansky, “Group Theory for Unified Model Building,” Phys. Rept. **79**, 1 (1981).
- [86] L. B. Anderson, J. Gray, A. Lukas and E. Palti, “Heterotic Line Bundle Standard Models,” JHEP **1206**, 113 (2012) [arXiv:1202.1757 [hep-th]].
- [87] L. B. Anderson, J. Gray, A. Lukas and E. Palti, “Two Hundred Heterotic Standard Models on Smooth Calabi-Yau Threefolds,” Phys. Rev. D **84**, 106005 (2011) [arXiv:1106.4804 [hep-th]].
- [88] L. B. Anderson, A. Constantin, J. Gray, A. Lukas and E. Palti, “A Comprehensive Scan for Heterotic SU(5) GUT models,” JHEP **1401**, 047 (2014) [arXiv:1307.4787 [hep-th]].
- [89] L. B. Anderson, A. Constantin, S. J. Lee and A. Lukas, “Hypercharge Flux in Heterotic Compactifications,” Phys. Rev. D **91**, no. 4, 046008 (2015) [arXiv:1411.0034 [hep-th]].
- [90] L. B. Anderson, J. Gray and B. Ovrut, “Yukawa Textures From Heterotic Stability Walls,” JHEP **1005**, 086 (2010) [arXiv:1001.2317 [hep-th]].

- [91] M. Kuriyama, H. Nakajima and T. Watari, “Theoretical Framework for R-parity Violation,” *Phys. Rev. D* **79**, 075002 (2009) [arXiv:0802.2584 [hep-ph]].
- [92] J. Gray, Y. H. He, A. Ilderton and A. Lukas, “STRINGVACUA: A Mathematica Package for Studying Vacuum Configurations in String Phenomenology,” *Comput. Phys. Commun.* **180**, 107 (2009) [arXiv:0801.1508 [hep-th]].
- [93] P. Candelas, X. de la Ossa, Y. H. He and B. Szendroi, “Triadophilia: A Special Corner in the Landscape,” *Adv. Theor. Math. Phys.* **12**, no. 2, 429 (2008) [arXiv:0706.3134 [hep-th]].
- [94] P. Berglund and P. Mayr, “Heterotic string / F theory duality from mirror symmetry,” *Adv. Theor. Math. Phys.* **2**, 1307 (1999) [hep-th/9811217].
- [95] C. T. C. Wall, “Classification problems in differential topology”. V. *Invent.Math.*,**1**,(1966) 355-374
- [96] L. B. Anderson, C. Clossett, J. Gray, and S. J. Lee, “GLSMs for gCICYs”. To appear.
- [97] I. V. Melnikov and E. Sharpe, “On marginal deformations of (0,2) non-linear sigma models,” *Phys. Lett. B* **705**, 529 (2011) [arXiv:1110.1886 [hep-th]].
- [98] L. B. Anderson, F. Apruzzi, X. Gao, J. Gray and S. J. Lee, “Instanton superpotentials, Calabi-Yau geometry, and fibrations,” *Phys. Rev. D* **93**, no. 8, 086001 (2016) [arXiv:1511.05188 [hep-th]].
- [99] L. B. Anderson, F. Apruzzi, X. Gao, J. Gray and S. J. Lee, “A new construction of Calabi-Yau manifolds: Generalized CICYs,” *Nucl. Phys. B* **906**, 441 (2016) [arXiv:1507.03235 [hep-th]].
- [100] P. Berglund and T. Hubsch, “On Calabi-Yau generalized complete intersections from Hirzebruch varieties and novel K3-fibrations,” arXiv:1606.07420 [hep-th].
- [101] J. Li and S. T. Yau, “The Existence of supersymmetric string theory with torsion,” *J. Diff. Geom.* **70**, no. 1, 143 (2005) [hep-th/0411136].
- [102] P. Candelas and X. C. de la Ossa, “Comments on Conifolds,” *Nucl. Phys. B* **342**, 246 (1990).

- [103] M. R. Douglas and C. g. Zhou, “Chirality change in string theory,” JHEP **0406**, 014 (2004) [hep-th/0403018].
- [104] L. B. Anderson, J. Gray, N. Raghuram and W. Taylor, “Matter in transition,” JHEP **1604**, 080 (2016) [arXiv:1512.05791 [hep-th]].
- [105] D. Huybrechts, ”Fourier-Mukai Transforms in Algebraic Geometry”, Oxford University Press Inc, 2007.
- [106] C. Bartocci, U. Bruzzo, D. Hernández Ruipérez, ”Fourier-Mukai and Nahm Transforms in Geometry and Mathematical Physics”, Springer, 2009.
- [107] R. Hartshorne, “Algebraic Geometry,” Springer-Verlag (1977) [ISBN 0-387-90244-9].
- [108] C.A. Weibel, “An introduction to homological algebra,” Cambridge University Press (1994) [ISBN 0-521-55987-1].
- [109] R. Friedman, “Algebraic Surfaces and Holomorphic Vector Bundles,” Springer-Verlag (1998) [ISBN 0-387-98361-9].
- [110] M.F. Atiyah, “Vector Bundles over an Elliptic Curve,” London Mathematical Society (1957)
- [111] P.S. Aspinwall, “Aspects of the Hypermultiplet Moduli Space in String Duality,” (1998) [hep-th/9802194v1].
- [112] G. Curio and R. Y. Donagi, “Moduli in N=1 heterotic / F theory duality,” Nucl. Phys. B **518**, 603 (1998) [hep-th/9801057].
- [113] F. Denef, “Les Houches Lectures on Constructing String Vacua,” Les Houches **87**, 483 (2008) [arXiv:0803.1194 [hep-th]].
- [114] R. Donagi and M. Wijnholt, “Model Building with F-Theory,” Adv. Theor. Math. Phys. **15**, no. 5, 1237 (2011) [arXiv:0802.2969 [hep-th]].
- [115] T. Weigand, “F-theory,” PoS TASI **2017**, 016 (2018) [arXiv:1806.01854 [hep-th]].
- [116] M. B. Green, J. H. Schwarz and E. Witten, “Superstring Theory Vol. 2 : 25th Anniversary Edition,”

- [117] L. B. Anderson and M. Karkheiran, “TASI Lectures on Geometric Tools for String Compactifications,” PoS TASI **2017**, 013 (2018) [arXiv:1804.08792 [hep-th]].
- [118] L. B. Anderson, X. Gao, J. Gray and S. J. Lee, “Fibrations in CICY Threefolds,” JHEP **1710**, 077 (2017) [arXiv:1708.07907 [hep-th]].
- [119] L. B. Anderson, X. Gao, J. Gray and S. J. Lee, JHEP **1611**, 004 (2016) [arXiv:1608.07554 [hep-th]].
- [120] L. B. Anderson, X. Gao, J. Gray and S. J. Lee, “Multiple Fibrations in Calabi-Yau Geometry and String Dualities,” JHEP **1610**, 105 (2016) [arXiv:1608.07555 [hep-th]].
- [121] P. Deligne. ”Courbes elliptiques: formulaire d’après J. Tate in Lecture Notes in Mathematics. Vol. 476: Modular functions of one variable”, 1975. Springer. IV Berlin Germany , pg. 53.
- [122] N. Nakayama, ”On Weierstrass Models, in Algebraic Geometry and Commutative Algebra”, Vol. II, Kinokuniya, Tokyo Japan, 1987 pg. 405.
- [123] W. Taylor, “TASI Lectures on Supergravity and String Vacua in Various Dimensions,” arXiv:1104.2051 [hep-th].
- [124] D. R. Morrison and C. Vafa, “Compactifications of F theory on Calabi-Yau threefolds. 2.,” Nucl. Phys. B **476**, 437 (1996) [hep-th/9603161].
- [125] M. J. Duff, R. Minasian and E. Witten, “Evidence for heterotic / heterotic duality,” Nucl. Phys. B **465**, 413 (1996) [hep-th/9601036].
- [126] M. Bershadsky, T.M. Chiang, B.R. Greene, A. Johansen, C.I. Lazaroiu “F-theory and Linear Sigma Models,” (1998) [hep-th/9712023v2].
- [127] R. Friedman, J. Morgan, E. Witten, “Vector Bundles over Elliptic Fibration,” (1997) [hep-th/9709029v1].
- [128] P. S. Aspinwall and R. Y. Donagi, “The Heterotic string, the tangent bundle, and derived categories,” Adv. Theor. Math. Phys. **2**, 1041 (1998) [hep-th/9806094].
- [129] R. Donagi and M. Wijnholt, “Gluing Branes, I,” JHEP **1305**, 068 (2013) [arXiv:1104.2610 [hep-th]].

- [130] R. Donagi and M. Wijnholt, “Gluing Branes II: Flavour Physics and String Duality,” *JHEP* **1305**, 092 (2013) [arXiv:1112.4854 [hep-th]].
- [131] C. Beasley, J. J. Heckman and C. Vafa, “GUTs and Exceptional Branes in F-theory - I,” *JHEP* **0901**, 058 (2009) [arXiv:0802.3391 [hep-th]].
- [132] T. Shioda. “On elliptic modular surfaces.” *J.Math.Soc.Jap.*,24,20, 1972
- [133] T. Shioda. “Mordell-Weil lattices for higher genus fibration over a curve. In New trends in algebraic geometry (Warwick, 1996).” *Lond.Math.Soc.Lect.Note Ser.*,264,359
- [134] R. Wazir. “Arithmetic on elliptic threefolds.” *Compos.Math.*,140,567, 2004
- [135] R. Donagi and M. Wijnholt, “Higgs Bundles and UV Completion in F-Theory,” *Commun. Math. Phys.* **326**, 287 (2014) [arXiv:0904.1218 [hep-th]].
- [136] L. B. Anderson, “Spectral Covers, Integrality Conditions, and Heterotic/F-theory Duality,” arXiv:1603.09198 [hep-th].
- [137] V. Sarkisov, “Birational Automorphisms of Conic Bundles,” *Math.USSR Izv.* 17, 177 (1981).
- [138] J. Distler and S. Kachru, “(0,2) Landau-Ginzburg theory,” *Nucl. Phys. B* **413**, 213 (1994) [hep-th/9309110].
- [139] E. Witten, “On the Landau-Ginzburg description of N=2 minimal models,” *Int. J. Mod. Phys. A* **9**, 4783 (1994) [hep-th/9304026].
- [140] P. Fre, L. Girardello, A. Lerda and P. Soriani, “Topological first order systems with Landau-Ginzburg interactions,” *Nucl. Phys. B* **387**, 333 (1992) [hep-th/9204041].
- [141] C. Beasley and E. Witten, “Residues and world sheet instantons,” *JHEP* **0310**, 065 (2003) [hep-th/0304115].
- [142] C. Beasley and E. Witten, “New instanton effects in string theory,” *JHEP* **0602**, 060 (2006) [hep-th/0512039].
- [143] M. Bertolini and M. R. Plesser, “Worldsheet instantons and (0,2) linear models,” *JHEP* **1508**, 081 (2015) [arXiv:1410.4541 [hep-th]].

- [144] S. Blesneag, E. I. Buchbinder, P. Candelas and A. Lukas, “Holomorphic Yukawa Couplings in Heterotic String Theory,” JHEP **1601**, 152 (2016) [arXiv:1512.05322 [hep-th]].
- [145] E. I. Buchbinder, A. Constantin, J. Gray and A. Lukas, “Yukawa Unification in Heterotic String Theory,” arXiv:1606.04032 [hep-th].
- [146] L. B. Anderson, J. Gray, D. Grayson, Y. H. He and A. Lukas, “Yukawa Couplings in Heterotic Compactification,” Commun. Math. Phys. **297**, 95 (2010) [arXiv:0904.2186 [hep-th]].
- [147] R. Donagi, J. Guffin, S. Katz and E. Sharpe, “(0,2) quantum cohomology,” Proc. Symp. Pure Math. **85**, 83 (2012).
- [148] C. Closset, W. Gu, B. Jia and E. Sharpe, “Localization of twisted  $\mathcal{N} = (0, 2)$  gauged linear sigma models in two dimensions,” JHEP **1603**, 070 (2016) [arXiv:1512.08058 [hep-th]].
- [149] L. B. Anderson, L. Fredrickson, M. Esole and L. P. Schaposnik, “Singular Geometry and Higgs Bundles in String Theory,” SIGMA **14**, 037 (2018) [arXiv:1710.08453 [math.DG]].
- [150] L. B. Anderson and W. Taylor, “Geometric constraints in dual F-theory and heterotic string compactifications,” JHEP **1408**, 025 (2014) [arXiv:1405.2074 [hep-th]].
- [151] M. Cvetič, A. Grassi and M. Poretschkin, “Discrete Symmetries in Heterotic/F-theory Duality and Mirror Symmetry,” arXiv:1607.03176 [hep-th].
- [152] M. Cvetič, A. Grassi, D. Klevers, M. Poretschkin and P. Song, “Origin of Abelian Gauge Symmetries in Heterotic/F-theory Duality,” JHEP **1604**, 041 (2016) [arXiv:1511.08208 [hep-th]].
- [153] P. Griffiths, J. Harris, “Principles of algebraic geometry,” 1978.
- [154] P. S. Aspinwall, B. R. Greene and D. R. Morrison, “Calabi-Yau moduli space, mirror manifolds and space-time topology change in string theory,” Nucl. Phys. B **416**, 414 (1994) [hep-th/9309097].